A putative interaction between mitochondrial cytochrome c oxidase subunit II (COX II) to lamin A/C and LAP2α in colon epithelial cells.

ALZOGHAIBI, FAHAD

University of Durham
School of Biological and Biomedical Sciences

A putative interaction between mitochondrial cytochrome c oxidase subunit II (COX II) to lamin A/C and LAP2α in colon epithelial cells.

Fahad Abdullah Al-Zoghaibi

Thesis submitted for the degree of Doctor of Philosophy

July 2009

Abstract:

The lamina is a cage-like structure, composed of lamins, found underneath the inner nuclear membrane (INM). In mammals, Lamins are type V intermediate filaments. Three genes encode seven different lamin proteins. These genes are LMNA, LMNB1 and LMNB2. Lamins are classified into A- and B-types. A-type lamins, Lamin A, Lamin C, Lamin Aδ10 and Lamin C2, are mainly expressed in differentiated tissues. All encodes by the LMNA gene and products of alternative splicing. Recent studies have shown the expression of Lamin A/C in colon crypt epithelia cells. This expression was greater in differentiated epithelial and stem cells than in the proliferation zone. Since 1999, mutations in LMNA have been shown to cause several different inherited diseases in muscle, fat, bone, skin and nerve tissues. LAP2α is one of the strong binding partners to Lamin A/C. LAP2α has a specific function as a non-membrane protein associated with the nucleoskeleton and may help to organize higher order chromatin structure by interacting with Lamin A/C.

To understand more about Lamin A/C and LAP2α in colon epithelial development, a Yeast 2-hybrid screen was used to look for novel protein interactions to Lamin A/C and/or LAP2a. It was found Cytochrome c oxidase subunit II (Cox2) is a putative binding partner to Lamin A/C and LAP2 α. Cox2 is encoded by the mitochondrial genome and imported into complex IV (COX) of the mitochondrial respiratory chain (MRC). The majority of mitochondrial proteins are encoded by nuclear DNA. However, 13 essential subunits of the MRC are encoded by mtDNA. The MRC is composed of five multi-subunit complexes (I-V). MRC is implicated in ATP generation and is involved in apoptosis in response to different stimuli. Deficiency in COX in colon cancer cells results in resistance to apoptosis and increases in reactive oxygen species (ROS). Biochemical assays like Co-immunopreciptation (IP) and western blot (WB) and Immuno-gold labeling (TEM) were used. IP confirmed the putative interaction of Cox2 to Lamin A/C and LAP2 α. WB showed the expression of lamin A/C and LAP2α in the mitochondrial and nuclear fractions but not in cytosol. TEM is alternative method showed the distribution of lamin A/C and LAP2α in the nucleus and mitochondria.

DECLARATION

I declare that this thesis is of my own work, the experiments and results presented in this thesis are of my investigations conducted by myself at the School of Biological and Biomedical Sciences, University of Durham under the supervision of Prof. C.J. Hutchison and Dr. M.D. Watson. No material has previously submitted for a higher degree at this or any university. The copyright of this thesis rests for the author. No quotation from it should be published in any format, including electronic and the internet without the author's prior written consent. All information derived from this thesis must be acknowledged appropriately.

Fahad A. Al-Zoghaibi

Acknowledgements

First of all, I would like to express my sincerely thanks to god, who awarded me health and time to continue my post grade.

I have to mention that this scholarship was funded by King Faisal Specialist Hospital and Research Centre.

I would also like to express my sincerely thanks to my supervisors Prof. C.J. Hutchison and Dr. M.D. Watson for their full support and guidance given to me throughout my Ph.D. and particularly during my writing up process. Additionally I am grateful to Dr. S. Al-Sedyri, Executive Director of Research Center. Dr F. Al-Muhana, Deputy Director of Research Center. Dr. K.S. AbuKabar, Principle Scientist / Head of Interferon and Cytokines Research Unit; for giving me this opportunity to pursue my postgraduate degree.

I am grateful to Prof. R. Quinlan for his guidance. Dr. R.Croy for his support in helping me with my bioinformatics studies. Dr. A. Benham and Dr. A. Smertenko for their full support. Dr. M.W. Goldberg and Mrs A. Christine Richardson for their invaluable experience in TEM. I am indebted to many of the researchers and technical staff working at the School of Biological and Biomedical Sciences, University of Durham during my period of study.

Great appreciation must also go to friends and colleagues at School of Biological and Biomedical Sciences; Mr Syed-ur-Fida Rahman-Casans who has provided me the colon tissue. Dr. N. Willis and Dr. G. Salpingidou for their help in immunoflurescence. Dr. E. Markiewicz, Dr. S. Fenyk and Dr. V. Pekovic for all their help in immunoprecipitation and western blot. Mrs P. Ritchie for her superb technical support. Mr T. Gibbons and Dr. F. Tholozan for their friendly help. Best wishes to all of my friends in the school whom help me and I didn't mention their name.

My special thanks to my wife for her full and non-stopped support. Great thanks to my children to make my life cheerful.

I would also like to extend my thanks to all of those who have personally supported me along the way.

TABLE OF CONTENTS

CHAPTER 1: INTRODUCTION

CHAPTER5: Localization and functional assay of Lamin A/C and LAP2α in mitochondria.

TABLE OF FIGURES

CHAPTER 1

CHAPTER 2

CHAPTER 3

CHAPTER 4

CHAPTER 5

CHAPTER 6

ABBREVIATIONS

AD	Alzheimer's Disease
AD-EDMD	Autosomal dominant Emery-Dreifuss muscular dystrophy
ADP	Adenosine diphosphate
AGE	Advance Glycation End
AIF	Apoptosis Inducing Factor
AMV-RT	Avian Myeblastosis Virus – Reverse Transcriptase
ANT	Adenine nucleotide translocase
APL	Acquired Partial Lipodystrophy
AP	Amonium persulfate
AR-EDMD	Autosomal recessive Emery-Dreifuss muscular dystrophy
ATP	Adenosine triphosphate
BAF	Barrier-to-autointegration
BBB	Blood Brain Barrier
BMP	Bone morphgenic protein
bp	Base pair
BRB	Blot rinse buffer
BSA	Bovine serum albumin
BTF	BCL2-associated Transcription Factor
CaCl2	Calcium chloride
cDNA	Complementary DNA
cdc	Coding region
CIAP	Calf Intestinal Alkaline Phosphatase
CMD-1A	Dilated cardiomyopathy-1A
CMT2	Charcot-Marie-Tooth-2
Co_2	Carboxyl dioxide
CoA	Coenzyme A
CoQ	Coenzyme Q
COX	Cytochrome c Oxidase (Complex IV of MRC)
Cox2	Cytochrome c Oxidase subunit II

Cu_2	Copper
Cu, Zn-SOD	Copper Zinc Superoxide dismutase
DCM-CD	Dilated Cardiomyopathy with conduction system defects
ddH_2O	Double distilled water
DEPC	Diethyl pyrocarbonate
dH_2O	Distilled water
D-MEM	Dulbecco's Modified Egale Medium
DMSO	Dimethyl sulphoxide
DNA	Deoxyribonucleic acid
DNA-BD	DNA-Binding Domain
DNA-AD	DNA-Activating Domain
dNTP	Deoxynucleotide Triphospate
DTT	Dithiothreitol
dUTP	2'-Deoxyuridine 5'-Triphosphate
ECACC	European Collection of Cell Cultures
ECL	Enhanced chemiluminescence
EDTA	Ethylenediaminetetraacedic acid
EGFP	Enhanced Green Fluorescent Protein
EM	Electron Microscopy
ER	Endoplasmic Reticulum
EST	Expression Sequence Taq
EtBr	Ethidium bromide
ETC	Electron transport chain
FBS	Foetal bovine serum
FITC	Fluorescein isothiocyanate
FS	Forward Scatter
FPLD2	Familial partial lipodystrophy type 2
g	Gram
GFP	Green Fluorescent Protein
GSH	peroxide and glutathione reductase
GFAP	Glial fibrillary acidic protein
GCL	Germ cell less

H^+	Proton
H_2O	Water
H_2O_2	Hydrogen peroxide
HCl	Hydrochloric acid
HDAC3	Histone deacetylase 3
HGPS	Hutchinson-Gilford progeria syndrome
HRP	Hours-radish peroxidase
IF	Intermediate filaments
IFNγ	Interferon gamma
INM	Inner nuclear membrane
Kb	Kilobases
KDa	Kilodaltons
LAP	Lamina-associated polypeptide
LiAc	Lithium Acetate
LB	Luria-Bertani (media/ agar)
LBR	Lamin Binding Receptor
LD-PCR	Long-Distance-PCR
LEM	LAP2, Emerin, MAN1 domain
LGMD 1B	Limb-girdle muscular dystrophy type 1B
LPS	Lipopolysaccharide
LSB	Laemmli Sample Buffer
M	Molar
mAB	Monoclonal antibody
MAD	Mandibulo-Acral Dystrophy
MDa	Megadalton
mtDNA	Mitochondria DNA or genome
$MgCl_2$	Magnesium chloride
$MgSO_4$	Magnesium sulphate
ml	Millilitre
mM	Millimolar
MIM	Mitochondrial Inner Membrane
mtΔψ	Mitochondrial membrane potential

MnSOD	Manganese Superoxide dismutase
mNOS	Mitochondrial Nitric Oxidase
MOK2	Kruppel-like protein
MOM	Mitochondrial Outer Membrane
MOMP	Mitochondrial Outer Membrane Permeabilization
MOM-R	Mitochondrial Outer Membrane Receptor
MPT	Mitochondrial Permeability Transition
mRNA	Messenger Ribonucleic Acid
MRC	Mitochondrial Respiratory Chain
MSF	Mitochondria-import stimulation factor
MTS	Mitochondrial Targeting Sequences
MTOC	Microtubule Organization Center
MW	Molecular weight
NaCl	Sodium chloride
NAD+	Nicotinamide adenosine dinucleotide
NADH	reduced form of NAD+
NaOAc	Sodium acetate
NaOH	Sodium hydroxide
nDNA	Nuclear DNA
NE	Nuclear Envelope
NETs	Nuclear Envelope Transmembrane proteins
NF	Neurofilament
NF_kB	Nuclear Factor $_kB$
ng	Ninogram
NHF	Normal Human Fibroblast cell line
NL	Nuclear Lamina
NLS	Nuclear localization signal sequence
nm	nanometre
NPC	Nuclear pore complex
NO	Nitric oxide
NOS	Nitric Oxide Synthase
nNOS	Neuronal Nitric Oxide Synthase

Nup153	Nuclear Pore Complex Protein 153
O_2	Oxygen molecule
O_2^-	Superoxide
ONM	Outer Nuclear Membrane
oxLDL	Oxidizing Low Density Lipoprotein
P	Probability-Student's *t*-test (p value)
PBS	Phosphate buffer saline
PCR	Polymerase Chain Reaction
PD	Parkinson Disease
PEG	Polyethylene Glycol
PI	Protease inhibitor
PKA	Protein Kinase A
PKC	Protein Kinase C
pmol	Picomolar
Rb	Retinoblastoma protein
RD	Restrictive dermopathy
RNA	Ribonucleic acid
ROS	Reactive oxygen species
rRNA	ribosomal RNA
RT	Room Temperature
RT-PCR	Reverse Transcriptase - Polymerase Chain Reaction
s.d.	Standard deviation
SD	Synthetic Defined (media/ agar)
SDS	Sodium Dioecyl Sulphate
SDS-PAGE	Sodium Dioecyl Sulphate–Polyacrylamide Gel Electrophoresis
Smac/DIABLO	Second mitochondrial-derived activator of caspase / direct IAP-binding protein
SOD	Superoxide dismutase
SREBP1	Sterol Response Element-binding Protein 1
SS	Side Scatter
2D	Two dimension
t	t value – Student's *t*-test

TAE	Tris-acetate EDTA
TBE	Tris-borate EDTA
TBST	Tris-Buffer Saline Plus Tween
TEM	Transmission Electron Microscope
TEMED	N,N,N',N'-tetramethylethylenediamine
TGFβ	Transforming Growth Factor β
Tm	Melt temperature
TRITC	Tetramethyl rhodamine isothiocyanate
tRNA	Transfer RNA
TNF	Tumor Necrosis Factor
V	Volt
XL	X-linked
XL-EDMD	X-linked Emery- Dreifuss muscular dystrophy
ug	Microgram
ul	Microlitre
um	Micrometre
umol	Micromolar
YPDA	Yeast Peptone Dextrose Adenine (media/agar)

Chapter 1: Introduction

1.1 Nuclear biology in health and diseases:

1.1.1 The nuclear envelope.

In higher eukaryotic cells, the nucleus is a complex organelle which contains a majority of the genetic information and is the site of DNA replication, RNA transcription and processing, and ribosome assembly. It is surrounded by the nuclear envelope (NE) which separates the nuclear content from the cytoplasm. The NE is composed of three parts: the nuclear membranes (inner, outer, and pore) the nuclear pore complexes (NPCs), and the nuclear lamina **(Figure 1.1)** (Broers *et al.*, 2006). The outer nuclear membrane (ONM) is continuous with the rough endoplasmic reticulum (ER). However the inner nuclear membrane (INM) is linked to the nuclear lamina by integral membrane proteins termed nuclear envelope transmembrane proteins (NETs) and lipid modifications. The luminal space is the space between INM and ONM which is about 100nm in width. The NPCs are composed of multiple proteins that form a complex. In vertebrates, the NPC is ~120 MDa protein complex made of ~30 different proteins. The NPCs regulate the passage of macromolecules in and out of nucleus (Goldberg, 2004). The nuclear lamina is a fibrous meshwork composed of type V intermediate filament proteins termed lamins (Muchir and Worman, 2004).

For many years, the NE was thought to function mainly as an architectural stabilizer for the nucleus, participating in assembly and disassembly processes during mitosis and to separate the DNA from the cytoplasm. However, recent findings demonstrate that NE proteins are involved in fundamental nuclear functions, such as gene regulation and DNA replication, and that inherited or *de novo* mutations in NETs cause human diseases. If the mutations are in INM or NPC proteins the diseases are termed “nuclear envelopathies”, whereas if the mutations are in lamins then the diseases are termed “laminopathies”. These finding emphasize the importance of understanding the function of this cellular domain, in both physiological and pathological states (Somech *et al.*, 2005a).

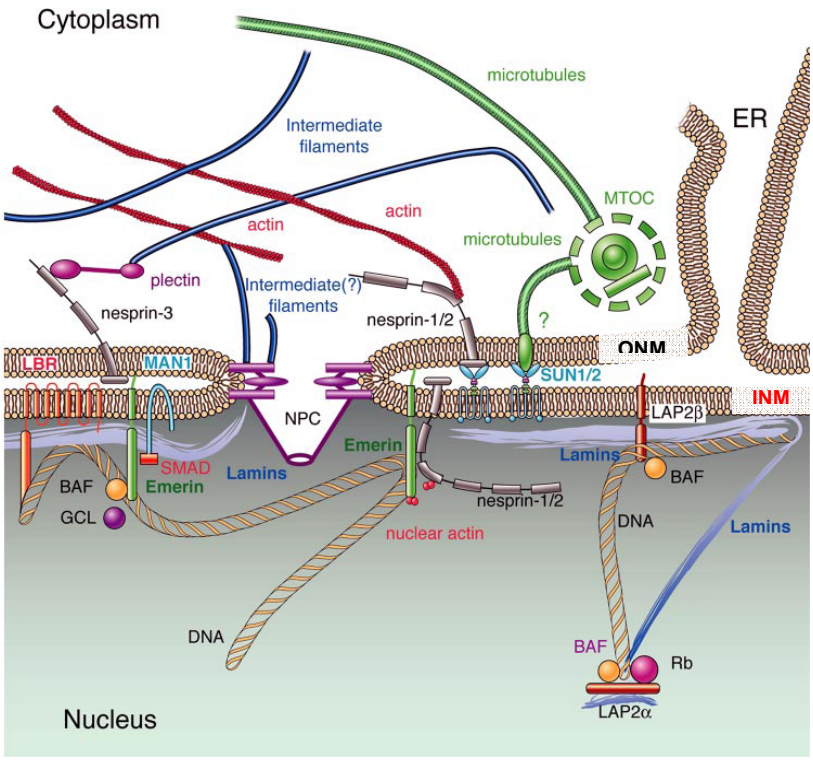

Figure 1.1: Model of the location of nuclear lamins and their interaction with nearby localized proteins. Lamins bind directly to lamina-associated proteins (LBR, LAP2, emerin, MAN1, nesprins-1 and -2), but also to BAF, Rb, SREBP1, histone proteins, and DNA, and thereby mediate association with a scala of interacting structural proteins, including SUN1, actin, and possibly tubulin and intermediate filament proteins. Question marks indicate suggested but not yet proven interactions (Broers *et al.*, 2006).

1.1.2 Intermediate filaments and the nuclear lamina.

The nuclear lamina is a cage-like structure found underneath the INM and is composed of lamins. The lamina is interconnected with integral membrane proteins and NPCs and together these interactions constrain nuclear size and shape (Moir *et al.*, 2000a; Hutchison, 2002; Herrmann and Foisner, 2003; Hutchison and Worman, 2004).

In mammals, the cell cytoskeleton is composed of three main parts: microtubules, actin filaments and intermediate filaments (IF). The intermediate filament super gene family comprising of more than 70 genes are divided into six groups, five of which (I-IV & VI) are cytoplasmic. The acidified and basic keratins (type I and II) are expressed in epithelial cells. The type III IFs are: vimentin that is expressed in mesenchymal cells, desmin which is expressed in muscle cells, glial fibrillary acidic protein (GFAP) which is expressed in glia and astrocytes and peripherin which is expressed in neurons of peripheral nervous system. The type IV neurofilament triplet proteins which are NF-L, NF-M, and NF-H and α-internexin are expressed in neurons of the central nervous system. Lamins make up group (V) of the IF family (Strnad *et al.*, 2008). The main functions of IFs are to maintain cell integrity and shape.

The nuclear lamins have the typical domain structure of the cytoplasmic IFs. All IF proteins have four central rod domains (α-helical-coiled-coil dimerization domain 1A, 1B, 2A and 2B), consisting of a heptad repeat which is characteristic of proteins forming an α-helix structure. They are separated by flexible linker regions

and flanked by N-terminal (head) and C-terminal (tail) globular domains of variable size. The major differences between lamins and cytoplasmic IFs in the protein structure are, IFs have an α-helix pre-coil domain (PCD) just before 1A of α-helix coiled-coil domain which is probably not involved in coiled-coil formation. However in lamins the head domain is ~47 amino acid shorter; there is a six heptad extension within coil 1B; the globular tail domain is longer and possesses a Nuclear-localization signal sequences (NLS) and carboxyl terminal tail CaaX motif which is the target for carboxyl methylation, farnesylation and proteolytic cleavage **(Figure 1.2)** (Herrmann *et al.*, 2007). Lamins like cytoplasmic IFs assemble into polymeric structures that are resistant to solubilization under a variety of conditions (Moir *et al.*, 2000a).

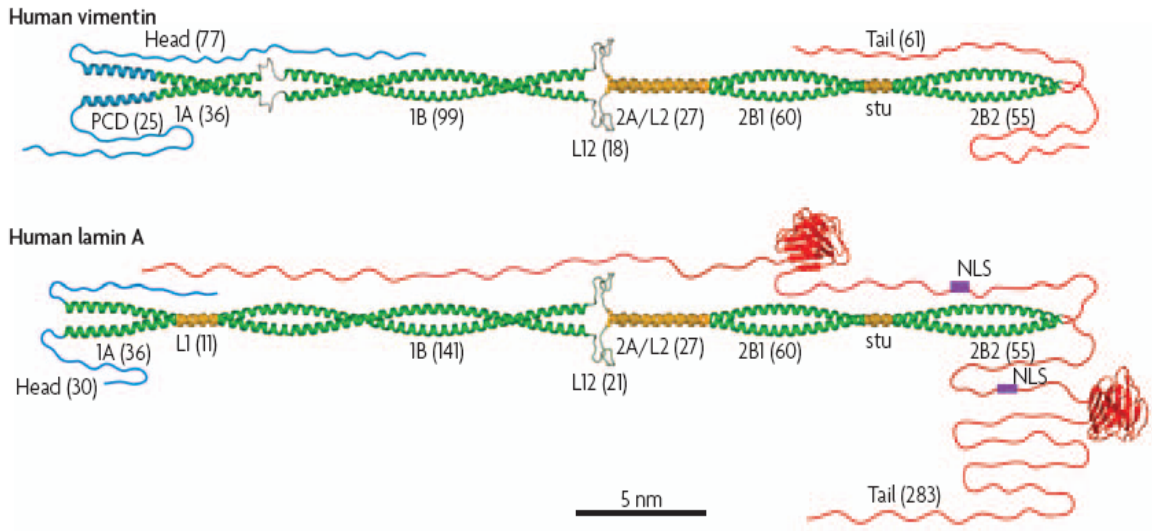

Figure 1.2: Structural model of cytoplasmic and nuclear intermediate filament protein dimers. Modelling of the human vimentin and the lamin A dimers, on the basis of structural data and structure prediction, revealed that the central α-helicalrod domain of the individual molecules is subdivided into the coil segments 1A, 1B, 2A, 2B1 and 2B2. The vimentin coil 1A ispreceded by an α-helical pre-coil domain (PCD), which is probably not engaged in coiled-coil formation. Linker segments that connect the individual α-helical segments are indicated: L1, L12 and L2. Left-handed coiled-coil segments are shown in green. Regions that are predicted to form nearly parallel α-helical bundles as well as the so-called stutter (stu) region in the heptad repeat pattern are represented in yellow. Non- α-helical linkers are shown in grey. The non- α-helical N- (head) and C-terminal (tail) domains are coloured blue and red, respectively. Parts of the α-helical coiled coils of vimentin and lamin A have been solved by X-ray crystallography9. The structure of the immunoglobulin-fold domain in the tail domain of lamin A (red wide arrows) has been solved both by X-ray crystallography and by NMR9. The numbers in brackets refer to the number of amino acids in each respective domain. Scale bar, 5 nm. NLS, nuclear localization signal (Herrmann *et al.*, 2007).

1.1.3. Nuclear Lamins.

1.1.3.1 Lamin structure.

In mammals, three genes encode seven different lamins protein. These genes are LMNA, LMNB1, and LMNB2 (Hutchison, 2002). Lamin proteins are classified into A-type and B-type lamins.

B-type lamins are expressed in all cells and are essential for cell survival (Harborth *et al.*, 2001). There are three different B-type lamin proteins. Lamin B1 is encoded by the LMNB1 gene, Lamin B2 and B3 are encoded by alternatively spliced LMNB2. Lamin B1 and B2 are expressed in most cells, while Lamin B3 is expressed in germ cells (spermatocytes and oocytes) possibly reflecting the distinct organization of nuclei of these cells (Bridger *et al.*, 2007).

A-type lamins (Lamin A, Lamin C, Lamin Aδ10, and Lamin C2) are mainly expressed in differentiated tissues (Hutchison *et al.*, 2001). Lamin C2 is expressed in germ cells (spermatocytes and oocytes) possibly reflecting the distinct organization of nuclei of these cells (Bridger *et al.*, 2007). Lamin Aδ10 is an alternative lamin protein that is expressed in tumor and several normal cell types (Machiels *et al.*, 1996).

B-type lamins are acidic and A-Type lamins are basic as demonstrated by isoelectric focusing in conventional two dimensional polyacrylamide gel

electrophoresis (Lehner *et al.*, 1986). All lamins contain a carboxyl-terminal CaaX motif except lamin C, ("C" is cysteine, "a" is commonly an aliphatic amino acid, and "X" can be different amino acids). The CaaX sequence in prelamin A is CSIM and in lamin B1 is CAIM (Stewart *et al.*, 2007). Lamin A and C proteins are identical for the first 566 amino acids but are distinct at their carboxy-terminal ends. Lamin C has six unique carboxy-terminal amino acids (Lin and Worman, 1993).

1.1.3.2 Lamin translation and post translational modifications.

Prelamin A is the precursor to mature lamin A. Prelamin A undergoes specific post translational processing to produce mature lamin A. This process starts by adding farnesyl lipid to the cysteine of the caboxy-terminal CaaX box of the protein by a cytosolic enzyme protein farnesyltranssferase. Subsequently, the last three amino acids of the protein –aaX are clipped off by RCE1 and ZMPSTE24. This will be followed by a methylation step via methyltransferase ICMT. These three modifications render the carboxyl-terminal domain of lamin A, B1 and B2 more hydrophobic, and this hydrophobicity could facilitate lamins to associate in INM (Young *et al.*, 2006). The post translational processing of B type lamin proteins follows the same steps of prelamin A (Rusinol and Sinensky, 2006; Stewart *et al.*, 2007). The only difference in post translational processing is that prelamin A expose to a second endoproteolatic cleavage by ZMPSTE24. This process is ended by clipping off the last 15 amino acids including the farnesyled methylated cysteine which will release mature lamin A **(Figure 1.3A).** This process occurs 30-

60 minutes after assembly into nuclear lamina (Bergo *et al.*, 2002; Pendas *et al.*, 2002).

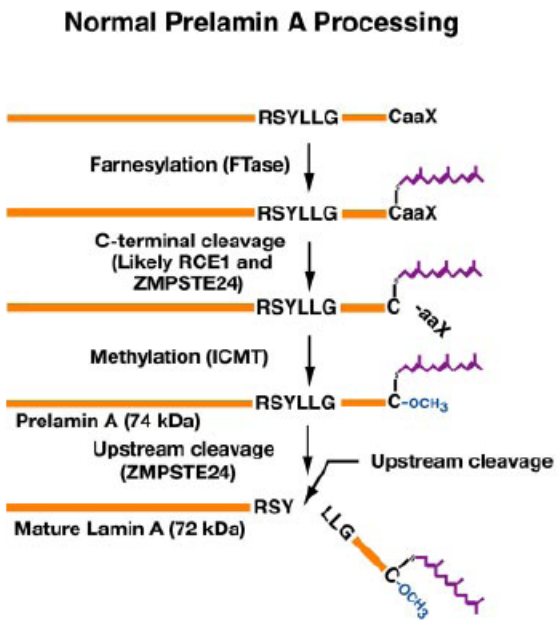

Figure 1.3A: The maturation step of Lamin A posttranslation in normal cells (Young *et al.*, 2006).

Mutation in this cleavage site leads to accumulation of permanently isoprenalyted lamin A that cause progeria (Young *et al.*, 2006). Lamin C lacks the CaaX motif and is never undergoes post-translation process **(Figure 1.3B)** (Hutchison *et al.*, 2001). But it still be found at the NE, which may show the post translation process is not essential for NE localization (Goldberg *et al.*, 2008a).

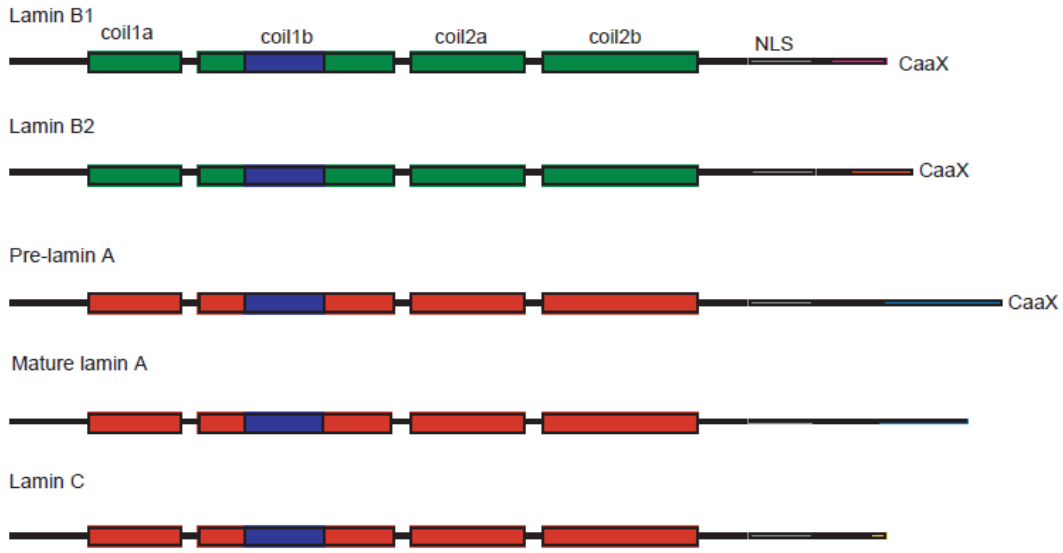

Figure 1.3B: Schematic representation of somatic cell lamins. Coloured rectangles represent α-helical coiled-coil domains; B-type lamins are shaded in green, and A-type lamins are shaded in red. The blue shaded NLS=nuclear localization signal sequence; CaaX is the site for carboxy methylation, prenylation and proteolytic cleavage. Coloured regions in the C-terminal tail domains show the major sites of amino acid residue variation among the lamin subtypes (Hutchison *et al.*, 2001).

1.1.3.3 Lamin polymer assembly.

In somatic cells lamina structure is more complex because of its interactions with intranuclear structures proteins. Because of this it is difficult to access and to judge the relevance of in vitro structures (Goldberg *et al.*, 2008a). An intermediate approach has been taken to study lamina structure in vitro using *Xenopus* oocytes. Accumulated evidence helped investigators to imagine three steps for the assembly of lamina structure. The first evidence showed the in-vitro assembly of B-type lamin to form a 10-13nm diameters filament was performed in *Xenopus* oocytes (Aebi *et al.*, 1986). However, in vitro experiments showed A-type lamin form a thicker (>13nm) diameter structure (Quinlan *et al.*, 1995)(Goldberg *et al.*, 2008b). Lamin assembly was studied using EM analysis of purified recombinant wild-type and mutant lamin and chemical cross-linking within the native lamina

(Stuurman *et al.*, 1998). These studies suggested that lamin assembly in-vitro involved lateral interaction via coiled-coil associations of α-helical rod domains of two lamin chains to form homodimers.

It was also suggested that lamins interact longitudinally to form head-to-tail polymers. Several studies on the mutant *Drosophilla* lamins have shown that amino acid residue of N-terminal end of coil 1A associated with the amino acid residues of C-terminal end of coil 2A, that suggest the head-to-tail polymerization (Heitlinger *et al.*, 1991; Moir *et al.*, 1991).

A model was suggested to explain how tetramers of B-type lamin form. This model showed that beside the lateral interaction of two lamin chains and head-to-tail polymerization (see above), B-type lamins are involved in N-N half anti-parallel tetramer structure of two polymers. This model was based on studies confirmed the binding of LAP2β with coil 1B of B-type lamins (Yang *et al.*, 1997a, 1997b; Mical and Monteiro, 1998; Gant *et al.*, 1999). Moreover the implication of LBR as an isoperen receptor, after confirmed binding CaaX motife to LBR (Mical and Monteiro, 1998).

A cartoon model was developed to show how a 2D lamina array forms in the INM **(Figure 1.4).** Since A-type lamins are not expressed in embryonic cells, it was proposed that the B-type lamin is the base of lamina structure. It was demonstrated that a tetramer of B-type lamin anchors to the NE by interacting with NETs such as LBR and LAP2β (Yang *et al.*, 1997b, 1997a).

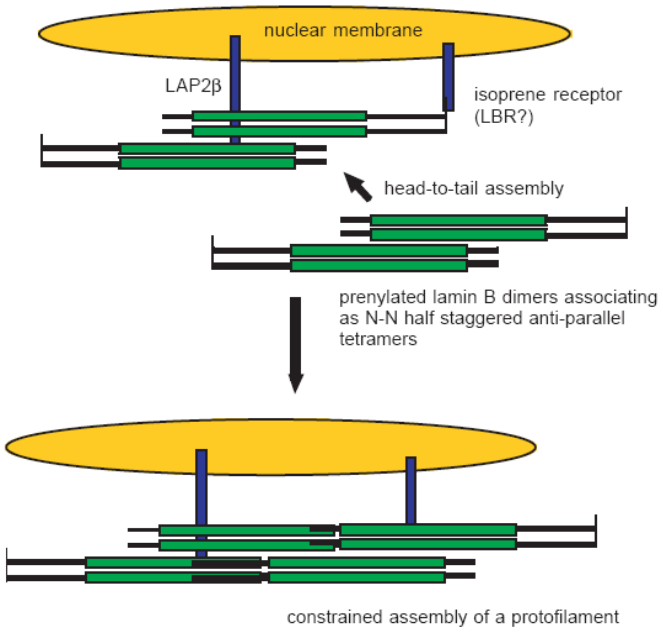

Figure 1.4: Cartoon showing the constrained polymerisation of B-type lamin filaments at the INM. Tethering of B-type lamins to the INM in this model is through association with LAP2 through coil 1b and through an isoprene receptor (possibly LBR). Lamin B dimers form NN half-staggered anti-parallel associations to make tetramers and head-to-tail associations to form higher-order structures such asproto-filaments (Hutchison *et al.*, 2001).

Several experiments showed the aggregation of A-type lamin in the nucleoplasm in the B-type lamin null cells (Dyer *et al.*, 1999). But, how A-type lamin interacts with B-type lamin is a big issue that needs to be investigated.

Several studies implicated lamin A in anchoring lamin C into the NE. In cancer cell lines that do not express lamin A, lamin C was located in the nucleolus instead of the NE (Vaughan et al., 2000; Venables et al., 2000). A cartoon model was developed to demonstrate how lamin A/C tetramer associate with B-type lamin dimers through anti-parallel associations at the NE **(Figure 1.5)** (Hutchison *et al.*, 2001).

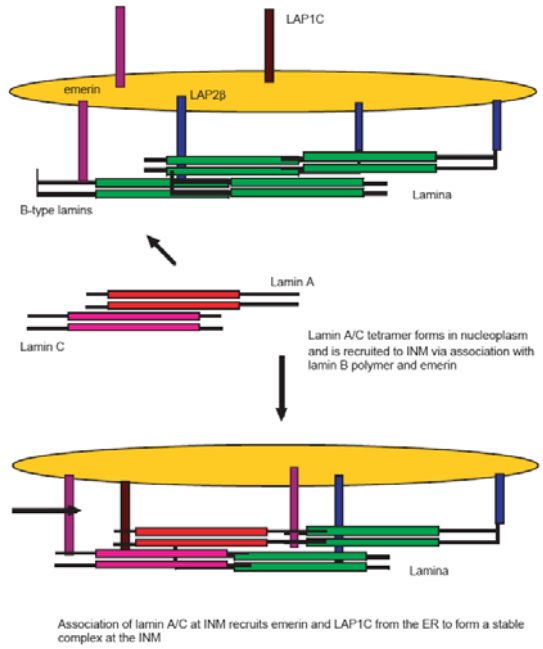

Figure 1.5: Incorporation and stabilisation of A-type lamins at the INM. A-type lamin tetramers are incorporated into the INM by head-to-tail and anti-parallel associations with B-type lamin filaments. Recruitment of these lamins to the INM leads to further recruitment of emerin and LAP1C from the ONM/ER to the INM, stabilising the A-type lamins. 'Lamina' indicates where lamin filaments are assembling.

1.1.3.4 Lamins in mitotic disassembly and assembly.

During interphase, it was believed that the nuclear lamins have important roles in the NE integrity and chromatin organization. At mitosis a complete disassembly and reassembly of the NE occurs (Vaillant and Paulin-Levasseur, 2008). Disassembly of nucleus was classified into three main independent steps: chromosome condensation, nuclear lamina depolymerization, and nuclear envelope breakdown (NEBD) (Newport and Spann, 1987). NEBD would define the end of prophase and the beginning of prometaphase (Vaillant and Paulin-Levasseur, 2008). Disassembly of nuclear lamina correlates with its hyperphosphorylation (see below). It was also believed that number of integral and

peripheral NE proteins, including LBR, LAP2α and LAP2β are involved in hyperphosphorylation by cyclin B and cdk during prophase (Dechat *et al.*, 1998). It was thought that phosphorylation step is important to abolish the structural protein-protein integrity of the NE, and to promote membrane release from chromatin (Vaillant and Paulin-Levasseur, 2008). The release of NPCs was implicated in nuclear disassembly, leading to a fenestration of the NE before NEBD (Collas, 1998).

At the G2/M transition, the localization and attachment of dynein to NE has been shown (Busson *et al.*, 1998; Salina *et al.*, 2002). It was speculated that dynein binds with NPC proteins which could serve as an attachment site for microtubules (Daigle *et al.*, 2001; Salina *et al.*, 2002). At the end of prophase and beginning of prometaphase microtubules bind to the nuclear membrane via dynein/dynactin and NPC proteins and tear away the membrane fragments out of the nucleus to generate NEBD. After NEBD, microtubules would stay attached to NPC and dynein and pull NE fragments away from the chromosome surface towards the centrosomes (Beaudouin *et al.*, 2002). The timing of disassembly of A- type and B-type lamins are different. A-type lamin are released to the nucleoplasm in early prophase before B-type lamin (Georgatos *et al.*, 1997). It was shown that B-type lamins solubilized rapidly within 5-10mins after NEBD. A kinetics experiments were performed on NE proteins dispersion including LBR, LAP2β, POM121 and Lamin B correlated to NEBD. The results demonstrate that all NE proteins tested except for LBR were dispersed only after NEBD. All three NE proteins were equilibrated with ER except B-type lamin appeared to be soluble in the cytoplasm (Ellenberg *et al.*, 1997; Daigle *et al.*, 2001; Beaudouin *et al.*, 2002). A-type lamins completely

solubulized during mitosis (Gerace and Blobel, 1980). Several key elements that control G2 to metaphase in the eukaryotic cell cycle have been found. Among these is the protein complex of cdc2 kinases that is composed of at least two subuints: p34cdc2 the 34 Kd product of the cdc2/cdc28 gene, and a 45-62 Kd protein known as cyclin B (Norbury and Nurse, 1989). The relationship between cdc2 and nuclear lamins were subjected for further studies. It was demonstrated that both chicken lamins B1 and B2 were phosphorylated by purified cdc2 kinase in vitro. It was confirmed that the sites of phosphorylation in vitro is the same one in vivo. This study was able to identify one of the M-phase specific phosphoacceptor sites of cdc2 kinase as an evolutionarily conserved serine residue in the N-terminal head domain of all lamins. Protein kinase A and C are among several lamin kinase proteins that have been implicated in lamins phosphorylation (Collas *et al.*, 1997). Binding of lamin A with PKA was identified and occurs through both the V5 region and a portion of the C2 region of the kinase (Martelli *et al.*, 2002). Down-regulation of PKA has been implicated in lamina disassembly (Lamb *et al.*, 1991). At interphase, PKC has been implicated in phosphorylation of chicken lamin B2, a process thought to regulate lamin import into the nucleus (Hennekes *et al.*, 1993).

At the end of mitosis, the NE proteins reassemble around chromatin to rebuild the nucleus structure (Gant and Wilson, 1997). Immunodepletion of lamins using antibodies in *Xenopus* nuclear assembly extracts did not affect nuclear envelop formation (Meier *et al.*, 1991), the nuclei have a full membrane structure. This suggested that lamins do not have an important role in rebuilding the nuclear envelop but may they have critical roles in its function. However, one study showed NPC clustering and small nuclei in immunodepletion of lamin B3 in *Xenopus*

extracts (Goldberg *et al.*, 1995). A different study showed that lamins start to assemble after the nuclear membranes have formed (Wiese *et al.*, 1997). Lamin polymerization appears to be necessary for the growth of the nucleus and the maintenance of nuclear shape during interphase (Moir *et al.*, 2000a).

1.1.3.5 Lamina functions in health and disease.

To understand the function of lamins in health and disease, we need to understand their structure at the gene and protein level. For over a decade, the investigators have focused on two areas; the role of lamins as building blocks and transcriptional regulators.

Since 1999, mutations in LMNA have been shown to cause several different inherited diseases; in muscle, fat, bone, skin and nerve. These observations have forced cell biologists to consider the nuclear lamina in a new light (Worman and Courvalin, 2002, , 2004). ~220 mutations have been discovered in LMNA (Gruenbaum *et al.*, 2005), which are linked to at least 12 diseases, including Hutchinson-Gilford progeria, striated muscle diseases including muscular dystrophies and dilated cardiomyopathies, lipodystrophies affecting adipose tissue deposition and a peripheral neuropathy (Stewart *et al.*, 2007) a database of nuclear envelopathies can be found at http://www.umd.be/.

As B-type lamins are essential for cell survival, loss of either lamin B1 or B2 is lethal to dividing cells (Harborth *et al.*, 2001). However, a duplication of lamin B1

gene was reported to be associated with the neurodegenerative disease autosomal-dominant leukodystrophy that is caused by myelin loss in the central nervous system (Padiath *et al.*, 2006). Recently, 3 rare mutations in lamin B2 genes were reported in patients with acquired partial lipodystrophy (APL). Two of these mutations result in amino acid substitutions. As there were no associations of these mutations in other APL patients, the relationship of these mutations to this disease is not yet understood (Hegele *et al.*, 2006).

Accumulation of different studies reported mutations in A-Type lamins. How mutations in A-type lamin proteins that are expressed in virtually all somatic cells cause different tissue-specific diseases were not understood yet. Therefore, several investigators in this field have converged on two types of hypothesis: gene expression and mechanical stress (Worman and Courvalin, 2004).

The gene expression hypothesis states that A-type lamins are considered to be essential in maintaining tissue-specific expression of certain genes. Thus, a pathogenic mechanism of some laminopathy diseases might be a change in gene expression caused by mutations in lamin A /C (Worman and Courvalin, 2002).

The mechanical stress hypothesis states that mutations in lamins A/C weaken the structural integrity of an integrated nucleocytoplasmic skeletal network (Worman and Courvalin, 2002). This weakness seems to be involved in physical damage to cells and tissues (Hutchison and Worman, 2004).

1.1.3.5.1 LMNA Mutations.

Mutations in A-type lamins were sub-classified into primary and secondary laminopathy diseases. The primary is the mutations in the LMNA. The secondary is the mutations in the enzyme (ZMPSTE24) that is involved in the posttranscriptional processing of lamin A /C.

Primary laminopathies affecting striated muscle: Numerous different mutations along LMNA which are mainly heterozygous substitutions were identified in the autosomal dominant form of Emery-Dreifuss Muscular Dystrophy (AD-EDMD) that are associated with clinical and biological features of early contractures of ankles, elbows and cervical spine, slow progressive humero-peroneal muscle weakness and wasting, and cardiac conduction defects and dysrhythmia in adult (Bonne *et al.*, 1999). Similar mutations were associated with limb-girdle muscular dystrophy type 1B (LGMD 1B), and associated with clinical and biological features of slow progressive proximal muscle weakness and wasting and frequent conduction defects (Muchir *et al.*, 2000). LMNA mutations were also identified in dilated cardiomyopathy with conduction system defects (DCM-CD), and associated with clinical and biological features of cardiac failure, cardiac conduction and rhythm disturbances and dilated cardiomyopathy (Fatkin *et al.*, 1999).

Primary laminopathy affecting axonal myelination: Homozygous R298C substitution mutation in the rod domain of lamin A was identified in Charcot-Marie-Tooth axoanal neuropathy type 2B1 (CMT 2B1), and associated with clinical and

biological features of absent deep-tendon reflexes, distal amyotrophy and loss of large myelinated nerve fibers (De Sandre-Giovannoli *et al.*, 2002).

Primary laminopathies affecting adipose and skeletal tissue: A heterozygous substitution mutation on codon R482G was reported in familial partial lipodystrophy of the dunnigan type (FPLD2), and associated with clinical and biological feature of loss of subcutaneous white adipose tissue in limbs and trunk and accumulation in face, neck and abdominal regions that begin at puberty which may not be recognized in children (Shackleton *et al.*, 2000). Several heterozygous substitution mutations at codon 482 (R482W/Q/L) were identified. Other mutations like: G465D, K486N, R582H and R584H were also associated with FPLD (Vigouroux and Capeau, 2005). Heterozygous C591F and R439C substitution missense mutations were also reported in FPLD2 patients (Araujo-Vilar *et al.*, 2008; Verstraeten *et al.*, 2009) respectively. Homozygous mutation R527H or A529V was identified in Mandibulo-Acral Dysplasia (MAD) and associated with clinical and biological features of the metabolic and fat depot, osteolytic lesions, and skeletal abnormalities of craniofacial region and clavicles, insulin resistance and hypertriglyceridermia (Simha *et al.*, 2003). A unique LMNA mutation (G602S) was reported in a nonobese 24-yr-old woman. This mutation was associated with polycystic ovary syndrome that including severe hyperandrogenism, acanthosis nigricans, and type A insulin resistance (Young *et al.*, 2005). Restrictive dermopathy (RD) is a rare disorder mainly associated by growth retardation, tight and rigid skin with erosions, prominent superficial vasculature and epidermal hyperkeratosis, sparse or absent eyelash and eyebrow, multiple joint contractures and an early neonatal lethal within the first week of life. It is caused by a

heterozygous mutation in the LMNA gene, that leads to form in-frame encoding resulting a truncated prelamin A (Navarro *et al.*, 2004). Lethal fetal akinesia, one case was found with a homozygous LMNA nonsense mutation (Y259X). It was associated with a lethal phenotype including dismaturity, facial dismorphism with retrognathia, severe contractures of the fingers and the toes and severe generalized muscular dystrophy (Mounkes *et al.*, 2003).

Primary laminopathies and progeroid syndromes: A heterozygous substitution mutation G608G that produces a truncated prelamin A or a homozygous substitution mutation K542N were identified in Hutchinson-Gilford Progeria (HGPS) and associated with clinical and biological features of generalized severe growth retardation, loss of subcutaneous fat (lipoatrophy), reduction in bone density (osteodystplasia), poor muscle development and artherosclerosis. The average age of death in this disease is 12-15 years because of artheroslerosis resulting myocardial infarction (Sarkar and Shinton, 2001).

A second mutation that causes premature aging is Werner's syndrome. It is an autosomal recessive mutation in WRN gene, which is one of RecQ DNA helicase-exonuclease that unwinds DNA and cleaves nucleotides from DNA termini. The disease associated with early-onset cataracts, arthrosclerosis, type-II diabetes, premature graying and loss of hair, cancer, death in the late 40's from myocardial fraction. 83% 0f Werner's patients have defects in the WRN locus, a few of them do not. However, mutations in LMNA were found in 15% of the Werner's patients (Stewart *et al.*, 2007).

Secondary laminopathies affecting skeletal muscle or skin tissue: Heterozygous mutations were identified in the ZMPSTE24 gene that encodes the protease involved in posttranslational process to produce mature lamin A. These mutations were found in Mandibulo-Acral Dystrophy (MAD) and restrictive dermopathy (RD) patients, and associated with exact MAD's clinical and biological features or with tight and rigid skin with epidermal hyperkeratosis, pulmonary hypoplasia, joint contractures and early neonatal mortality in the first week (Donadille *et al.*, 2005). Mutations in ZMPSTE24 were reported in neonates associated with RD symptoms. Accumulation of prelamin A and complete absence of ZMPSTE24 and mature lamin A were found in these patients (Navarro *et al.*, 2005).

1.1.3.5.2 Cancer development.

The expression levels of lamins have been correlated with tumors. Down regulated expression of lamin A/C have been associated with different cancers, such as lymphoma and leukemia (Agrelo *et al.*, 2005), lung cancer (Broers *et al.*, 1993) and colon cancer which suggested that down regulation of lamin in colon cancer could be a biological marker of malignancy (Moss *et al.*, 1999). One study in colorectal cancer showed that the expression of A-type lamin in tumors leads to a more aggressive form. Lamin A expression was associated with high motility, loss of cell adhesion which become more invasive and a stem cell-like phenotype (Willis *et al.*, 2008). The expression of A-type and B-type lamins were investigated in skin normal and tumor tissue. It was concluded that down expression of lamin A is

correlated to rapid growth within the tumor, while down regulated expression of lamin C is correlated with slow growth within the tumor. These findings suggest that lamin A has a negative influence on cell proliferation (Venables *et al.*, 2001; Tilli *et al.*, 2003).

1.1.3.5.3 DNA replication.

It has been reported that lamins are not only found in the NE or nucleoplasm but they are located at sites of DNA synthesis. The first reports that implicated lamins in DNA replication was when small nuclei that failed to replicate DNA were assembled in lamin depleted *Xenopus* egg extracts (Newport *et al.*, 1990; Meier *et al.*, 1991). It was also shown that lamin B1 binds to DNA and histones (Taniura *et al.*, 1995). Two further studies demonstrated that disruption of lamina structure in nuclei affects the initiation phase but not the elongation phase of DNA replication. These results were performed when two constructs of GST-lamin mutant fusion proteins were used as a dominant negative protein in *Xenopus* egg extracts (Ellis *et al.*, 1997; Izumi *et al.*, 2000). It was also shown that complexes of nuclear proteins like LAP2β and HA95 have important roles in the initiation but not elongation phase of DNA replication. It was found that this complex protects the initiation protein cdc6 from destruction by the proteasome (Martins *et al.*, 2003). As B-type lamins bind to LAP2β, it is thought that B-type lamins may tether the complex of LAP2β/ HA95 to the NE to stabilize cdc6 (Broers *et al.*, 2006).

1.1.3.5.4 RNA transcription.

Both A-type and B-type lamins have important functions in transcription regulation. Several experiments have been designed to investigate the exact role of B-type lamins in gene expression. RNAi knockdown of either lamin B1 or lamin B2 in cultured cells inhibited cell growth and promoted apoptosis, which suggested both lamin B1 and B2 genes are important for gene expression (Harborth *et al.*, 2001). It was also found that B-type lamins bind to RNA polymerase II, which implicated B-type lamins in RNA synthesis (Spann *et al.*, 2002). In mammalian cells, recent studies show low expression of lamin B1 but not lamin A/C has a critical role in RNA synthesis, which was associated with morphological changes in nuclear compartments, nuclei and nuclear speckles. These results elucidated that lamin B1 is important to maintain RNA synthesis (Tang *et al.*, 2008).

A-type lamins can move between the NE and nuclear bodies so may have positive and negative influences on gene expression, while B-type lamins are located in the NE only which suggested they may have a specific effect on gene silencing (Hutchison, 2002). There is also strong evidence that A-type lamins have roles in RNA transcription regulations and processing. It has been reported that four different transcription regulators can bind strongly to A-type lamins: the kruppel-like protein (MOK2), the sterol response element-binding protein (SREBP1), Retinoblastoma (Rb) and c-Fos (Ozaki *et al.*, 1994; Dreuillet *et al.*, 2002; Lloyd *et al.*, 2002; Ivorra *et al.*, 2006).

On the other hand the influences of A-type lamins were not clear; some studies show that lamin A was not crucial in gene expression but other show that lamin A has role in gene expression (Wilson *et al.*, 2001). In fact, the binding of transcription regulators may explain their influences on gene expression at transcriptional or post-transcriptional level (Hutchison, 2002).

1.1.3.5.5 Nuclear envelope shape and size.

A-type lamins have a role in determining the nuclear shape. Alteration in nuclear morphology has been reported in fibroblasts from patients with lamin A/C mutations (Vigouroux *et al.*, 2001). The same phenomena was seen in cell lines knocked down using siRNA for Lmn-1 in *C.elegans* (Liu *et al.*, 2000). Small nuclei were formed in the presence of dominant negative lamin mutants in *Xenopus* eggs extract (Spann *et al.*, 1997). Many experiments have revealed the role of lamins in resisting deformation of the nuclear envelope, green fluorescent protein (GFP)-lamin was used to look for lamina assembly properties of living cells. The experiment showed that the original shape of the NE was quickly restored (Broers *et al.*, 1997; Moir *et al.*, 2000b). In fact the presence of lamins helps the nucleus to take its shape, size and the strength of the nuclear envelope (Hutchison, 2002).

One of the important functions of the lamina is anchoring the nuclear envelope's elements to the right position. B-type lamin was confirmed to interact to nuclear-pore protein nucleoprotein 153 (Nup153): when lamina assembly is prevented in

Xenopus egg extract using a dominant negative lamin mutant, Nup153 did not incorporate into NPCs (Smythe *et al.*, 2000).

1.1.3.5.6 Cytoskeleton organization.

Growing evidence demonstrate the links between the lamina and the cytoskeleton. These links were through the interaction of nuclear lamins with proteins located at the INM and ONM to join the lamina with the cytoskeleton (Broers *et al.*, 2006).

A complex of proteins was found at the INM and ONM. Three SUN domain proteins called UNC-83, UNC-84 and SUN1 were found located at the INM and ONM in C. elegans (Starr *et al.*, 2001; Lee *et al.*, 2002; Malone *et al.*, 2003). A putative interactions between UNC-84 and SUN1 to lamin A were found, this demonstrates the localization of both of them at the INM. Two additional protein ZYG-12 and ANC-1 are anchored to the ONM by SUN1 and UNC-84 respectively (Malone *et al.*, 1999; Starr and Han, 2002). ZYG-12 is a microtubule binding protein. ANC-1 is a homolog of nesprin-1 which interacts with the actin cytoskeleton. These findings emphasise that the tethering of UNC-84 and SUN1 by lamins will maintain two independent protein complexes at the ONM which interact with microtubules and the microtubule organization center (MTOC).

Further studies were done on the mammalian cells which concluded that a family of proteins homologous to ANC-1 termed nesprin-1 and 2 are localized at the NE (Mislow *et al.*, 2002; Libotte *et al.*, 2005; Zhang *et al.*, 2005). It was found that

nesprin-1 interacts with emerin and lamin A in vitro (Mislow *et al.*, 2002). Nesprin-1 interaction to actin bundling protein was also found in vivo and in vitro (Padmakumar *et al.*, 2004). Several studies also showed the interaction of nesprin-2 to lamin A/C and emerin. These studies suggested that a complex of nesprin-2 and lamin A/C is necessary for anchoring emerin to the INM, whereas dominant mutants of nesprin-2 showed mislocalization of emerin to the ER (Libotte *et al.*, 2005). However, different studies showed that A-type lamins are not involved in anchoring nesprin-1 or 2 into the NE. These studies showed SUN1 interacts to nesprin-1 and 2. Moreover, small interfering (si)RNA knockdown of SUN1 leads to mislocalization of nesprin-2 (Padmakumar *et al.*, 2005). The third member of nesprin family nesprin-3 was identified. It's interaction to lamin A was confirmed. It has also been reported to interact to IFs (Wilhelmsen *et al.*, 2005). These finding may implicate A-type lamin in maintaining three independent protein complexes at ONM by interconnecting the microtubules, MTOC or actin and IFs to NE.

A study showed that lack of A-type lamin disrupts a macromolecular complex that spans the nuclear envelop and connects the nucleoskeleton to cytoskeleton (Crisp *et al.*, 2006). A recent study showed that lamin A/C deficiency induced significant separations of the MTOC from the nuclear envelope. In addition, the elasticity and viscosity of the cytoplasm in $Lmna^{-/-}$ cells were reduced; the same results were found when either actin filaments or microtubule networks were disassembled in wild-type cells. Investigators implicated the mechanical properties of cytoskeleton and cytoskeleton-based processes, including cell motility, coupled MTOC and nuclear dynamics, and cell polarization depend on the integrity of the nuclear

lamina which may explain the connection between the nucleus and cytoskeleton (Lee *et al.*, 2007).

One more study implicated B-type lamins in nuclear dynamics and in anchoring the nucleus to the cytoskeleton. By using time-lapse video-microscope, investigators were able to show the nuclear rotation in laminB1$^{-/-}$ cells verses wild-type fibroblast. The rotation involved the nuclear interior as well as the nuclear envelope. This rotation was eliminated by expressing lamin B1 in the cell (Ji *et al.*, 2007).

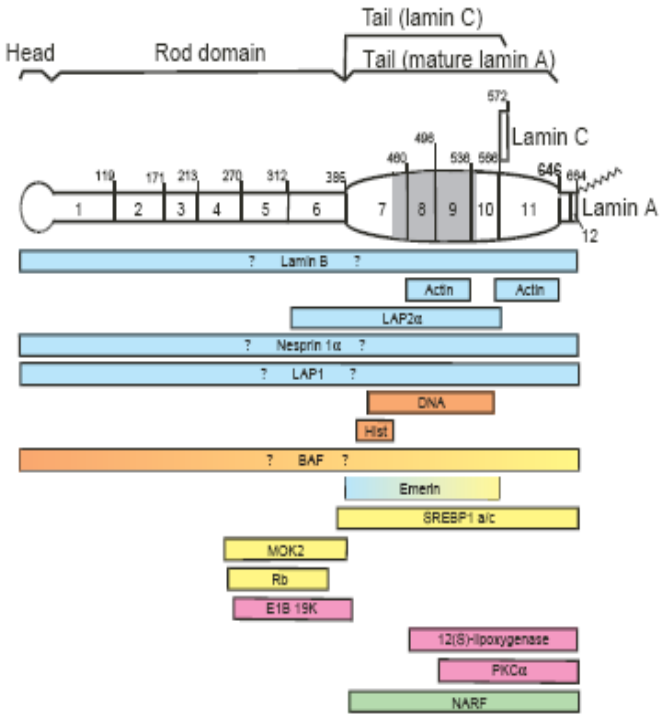

Figure 1.6: Regions in A-type lamins to which partners bind (Zastrow et al., 2004).
Regions in lamins A andC to which partners bind. Thestructural domains (head, rod,tail) of prelamin A are shown.Exons 1-12 encoding residues 1-664 are numbered; the last residue encoded by each exon (except exon 11) is given above. The Ig-fold domain, which includes exons 8 and 9, is shaded gray. Residues 1-566 of lamin A and lamin C are identical. Unique lamin C tail residues 567-572 are produced by alternative mRNA splicing; thus the extreme C-terminal regions of lamins A and C may have distinct binding properties. The zigzag represents the farnesyl moiety on prelamin A; the farnesylated C-terminal peptide is normally removed by proteolytic cleavage after residue 646 (bold; dotted line) togenerate mature lamin A. Colored bars indicate the region(s) in lamins A and C required for each named partner to bind, as detailed in Table 1 (e.g. actin can bind two different regions in the tail). For partners with question marks, the binding region in lamin A/C is unmapped. Based on current incomplete knowledge, interactions were loosely color-coded (top to bottom) as blue (architectural), orange (chromatin), yellow (gene regulation), pink (signaling) and green (unknown). Some partners (e.g. BAF) will continue to defy categorization until more is known about their functions.

1.1.4 Lamin A Binding Partners.

To understand more about the function of the lamina we need to know more about the proteins that binding to lamins. Some studies showed A-type lamins bind to other proteins, some of them showed in two-hybrid assays and in vitro, but in vivo significances remain untested.

These proteins were classified into four groups; some of these proteins are linked in different function. Architectural partners are LAP1, Nesprin 1α, LAP2α, Actin and Lamin B. Chromatin partners are Histone, and BAF. Gene regulatory partners are BAF, SREBP1a, SREBP1c, MOK2, LAP2α and Retinoblastoma (Rb). Signaling partners are E1B 19K, 12(S)-lipoxygenase and PKCα. Some of them have unknown function like NARF **(Figure 1.6)** (Zastrow *et al.*, 2004).

A recent proteomics analysis suggests that as many as eighty transmembrane proteins are localized to the INM in interphase cells (Schirmer *et al.*, 2003). Only a few of these proteins have been characterized in detail as interaction with nuclear lamina **(Figure 1.1)** (Broers *et al.*, 2006).

It was suggested that BAF may be function as a modulator of cell proliferation by influencing S-phase progression. Because, many nuclear proteins do not exist in unicellular eukaryotics but they do in multicellular metazoan including *C. elegans*. It was thought that in multicellular organisms, BAF through it's interaction with nuclear envelope proteins may regulate DNA synthesis and/or cell proliferation in

particular cells to produce specific type of tissues and organs (Haraguchi *et al.*, 2007).

1.1.4.1 Lamina-associated polypeptide 2 (LAP2).

LAP2 (also called thymopoietein) is a family of alternatively spliced proteins derived from a single gene. Three isoforms (lap2-α,β,γ) have been identified in humans at the protein and mRNA level (Harris *et al.*, 1994). Seven isoforms (lap2-α,β,β',γ,δ,ε,ζ) were identified in mouse (Berger *et al.*, 1996).

1.1.4.1.1 LAP2 isoforms structure.

LAP2β is a type II NET containing a N-terminal nucleoplasmic domain, a single transmembrane region, C-terminal domain located in the luminal space between INM and ONM (Dechat *et al.*, 2000) and N-terminal domain sharing a common structure motif of an 40 aa which is found in all LAP2, Emerin, and MANI proteins and called (LEM domain) (Lin *et al.*, 2000). LAP2-γ,δ and ε are slightly shorter than LAP2β, but they are very closely related in structure. They only lack a short region of 109, 72, and 40 amino acids respectively. LAP2ζ and LAP2α don't contain a potential transmembrane region. LAP2ζ represent the first 219 N-terminal residues of LAP2β and five additional C-terminal amino acids. LAP2α is different in the structural and function compared with other LAP2 isoforms. It shares only 187 amino acids at the N-terminal, but contains a unique C-terminal of 506 amino acids

(Foisner, 2003). The following figure shows the different LAP2 isoforms and how they attached to the INM (Dechat *et al.*, 2000) **(Figure 1.7)**. LAP2 α and β have been shown to be resistant to NE treatment with Triton X100 and high salt suggesting that they make a very tightly complex associated with the Lamina (Dechat *et al.*, 1998).

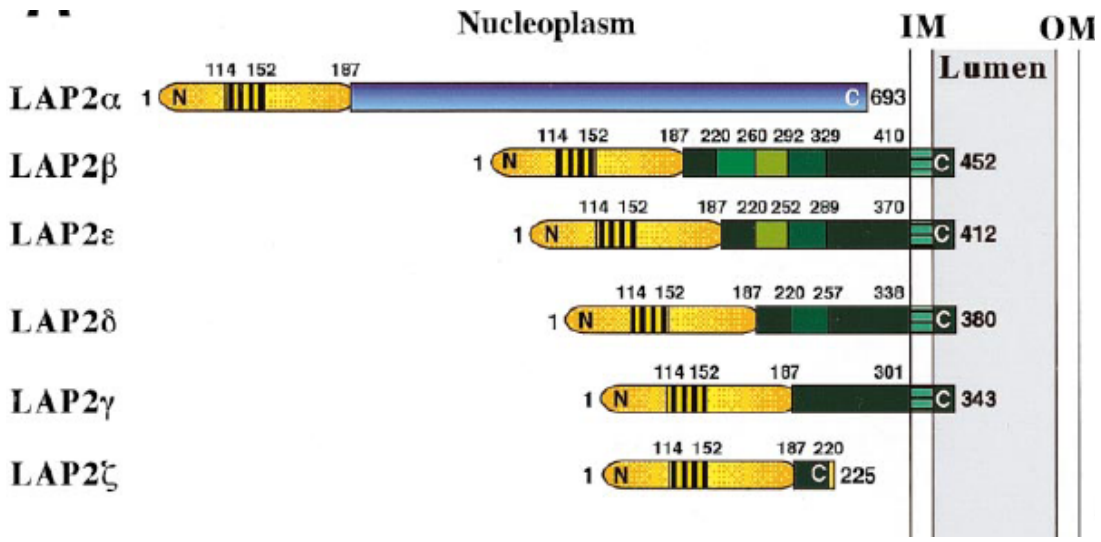

Figure 1.7: *This figure shows us the matching between different LAP-2 isoforms and their structures (Dechat et al., 2000).*

1.1.4.1.2 LAP-2 α and β function.

Studies have shown that LAP2α assembles around chromosomes earlier than LAP2β, suggesting that it is the first protein among the NE/nucleoskeleton components to associate with chromosomes during NE assembly (Foisner, 2003).

The unique C-terminus of LAP2α may add a specific function as a non-membrane protein associated with the nucleoskeleton and may help to organize higher order

chromatin structure by interacting with Lamin A/C (Dechat *et al.*, 2000) . LAP2α is one of the binding partners of Lamin A/C, which also bind strongly to pocket C and weakly to pocket B of retinoblastoma protein (Rb) (Markiewicz *et al.*, 2002). Four possibilities were suggested to explain how Lamin A/C-LAP2α complexes regulate Rb (Dorner *et al.*, 2006): first, LAP2α may regulate Rb phosphorylation by preferential binding to Rb phosphorylated on serine 780 which is the first serine to be targeted during the G1-S phase. The interaction of lamin A/C-LAP2α with Rb may delay the phosphorylation of Rb and leads to stop Rb function. Second, Lamin A/C-LAP2α may recruit regulatory proteins to the Rb complex. Third, Lamin A/C-LAP2α may recruit Rb-E2F complexes to subnuclear compartment or chromatin regions. Fourth, the interaction of Lamin A/C-LAP2α complexes with Rb may stabilize the Rb protein. In $Lmna^{-/-}$ fibroblasts Rb protein was destabilized by proteasomal degradation (Johnson *et al.*, 2004). The function of LAP2α in cell cycle progression and differentiation was studied. A decrease in expression of LAP2α negatively affects growth arrest response of fibroblast to serum starvation. Increased LAP2α expression delays the transition from G1 to S phase. This function of LAP2α in the cell cycle requires Rb and involves regulation of the activity of E2F transcription factors (Dorner *et al.*, 2006). When LAP2α was immunoprecipitated from nuclear fractions, lamins A/C and hypophosphorylated Rb were co-precipitated efficiently (Markiewicz *et al.*, 2002). This study confirmed the importance of Lamin A/C-LAP2α complexes to anchor Rb protein to the nucleus.

Other studies showed that entry of HDFs into G0 is correlated with low expression of LAP2α. HDFs Lamin A/C null cells result in LAP2α aggregates, which is correlated with cell cycle arrest (Pekovic *et al.*, 2007). However, embryonic

fibroblast from a $lmna^{-/-}$ mouse (MEFs) display a rapid growth phenotype (Johnson *et al.*, 2004). One author justified the difference in LAP2α function. HDFs are able to respond to stimuli by inducing a checkpoint arrest, while this checkpoint in cell lines like MEFs or transformed cell lines does not exist (Pekovic *et al.*, 2007).

LAP2β has the ability to bind to Lamin B via specific Lamin B binding domain (Furukawa and Kondo, 1998). LEM domain was found to bind not only to lamins but to BAF as well (Segura-Totten and Wilson, 2004; Gruenbaum *et al.*, 2005). The interaction of HA95 with LAP2β was reported via two distinct domains. This association was implicated in regulating the initiation phase of DNA replicating after the association was disrupted (Martins *et al.*, 2003). There was also found to be a strong interaction between LAP2β and the transcriptional repressors germ cell less (GCL) (Nili *et al.*, 2001), and histone deacetylase 3 (HDAC3) resulting in the latter case in deacetylation of histone 4 (Somech *et al.*, 2005b). One study has been shown that under certain unknown physiological conditions, NE proteins such as LAP2β and LBR are involved in the modification of the chromatin in order to induce gene silencing. To understand how this is happened, investigators have suggested that two complexes are formed and anchored at NE. One complex is LAP2β recruits the enzyme (HDAC3) while the other complex is LBR recruits the substrates (histone H3/H4) (Shaklai *et al.*, 2007).

1.1.4.2 MAN1 and Lamins.

MAN1 is one of INM proteins with two transmembrane spanning domains and N- and C- terminal nucleoplasmic domains. It share a ~40 amino acids residue conserved domain with LAP2 and emerin termed a LEM domain (Lin *et al.*, 2000). Beside the interaction between MAN1 and lamin A, it was shown that MAN1 interacted with certain transcription factors. Recent studies show the interaction between Smad4 transcription factor and MAN1 (Bengtsson, 2007; Cohen *et al.*, 2007). It was shown that MANI functions as an antagonist to transforming growth factor-β (TGFβ) and bone morphgenic protein (BMP). Smads4 are crucial regulators of TGFβ and BMP. Activation of TGFβ and BMP lead to phosphorylation to receptor-mediated R-smads which will be oligomerized with Smads4, subsequently translocated to the nucleus where they bind to DNA and regulate transcription (Bengtsson, 2007). It was thought that MAN1 acts as a nuclear scavenger, sequestering R-smads that illegitimated enter the nucleus (Heessen and Fornerod, 2007). It also interacts with several transcription factors including GCL, the BCL2-associated transcription factor (BTF) and BAF, although the function of these interactions are not yet understood (Heessen and Fornerod, 2007).

1.1.4.3 Emerin and Lamins.

Emerin is a type II integral membrane protein of the inner nuclear membrane (INM). It is a 254-residue (34 kda) protein encoded by the EMD gene located on

the human X-chromosome (Yorifuji *et al.*, 1997; Gruenbaum *et al.*, 2005). It contains an ~40-residue motif at N-terminus termed the LEM domain (Lin *et al.*, 2000), which is homologous to LAP2 and MAN1 proteins. Second homology between emerin and LAP2β have been reported at the transmembrane domain (Foisner and Gerace, 1993). It has also been found that emerin has 2 functional domains, LEM and the central domains. These let investigators suggest that emerin may have additional functional domains which bind to different partners related to diseases (Lee *et al.*, 2001). The interaction of emerin to lamin A by the central domain of emerin and to lamin B was confirmed (Fairley *et al.*, 1999; Clements *et al.*, 2000). The interaction of emerin to barrier autointegration factor (BAF) by the LEM domain has also been confirmed (Lee *et al.*, 2001). It was also found that the interaction of emerin to cytoskeleton organization through direct binding to α and β actin or indirect binding through its association with nesprin 1 and 2 (Mislow *et al.*, 2002; Lattanzi *et al.*, 2003; Libotte *et al.*, 2005). Emerin through its interaction to β-catenin was implicated in preventing nuclear accumulation of β-catenin which leads to inhibit its transcriptional activity (Markiewicz *et al.*, 2006). The localization of emerin at the INM is critical for its function, since a mutation that inhibits emerin to reach its position at nuclear rim causes disease (Fairley *et al.*, 1999). The known disease caused by mutations in EMD is the X-linked form of EDMD (X-Linked EDMD) (Gruenbaum *et al.*, 2005).

1.2 Mitochondria.

Mitochondria are central organelles in the cell that have a critical function, producing cellular energy ATP and acting as signaling organelles. Mitochondria are the same size as an E. coli bacterium, which is 1-2um in length and 0.1-0.5um width. Mitochondria occupy up to 25% of the volume of the cytoplasm. The main function of mitochondria is producing energy (ATP) via aerobic metabolism that will be utilized for cell activity **(Figure 1.8)**.

Division of mitochondria in the cell is not coupled to the division of the cell. Mitochondria grow by the incorporation of proteins and lipid that are localized in the mitochondrial membranes. It increases in size, then one or more daughters pinch off in a similar to the way to bacterial cell growth and division (van der Bliek, 2000).

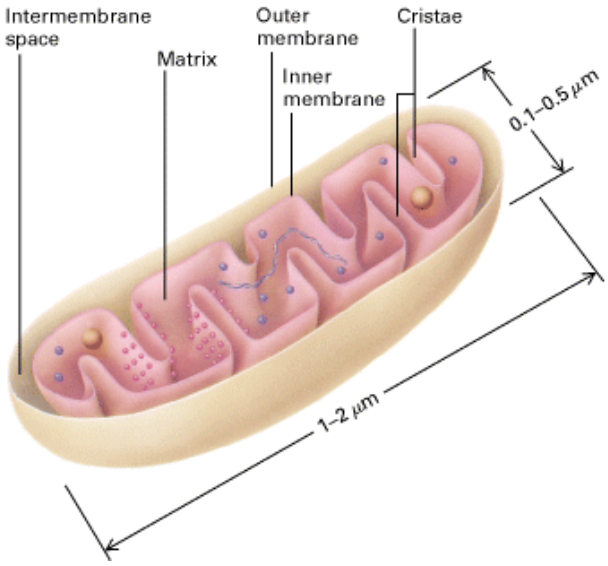

Figure 1.8: *A three dimension diagram of mitochondria [From Lodih H. Molecular Cell Biology, 4th edition, p. 622].*

1.2.1 Mitochondrial structure.

Mitochondria are unique in their double genetic origin; proteins are encoded via nuclear DNA (nDNA) and mitochondrial DNA (mtDNA). They contain two membranes mitochondrial outer membrane (MOM) and mitochondrial inner membrane (MIM), which are separated by an intermembrane space. Inside the MIM there is the matrix **(Figure 1.8)**.

The MOM is composed of about half lipid and half protein which let molecules move across easily. It contains mitochondrial porin a transmembrane channel protein that allows molecules to pass through if it has a molecular weight less than 10 kDa.

The MIM is composed of about 20 percent lipid and 80 percent proteins and is much less permeable than the outer membrane. The surface area of the MIM increases by infoldings (cristae). In the MIM there are the proteins of mitochondrial respiratory chain (MRC), transport proteins important in importing or exporting molecules like ADP, P, Fatty acid, and pyruvate or a shuttle protein that transports electrons from the cytosol to matrix to reduce NAD+ to NADH and FAD to $FADH_2$ **(Figure 1.9)**.

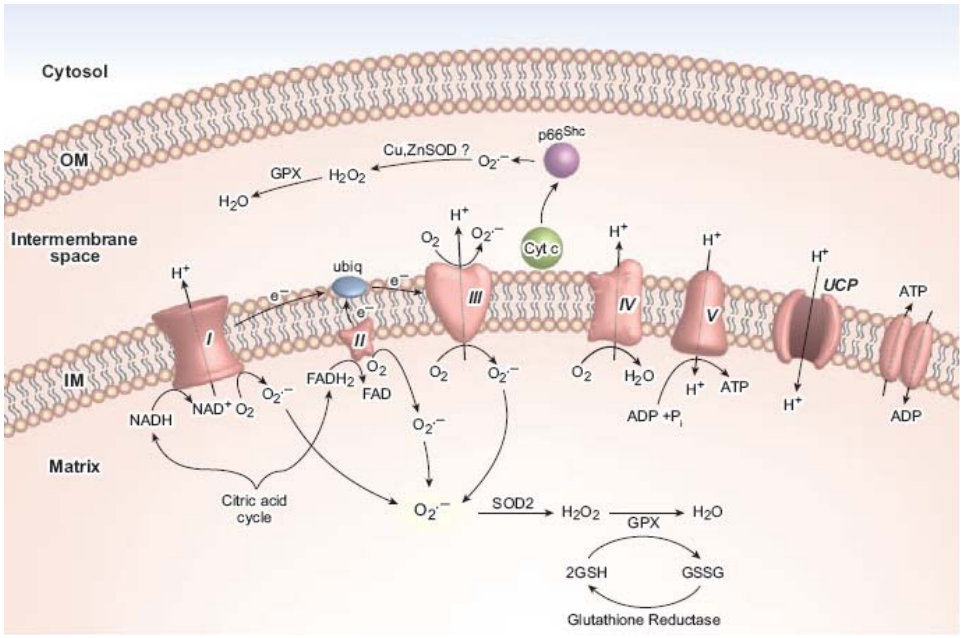

Figure 1.9: *ATP generation. Electrons donated from NADH and FADH2 through (ETC) of complex I and II respectively. Then the electrons pass from complex I, II, III to cytochrome c which will move to complex IV. Associate to transfer electrons the protons will across the inner membrane through complex I, III and IV which will create an intermembrane potential Δψ. The gradient of protons dissipate by reenter of protons to the matrix through complex V (Madamanchi and Runge, 2007).*

1.2.2 Mitochondrial genome and the genetic code.

The matrix is the place where the mitochondrial genome is located and the proteins are encoded. Each mitochondrion contains 5 to 10 copies of mtDNA. Thus the total amount of mtDNA is depend on the number of mitochondria in the cell, the number of mtDNA and the size of mtDNA per mitochondria (Wallace, 1999).

Human mtDNA is a circular molecule that contain 16,569 base pairs which is self replicating and present in multiple copies in the mitochondrial matrix (Madamanchi and Runge, 2007) **(Figure 1.10).** The mitochondrial genome has been fully sequenced. In-side this genome there are thirteen sequences that start with ATG

(methionine) codon and end with stop codon. They are long enough to encode a molecule of polypeptide more than fifty amino acids. MtDNA lack introns and long non-coding sequences. Unlike the nuclear genome, mtDNA is continuously replicated, independently of the cell cycle (Bogenhagen and Clayton, 1977). The only polymerase that is required for mtDNA replication in human is poly-γ (Kaguni, 2004). poly-γ 195 kDa heterotrimer compose of catalytic subunit (p140, coded by *POLG* on chromosome 15q25), and two identical accessory subunit (p55, coded by *POLG2* on chromosome 17q) (Longley *et al.*, 1998).

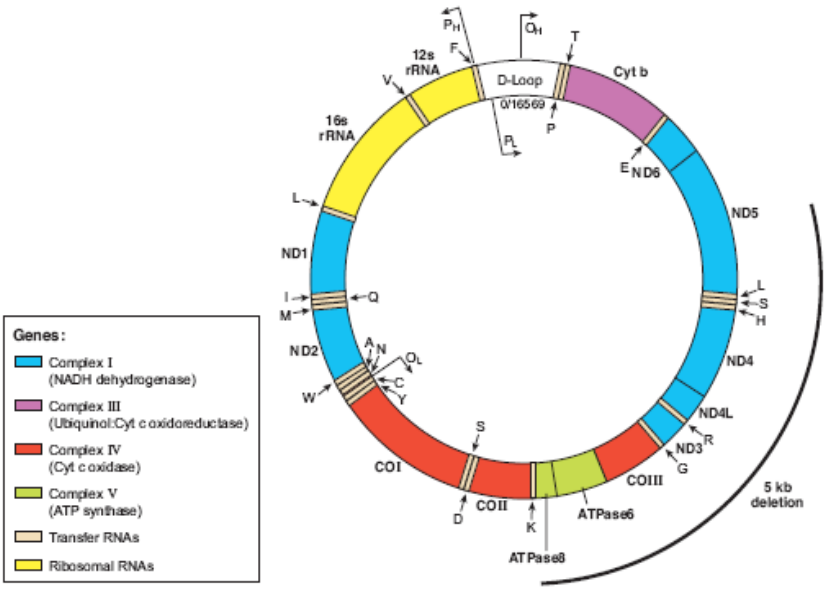

Figure 1.10: *Human Mt.DNA encodes 37 genes (13 polypeptides, 22 tRNAs, and 2 rRNAs). Each mitochondrial contains of several circular DNA bound to the inner membrane at the matrix side. The 13 proteins that encode of Mt.DNA are involve in different subunit of mitochondria respiratory chain complex as follow: 7 polypeptides of 43 subunit of complex 1 (NADH dehydrogenase), 1 of 11 subunits of complex III, 3 of 13 subunits of complex IV, and 2 of 16 subunits of complex V(Madamanchi and Runge, 2007).*

1.2.3 Synthesis and targeting protein to mitochondria.

The majority of mitochondrial proteins are encoded by the nuclear genome (nDNA) and transported into mitochondria. MtDNA encode; thirteen essential subunits of mitochondrial respiratory chain (MRC), two ribosomal RNA (rRNAs), and twenty two transfer RNA (tRNAs). MtDNA transcribe and translate within mitochondria (Attardi and Schatz, 1988).

As far as is known, mitochondria have their own transcription-translation machinery. All RNA transcripts of mtDNA and their translated products remain in the mitochondria. All of mitochondria proteins that are encoded by mtDNA are synthesized on mitochondrial rRNA, and all of tRNA used for protein synthesis in mitochondria are encoded from mtDNA. However, the genetic codes that are used in mtDNA are different from nDNA. UGA is used as a stop codon in the nDNA but is read as tryptophan in the mtDNA. AGA and AGG are codons for arginine in nDNA but they are stop codons in mtDNA (Fox, 1979).

Mitochondrial proteins that are encoded by the nuclear genome are translated in the cytosol and transferred to mitochondria. These proteins should contain a specific sequence at the N-terminus called the mitochondrial targeting sequence (MTS). By using gene engineering techniques, the MTS of alcohol dehydrogenase was fused to the N-terminal of such protein that usually localize in the cytosol like dihydrofolate reductase which then re-localized in mitochondria. Mutation in the MTS of these proteins stopped their localization into the matrix and increased their

accumulation in the cytosol (Rassow *et al.*, 1990), which illustrated the importance of MTS to import these proteins into mitochondria **(Figure 1.11).**

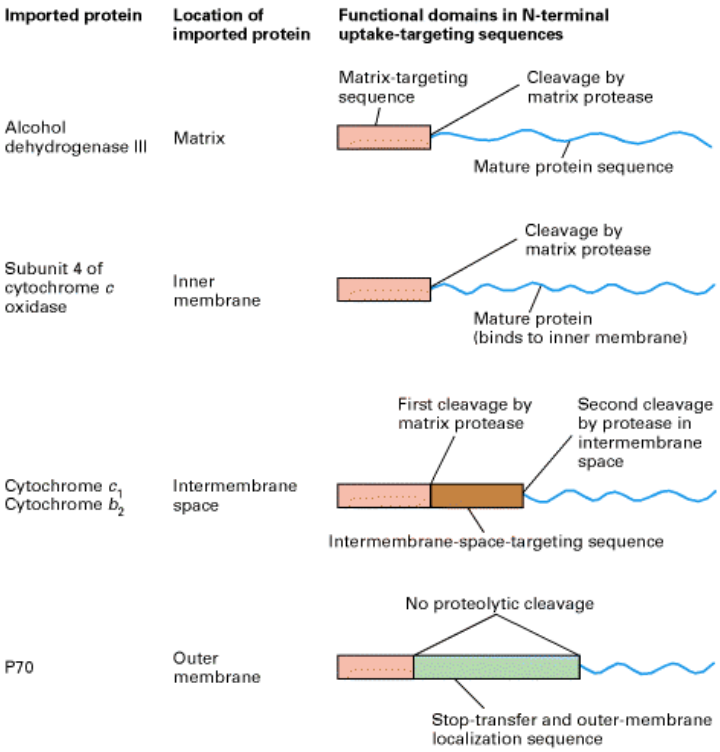

Figure 1.11: ***Uptake targeting sequences of imported mitochondrial proteins.*** *All proteins encoded by cytosolic machinery and transfer into mitochondria has a unique precursor allow them to import and localized in specific area of the mitochondria [From Lodish H. Molecular Cell Biology, 4th edition, p. 622].*

Two mechanisms are involved in importing proteins into mitochondria. These mechanisms involve two cytoplasmic chaperones which are cytosolic Hsc70 (Fan *et al.*, 2006) and mitochondrial-import stimulation factor (MSF) (Komiya *et al.*, 1997). The proteins that synthesize in the cytosol and transfer into mitochondria need to bind to a specific receptor on the MOM. These receptor proteins are able to recognize MTS at the N-terminus of the protein that should be moved into mitochondria.

The main function of chaperones is to prevent the targeted proteins from aggregation and is to bind them to one of the receptor that found on the MOM (MOM-R). These receptors will recognize the MTS domain on the targeted proteins. This process needs ATP to be complete (**Figure 1.12)**.

So, after the proteins are synthesized, they will bind to one of the chaperone proteins. The protein that binds to MSF travels and binds to a set of MOM-R called Tom70/Tom37. Then, this protein releases from MSF and binds to a second set of MOM-R called Tom20/Tom22. The protein that binds to cytosolic Hsc70 travels directly to MOM and binds to Tom20/Tom22. After this protein is bound to Tom20/Tom22, it was suggested that this receptor has a mechanism to pass this protein through the channel at the MOM that called Tom40. These channels are 1.5 to 2.5 nm wide that allow non-aggregated proteins to pass through to the intermediate space. If the protein is to be located in the matrix, it needs to proceed through an additional channel located on MIM that is composed of different trans-membrane proteins called Tim44, Tim23 and Tim17 (**Figure 1.12)** (Komiya *et al.*, 1997; Fan *et al.*, 2006).

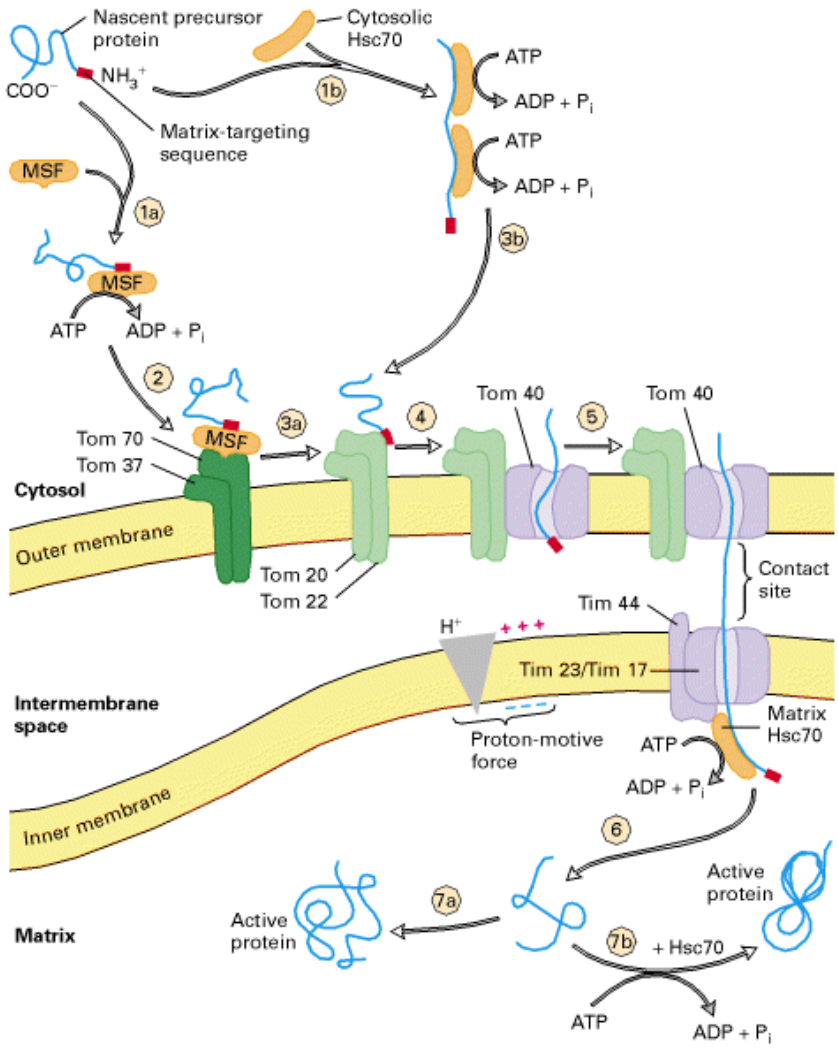

Figure 1.12: ***The pathway of protein import into mitochondrial matrix.*** *Such protein encoded in cytoplasim bind to a specific carrier, that bind to the target sequences of that protein or to the whole protein sequences which need energy to keep them on the such receptors on the mitochondrial outer membrane. [From Lodish H. Molecular Cell Biology, 4th edition, p. 622].*

As far it was known, the imported protein must fold back once it has reached its final location. This procedure must be in the right manner to maturate/activate the target protein. Once the protein has entered the matrix, it binds to one of mitochondrial chaperone proteins like Matrix Hsc70 (mhsc 70) which locates close to the MIM channel. This step is to prevent protein aggregation or incorrect association within or between polypeptide chains during protein folding process.

Accumulated studies showed that different proteins use different strategies for folding in the matrix. Most of these proteins are folded without assistance, while some proteins need the assistance of matrix chaperones like Hsc60 **(Figure 1.13)** (Rospert *et al.*, 1996).

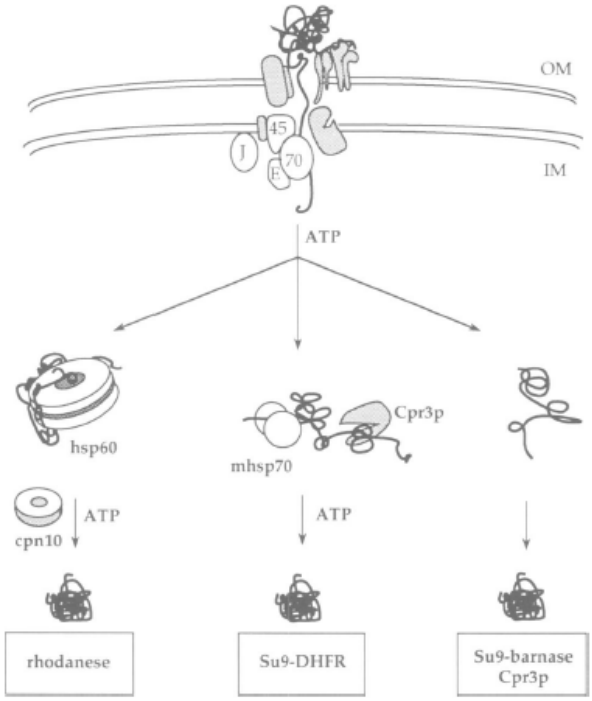

Figure 1-13: Model for folding pathway for some of imported protein to matrix, rhodanacse (Rospert et al., 1996).

1.2.4 The mitochondrial functions.

The main function of mitochondria is to produce ATP that will be used for the cell's mechanisms. Mitochondria are also implicated in cell signaling, inherited diseases, apoptosis and cancer.

1.2.4.1 Mitochondrial function in health.

Biologists noticed that mitochondrial morphology may change during their functions in health and disease. Increases in matrix volume are reported during ATP production (Halestrap, 1989; Lim *et al.*, 2002), ROS production (Garlid *et al.*, 2003), and apoptosis (Holmuhamedov *et al.*, 1998; Gogvadze *et al.*, 2004). The fabulous functions of mitochondria balance between the utilization and/or releasing of NO, H_2O_2, O^-_2 through ATP generation and redox system. This function responds to the needs of cell for proliferation, differentiation and apoptosis pathways in health and diseases (Huang *et al.*, 2000; Wang *et al.*, 2000).

1.2.4.1.1 ATP generation:

The most important function of mitochondria is ATP generation. The MIM and the matrix are the main part of mitochondria where most of the ATP producing reactions take place. The MIM with so many infoldings provide sufficient surface area for the reaction of MRC to occur.

The main fuels for ATP synthesis are fatty acids and glucose. 36 ATP molecules result from the complete aerobic degradation of glucose to CO_2 and H_2O. The glucose degradation process goes through two stages, the initial stage occurs in the cytosol (glycolysis). The terminal stages including oxidation and phosphorylation occur inside the mitochondrial matrix and cristae.

After, the glucose and fatty acid move across the cell membrane, the initial part of ATP generation will start. Inside the cytosol glycolysis of glucose starts to produce a little amount of ATP and converts one molecule of glucose to two molecules of pyruvate. A set of 10 enzyme reactions are involved in the glycolysis pathway. During this reaction the cell will lose two molecules of ATP and gain four molecules which will gain in the end two molecules of ATP and pyruvate.

The pyruvates need to react with coenzyme A (CoA) in order to be transport from the cytosol across the mitochondrial membranes to the matrix. This reaction produces CO_2 and intermediate acetyl CoA, and is catalyzed by pyruvate dehydrogenase. This reaction is highly exogenic and irreversable. Pyruvate dehydrogenase is located in the mitochondrial matrix, and is composed of three different proteins that form a complex of multi-enzyme.

Acetyl CoA is generated from pyruvate and is important in the oxidation of fatty acids and many amino acids. It is important in numerous biosynthetic reactions, such as transfer of acetyl groups to lysine residues in histone proteins and to the N-termini of other proteins.

The oxidation of acetyl CoA through the citric acid cycle or krebs cycle will produce CO_2, and the coenzymes (NADH, FADH2). Electrons are donated from NADH and FADH2 to oxygen through an electrons transport chain (ETC) consisting of complexe I (NADH dehydrogenase), II (succinate_ubiquinone oxidase) of MRC. The electrons then pass on to ubiquinol via coenzyme Q. The electrons pass to complex III (ubiquinol_cytochrome oxidoreductase), which in turn to cytochrom c.

Then move to complex IV (cytochrom c oxidase 'COX'). The movements of electrons will be associated with pumping of protons across MIM which will create a mitochondrial membrane potential Δψ. Then the protons will influx back into the matrix through complex V of MRC (complex F0-F1) where the ATP will be produced by adding a phosphate group to ADP (Madamanchi and Runge, 2007) **(Figure 1.9)**. ATP is then exchanged with cytosolic ADP through adenine nucleotide translocase (ANT).

1.2.4.1.2 Nitric oxide productions.

Nitric oxide (NO) is a free radical which functions as an intracellular and an intercellular messenger in regulating cell O_2 uptake and ATP production. Mitochondria were implicated in producing NO from arginine, NADH and O_2 by nitric oxide synthase (NOS) (Alderton *et al.*, 2001).

Recently, different investigations showed that different isoforms of NOS are expressed in different tissue. In rat four isoforms of NOS were found. These isoforms were classified according to the tissue-type [neuronal (NOS I or nNOS0, inducible (NOS II), endothelial (NOS III) and mitochondrial (mNOS)] (Ghafourifar and Richter, 1997; Giulivi *et al.*, 1998). It was found that mNOS is nNOS translocated into mitochondria. mNOS bind to mitochondrial PDZ domain of COX (Persichini *et al.*, 2005; Franco *et al.*, 2006). NOS I and III are constitutively expressed (Lamas *et al.*, 1992; Christopherson and Bredt, 1997). However, NOS II

expression is regulated by inflammatory stimuli like TNFα, IFNγ, and LPS (Taylor and Geller, 2000).

NO has been implicated in mitochondrial activities. Prolonged NO affects mitochondrial functions which may explain the link between NO, ROS and ATP production (Huang *et al.*, 2000). NO via high affinity binding to COX has a critical role on MRC activity, (Boveris *et al.*, 1999). NO binds to Cu^{2+} B center of COX leading to inhibited electron transfer to O_2 and reduces mitochondrial O_2 uptakes. Different studies showed the effect of NO on MRC, in rat heart, skeletal muscle, liver and synaptosome mitochondria (Cleeter *et al.*, 1994; Brown, 1995; Poderoso *et al.*, 1996; Boveris *et al.*, 1999). Different studies showed the implication of NO in cell processes. It was reported that the utilization of NO is associated with production of H_2O_2 and superoxide (Poderoso *et al.*, 1996; Cadenas *et al.*, 2000). In a different approach, high expression of mNOS was implicated in releasing cytochrome c from mitochondria to the cytoplasm and initiating apoptosis (Ghafourifar and Richter, 1999). The modulations in the NO concentration in mitochondria were linked to modulations in H_2O_2 and superoxide. At low NO concentrations the inhibition of COX will be low which increase O_2 consumption and ATP generation which will reduce superoxide and H_2O_2. Otherwise, at high concentrations of NO there is a block of COX consequently there is a block of complexes I, II, and III, which will lead to increase in superoxide and H_2O_2 (Carreras and Poderoso, 2007).

1.2.4.1.3 Mitochondria and Reactive Oxygen Species productions.

Reactive Oxygen Species (ROS) are a wide range of molecules that have important signaling functions. Free radicals are chemical species composed of one or more unpaired electrons. Hydrogen atoms have one unpaired electron while most metal ions, nitric oxide, and oxygen have two unpaired electrons (Halliwell, 1991). The unpaired electrons in the oxygen molecule react to make partially reduced highly reactive species that are classified as ROS including, superoxide O_2^-, hydrogen peroxide (H_2O_2), hydroxyl radical, and peroxynitrite (Fruehauf and Meyskens, 2007). The system of various enzymes including, mitochondrial transport chains, cytochrome P450, lipoxygenase, cyclogenase, the NADH oxidase complex, xanthine oxidase, and peroxisoms are involved in production of ROS from free radicals (Inoue *et al.*, 2003).

Over a decade, investigators have sought to understand how and why ROS is produced in cells. Scientists in this field elucidated two factors that cause ROS production which are: 1) when mitochondria do not produce ATP, this correlates with a high proton motive force (ΔP) and a reduced coenzyme Q (CoQ) pool, 2) when there becomes a high NADH/NAD+ ratio. But, in the normal mitochondria that are producing ATP the ROS level will be low, low proton motive force (ΔP) and normal NADH/NAD+ ratio (Murphy, 2009).

ROS was involved in several cell processes including redox system, apoptosis and mitochondria dysfunctions which will be explained below **(Figure 1.14)** (Murphy, 2009).

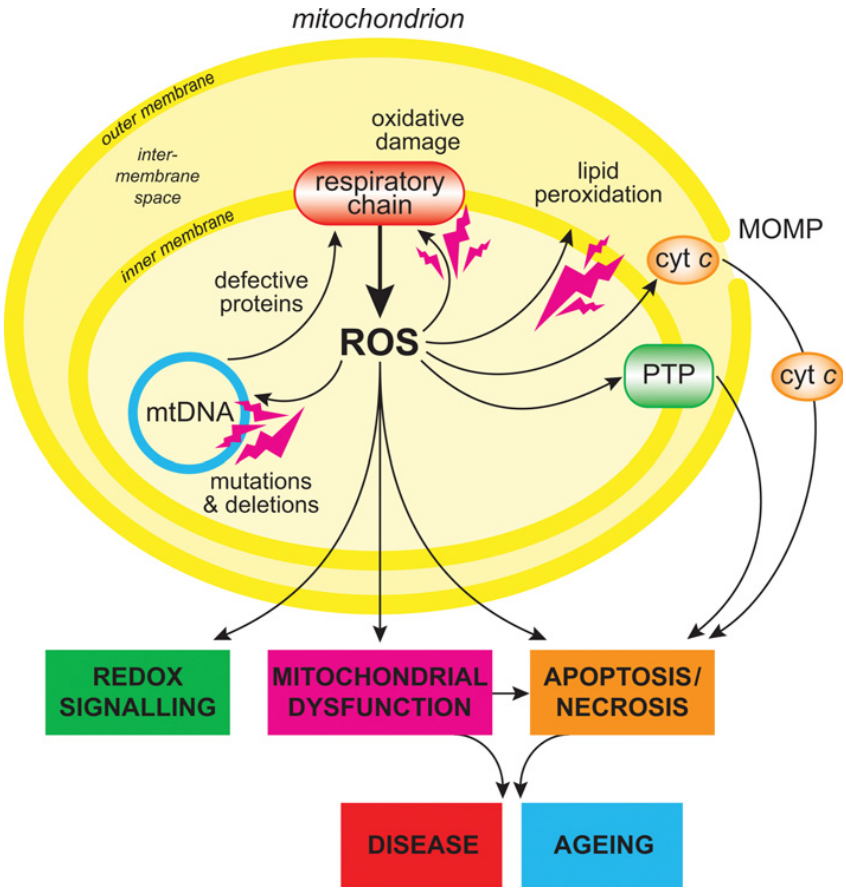

Figure 1.14: Overview of mitochondrial ROS production
ROS production by mitochondria can lead to oxidative damage to mitochondrial proteins, membranes and DNA, impairing the ability of mitochondria to synthesize ATP and to carry out their wide range of metabolic functions, including the tricarboxylic acid cycle, fatty acid oxidation, the urea cycle, amino acid metabolism, haem synthesis and FeS centre assembly that are central to the normal operation of most cells. Mitochondrial oxidative damage can also increase the tendency of mitochondria to release intermembrane space proteins such as cytochrome c (cyt c) to the cytosol by mitochondrial outer membrane permeabilization (MOMP) and thereby activate the cell's apoptotic machinery. In addition, mitochondrial ROS production leads to induction of the mitochondrial permeability transition pore (PTP), which renders the inner membrane permeable to small molecules in situations such as ischaemia/reperfusion injury. Consequently, it is unsurprising that mitochondrial oxidative damage contributes to a wide range of pathologies. In addition, mitochondrial ROS may act as a modulatable redox signal, reversibly affecting the activity of a range of functions in the mitochondria, cytosol and nucleus (Murphy, 2009).

1.2.4.1.4 Mitochondria and Redox balance system.

Redox process is the balance between oxidization and reduction reactions within the cell that takes place mainly inside mitochondria. It was found that redox has an important role in the regulation of cell signaling, including kinase and phosphatase activity and gene expression (Sen, 2000; Thannickal and Fanburg, 2000; Biswas *et al.*, 2006).

Redox balance is maintained via various enzymes (superoxide dismutase (SOD) glutathione peroxidase and glutathione reductase). Two different SODs were found in mitochondria. Manganese form (Mn-SOD) which is localized in the mitochondrial matrix or copper zinc form (Cu,Zn-SOD) which is localized in the mitochondrial intermembrane space.

SOD converts superoxide to hydrogen peroxide then to water via catalyses glutathione peroxidase coupled with glutathione reductase. There are varieties of scavengers including glutaredoxin, and thioredoxin coupled to thioredoxin reductase that use glutathione (GSH) as a substrate. GSH has a main role in maintaining redox homeostasis (Schafer and Buettner, 2001).

1.2.4.1.5 Mitochondria and Cell death pathways (Necrosis and Apoptosis).

Mitochondria play very important roles in cell death pathways. A balance between cell death and cell proliferation is essential for the development and maintenance of multicellular organisms.

Cell death divides into two main pathways namely apoptosis and necrosis. Necrosis occurs in response to infection while apoptosis occurs in normal tissue. Both pathways of cell death involve mitochondria (Fink and Cookson, 2005).

Necrosis is the un-controlled cell death program that leads to cellular break-up and irreversible damage. Necrosis results in the release of inflammatory cytokines such as TNF-α, giving rise to subsequent tissue damage.

Apoptosis is a controlled programmed cell death which occurs via signalling pathways that at certain steps is a reversible process (Fadeel and Orrenius, 2005). Apoptosis is important in physiological process throughout cell life, development and maintenance of multi-cellular organism. Two major initiating pathways trigger apoptosis, inner / intrinsic / mitochondrial and outer / extrinsic / mitochondrial pathways (Petak and Houghton, 2001; Green and Kroemer, 2004; Thorburn, 2004). Defects in apoptosis are linked to dysfunction of mitochondria. Defects in apoptosis may cause various diseases, such as tumors, autoimmune and neurodegenerative disorders.

The factors that initiate the intrinsic pathway include chemical and physical injuries (e.g. UV radiation, heat shock, osmotic shock, hypoxia), over expression of oncogenes and tumor suppressor genes (e.g. c-Myc, c-Fos, p53, PTEN), DNA damage, cytoskeleton structure disruption, growth factor / cytokine deprivation and accumulation of misfolded proteins (Klener *et al.*, 2006). All of the above lead to mitochondrial outer membrane permeablization (MOMP) and increased production of ROS, resulting in release of cytochrome c and other pro-apoptotic molecules such as AIF (apoptosis-inducing factor), Smac/DIABLO (second mitochondria-derived activator of caspase/direct IAP-binding protein) and endunuclease G to the cytoplasm (Susin *et al.*, 1999; Du *et al.*, 2000). In response to different stress stimuli at the mitochondria, a pro-apoptotic Bcl-2 members Bax/Bak form oligomers and react to MOM to make pores which increase MOM permeabilization. This permiblization will increase Cytochrome c accumulation in the cytoplasm which initiates the apoptotic pathway (Green and Kroemer, 2004). Studies showed that in response to specific stimulation, Ca_2^+ is released from the ER and accumulates in the mitochondria. This accumulation was associated with ROS production and opening of the mitochondrial permeablility transition (MPT) which was the cause of mitochondrial membrane dissipation, MOMP and releasing of pro-apoptotic molecules from mitochondria to cytoplasm (Brookes and Darley-Usmar, 2004).

Outer / extrinsic / mitochondria-mediated pathway starts when one of TNF super-family ligand binds to TNF receptor (TNF-R). This binding initiates the formation of a higher order complex at the intra cellular ligands of TNF-R. This formation helps the interaction of procaspase 8 with 10, that resulting in activation of caspase 3, Bid cleavage and Bax/Bak activation. Then Bax/Bak involved mitochondria by

causing MOM permeabilization and release of cytochrom c to the cytoplasm to increase in the induction of caspase 3 (Chinnaiyan *et al.*, 1996a; Chinnaiyan *et al.*, 1996b; Kischkel *et al.*, 2001).

1.2.4.2 Mitochondrial dysfunction.

Organ systems such as brain, heart, liver etc that have high ATP demands are most likely to be affected by mitochondrial dysfunction.

1.2.4.2.1 Reactive Oxygen Species and mitochondrial dysfunction.

1.2.4.2.1.1 ROS and Atherosclerosis:

Atherosclerosis is a vascular disease that causes death. The endothelium regulate the passage of macromolecules to tissue is a major target of oxidant stress (Faraci and Heistad, 1998). Most of the cell types including the endothelium are able to synthesize, store and release ROS in response to stimuli. Oxidant stress plays important role in the pathophysiology of several vascular diseases. MtDNA lacks protective histone and repair machinery found in the nuclear genome, which make It vulnerable for ROS damage (Clayton *et al.*, 1974; Yakes and Van Houten, 1997; Souza-Pinto *et al.*, 1999). Accumulation of oxidative damage to mitochondrial proteins lead to mitochondrial dysfunction that is associated with atherosclerosis

(Madamanchi and Runge, 2007). Accumulation of oxidant stress involves in: 1) interfering in nitric oxide (NO) function and endothelial relaxation; 2) increasing endothelial permeability and promoting leukocyte adhesion; 3) leading to alteration in endothelial signal transduction and blood flow (Lum and Roebuck, 2001).

1.2.4.2.1.2 ROS and Dyslipidemia.

Mitochondria play an important role in oxidizing Low Density Lipoproteins (oxLDL). OxLDL has been implicated in the induction of apoptosis in the endothelial layer of the effected vessel in the atherosclerotic patient (Hessler *et al.*, 1979; Alcouffe *et al.*, 1999). This process involves two special calcium-dependent pathways. One is mediated by activation of the cysteine protease calpain and release of tBid, a truncated form of Bcl2 family member Bid which will result to release of cytochrome c into the cytosol and induction/activation of caspase 3. The second pathway is mediated by activation of apoptotosis-inducing factor cytochrome c and AIF (Vindis *et al.*, 2005).

1.2.4.2.1.3 ROS and Hypertension.

Mitochondria also play an important role in high blood pressure. Mitochondrial ATP deficiency leads to arterial hypertension (Postnov Iu, 2001) and it was also shown that a mutation in mitochondrial tRNA is associated with hypertension (Wilson *et al.*, 2004).

1.2.4.2.1.4 ROS and Diabetes.

Mitochondrial superoxide levels increase in diabetic patients from two different stimulators (Insulin-resistance or hyperglycemia). Insulin resistance is associated with type II diabetes (Bonora *et al.*, 1998). Hyperglycemia was reported in diabetic patients (DeFronzo *et al.*, 1989). Hyperglycemia was also associated in different diseases like vascular damage. It was found that hyperglycemia induces superoxide in mitochondria that causes cell apoptosis and cell damage (Nishikawa *et al.*, 2000; Du *et al.*, 2003). Increase in superoxide will activate PKC and advanced glycation end (AGE), which in turn activates nuclear factor $_k$B (NF $_k$B) (Nishikawa *et al.*, 2000).

1.2.4.2.1.5 ROS and Aging.

Mitochondrial oxidation is a major contributor to aging (Ames and Liu, 2004). Mitochondrial respiratory and ATP generation dysfunction, ROS production, mtDNA damage and accumulation of mutations in mtDNA are all linked to aging (Harman, 1972; Trounce *et al.*, 1989; Cortopassi *et al.*, 1992; Hsieh *et al.*, 1994; Goodell and Cortopassi, 1998). Loss of mitochondria in the endothelial layer of cerebrovascular are also linked with aging because this leads to cerebral blood flow that cause cerebrovascular disfunction (Zhu *et al.*, 2007).

1.2.4.2.1.6 ROS and Carcinogenesis.

The most vulnerable target genome is mtDNA. ROS arising from mtDNA mutations are involved in carcinogenesis and malignant transformation (Singh, 2006; Valko *et al.*, 2006). MtDNA alterations were suggested to be a main cause of cancer (Jeronimo *et al.*, 2001; Kagan and Srivastava, 2005). MtDNA mutations are ten times higher than nuclear DNA in some cancers (Verma *et al.*, 2003). ROS mediates DNA damage. For example, hydroxyl radicals react with pyrimidines, purines, and chromatin proteins which result in base modifications, genomic instability, and altered gene expression. The main sources of pathological forms of ROS are chronic inflammation secondary to infections or chronic irritants. Defects in NOS and mtNOS have also been reported during tumor formation (Galli *et al.*, 2003).

Cancer cell has special cell death program called autophagy. Autophagy doesn't require activation of caspases (Gozuacik and Kimchi, 2004). Cancer cell use autophagy to survive nutrient limitation and low oxygen environments and may help cancer cells from ionizing radiation by removing damaged elements (Paglin *et al.*, 2001).

Tumors can survive in hypoxic environments. Studies showed that HIF1 (Hypoxia-inducible factor-1) act as a regulator of the hypoxic response (Jiang *et al.*, 1996; Huang *et al.*, 1998; Maxwell *et al.*, 1999). HIF1 is a heterodimer comprising HIF-1α and HIF-1β. HIF1α and HIF-1β translocate to the nucleus to associate with other proteins to initiate the transcription of more than 70 genes. HIF-1α is constitutively

expressed, but under normal conditions has a very short half life <5 min. Hydroxylation of HIF-1α proline residues by prolal 4-hydoxulases (PHD) that use 2-oxoglutarates and O_2 as substrates, marking HIF-1α for rapid degradation by the proteasome (Schofield and Ratcliffe, 2004; Semenza, 2004). Recent evidence implicated various oxygen species like H_2O_2 in promoting HIF1α stabilization by inhibiting (PHD) activity and nitric oxide (Metzen *et al.*, 2003; Bell *et al.*, 2005; Wallace, 2005). Increased HIF1α half life was associated with transcription of target genes that were involved in maintaining cell growth in low oxygen environments (Semenza *et al.*, 2006). In low oxygen environments mitochondrial superoxide accumulates and converts to H_2O_2 by Mn-SOD or Cu, Zn-SOD. Then, H_2O_2 effluxes into the cytosol that leads to inhibit PHD activity. This inhibition in PHD activity allows HIF1α to accumulate and dimerize with HIF1β and translocate into nucleus where it modulates the expression of target genes (Semenza *et al.*, 2006).

1.2.4.2.2 Neurodegenerative disorder and mitochondrial dysfunction.

1.2.4.2.2.1 Alzheimer's disease.

Alzheimer's disease (AD) is one of the neurodegenerative disease of the central nervous system that results in dementia (Selkoe, 2001). Intracellular neurofibrillary tangles and extracellular senile plaques in the neocortex, hippocampus and other subcortical region in the brains are involved and essential for cognitive function (Mattson, 2004).

There is strong evidence showing increased levels of oxidative stress in AD (Zhu *et al.*, 2005). It was reported that AD-samples have a decline in polyunsaturated fatty acid (Lovell *et al.*, 1998) and increase in lipid peroxidase (Smith *et al.*, 1996; Sayre *et al.*, 1997). Protein, DNA and RNA oxidation was also linked to alzheimer's diseases (Mecocci *et al.*, 1994; Smith *et al.*, 1995; Nunomura *et al.*, 1999; Nunomura *et al.*, 2004). Lower plasma antioxidant and alteration in the activity of antioxidant enzymes are associated at early stage of AD (Riviere *et al.*, 1998; Bourdel-Marchasson *et al.*, 2001).

Amyloid *β*-peptide (A*β*) *is* not synthesized in neurons but is abundant in the endothelial layer of blood vessels which explain the link between the blood brain barrier (BBB) and the AD. A*β* interacts on endothelial cells to produce free superoxide radicals that lead to oxidation and lipid peroxidation (Thomas *et al.*, 1996). In AD patients, it was reported that A*β* released from the blood vessels accumulates in neurons causing mitochondrial dysfunction and neuronal apoptosis (Kawai *et al.*, 1990; Alavi *et al.*, 1998; Kalaria, 1999). Neuronal death in AD patients is associated with A*β* deposition that results in oxidative stress and apoptosis (Colurso *et al.*, 2003). Deposition of A*β,* a 39-43 amino acid peptide derived by cleavage of the amyloid precursor protein (APP) is associated with plaque formation. A*β* fragment leads to inhibit the activity of cytochrome c oxidase, pyruvate dehydrogenase, α-ketoglutarate dehydrogenase, electron transport via mitochondrial respiratory complexes, and elevate Ca_2^+. A*β* fragments in aqueous solution may also generate free radical peptides (Hensley *et al.*, 1994). Different A*β* deposition molecules were used in vitro to establish the link between the depositions with different mitochondrial dysfunction phenomena. A*β* (25-35) and

A*β* (1-42) cause reduction in mitochondrial membrane potential (Abramov *et al.*, 2004). A*β* (1-42) via p53 cause release of cytochrome c which results in apoptosis in human neurons (Zhang *et al.*, 2002). Whereas, A*β* (25-35) limits its affects in reduction in ATP generation via inhibition in complex I of mitochondrial respiratory complex (Casley *et al.*, 2002). From these studies, it seems that increases in the level of A*β* is a major factor in AD, and has important roles in controlling apoptosis in neuronal cell (Takuma *et al.*, 2005).

1.2.4.2.2.2 Parkinson Disease (PD).

PD is an age-related chronic neurodegenerative disorder characterized by progressive resting tremor, rigidity, bradykinesia, gait disturbance, postural instability and dementia (Mandemakers *et al.*, 2007). Mitochondrial dysfunction has been linked to PD for many years. PD-like symptoms have been observed upon exposure to MPTP(1-methl-4-pheyl-1,2,3,6-tetrahydopyridine) a product of heroin (Langston *et al.*, 1983). MPTP enters dopaminergic neurons via the dopamine transporter and inhibits complex I of the mitochondrial respiratory chain which results in increased oxidative stress, elevated intracellular Ca_2^+ level and decreased ATP production which all contribute to PD-like symptoms (Vila and Przedborski, 2003). A similar effect has been shown on rodents treated with rotenone a complex I inhibitor (Sherer *et al.*, 2003).

Several studies showed mutations in mtDNA or nuclear-encoded mtDNA polymerase showed PD like symptoms (van der Walt *et al.*, 2003; Autere *et al.*,

2004; Pyle *et al.*, 2005). Other studies also showed that mtDNA polymorphisms and haplotypes are also associated with PD, mutation in nuclear-encoded mtDNA polymerase-G (POLG) cause PD-like symptoms (Luoma *et al.*, 2004; Pagnamenta *et al.*, 2006).

Other genes also have critical roles in PD. Parkin functions as an E3 uniquitin ligase (Shimura *et al.*, 2000) catalyzing the ubiquitylation of damaged proteins that lead to their degradation by the 26S proteasome (Ciechanover, 1998). The mechanism of parkin in regulating mitochondrial function is not yet understood, but there is a link between parkin and mitochondrial function showed in a different study. Parkin null *Drosophila* (park25) has reduced life spans, excessive apoptosis, flight muscle degeneration and male sterility. Microscopic images showed swollen and severe disruption of mitochondria (Greene *et al.*, 2003). Loss of parkin in mice results in an increase in dopamine levels and reduction in the synaptic excitability in straitum (Goldberg *et al.*, 2003). PINK1 (encoding the PTEN induced putative kinase 1) has specific functions in protecting the cell from mitochondrial induced apoptosis (Petit *et al.*, 2005). Homozygous mutations of PINK1 in primary fibroblast of patients was associated with increasing lipid peroxidation and expression of mitochondrial superoxide dismutase which explained the link between PINK, mitochondrial function and PD (Hoepken *et al.*, 2007).

1.2.4.2.2.3 Mitochondrial dynamics and neuronal disorder.

Mitochondria are dynamic organelles that undergo continuous cycles of fusion and fission. The balance between the fusion and fission not only play important roles in the morphology of mitochondria but has important roles in mitochondrial function (Chan, 2006).

Dynamin-related protein (Drp1) and fission1 (Fis1) are proteins involved in mediating mitochondrial fission. Fis1 is anchored to the mitochondrial outer membrane (MOM) by a hydrophobic domain with two tandem tetratrico-peptide repeat motifs facing the cytosol, which mediate protein-protein interactions between Fis1 and other proteins (Suzuki *et al.*, 2003; Dohm *et al.*, 2004). Fis1 is thought to be a receptor for Drp1. Drp1 is a large cytosolic GTPase which translocates to the mitochondria where it is implicated in fission (Smirnova *et al.*, 2001). The mitochondrial protein 18 (MTP18) and Ganglioside-induced differentiation associated protein 1 (GDAP1) have also been implicated in mitochondrial fission (Niemann *et al.*, 2005; Tondera *et al.*, 2005).

The dynamin-family members, optic atrophy 1 (OPA1) and mitofusins (MFN1 and 2) are involved in mitochondrial fusion. MFN1 and 2 are anchored to MOM which forms homo and hetero-complexes with each other. Their N-terminal GTPase domain is required for fusion and is oriented towards the cytosol. Their C-terminal coiled-coiled domain also faces the cytosol and coordinates the docking of mitochondria to one another through antiparallel binding to the C-terminal of MFN1 or 2 molecules on adjacent mitochondria (Koshiba *et al.*, 2004). OPA1 is a large

GTPase located on the mitochondrial inner membrane (MIM) facing the intermediate space (IMS). At least eight isoforms have been identified. Their role in mitochondrial fusion is not fully understood yet (Delettre *et al.*, 2000). They localize in the IMS of mitochondria and tight association with MIM was found (Olichon *et al.*, 2002; Cereghetti and Scorrano, 2006). The interaction of OPA1 with MFN1 was found and may explain the main function of this interaction in coordinating the fusion reaction of the outer and inner membrane (Cipolat *et al.*, 2004). These proteins are involved in localization as well as fusion of mitochondria. Over expression of MFN1 in neuronal primary cell culture decreased the localization of mitochondria to dendritic spines, whereas over expression of dynamin-1-like (Dnm1l or Drpl) resulted in relocalization of mitochondria to dendritic spines and is involved in mitochondrial fission (Li *et al.*, 2004). Coiled-coil protein Milton (Stowers *et al.*, 2002) and rho-related GTPase dMiro (Guo *et al.*, 2005) are implicated in moving mitochondria along microtubules.

Mutations in the proteins that are involved in mitochondrial dynamics cause neurodegenerative diseases (Mandemakers *et al.*, 2007). Mutations in GDAP1 cause Charcot-Marie-Tooth (CMT) type 4A, a severe autosomal recessive form of neuropathy associated with either demyelinating or axonal phenotypes. It was suggested that CMT4A disease is in fact a mitochondrial disorders caused by mutations in nuclear genes. This study postulates that GDAP1 may be related to the maintenance of the mitochondrial network (Pedrola *et al.*, 2005). Mutation in human mitofusin-2 (MFN2) occurs in Charcot-Marie-Tooth neuropathy type 2A disease (Zuchner *et al.*, 2004). Optic atrophy 1 (OPA1) is another protein that

involved in mitochondrial dynamics. Mutation in the gene that encodes OPA1 is a major cause of blindness (Delettre *et al.*, 2000).

1.3 The aim of this work.

LAP2α is one of the strongest interacting nuclear proteins that interact with Lamin A/C. The nucleoplasmic complexes of Lamin A/C/LAP2α are implicated in cell pathways by interacting with a tumor suppressor retinoblastoma (Rb), regulating the expression of Rb-E2F-dependent target genes and differentiation. Mutations in LMNA cause a heterogeneous group of inherited human disease called laminopathies, which affect different tissues, including cardiomyopathy. Mutations in LAP2α have been identified and linked to cardiomyopathy as well. To understand more about Lamin A/C and LAP2α in cancer, it was suggested to start searching for a novel protein partner binding to Lamin A/C and/or LAP2α in colon tissue and their function in cancer development.

Chapter 3 describes the generation of bait gene of lamin A/C and LAP2α, by cloning the full length of each one in frame with the Gal-4 DNA binding domain of the yeast expression vector (pGBKT7), in order to carry out yeast two hybrid screens to detect interactions. The generation of a cDNA library from normal human colon RNA, and clone them in the frame with the activating domain of yeast expression vector (pGADT7). Mating bait constructs to cDNA constructs resulted about 1000 positive colonies of lamin A/C and 40 positive colonies of LAP2α. Then simple bioinformatics analyses were applied on both of them which resulted in hundreds of hypothetical genes including cytochrome c oxidase subunit II (Cox2). Interestingly, Cox2 is an mtDNA encoded protein and associated in building complex IV of the mitochondrial respiratory chain (COX). Evidence implicated COX

in cancer. Because of this, it was interesting to understand this interaction in a colorectal cancer cell lines.

Chapter 4 focuses on the confirmation part. As the yeast 2-hybdrid system showed the in vivo binding between proteins encoded through the expression vector. In addition of the check point through the assay, it was important to think about an alternative method to confirm any outcome results. In-vitro biochemical assays were used to do so; western blots were performed from HT29 cell line fractions. These experiments were subjected for antibodies to Rb and LAP2β to check if the fractions are clear of cross contamination. Then the blots were subjected to probe by anti-lamin B antibody to answer the question of the possibility of a lamina structure in mitochondria as in the nucleus.

Chapter 5 uses alternative techniques to confirm these findings. Transmission Electron Microscopy (TEM) was used on different cell types. Cryo-sections of HT29 cells were labeled with different antibodies to lamin A, LAP2α and Cox2. To address if the results that were found in chapters 3&4 are not specific for colon tissue, new sections from different cell lines such as Normal Human Fibroblast (NHF), fibrosarcoma and brain cancer cells were labeled with anti-lamin A antibodies all of which showed the same phenomena. To address why lamin A/C are localized in mitochondria, functional assays such as Reactive Oxygen Species (ROS), mitochondrial mass and Cox2 protein expression were suggested in lamin null cells versus normal and nuclear protein null cell lines including Lamin$^{-/-}$, NHF, LBR$^{-/-}$, LBR$^{-/+}$ and Emerin$^{-/-}$.

Chapter 2: Materials and Methods

2.1 General Chemicals.

Unless otherwise stated, all general chemicals used in this work are from Sigma-Aldrich Company Ltd; BDH Laboratory Supplies (AnalaR or Molecular grade). All microbiological growth media was from DIFCO.

2.2 Tissue and cell culture.

2.2.a Normal Human Colon Tissue.

Human colon tissue was supplied to the laboratory after surgical procedure. One-centimeter squares were cut from the sample of normal human colon tissue found adjacent to the carcinoma. The tissue was washed three times with sterile RNAse free PBS **(see Appendix I)**. The sample was incubated overnight at 4^{o}C in 1 mg/ml Dispase (GIBCO) in RNAse-free PBS. The following day, under 20X magnification and sterile conditions the epithelial layer was teased from muscle and subsequently used for total RNA extraction.

2.2.b Cell lines.

Human Colon carcinoma cell lines (HT29), Fibro sarcoma (US913T), Lamin B receptor heterozygote ($LBR^{-/+}$), Lamin B receptor homozygote ($LBR^{-/-}$), $Emerin^{-/-}$ (KK), Lamin A/C null (Lamin $A/C^{-/-}$) and Normal Human Fibroblast (NHF) were found in lab's liquid nitrogen. Brain cancer cell line (U373) was a gift from Prof. Roy Quinlan. Cells were cultured in 25 ml or 75 ml tissue culture flasks under the following conditions:- HT29 cells were grown in McCoy's 5A medium (Sigma) supplemented with 10% Foetal Bovine Serum (FBS), 2mM L-Glutamine, 100 units/ml Penicillin and 100 units/ml Streptomycin (Invitrogen). U373, US913T, $LBR^{-/+}$, $LBR^{-/-}$, KK, Lamin $A/C^{-/-}$ and NHF cell lines were grown in DMEM (Invitrogen) supplemented with 10% FBS, 2mM L-Glutamine, 100 units/ml Penicillin and 100 units/ml Streptomycin.

All cultures were maintained in a humidified incubator at 37°C and 5% CO_2. Cells were maintained twice a week or when they became 80% confluent. Cells were washed twice with phosphate buffered saline (PBS) and detached in the presence of 0.25% trypsin, 0.5mM EDTA in PBS at 37°C for 2-4 min, then cells were split 1:3 or 1:4 in fresh medium and incubated for a further three or four days.

2.3 DNA and RNA preparation:

2.3.a Total RNA extraction.

Trizol reagent (Invitrogen) was used to extract total RNA from colon epithelial layer which was prepared from 1 cm^2 of normal colon tissue (see section **2.2.a**). One-centimeter squares of tissue were homogenized in 10ml of Trizol using a glass-Teflon homogenizer. After 5 minutes incubation at RT 2ml of Chloroform was added, followed by vigorous shaking for 30secs. The sample was then centrifuged at 12000g for 15min at 4^oC. For the precipitation step, the upper aqueous layer was transferred into a new sterile tube. Then 5ml of isopropyl alcohol was added and mixed by vortexing for 10secs. The mixture was then incubated at RT for 30min, centrifuged at 12000g for 10min at 4^oC. After decanting the supernatant, RNA pellet was washed twice with cold 75% ethanol as follows. 3ml of cold 75% ethanol was added to the pellet, vortexed then centrifuged for 5min at 12000g at 4^oC. After decanting the last washing buffer, RNA pellet was dried by standing it at RT for 30min, and then finally re-suspended in a minimal amount of RNAse free water. The sample of RNA was stored at -70^oC. The sample of RNA was quantified as described in section **(2.4.a)**, and run in 1.2% agarose to determine the quality and purity of RNA as described in section **(2.5.a).**

2.3.b Poly A+ mRNA extraction.

Poly A+ mRNA was purified from 300ug of total RNA extracted from colon tissue by using a Poly A+ mRNA extraction kit (Qiagen). The kit was used as described in the manufacture's instructions. The sample of Poly A+ mRNA was quantified using the RiboGreen method (see section **2.4.b**).

2.3.c Plasmid DNA mini-preparation.

Positive bacterial colonies were inoculated into 7 or 10ml of selective media and then incubated with shaking overnight at 37^{o}C. Two aliquots of 700ul of bacteria culture were used for glycerol stock by adding 300ul of 100% sterile glycerol, vortex, and stored in -70^{o}C for further need. The cultures were then centrifuged at 3000rpm for 5min at 4^{o}C. By using the Wizard® Plus SV Miniprep DNA Purification System (Promega), the plasmid DNA was prepared as described in manufacturer's instructions. DNA was quantified as described in section (**2.4.c)**. The plasmid DNA was stored at -20^{o}C. The sample of DNA was determined as described in section **(2.5.b).**

2.4 Nucleic Acid Quantitation.

2.4.a Total RNA quantitation.

2ul of RNA sample was mixed with 98ul of RNAse free water and the optical density at 260nm and 280nm determined. An optical density of 1 at 260nm is equivalent to 40ug/ml.

2.4.b Poly A+ mRNA quantitation.

RiboGreen RNA quantitation Reagents (Molecular Probes) was used to measure the concentration of poly A+ mRNA. The kit was used as described in the manufactures instructions.

2.4.c DNA quantitation.

2ul of DNA sample was mixed in 98ul of RNAse free water and the optical density at 260nm and 280nm determined. An optical density of 1 at 260nm is equivalent to 50ug/ml.

2.5 Nucleic Acid purity analysis.

2.5.a RNA quality and purity analysis.

The quality and purity of RNA extraction was determined by gel electrophoreses. 1.2% agarose gels were prepared as follows:- 1.2g of agarose (Sigma) and 79ml of RNAse free water were microwaved for 1-2 minutes then allowed to stand at RT for 10min to cool down. Then 10ml of 10 x MOPs (Chemicon) and 11ml of 37% formaldehyde (Sigma) were added to make the final concentrations of MOPs 1X and formaldehyde 4%. Running buffer was 1 x MOPs in RNAse free water. Samples were prepared as followed:- after quantitation, 5ug of RNA was mixed with 15ul of RNA Gel Loading Buffer (Sigma) and made up to 30ul with RNAse free water. The samples were denatured at 65^{o}C for 10min followed by 2min in ice. The gel was run at 80 Volts for 3-5 hours. RNA marker (Sigma) was used as a standard. Good quality RNA should show clean bands without signs of degradation between 4 kb and 2 kb, representing 28S and 18S rRNA respectively..

2.5.b DNA quality and purity Analysis.

TAE agarose gel electrophoreses was the standard method used to check DNA purity and quality. Agarose concentration depends on the expected size of the DNA. 1 - 1.5 % agarose gels were prepared as follows:- 1 - 1.5 grams of agarose was mixed with 100 ml 1 X TAE, microwaved for 2 min then allowed to cool down

at RT for 10 minutes. Then 10ul of 1mg/ml ethidium bromide was added before pouring the gel. Running Buffer was 1 x TAE. Samples were prepared as follows:- 5ul of DNA were mixed with 3ul of 10 x Blue Juice-loading Buffer (Invitrogen) and made up to 30ul with 1 x TAE. The gel was electrophoresed at 100 volts for 1-2 hours. A 1 kb DNA Ladder (Invitrogen) 0.5 ug/lane was used as a standard.

2.6 First strand cDNA generation.

Purified human colon total RNA sample was used to generate the 1st cDNA by using Avian Myeloblastosis Virus reverse transcriptase (AMV-RT). The method was as described by Invitrogen. 5ug of RNA was mixed with 1ul oligo dt_{20} (50uM), 2ul dNTP mix (10mM) and then made up to 12ul with RNAse free water. The mixed was denaturized at 65^{o}C for 5 minutes and then placed on ice. To the mix 4ul of 5x cDNA Synthesis buffer,1ul of 0.1M DTT, 1ul of RNase 40 U/ul, 1ul of RNAse free water and 1ul of Cloned AMV RT 15 U/ul. The reaction was incubated for 45min at 50^{o}C, followed by 30min at 55^{o}C, and finally 5min at 85^{o}C to stop the reaction.

2.7 Polymerase Chain Reaction.

All of the PCR reagents were purchased from Invitrogen. PCR master mixes were prepared fresh in a total volume of 25ul as follows:- 2.5ul of 10X PCR Buffer, 0.75ul of 50mM $MgCl_2$, 0.5ul of 10 mM dNTPs mix, 1.25ul of 10uM of upper and lower primers(Sigma), 1ul of 1 unit/ul of Platinum Taq polymerase and made upto

24ul with RNAse free water then 1ul of 200ng/ul cDNA or 2ul of plasmid DNA was added.

Different PCR programs were used. [*LD-PCR*, denaturation 95^{o}C for 30secs, then 30 cycles of: denaturation 95^{o}C for 15secs, annealing 65^{o}C for 3min, followed by long polymerization at 65^{o}C for 30min]. [*Gene specific RT-PCR*, denaturation at 95^{o}C for 5min, then 30 cycles of; denaturation at 95^{o}C for 40secs, annealing at 58^{o}C for 3min, polymerization at 72^{o}C for 2min, followed by a further polymerization at 72^{o}C for 10min]. [*Colony PCR program*, denaturation at 95^{o}C for 10min, then 25 cycles of; denaturation at 95^{o}C for 30secs, annealing at 55^{o}C for 1min, polymerization at 72^{o}C for 2min, followed by a further polymerization at 72^{o}C for 20min].

2.8 Phenol: Chloroform extraction and Ethanol precipitation.

2.8.a Phenol: Chloroform extraction.

An equal volume of phenol: chloroform: isoamyl alcohol (25:24:1) (Sigma) was added to the reaction. The mixture was vortexed then centrifuged at high speed at 4^{o}C for 5min. The aqueous layer was transferred to a fresh tube and re-extracted with an equal volume of chloroform and centrifuged as above. The aqueous layer was then transferred to a fresh tube for the ethanol precipitation step.

2.8.b Ethanol precipitation.

One tenth volume of 3M sodium acetate pH5.5 was diluted in three volume of 100% ethanol, this was then added to the reaction, mixed well and left at -70^{o}C for at least 30min or on dry ice for 10min. The mixture was centrifuged at high speed at 4^{o}C for 15min. The pellet was washed twice with cold 70% ethanol. The pellet was dried at RT for 30min and re-suspended in a minimal amount of RNAse free water. The sample was stored at -20^{o}C.

2.9 Gel extraction and purification.

The qiagen gel extraction and purification kit was used as described in the manufactures instruction. DNA samples were electrophoresis in 0.9% TAE agarose gel. The correct bands were excised using a sterile scalpel and transferred into 1.5ml eppendorf tube. The volume of the slice was calculated by weighting.

2.10 Transformation into *E.coli*.

Ligation mixes were transformated into E.coli DH5α chemically competent cells **(see Appendix III).** 2 ul of ligation mix was added to 50 ul of DH5α and incubated on ice for 30min. After a heat shock at 42^{o}C for 2min followed by 2min on ice, 250ul of S.O.C media was added **(see appendix II)**. The cells were incubated at 37^{o}C for 1 hour with agitation at 225 rpm. 30ul aliquots were spread onto LB-agar

supplemented with appropriate antibiotics **(see appendix II).** Plates were incubated overnights at 37^{o}C.

Single colonies were selected for inoculating overnight cultures of LB-media **(see Appendix II)** containing antibiotics. Plasmid DNA was purified as described in section (**2.3.c)**. The correct colonies were identified by using colony-PCR followed by DNA sequences and restriction analysis. Colony-PCR was performed by using T7 primers and a gene specific primers and 2ul of DNA plasmid, 5ul was sent for DNA sequence. Restriction analysis was performed using specific enzymes selected to cut internal to the insert and one in the vector to give ~ 75 % of the predicted insert size. In the case of incorrect orientation a fragment, 25% of the predicted insert sizes will results.

2.11 Yeast two-hybrid system.

2.11.a The principle.

The Matchmaker Library Construction and Screening Kit (BD Biosciences) was used to screen for novel proteins that bind to Lamin A/C and/or LAP2α.

The principle of this method is to express a full length cDNA of a gene of interest known as `bait` fused in-frame to the yeast Gal4 DNA-binding domain (DNA-BD).

This is co-expressed with a cDNA library fused in-frame to the yeast Gal4 activating domain (AD).

If there is an in-vivo interaction between one of the cDNA library expressed proteins and the bait fusion protein then this will allow interaction of the Gal4 DNA-BD with the Gal upstream activating sequence (AD). This interaction will activate the expression of reporter genes. Yeast strain AH109 has four reporter genes (ADE2, HIS3, MEL1, and LacZ) under the control of Gal Upstream Activating Sequences (Gal-UAS) and TATA boxes. This will allow yeast colonies to grow on Minimal SD Agar –ADE, and –HIS3 **(see Appendix II)**. The positive colonies will also generate a blue colony color on SD -ADE, -HIS + X-α-Gal, because of the activation of MEL1 that encodes α-galactosidase.

2.11.b Construction of `bait` vectors.

2.11.b.1 Primer design.

The primers that have been used to generate the bait gene were selected and checked using the Vector NTI software. For both Lamin A/C and LAP2α, the entire coding sequence was to be fused in-frame to the Gal4 DNA BD. The 5' end of the 5' forward primer begins at the ATG start codon and the 5' end of the 3' reverse primer begins just before the stop codon. Selected restriction sites were then added to the 5' end of each primer. The predicted PCR product when cloned into

pGBKT7 will create an in-frame fusion with the gal DNA BD. The PCR product was initially cloned into TOPO(TA)pCR2.1 (Invitrogen) and then subcloned into pGBKT7.

The primers were reconstituted in 100ul of RNAse free water and primer stock of 10mM concentration have been made and stored at -20^{o}C until be used for PCR reaction.

2.11.b.2 Cloning into TOPO-TA-pCR2.1.

The `bait` gene cDNA was prepared by RT-PCR (see section **2.6**), from RNA extracted from colon tissue (see section **2.3.**a). PCR primers were designed using the bioinformatics and gene engineering software Vector NTI (see section **2.11.b.1**). PCR primers were designed not to include the stop codon so that when sub-cloned into pGBKT7 it creates an in-frame fusion to Gal4 DNA-BD. In addition this set of PCR primers contained specific restriction sites that facilitate sub-cloning into pGBKT7 (see below). PCR reactions in a total volume of 25ul were set up as described in section (**2.7)**.

The PCR products were electropheresed in 1% TAE agarose gel. The correct band was excised and purified (see section **2.9**)**.** The purified PCR product was used for cloning into TOPO-TA-pCR2.1 (Invitrogen). A ratio of 3:1 insert to vector was mixed with 1ul Salt provided with the kit in a 0.2ml tube and kept at RT for ligation for 20min. The ligation mix was used for transformation into DH5α chemically

competent *E.coli* **(see Appendix III).** 2ul of ligation mix was used for transformation as described in section (**2.10)**. 30ul aliquots were spread on LB-agar contained 50ug/ml of Kanamycin **(see appendix II).** Plates were incubated overnight at 37^{o}C.

Single colonies were selected for inoculating overnight cultures of LB-media **(see Appendix II)** with 50ug/ml Kanamycin. Plasmid DNA was purified as described in section (**2.3.c)**. Colony-PCR was performed to check for clones with the correct orientation (section **2.10**).

2.11.b.3 Sub-Cloning into pGBKT7.

pGBKT7 is a yeast expression vector that has the Gal4 DNA-Binding Domain at the 5' prime end of the multi cloning site (MCS). This vector needs to be prepared for ligation with the prepared insert. 20ug of plasmid DNA of a correct clone **(**see section **2.11.b.2)** was digested with specific restriction enzymes that excise the PCR product from TA vector at the sites of the 5' and 3` primers. The digested DNA was electrophoresis in 1 x TAE agarose for 2 hours. The PCR insert band was excised and purified as described in section (**2.9)**.

16ug of pGBKT7 was digested with 16 units of the relevant enzymes (Promega). These were mixed in an eppendorf tube, the correct buffer was added and made up to 100ul with RNAse free water and then incubated at the recommended temperature for 1 hour.

The digested DNA was then dephosphorylated as follows:- 5ul of Calf Intestinal Alkaline Phosphatase (CIAP) was added with 10ul of 10x dephosphorylation buffer (Invitrogen) and then incubated at 37^{o}C for 30 min. Followed with incubation at 85^{o}C to stop the reaction. Then the plasmid DNA was cleaned out of restriction enzymes by using phenol: chloroform extraction followed ethanol precipitation as described in section (**2.8)**. The following formula was used to calculate how match of insert need to be mixed with 100ng/ul of vector to get a ratio of 3:1 insert: vector. 100ng vector X z Kb insert / y Kb vector X 3/1= v (ug of insert the equal 3x of 100ng of vector). After calculation 2ul of 100ng/ul of digested vector and 2ul of 100ng/ul of prepared insert mixed with 1x ligase buffer and 1 unit of T4 DNA ligase (Invitrogen) incubated at 14^{o}C overnight. 2ul of ligation mixture was used for transformation as described in section (**2.10)**. 30ul of transformed cells were spread on LB-agar containing 50ug/ml of Kanamycin **(see appendix II).** Plates were incubated overnight at 37^{o}C. Single colonies were selected for inoculating overnight cultures of LB-media **(see Appendix II)** with 50ug/ml Kanamycin. Plasmid DNA was purified as described in section (**2.3.c)**. Colony-PCR, restriction digestion and sequencing were used to check for the correct clones.

2.11.b.4 Test the bait gene for transcriptional activation.

As described in the principle of the yeast two hybrid system above, `bait` sequences are expressed proteins fused to the Gal 4 BD. These alone should not activate transcription of the reporter genes in yeast strains AH109 or Y187. However, some times the `bait` gene or part of its sequence has a transcription

factor-like domain which will activate the transcription of the reporter genes even in the absent of an interacting partner. For this reason we need to test the bait gene for autonomous activation of transcription before starting the search for novel protein interactions. The cloned bait gene and empty control vector (pGBKT7) were transformed into AH109, and Y187 yeast strains **(see appendix III).** The transformed cells were spread on the following media: SD/-Trp/X-α-gal, SD/-His/-Trp/ X-α-gal, and SD/-Ade/-Trp/ X-α-gal. These plates were incubated at 30^{o}C for 3-5 days or until the colonies appeared. If the `bait` gene is inactive as a transcriptional activator, we should see white colonies only on SD/-Trp/ X-α-gal plates for both the empty control vector and the bait gene construction. If the `bait` gene is an active transcriptional factor, then blue colonies will appear on all of the plates but not on the empty control vector cells. If these colonies appear on all plates except the SD/-Ade then this background growth could be eliminated by adding 3-AT to the media. If however, they grow even on SD/-Ade then a new bait gene construct, lacking the transcription activating sequences would have to be made.

2.11.b.5 Test the bait gene for toxicity.

It is possible that some of the bait gene constructions are toxic in yeast. They will grow on selective plates but have weak growth in selective liquid media. To check this, the growth of cells with the empty control vector was compared with cells with the bait gene construct after overnight culture in selective liquid media. If the cells had comparable growth, then they can be processed to mate them with cDNA

library. If however, the growth was slower than 5 colonies were picked from selective plates and mixed with 1ml of 0.5 x YPDA media and then spread on five SD/-Trp plate. After colonies will appear, they were harvested in 5 ml of 0.5 YPDA and the number of yeast cells determined. If this was $\geq 1x10^9$cells/ml then they can be used for mating to cDNA library (see below).

2.11.c Construction of a cDNA Library into pGADT7.

2.11.c.1 Generation of cDNA.

First strand synthesis was achieved by taking 4ul (0.1 ug) of human colon Poly A+ mRNA (25 ng / ul) and treating it with PowerScript Reverse Transcriptase (BD Bioscience). The primer was CDSIII oligo-dt provided with the kit. This primer has oligo-dt and a unique sequence at the 5' end called CDSIII which matches with the 3'end of the MCS in pGADT7. In most cases the first strand cDNA will terminate with CCC, the BD Smart III oligonucleotides were used prime synthesis of the second strand. BD smart III has unique sequences at the 5'end that match with the 5'end of the MCS in the pGADT7 and GGG at the 3'end. After this step we have cDNA Library from poly A+mRNA that starts with BD Smart III and end with CDSIII.

This library was now amplified by LD-PCR using the advantage-2 PCR kit (BD Biosciences) as follows: 2ul of the cDNA library, 80ul DD-water, 10ul of 10 x BD Advantage-2 PCR Buffer, 2ul of 50 x dNTP Mix, 2ul of 5' PCR primer and 3' PCR

primer, 2ul of 50x BD Advantage-2 Polymerase Mix. The PCR program was used as described in section (**2.7)**.

The cDNA was size fractionated after LD-PCR by using BD CHROMA spin Columns TE-400 which is included in the kit. These are packed with resins that fractionate molecules based on size. This column selects DNA molecules >200 bp. By following the manufacturer's instructions, the LD-PCR products were purified and concentrated into 20ul of elution buffer.

2.11.c.2 Construction the LD-PCR product with pGADT7 into Yeast.

Co-transformation of yeast with purified LD-PCR product cDNA and Sma I linearized pGADT7-Rec allows in-vivo recombination of the two to yield a complete Gal4 AD expression library.

Yeast strain AH109 was made competent as described in **(Appendix III).** 20ul of the purified LD-PCR was mixed with 6ul of pGADT7-Rec (0.5ug/ul) and 20ul of denatured Herring testes carrier DNA (10mg/ml) this was added to 600ul competent yeast cells. The contents were gently mixed and then 2.5ml PEG/LiAc was added **(see Appendix I).** The cells were mixed and incubated at 30^{o}C for 45 min. The cells were gently mixed every 10-15min. 160ul DMSO (Sigma) was added, mixed, and then the cells placed at 42^{o}C for 20min. The cells were gently mixed every 10 min. The cells were then centrifuged at 700xg for 5min. The supernatant were discarded and the pellet re-suspend in 3ml of YPD-Plus Liquid

Medium provided in the kit. The cells were then incubated at 30^{o}C with shaking for 90min. After that the cells were centrifuged at 700xg for 5min. The supernatant was discarded and the cell pellet re-suspended in 30ml of 0.9% NaCl solution **(see appendix I).**

The transformed cells were spread on 180 SD/-Leu plates of 150mm diameter 200ul/plate. For calculation of the transformation efficiency, 1:100, 1:1000, and 1:10,000 dilutions of transformed cells were spread onto 100mm SD/-Leu plate as 100 ul/plate. The plates were then incubated at 30^{o}C for 3-6 days or until colonies appeared.

After colonies were appeared, they were harvested as follows:- the plates were chilled at 4^{o}C for 4 hours. Batches of plates were taken and placed on ice, 5 ml of freezing medium **(see appendix II)** was added to each plate. Using glass beads the colonies were gently scraped and pooled into a sterile flask. 2ml aliquots were stored at -80^{o}c.

2.11.d Yeast two hybrid screening.

2.11.d.1 Mating Bait-gene constructs into the cDNA library.

On the day of mating, `bait` construction transformed Y187 cells and a 2ml aliquot of cDNA library AH109 cells were counted using a hemocytometer. Both cell types

were mixed in equal numbers in a sterile two liter flask, then 45ml of 2X YPDA/Kan (50 ug/ml) was added. The mixture was incubated at 30^{o}C for 20-24 hours with gently agitation at 50 rpm. After 20 hours one drop of mating mixture was tested under a phase-contrast microscope at 400 x powers for zygote formation this typically has a three-lobed shape, the lobes representing the two haploid parents and the third lobe the budding diploid cell. If at 20 hours incubation zygotes were present in the culture the cells were incubated four hours more. Then a further drop was checked again to determine if more than 90% of the cells had separated as single diploid cells. At this point, the cells were transferred to two 50ml falcon tubes (25ml of culture/tube) then centrifuged at 1000xg for 10min. Meanwhile, the 2-liter culture flask was rinsed twice with 50ml of 0.5x YPDA/Kan (50ug/ml). This was centrifuge of as before and all of the pellets combined and resuspended in 10ml of 0.5 ml YPDA/Kan.

The cells suspension were plated on 150mm diameter SD/-Trp/-Leu/-His/-Ade plate, and 200 ul/plate, incubated at 30^{o}C until colonies appeared. For calculation of the mating efficiency, the cells suspension were diluted 1:10, 1:100, 1:1000 and 1:10,000 and spread on 100mm diameter selective agar: SD/-Leu, SD/-Trp, and SD/-Leu/-Trip at 100ul/plate. After few days incubation at 30^{o}C colonies were appeared. Colonies from the experimented plates were re-streaked on SD/-Trp/-Leu/-His/-Ade/x-α-gal. This step is to reduce the background and to test for MEL1 expression. The mating efficiency was calculated as in formula 2 **(Table 2.1).**

Table 2.1 Formula.

Formula No 1:

To quantify nucleic acids.

(OD_{260} X DF X N)/ 1000= concentration ug/ul

N; is a constant concentration at 1 OD_{260} for RNA 40ug/ml, for DNA 50ug/ml for ss DNA 30ug/ml. DF; Dilution Factor of the sample.

Formula No 2:

Yeast mating efficiency.

1. Count the colonies (cfu*) on the SD/-Trp; SD/-Leu; and SD/-Trp/-Leu in plates that have 30-300 cfu.
2. Calculate the viable cfu/ml on each type of SD medium:

(**Cfu / Vol.plated (ml)) x dilution factor= viable cfu/ml**

cfu/ml on SD/-Trp = Viable AH109 cells.

cfu/ml on SD/-Leu = Viable Y187 cells.

cfu/ml on SD/-Trp/-Leu= Viable diploids.

3. The strain with the lower viability is the “limiting partner”. In this protocol, the AH109 [library] strain is the ‘limiting partner”.
4. Calculate the mating efficiency (% Diploid):

(cfu/ml of diploids) / (cfu/ml of limiting partner) x 100 = % Diploid

If the mating efficiency was <2%, the protocol was repeated.

*Colony Formation Units (cfu).

2.12 DNA sequencing and Bioinformatics analysis.

2.12.a DNA sequencing of yeast two-hybrid colonies..

Positive colonies were incubated at 30^{o}c overnight in SD –Trp/-Leu selective media. Colony PCR was performed by mixing 5ul of overnight culture with 45ul of PCR master mix (see section **2.7**), using the pGADKT7-LD-insert forward and reverse primers. The PCR program used as described in section (**2.7)**. 5ul of the PCR product was electrophoresed in 1% agarose gels and 5ul was sent, with pGADKT7-LD-insert forward and reverse primers to the DNA sequencing core facility.

2.12.b Bioinformatics and sequences analysis.

Invitrogen Vector NTI bioinformatics software was used for sequence compilation and editing. Raw sequence files were imported into Vector NTI using the contig express feature. Sequence files were corrected of mismatches. Any mismatches edited by viewing the relevant chromatogram. Sequence files were then assembled into contigs. Each contig was then screened for open reading frames (ORFs). Suitable ORFs were then screened against the human EST databases using a BLASTN search engine.

Table 2.2 Primers design sequences.

Gene	Accession Number	Primer direction 5'----------3'	Start	Primer sequences	Product size (bp)
Lamin A/C	NM_170707	Sfil 170707 forward	213	TCTGGCCATGGAGGCCATGGAGACCCCG	1992
		Sall 170707 reverse	2204	GTTGTCGACCATGATGCTGCAGTT	
LAP2α	NM_U09086	Sma I- U09086 forward	205	CCAGCCCGGGGATGCCGGAGTTCCTGGAA	2082
		Sall U09086 reverse	2286	CAGAGTCGACGTGTTTATTTCCACGCTT	
pGADKT7	AD – expression vector	AD LD-Insert Seq forward primer	1858	CTATTCGATGATGAAGATACCCCACCAAACC	
		AD LD-Insert Seq reverse Primer	2175	GTGAACTTGCGGGATTTTTCAGTATCTACGATT	
β actin	NM_001101	Sense	257	GGCACCACACCTTCTACAATGAGC	834
		Anti-Sense	1090	CGTCATACTCCTGCTTGCTGATCCAC	
Contig5/ Cox2	_____	Sense	__	ATGGCACATGCAGCGCAAG	~500
		Anti-Sense	__	GTTTAGACGTCCGGGAATTG	
LAP2α Seq8	_____	Sense	___	TTACGCTCTTATGGCCATGGAG	~500
		Anti-Sense	___	CCCCGACCCGCATCTCTTTC	

2.13 Protein Analysis.

2.13.1 Protein extraction.

2.13.1.1 Total cell extract.

Cell lines cultured as described in section (**2.2b)**. On the day of experiment, the cell monolayer were washed twice with cold PBS then harvested with a cell scraper and centrifuged at 1000 rpm for 5 minutes at 4^{o}C. The cell pellet was re-suspended in 0.5 ml/flask of hypotonic solution **(see Appendix I)** containing 0.5 mM DTT, 1x of Protease Inhibitor (Sigma) and 50u/ml DNAse1 (Sigma). The cell suspension were incubated on ice for ~20 min followed with vortex every. The total extract was subjected for protein measurements see section **2.13.3**.

2.13.1.2 Cell fractionation.

Cell lines cultured as described in section (**2.2b)**. On the day of experiment, the cell monolayer were washed twice with cold PBS then harvested with a cell scraper and centrifuged at 252g for 5 minutes at 4^{o}C. The cell pellets were re-suspended in 0.5 ml/flask of hypotonic solution **(see Appendix I)** containing 0.5 mM DTT and 1x of Protease Inhibitor (Sigma). The cell suspension were incubated on ice for 15min then harvested by homogenization. The nuclear pellet was isolated from the suspension by centrifugation at 1000g for 5 minutes at 4^{o}C. This step was

repeated to remove any nuclear contamination from the sample. The supernatant was then used for mitochondrial extraction by centrifugation 13552g for 20 min at 4^{o}C. The nuclear pellets were combined and re-suspended in 500ul of Hypertonic solution **(see Appendix I)** with 0.5mM DTT and 1x Protease Inhibitor and incubate on ice for 10 min then centrifuged at 21918g for 5min at 4^{o}C. The supernatant was either transferred into a dialysis tube to incubate in 1 liter cold PBS in magnetic stir at 4^{o}C room for co-immunoprecipitation or transferred into new tube and stored at -20^{o}C until used. The mitochondrial pellet was washed three times, in each time it was re-suspended in 300ul of hypotonic solution followed by centrifugation 13552g for 20 min at 4^{o}C. Then the mitochondrial pellet was solubilized in 200ul of NP-40 **(see appendix I)** plus 0.5mM DTT and 1x Protease Inhibitor and stored at -20^{o}C until used. The post-mitochondrial supernatant was centrifuged at 469280g for 1 hour at 4^{o}C for isolation of the cytosolic fraction. The pellet was washed once in cold PBS and re-suspended in 200ul of NP-40 and stored at -20^{o}C until used.

2.13.2 Co-Immunoprecipitation.

For each immunoprecipitation 50ul of Dynabeads coated with sheep anti-mouse IgG antibodies (Invitrogen) was washed three times with 500ul cold PBS-1% BSA. Each aliquot of Dynabeads was then incubated with 50ul of diluted specific antibody **(see Table 2.3)**, and incubated with low speed agitation overnight at 4^{o}C. The following day, the incubated beads were washed twice in PBS-0.1% Triton x-100 for cross linking. Fractioned proteins extractions **(see section 2.13.1.2)** were measured by using the BCA as described in section **(2.13.3).** 100 ug of dialyzed

nuclear extract or mitochondrial extract were mixed with the beads and agitated at low speed for 4 hours at 4^{o}C. The beads were then centrifuged at 12000g for 1 min at 4^{o}C. The supernatant was precipitated with an equal volume of cold Methanol: Acetone 1:1 and incubated at -20^{o}C for 15 minutes. The precipitated was collected by centrifugation at 12000g for 5 minutes then washed two times with cold PBS-0.1 % Triton x-100. Finally, the pellet was re-suspended in 50ul of 2x sample buffer and denaturated at 95^{o}C for 3 minutes then placed on ice. This was labeled as the unbound (S) fraction. The beads were washed twice in cold PBS- 0.1% Triton x-100 by using the magnetic rack. The beads were resuspended in 50ul of 2x sample buffer and denaturated at 95^{o}C for 3 minutes then placed on ice. This was labeled as the bound (IP) fraction. 10 ul of each sample were resolved using 10 or 12 % one dimensional SDS-PAGE (See below).

2.13.3 Protein concentration determination.

Protein quantification was determined by use of the BCA Protein Assay Kit (Pierce). 5 mg/ml of Bovine Serum albumin in 1 x Laemmli Sample Buffer was prepared **(see Appendix I).** Stock Standards of 0, 0.1, 0.25, 0.5, 1, 1.5, and 2 mg/ml BSA were prepared from this by dilution in 1 x Laemmli sample buffer and stored at 4^{o}C until used. On the day of assay, 10ul of each standard was mixed with 40ul of DD-water, and 2ul of sample extracts with 48ul of DD-water. Then 1/50 dilution of reagent b to reagent A was prepared. 950ul of diluted reagent B and A were added on each tube and incubated at 37^{o}C for 20 min. The optical density of each sample at 545 nm was now determined.

2.13.4 SDS-PAGE.

SDS-PAGE gels were prepared using the Bio-Rad mini-gel apparatus. 10 or 12% of resolving was made as described in **(Appendix II.8.I).** Stacking gel was made as described in **(Appendix II.8.II).** Samples were run at 100 V for about 2 hours (when the loading dye reach of the gel) in 1X running buffer as described in **(Appendix I).**

2.13.5 Immunoblotting.

Nitrocellulose membrane (Protran, grade BA85, Schleider and Schuell BioScience) was cut same size of the gel and soacked in 1X transfer solution **(see Appendix I)**. The resolving gel was laid on the membrane and the two sandwiched between one layer of 3MM filter paper and sponge. The apparatus was assembled and ran at 100 V for 1.5 hours at RT using ice pack to cool the transfer buffer. The nitrocellulose membrane was stained with Pounco dye to check the transfer quality. The membrane was washed in 2x TBST **(see Appendix I)** and blocked in blocking buffer (5% Milk powder w/v 2x TBST) for 1-2 hours at room temperature. After blocking, the membrane was incubated in exact dilution of primary antibody in 1 Milk powder w/v 2x TBST **(see Table 2.3)** for 2 hours at RT or overnight at 4^{o}C room with shaking. After primary antibody incubation the membrane was washed 3 times at RT, 15 min each, in 2x TBST. Then the membrane was incubated with a 1/2000 dilution of secondary – HRP antibody in 1% Milk powder w/v 2x TBST **(see Table 2.3)** for 1 hour at RT with shaking. The membrane was washed 3 times at

RT, 15 min each, in 2x TBST. The nitrocellulose membrane was then exposed to 1:1 mix of ECL™ Western Blotting Reagents 1 and 2 (Amersham Biosciences, Buckinghamshire, UK) for 1-4 minutes and immunoreactivity was measured by detecting the chemiluminescence on Hyperfilm™ ECL (Amersham Biosciences). The film was developed in a compact X4 Automatic X-ray Film Processor (Xograph Imaging System Ltd) or by recording the signal in a Fuji film imagining camera.

Then by using ImageJ software, selected images were opened. After the image was inverted, a box was draw around the biggest band. Then, the mean of the histogram of background alone and the band was taken. The mean of band was subtracted from the mean of background. As the band represents the expression level of the protein in the amount of protein was loaded on the gel, not from the total amount of protein in the fraction. So, the dilution factor was used to calculate the amount of the protein expression in the sample. Because the nuclear pellets were re-suspended in 500ul and both of cytosol and mitochondrial pellets were re-suspended in 200ul, so the dilution factor is 2.5 between nuclear and other fractions. Because of that the mean histogram of nuclear band will multiply by 2.5.

Table 2.3 Primary and secondary antibodies used and their dilutions.

Primary Antibodies	Target	Type	Reference	WB	IP	EM	IF
Jol2	Lamin A/C tail	Mouse- M	In house	1:200	1:10	-	1:50
R-Lamin A	Lamin A	Rabbit-R	Sigma	-	-	1:600	1:500
M-Lamin A/C	Lamin A/C	Mouse-M	Santa Cruz	-	-	1:10	-
M-Lamin A	Lamin A	Mouse-M	Novus	-	-	1:5	-
LAP15	LAP2α	Mouse- M	Gift from Dr. Foisner	1:100	1:10	1:50	1:100
R-LAP2α	LAP2α	Rabbit-R	ImmuQuest	1:1000	-	1:300	1:500
LAP17	LAP2β	Mouse- M	Gift from Dr. Foisner	1:10	-	-	-
IF-8	Retinoblastoma	Mouse- M	In house	1:100	-	-	-
Mt.COX2	Cytochrom C Oxidase	Mouse- M	Invitrogen	1:500	1:100	1:50	1:300
Lamin B	B1 and B2	Mouse-M	ImmuQuest	1:50	-	-	-
Lamin B2	B2	Mouse-M	Abcam	-	-	1:50	-
B-Actin	AC-40	Mouse-M	Sigma	1:1000	-	-	-
Secondary Antibodies	Target	Type	Reference	WB	IP	EM	-
Donkey anti-Mouse	Mouse primary antibodies	HRP	Stratech	1:2000	-	-	-
Donkey anti-Rabbit	Rabbit primary antibodies	HRP	Stratech	1:2000	-	-	-
Goat anti-mouse IgG	Mouse primary antibodies	Gold 5, 10 or 20 nm	British Biocell International	-	-	1:20	-
Goat anti-Rabbit IgG	Rabbit primary antibodies	Gold 5, 10 or 20 nm	British Biocell International	-	-	1:20	-

WB-western blot, IP-immunoprecipitation, EM-electron microscope, HRP-Horse-radish peroxidase.

2.14 Transmission Electron Microscope (TEM).

Cells were grown in 100mm culture dishes. Media was replaced with 3mls of new growth media one day before fixation. On the day of fixation, medium was replaced with 3mls of double strength fixation buffer **(see Appendix I)** mixed gently and quickly for 2mins**.** Then fixation was replaced with 3mls of single strength fixation buffer **(see Appendix I)** for 2 hours at room temperature. Cells were washed three times with PBS-0.1% glycine 15mins each time. Cells were incubated with 3mls of PBS-1% glycine at 37^{o}C for 10mins. Cells were scraped from dish and centrifuged down at 200g for 5mins. Cells pellets were re-suspended in 5mls of PBS-10% gelatin and incubated at 37^{o}C for 10mins. Cells were re-centrifuged down and incubated on ice for gelatin sets. The tips of the eppendorf tube containing cells were cut off by using a razor blade. By using 2.3M sucrose as a lubricant the tip of the eppendorf tube was cut half, and the separated of the cell pellet. Small blocks of cell pellets was prepared in pyramids (1x1x1mm) and stored in 2.3M sucrose at 4^{o}C until the cryosectioning was prepared. The cryosection was then fixed on grids. The grids were put on cold 2%gelatin and melted under a lamp. Grids were incubated on the melted gelatin at 37^{o}C for 30mins. The grids were rinsed 5 times with PBS-0.1% glycine 1min each, then one time with PBS-1%FBS for 3mins. Then 5 droplets of specific antibody concentration in PBS-1%FBS was added for one hour at room temperature or over night at 4^{o}C. Grids were rinsed 4 times with PBS-1%FBS 2min each. Then the grids were rinsed 3 times with PBS, followed with 4 times washing with PBS 2mins each. The grids were incubated in stabilizer PBS-1% gluteraldehyde for 5mins. The grids were washed 10 times with distilled

water 1min each. The grids were rinsed quickly with two drops of cold MC/UA pH4 on ice, followed with 5mins incubation with fresh drops of cold MC/UA pH4 on ice. The grids were let for air dry for 10mins and kept until used.

2.15 Gold particles count and analysis.

Image Processing and Analysis in Java software (ImageJ software) was downloaded free from web site. The scale was set on each opened image according to the scale bar provided with the image. In order to quantify the density of labeling of A-type lamins at the NE, a region was defined that enclosed the NE and the gold labels that were associated with it. In case of B-type lamins and LAP2α, because they express all over the nucleus, the size of the whole nucleus was taken. In case of Cox2, because there were no gold particles in the nucleus, the size of the whole nucleus was taken. The size of the whole mitochondria was taken for each labeling. The size of cytoplasm was taken by subtracting the size of the whole nucleus and mitochondria of each image. After that the gold labels were counted on each selected cell compartments. By using excel, a chart was draw to represent the value of the density of gold labeling expressed as the mean $\pm$ SD (n= 30 images, 10 images of each cell pellet). At least ten images per cell compartments were analyzed. The average of the gold labeling was divided by the average of the surface area. The density of gold labeling was evaluated by calculating the gold particles/um^2. Significance was calculated using the Student *t*-test $P < 0.05$ which Comparing mitochondria or nucleus to cytosol**.**

2.16 Reactive Oxygen Species (ROS) measurement.

To measure ROS, CM-H_2DCFDA (Molecular Probes, Invitrogen) was used. The dye makes covalent binding to mitochondrial inner membrane. Fluorescent will generate when the acetate groups remove by oxidation.

Cell lines were seeded in a density of $5X10^4$ cell/well of 12 well plate. Cells were grown for 48 hours. Then, cells in particular wells were treated for 12 hours by 1% DMSO (-ve control to show that DMSO that used for solving the reagent and dye has no affect on the ROS production) and for 12 hours by 5uM Valinomycin (+ve control and to show that the protocol is working). At the day of measurement, cells were washed once with PBS and incubated with 10mM CM-H_2DCFDA in DMEM-Low glucose Phenol red free and serum free (DMEM-PR-FBS) for 45 minutes at 37^{o}C incubator. Then, cells were trypsinized and centrifuged down at 1000 rpm for 5 minutes at 4^{o}C. The cell pellet was re-suspended in 1ml of DMEM-PR followed by flow cytometry (FACS) FL1.

Flow cytometric analyses were carried out using Coulter® EPICS XL-MCL™ Flow Cytometer (Beckman Coulter, Inc., Fullerton, CA) installed with System II™ version 3.0 software.

The template page was set with 4 histograms. One for forward scatter (FS) and side scatter (SS), one for Filter 1 (FL1) green filter and event, one for filter 2 (FL2) red filter and the last one was FL1 and FL2 X and Y axis respectively. Then, the

parameter was set for FS and SS of the light as cells pass through laser by using cell suspension without dye (no green fluorescence), where the peak of the cell population will be close to zero for both filters. The counter was set for 10,000 events.

FlowJo was used to analysis the FACS data. The median of FL1 value of wild-type was made 100% as a basal level. Then the FL1 values of other samples were calculated based on this. The experiments repeated at least three times. The chart representing the percentage of the ROS level as the mean $\pm$ SD (n= 3).

2.17 Mitochondria mass measurement.

To monitor the mitochondrial mass of specific cells, fluorescent dye 10-*n*-nonyl-acridine orange (NAO; Molecular Probes, Eugene, Oreg., USA) was used. This dye binds specifically to the negatively charged cardiolipin (diphosphatidylglycerol) in the mitochondrial inner membrane independently of the membrane potential.

On the day of the experiment, Cells were trypsinized and counted. Then 200,000 cells were re-suspended in 1 ml of DMEM no serum containing 10uM NAO. After incubation for 10 minutes at 37°C in the dark, cells were centrifuged at 1600rpm 2min and supernatant discarded. The cell pellet was re-suspended in 3ml of DMEM without serum. Then, Cell were analyzed by flow cytometry and green

fluorescence was recorded FL1, using the same parameter that mentioned in section **2.16**.

FlowJo was used to analysis the FACS data. The median of FL1 value of wild-type was made 100% as a basal level. Then the FL1 values of other samples were calculated based on this. The experiments repeated at least three times. The chart representing the percentage of the mitochondrial mass as the mean $\pm$ SD (n= 3).

2.18 Immunofluorecscence (Confolcal).

HT29 cell line was seeded at an density of $4x10^5$ cells/ml. 500ul of cells were loaded/well on 24 tissue culture well plats. Each well contains 1x13mm diameter glass cover slips pre-autoclaved. Cells were grown overnight, replaced with phenol free medium contains 500nM MitoTracker Red CMXRos probe (Invetrogen M7511) and incubated for 30 minutes at cell culture incubator. Then cells were washed three times in 1x PBS pH 7.4, followed by fixation in pre-warmed at 37^oC and fresh made 3.7% Para-formaldehyde in PBS pH 7.4 for about 12 minutes at RT with shaking. Permeablization step in 0.5 % triton X-100 in PBS for 5 minutes and followed with three times washing in PBS 5 minutes each at RT and shaking. Cover slips were then blocked in 1% New Born Serum in PBS (NCS-PBS) for 30 minutes at RT. Cover slips were washed twice in PBS and kept at 4^oC or used immediately.

Cells were stained single with primary antibodies (50 ul/cover slip) for one hour at RT in humidified condition (Table 2.3). Followed by washing three times in PBS and dried on tissue by touching the cover slip at 45^{o} angle. Fluoescein (FITC)-conjucated IgG secondary antibodies were used in 1:50 dilution and incubated for one hour at RT in humidified condition. Cover slips were washed three times in PBS and dried. Cover slips were mounted in Mowiol mounting media containing 2.5 % DABCO and 1 ug/ml DAPI.

Chapter 3: Yeast 2-Hybrid analysis of proteins binding to Lamin A/C and LAP2α.

3.1 Introduction.

3.1.1 Lamin A/C binding protein.

Many studies have shown that there are hierarchies of lamin-lamin associations at the Inner Nuclear Membrane (INM) to form the nuclear lamina. After the lamina has formed, it will interact with integral proteins of the INM to determine the size and shape of the nucleus and aid the distribution of nuclear pore complexes (NPC), as well as other more poorly defined functions.

To understand the function of the lamina we need to know more about the proteins that bind to lamins. Studies *in-vitro* and two-hybrid assays have shown that A-type lamins bind to other proteins, but the *in-vivo* significances remain untested see Table 1 in (Zastrow *et al.*, 2004), which have been classified according to their function when interacting with A-type lamins.

3.1.2 Colon Crypt development.

A cross-section of the colon shows that it is composed of three main layers. The mucosa is composed of epithelial cells, 90% of these are found in crypts and the remaining 10% found in the flat surface. There is a sub-mucosa and two layers of smooth muscle. The mucosal crypt has stem and proliferating precursor cells occupy the bottom two thirds, whereas differentiated cells occupying the top third and the flat surface epithelial layer (Kirchhoff and Geibel, 2006; Prendergast et al., 1996). The main functions of the colon crypts are to absorb and secrete fluid to maintain normal salt and water homeostasis (Kirchhoff and Geibel, 2006).

3.1.3 Lamin A/C expression in Colon Crypt.

Recent studies have shown the expression of Lamin A/C and Lamin B1 in the crypt epithelia cells. The expression of Lamin A/C is greater in differentiated epithelia and stem cells than in the proliferation zone. This expression is decreased in colonic adenocarcinoma tissues as well as at an intermediate stage of neoplasm in the same organ. This phenomena may be because of contamination of non-epithelial cells in cancer sections, or it could be due to aberrant cytoplasm but there is no explanation as to why this is happening (Moss *et al.*, 1999). However, one author linked the expression of lamin A/C in colorectal cancer (CRC) in promoting the reorganization of the cytoskeleton (Willis et al., 2008), whereas lamin A/C expression in CRC promoted invasiveness through up-regulation in the

expression of the actin-bundling protein (T-plastin), which down regulated the cell adhesion molecule (E-cadherin).

3.1.4 LAP2α expression in Colon Crypt.

There are no studies showing LAP2α expression in the crypt of normal human colon tissue. There has been only one study showing the over expression of LAP2α in different cancer tissues from larynx, lung, stomach, breast, and colon. This expression is under the control of the E2F transcription factor (Parise *et al.*, 2006).

3.2 The aim of this study.

As described above LAP2α is one of the strongest binding partners to Lamin A. In this chapter we would like to understand more about the role of Lamin A/C and LAP2α in controlling cellular function in colon tissue. To do so, we need to search for novel protein binding partners to Lamin A/C and/or LAP2α. In this chapter we describe the search for these binding partners using the yeast two-hybrid assay.

3.3 Results:

3.3.1 cDNA library construction and cloning into the Gal4-Activating Domain vector.

A cDNA library of colon epithelia is not available commercially therefore we had to construct our own. Total human RNA was extracted from 1cm^2 of the epithelial layer of normal human colon **(sections 2.2.a, 2.3.a).** Quality of the RNA extraction was checked by electrophoresis run in a 1.2% formaldehyde agarose gel **(Figure 3.2.a)**. β-actin PCR was performed on 0.5ug of total RNA to check for DNA contamination **(Figure 3.2b)**. Poly A+ mRNA was purified from 300ug of total RNA **(section 2.3.b)** and after quantification **(section 2.4.b)** 100ng of poly A+ mRNA was used to generate the cDNA library **(section 2.11.c.1).** LD-PCR was used to amplify a selection of cDNAs ranging from 300 to 3000 bp in length **(section 2.11.c.1) and Figure 3.2c.** The purified LD-PCR products were ultimately cloned into pGADT7 before transformation into yeast strain AH109 **(section 2.11.c.2) and Figure 3.5.a.**

3.3.2 Lamin A/C-Gal4 DNA Binding Domain Construction.

In the databases there are different variants of lamin A/C mRNA sequence. The one that was used in this study is Lamin A/C transcription variant 1 with accession no. NM_170707. The full length of the lamin A coding sequence was required. Primer design was described in section **2.11.b.1**. The PCR primers must not

generate a stop codon when ultimately sub-cloned into pGBKT7 where it will be fused to the Gal4 DNA-BD. Both PCR primers have specific restriction enzyme sites at the 5' ends which are not in the MCS of TOPO-TA pCR2.1 intermediate vector, that will allow later in sub-cloning into pGBKT7. The SfiI-170707 forward primer is 28 nucleotides in length; 3 nucleotides as cozak plus a 13 nucleotide SfiI site plus 12 nucleotides which are gene specific from the ATG start codon at mRNA sequence position 213 **(see Table 2.2)**. The SalI-170707 reverse primer is 24 nucleotides in length; 3 nucleotides as cozak plus a 6 nucleotide SalI site plus 15 nucleotides which are gene specific starting prior to the stop codon at mRNA sequence position 2204 **(see Table 2.2)**.

5ug of total RNA was used as a template for RT-PCR **(section 2.11.b.2)** to amplify Lamin A/C **(Figure 3.3.a)**. The PCR fragment was excised from the agarose gel extracted, purified **(section 2.9)** and quantified **(Table 2.1)**. 2.5ul of purified PCR product (~30ng) was mixed with 1ul of salt solution, 1ul of TOPO-TA-pCR2.1 vector (10ng/ul), and made up to 6ul with DD-water. This mixture was incubated for ligation and transformation **(section 2.11.b.2)**. After transformation 5 colonies were selected and DNA minipreps made from them. These minipreps were digested as follows: 5ul of each miniprep, 3ul of 10X Buffer B, 1ul of SfiI (1u/ul) and made up to 30ul with DD-water and then incubated at 37^{o}C for 1 hour. Then 3ul of 10X Buffer D and 1ul of SalI (1u/ul) was added and incubated at 37^{o}C for 1 more hour. After the gel electrophoresis, the correct band was detected in all of the 5 colonies **(Figure 3.3.b).** A large scale digestion was applied to clone # 1 as described above except 5ul of each enzyme and a total of 100 ul was used. After the gel

electrophoresis the correct band was excised, purified and quantified **(Figure 3.3.b).**

Vector pGBKT7 was prepared as described in section **2.11.b.3.** pGBKT7 was digested and dephosphorylated by using SfiI , SalI and CIAP**.** The prepared Vector was then quantified**.** 100ng of digested Lamin A/C were mixed with 100ng of prepared pGBKT7 in a ratio of 3:1. This mixture was then ligated and transformated into *E.Coli* DH5α **(section 2.11.b.3)**. 5 transformed colonies were selected and plasmid minipreps made. The plasmids were then digested to double check for the correct orientation. ApaI and SalI were used as follows: 5ul of each miniprep, 3 ul of 10X Buffer A, 1ul of ApaI (1u/ul) and then made up to 30ul total volume with DD-water then incubated at 37^{o}C for 1 hour. After this 3ul of 10X Buffer D, 1ul of SalI (1u/ul) was added and incubated at 37^{o}C for 1 more hour. All of the colonies were in the correct orientation **(Figure 3.3.c).** One of the plasmid was selected for DNA sequence as an alternative method to check the full open reading frame cloning into pGBKT7 **(Appendix IV-1b).**

3.3.3 LAP2α-Gal4 DNA Binding Domain Construction.

The construction of the LAP2 α-Gal4 bait vector follows the same protocol that was used for lamin A/C **(section 3.2.2).** The GenBank accession used for the design of primers was U09086. The full length codon sequence was required. The primers designed were described in section **2.11.b.1.** The primers must not generate a stop codon when ultimately subcloned into pGBKT7 where it should be fused to the

Gal4 DNA-BD. Both primers have a restriction enzyme sites that will be used for later sub-cloning into pGBKT7. The SmaI U09086 forward primer is 29 nucleotides in length; 4 nucleotides as cozak plus a 7 nucleotide SmaI site plus 18 nucleotides which are gene specific from the ATG start codon at mRNA sequence position 205 **(see Table 2.2)**. The SalI-U09086 reverse primer is 28 nucleotides in length; 4 nucleotides as cozak plus a 6 nucleotide SalI site plus 18 nucleotides which are gene specific starting prior to the stop codon at mRNA sequence position 2286 **(see Table 2.2)**.

Preparation of RNA, RT-PCR, ligation into TOPO-TA-pCR2.1 and transformation into *E.Coli* DH5 α are all as described for lamin A/C **(section 3.2.2) (Figure 3.4.a).** Analysis of transformants were also carried out in an identical manner, except miniprep plasmids DNA were cut with SmaI using appropriate buffers. The correct fragment was detected in all cases **(Figure 3.4.b).** A large scale digestion of LAP2α clone#1 was made and ligated into prepared pGBKT7 vector as described in section **3.2.2** except that SmaI and SalI were used. Analysis of selected transformants were made by restricting miniprep plasmid DNA with NcoI, the correct orientation was found in all of them **(Figure 3.4.c).** One of the plasmid was selected for DNA sequence as an alternative method to check the full open reading frame cloning into pGBKT7 **(Appendix IV-2b).**

3.3.4 Screening of the cDNA Library with the LaminA/C-bait-construct

Before using the bait constructs in cDNA library screening, they must be tested for transcriptional activation and toxicity (see sections **2.11.b.4 and 2.11.b.5** respectively). The lamin A/C bait-gene was tested for transcriptional activation. The colonies were white and only grew on SD/-Trp media. This means that the construct does not activate transcription. However, in separate tests it did show toxicity. This was overcome by using the strategy described in section **2.11.b.5**. After harvesting the lamin A/C bait gene containing cells, they and the cDNA library containing cells were counted by using a hemocytometer. 2 ml of cDNA library-pGADT7 in yeast strain AH109 cells **(section 2.11.c.2)** and 5 ml of harvested lamin A/C bait-gene in yeast strain Y187 were mixed **(section 2.11.d.1).** After 24 hours of incubation the mating mixture was tested for zygote formation **(Figure 3.5.b)**. The mating efficiency was 9.3%.

After 8 days growth on selective media 1000 positive colonies were re-streaked onto the master plates to test for MEL1 expression and blue colony formation. Colony PCR was applied to these 1000 colonies by using the vector out AD LD-insert primer set **(Table 2.2) (Figure 3.6).**

3.3.5 Screening of the cDNA Library with the LAP2α-bait-construct

As described above the LAP2α-bait-gene was also tested for transcriptional activation and toxicity. It was found not to activate transcription but it was toxic. So,

the strategy described in section **2.11.b.5** was used. The cells were prepared for mating to cDNA library containing cells in an identical manner to that described above in section **3.2.4.** After 20 hours incubation the mating mixture was tested for zygote formation as mentioned in section **3.3.4** and (**Figure 3.5.b**). The mating efficiency was 9.3%.

After 8 days growth on selective media 42 positive colonies were re-streaked onto the master plates to be tested for MEL1 expression and blue colony formation. Colony PCR was applied for these 42 colonies by using the vector out AD LD-insert primers set **(Table 2.2) (Figure 3.7).**

3.3.6 DNA sequencing and bioinformatics study.

5ul of product from the colony PCR reactions for both the 1000 positive colonies resulting from the lamin A/C screening **(section 3.2.4)** and the 42 positive colonies resulting from the LAP2α screening **(section 3.2.5)** were sent to the DNA sequencing facility to perform sequence analysis **(section 2.12.a).**

Sequences data was used in a Bioinformatics study **(section 2.12.b)**. By excluding small sequences off less than 200bp and poor sequence data, 11 contigs and 263 individual sequences resulted from the lamin A/C mating with the cDNA library **(Table 3.1)**. 3 contigs and 3 individual sequences resulted from LAP2α mating with the cDNA library **(Table 3.2)**. One of the sequences that matched from both studies above was Cytochrome c Oxidase subunit II (Cox2) **(Figure 4.1).**

3.4 Discussion.

One of the approaches to study the function of a protein is to investigate if this protein works in conjunction with others or alone. Are these interactions important in the localization or expression of the protein? It was shown before that LAP2α binds to lamin A/C. Therefore, it was important to investigate novel protein binding to lamin A/C and/or LAP2α. The yeast 2-hybrid technique was employed for this study.

A cDNA library was generated from total RNA purified from the epithelial layer of normal human colon tissue. Poly A+mRNA was purified from the total RNA this was followed by LD-PCR. 0.3-3 kb fraction of the cDNA was co-transformed with pGADT7 into AH109 yeast cells.

Full length cDNA of lamin A/C and LAP2α were separately cloned into pGBKT7. Lamin A/C-pGBKT7 or LAP2α-pGBKT7 transformed into Y187 yeast cells were mated with the cDNA library transformed into AH109 yeast cells. Positive colonies from each mating were re-streaked onto master plates for Mel1 reporter gene testing and to reduce the background. Each positive colony was amplified using the colony-PCR technique. The PCR products were electrophoresed on 1% agarose gels. More than 1000 positive colonies resulted from the lamin A/C and cDNA library mating. Most of the PCR products were approximately 1000bp in size. These PCR products were sent for DNA sequencing. About 42 positive colonies resulted from LAP2α and cDNA library mating. The PCR products were

between 200bp-400bp in size. Again these PCR products were sent for DNA sequencing.

Bioinformatics studies on the DNA sequences from lamin A/C interacting colonies were performed. After analysis, 11 contigs and 263 individual sequences were resulted. Contig 5 is assembled of 6 sequences out of 366 total sequences. Contig 5 is 600bp in size and is identical to cytochrome c oxidase subunit II (Cox2). Bioinformatics studies on the DNA sequences of LAP2α interacting colonies were also performed. After analysis, 3 contigs and 3 individual sequences were resulted. Sequence 8 is 521bp in size and is also identical to cytochrome c oxidase subunit II (Cox2).

Cox2 is a mitochondrial protein which is encoded by mtDNA. According to the Gene Bank (X15759) see **(Appendix IV-3c)**, its sequence contains on poly A tail and rich of poly A nucleotides in the medial. This may be the target of cDNA library and LD-PCR generation. It localizes into the mitochondrial inner membrane in a complex with other proteins to form complex IV (COX) of the mitochondrial respiratory chain (MRC). COX is composed of thirteen subunit polypeptides, three of which are encoded by mtDNA while the rest are encoded by the nuclear genome. Cox2 is the smallest subunit found in COX. It contains on a copper centre that has a critical function in receiving electrons from cytchrome c (Capaldi, 1990; Tsukihara *et al.*, 1996).

COX deficiency was linked to different diseases including Alzheimer disease (AD) (Ojaimi and Byrne, 2001). It was found that reduction in COX activity is associated with elevation in reactive oxygen species (ROS) and a reduction in ATP production in mitochondria from AD derived cells (Cardoso *et al.*, 2004). LMNA mutations were implicated in cell stress and ROS production (Caron et al., 2007). LMNA mutations such as R439C and R482W were reported in FPLD2 patient and implicated in increasing ROS (Verstraeten et al., 2009). Because of that it was interesting to focus on the interaction of lamin A/C and LAP2α with Cox2.

Several questions may be asked. Is this interaction real or not? If yes, does Cox2 localize in the nucleus as well as the mitochondria, or do lamin A/C and/or LAP2α localize to the mitochondria as well as the nucleus? To answer these questions, western blot analysis following co-immunoprecipitation, immunofluorescence and TEM were employed.

3.5 Figures.

Figure 3.1:

Yeast 2-Hybrid Principle:

A) DNA- Binding Domain Construction:

The bait gene should be cloned in-frame to the Gal-4 binding domain (BD) in plasmid pGBKT7. The construct is then transformed into yeast Y187 and AH109 to be tested for toxicity and transcriptional activation respectively. The Gal4 DNA Binding Domain of the construct protein binds to Gal4 upstream activating sequences (UASs) and TATA boxes of the AH109 genome. If it is not a transcriptional activator, the reporter genes (His3, Ade2, LacZ and Mel1) will not be transcribed and the colonies will grow on SD-Trp plates only. However, if the bait gene has any transcription factor function the colonies will grow in blue color on SD-Trp/-His3/-Ade2/-Mel1 plates. If this is the case we need to remove the activating domain and re-test.
If it is inactive, a toxicity test needs to be done on the bait gene construct transformed into Y187. Some strains do not grow well in liquid media compared with the empty vector alone.

B) cDNA Library-Activating Domain Construction:

Total or polyA+ mRNA was reverse transcribed to ss cDNA by using the CDS III oligo(dt) primer. This primer has oligo-dt sequences and a sequence named CDSIII at the 5' end. When the primer is mixed with the RNA it will hybridize to the 3' end of polyA+ mRNA and generate cDNA sequences with GGG at the 5' end. BD SMART III oliqonucleotide has a unique sequence terminating with CCC at the 3'end. When BD smart III is mixed with the cDNA it will generate cDNAs starting with the BD Smart III sequences and terminating with CDS III. Long-Distance PCR (LD-PCR) will be used to amplify these copies of cDNA by using primers that match with BD Smart III and CDS III. After the LD-PCR was performed, the cDNA was purified on a BD chroma spin TE-400 column. The whole purified cDNA library was mixed with pGADT7-rec Sma I linearized vector and co-transformed to AH109 yeast competent cells. The yeast repair enzymes will restore the Sma I-linearized vector to covalently closed circles by recombining sequences at the ends of the cDNA library with the homologous sequences at the ends of the vector. The outcome will be on open reading frame with the activating domain of the vector and in the correct orientation with the cDNA.

A) DNA-BD Construction

I- Clone Bait gene into pGBKT7 vector.

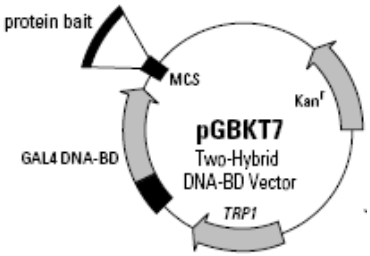

Transformed into *E. coli* DH5α

Transformed into Yeast (Y187 & AH109).

Test for transcriptional activation and Toxicity.

Count enough number of Y187 yeast transformed for mating.

B) cDNA Library construction.

I) cDNA library construction.

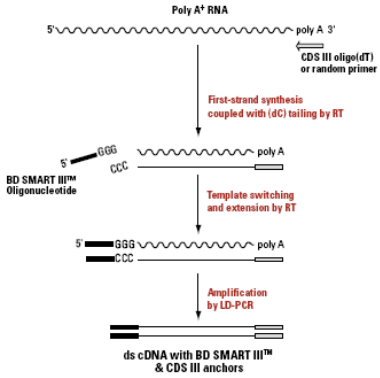

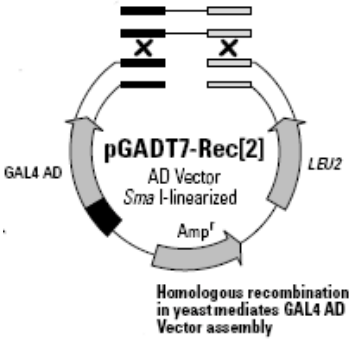

in-vivo recombination.

Transformed into Yeast (AH109).

Plated onto 180X 150mm SD-Leu plates. Harvesting & aliquots in 2ml and freeze.

Count enough number of aliquots cells for mating.

Plated onto SD –Leu/-Trp/His/-Ade

Figure 3.1

Figure 3.2:

cDNA library generation:

A) Total RNA extracted from two samples of epithelia layer of normal Human Colon Tissue. Sample # 2 was used for cDNA library generation.

B) PCR of β-actin applied to 0.5ug of Total RNA to check for DNA contamination.

C) LD-PCR performed on sample 2 RNA to generate the cDNA library. (S) cDNA generated from Poly A+ mRNA extracted from human colon epithelial tissue. (C) Poly A+ mRNA used as a control. (PCR-C) 3.5 Kb PCR fragment was used as reaction control for LD-PCR.

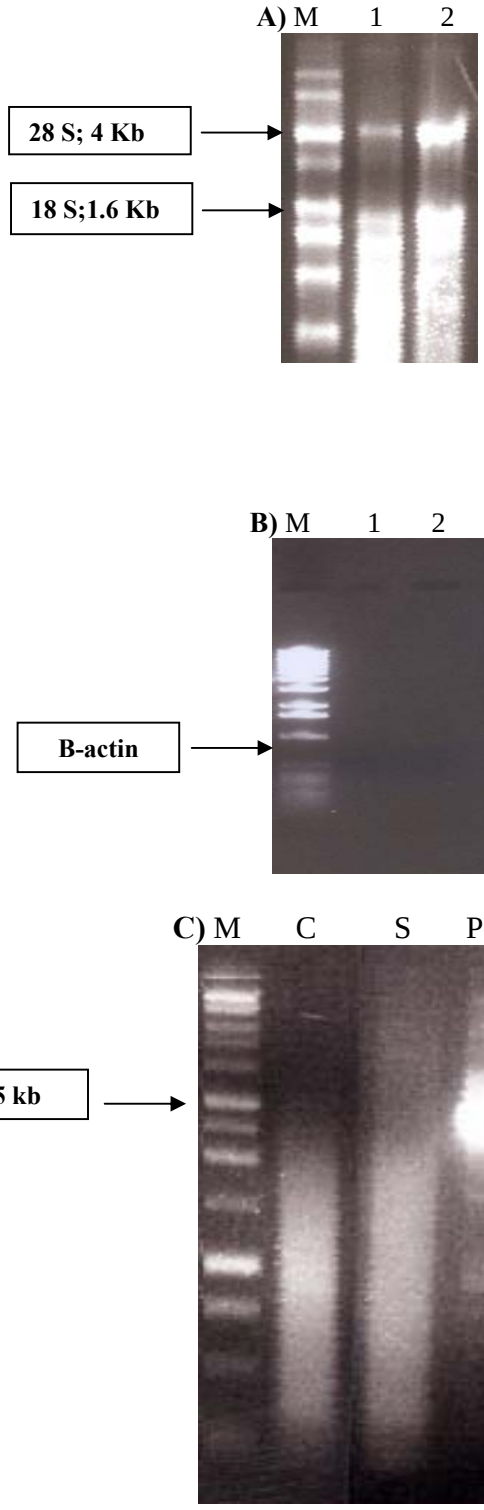
A) M 1 2
28 S; 4 Kb
18 S;1.6 Kb
B) M 1 2
B-actin
C) M C S PCR.C.
3.5 kb
- M, Marker 0.2-10Kb
- C, Poly A+ mRNA controls.
- S, Poly RNA Sample,
- PCR C, LD-PCR controls.

Figure 3.2

Figure 3.3:

Lamin A-Gal4 DNA Binding Domain Bait Construction (LaminA-BD-pGBKT$_7$).

A) Two RT-PCR reactions of 50ul each were performed from poly A+ mRNA. The resultant bands were excised to be used for cloning into TOPO-TA-pCR2.1 **(Table 2.2).**

B) 40ul of correct clone # 1 of Lamin A+Topo (TA)-pCR2.1 digested with Sfil and Sall for gel extraction and purification to be used for sub-cloning into prepared pGBKT7.

C) 4 correct clones were selected from sub-cloning Lamin A into pGBKT7. These were digested with Apal and Sfil to check for the correct orientation which should give a 1.2 kb product.

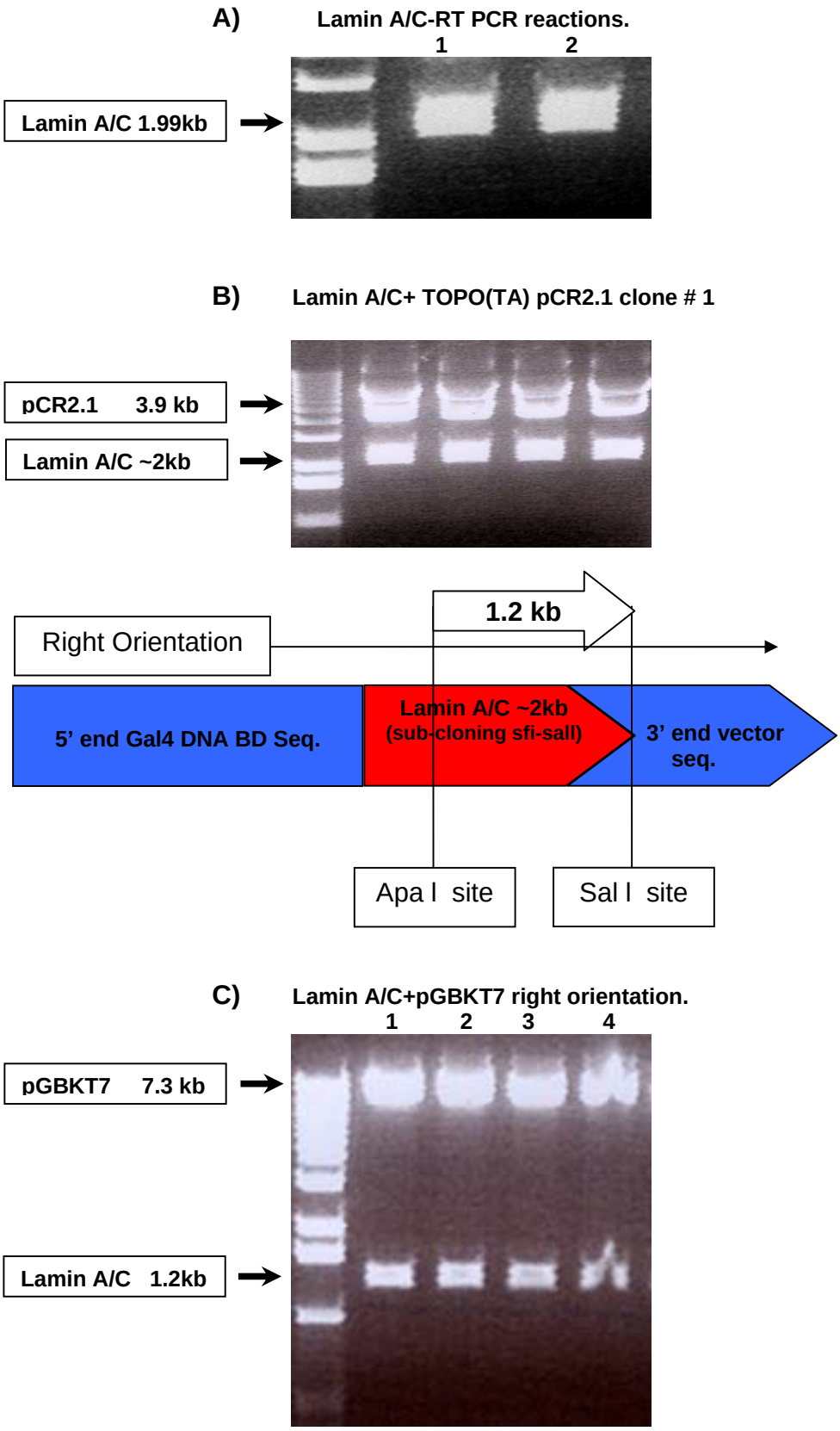
A)
Lamin A/C-RT PCR reactions.
1
2
Lamin A/C 1.99kb
B)
Lamin A/C+ TOPO(TA) pCR2.1 clone # 1
pCR2.1 3.9 kb
Lamin A/C ~2kb
1.2 kb
Right Orientation
5' end Gal4 DNA BD Seq.
Lamin A/C ~2kb
(sub-cloning sfi-sall)
3' end vector seq.
Apa I site
Sal I site
C)
Lamin A/C+pGBKT7 right orientation.
1
2
3
4
pGBKT7 7.3 kb
Lamin A/C 1.2kb

Figure 3.3

Figure 3.4:

LAP2α-Gal4 Binding Domain Bait Construction (LAP2α-BD-pGBKT$_7$):

A) Three RT-PCR reactions of 50 ul each were performed from poly A+ mRNA. The resultant bands were excised to be used for cloning into TOPO-TA-pCR2.1 **(Table 2.2).**

B) 40ul of correct clone # 1 of LAP2 α + Topo(TA)-pCR2.1 digested with Sma I and SalI for gel extraction and purification to be used for sub-cloning into prepared pGBKT7.

C) 5 correct clones were selected from sub-cloning LAP2α into pGBKT7. These were digested with NcoI to check for the correct orientation which should give a 1.95 kb product.

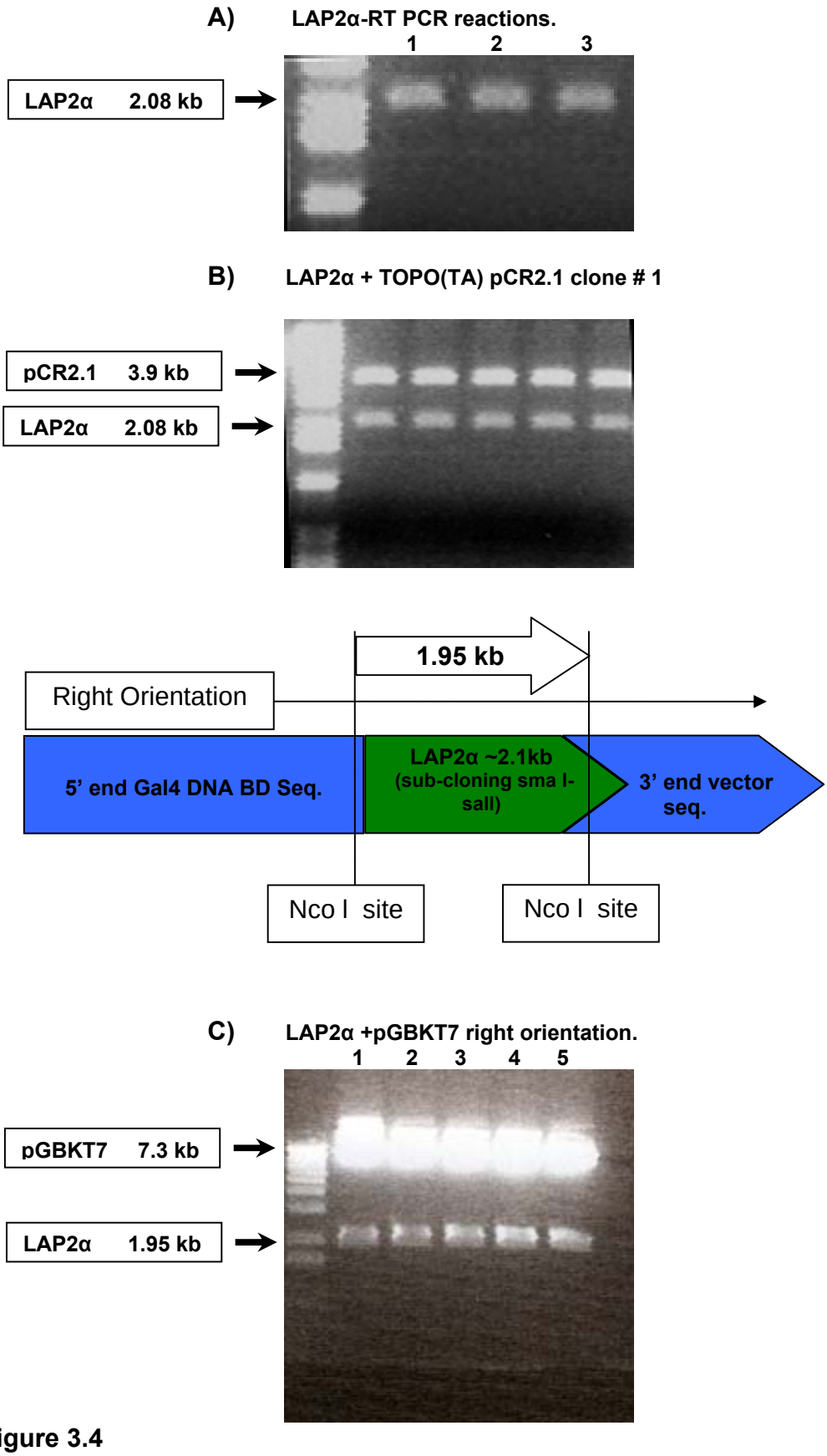
A)
LAP2α-RT PCR reactions.
1
2
3
LAP2α 2.08 kb
B)
LAP2α + TOPO(TA) pCR2.1 clone # 1
pCR2.1 3.9 kb
LAP2α 2.08 kb
1.95 kb
Right Orientation
5' end Gal4 DNA BD Seq.
LAP2α ~2.1kb
(sub-cloning sma I-
sall)
3' end vector
seq.
Nco I site
Nco I site
C)
LAP2α +pGBKT7 right orientation.
1
2
3
4
5
pGBKT7 7.3 kb
LAP2α 1.95 kb

Figure 3.4

Figure 3.5:

cDNA Library Activating Domain (AD)-pGADT7 Construction (cDNA library(AD)pGADT7):

A) Purified LD-PCR product of the cDNA library was co-transformed with SmaI linearized pGABT7-Rec into AH109 yeast competent cells and plated on SD/-Leu plates (~180 plates total of 150-mm size). After 5 days colonies appeared and were harvested **(section 2.11.c.2).**

B) Zygote formation after mating one of the bait (BD)-pGBKT7 constructs in Y187 with cDNA (AD) pGADT7 constructs in AH109. After 20-24 hours incubation with gentle agitation at 50rpm, the cells were observed by phase-contrast microscopy at 400x power. When two yeast cells are matted, the parent cells will attach and form third loupe, this formation called (Zygote). The third loupe called daughter (Diploid) which will separate from the parents. After 20 hours most of the cells showed zygote formation (Z), after 4 more hours incubation the diploid cells were appeared (D).

Scale bar = 10um.

A)

B)

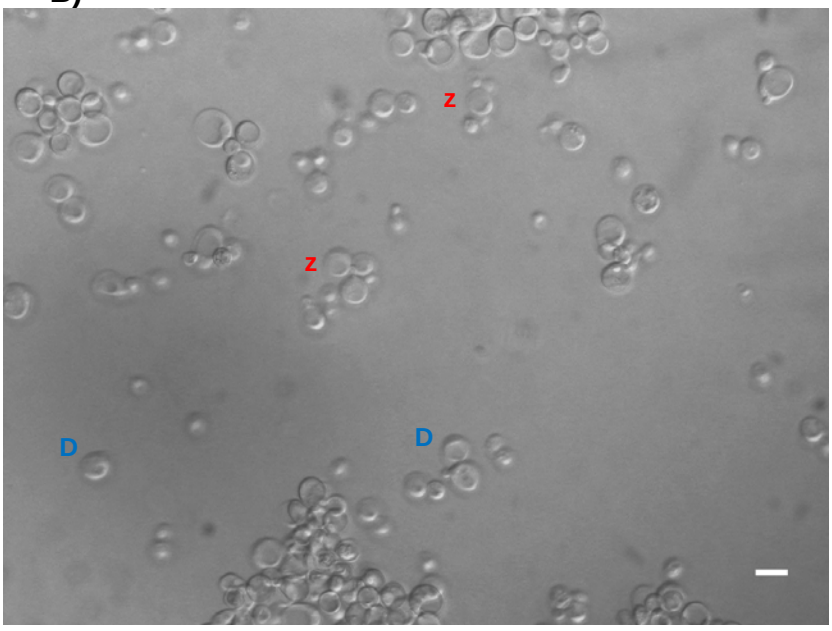

Figure 3.5

Figure 3.6:

Analysis of positive colonies resulting from mating the cDNA Library-AD-pGADT$_7$ with LaminA-BD-pGBKT$_7$:

More than 1000 positive colonies were produced from mating Lamin A/C and cDNA library constructs. Colony-PCR was applied to all of them **(section 2.12.a)**. This figure shows part of the PCR results. We see a primer dimer (Red arrow 100bp) in each reaction plus many have indicated inserts (Black arrow 1000bp).

Colony PCR of selected positive colonies generated.

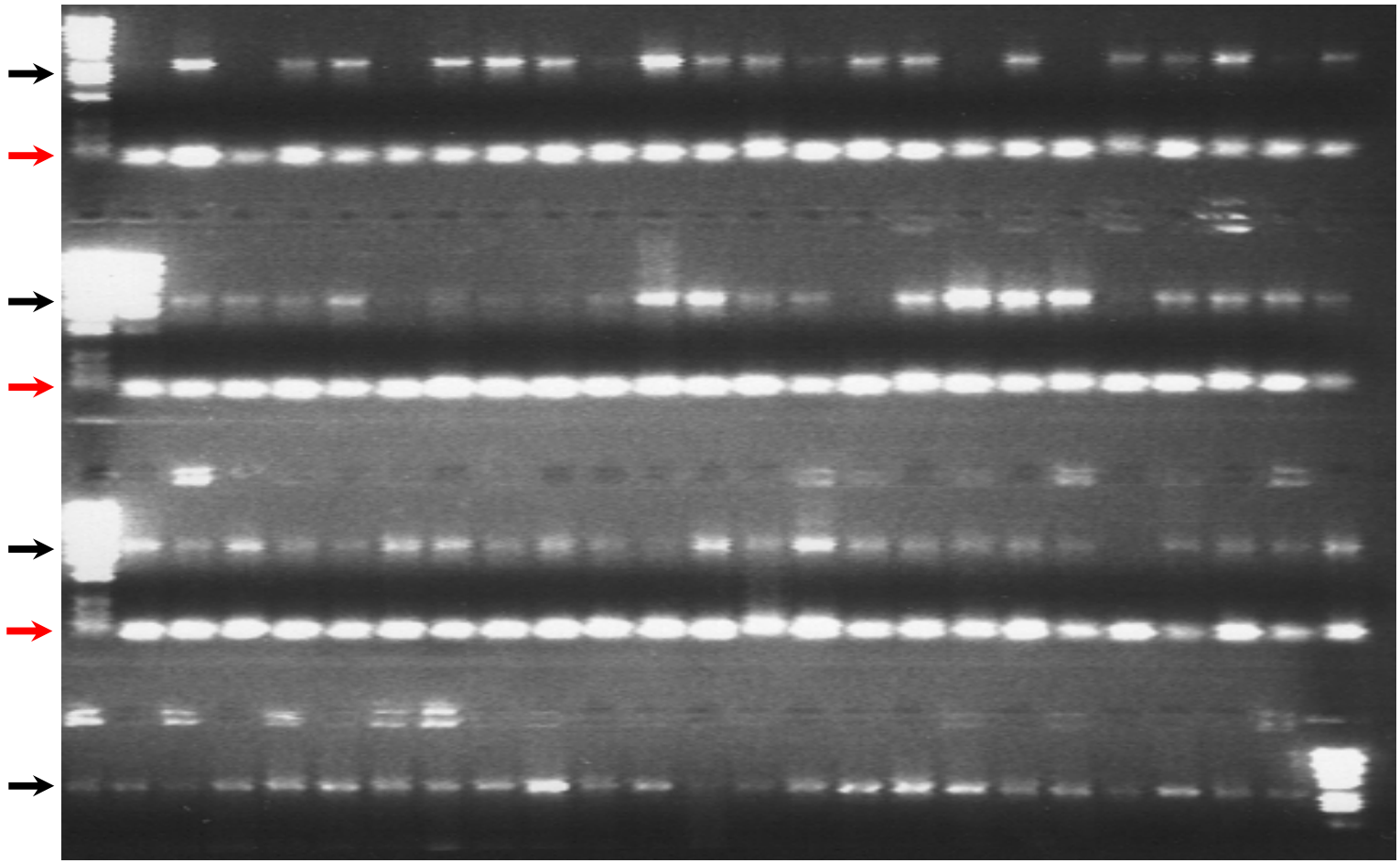

Figure 3.6

Figure 3.7:

Analysis of positive clones resulting from mating the cDNA Library-AD-pGADT$_7$ with LAP2α-BD-pGBKT$_7$:

42 positive colonies were produced from mating LAP2α and the cDNA library construct. Colony-PCR was applied to all of them **(section 2.12.a)**. This figure shows part of the PCR results. Primer dimer (Red arrow 100bp) and PCR product (Black arrow 200-600bp)

Colony-PCR of selected positive colonies generated.

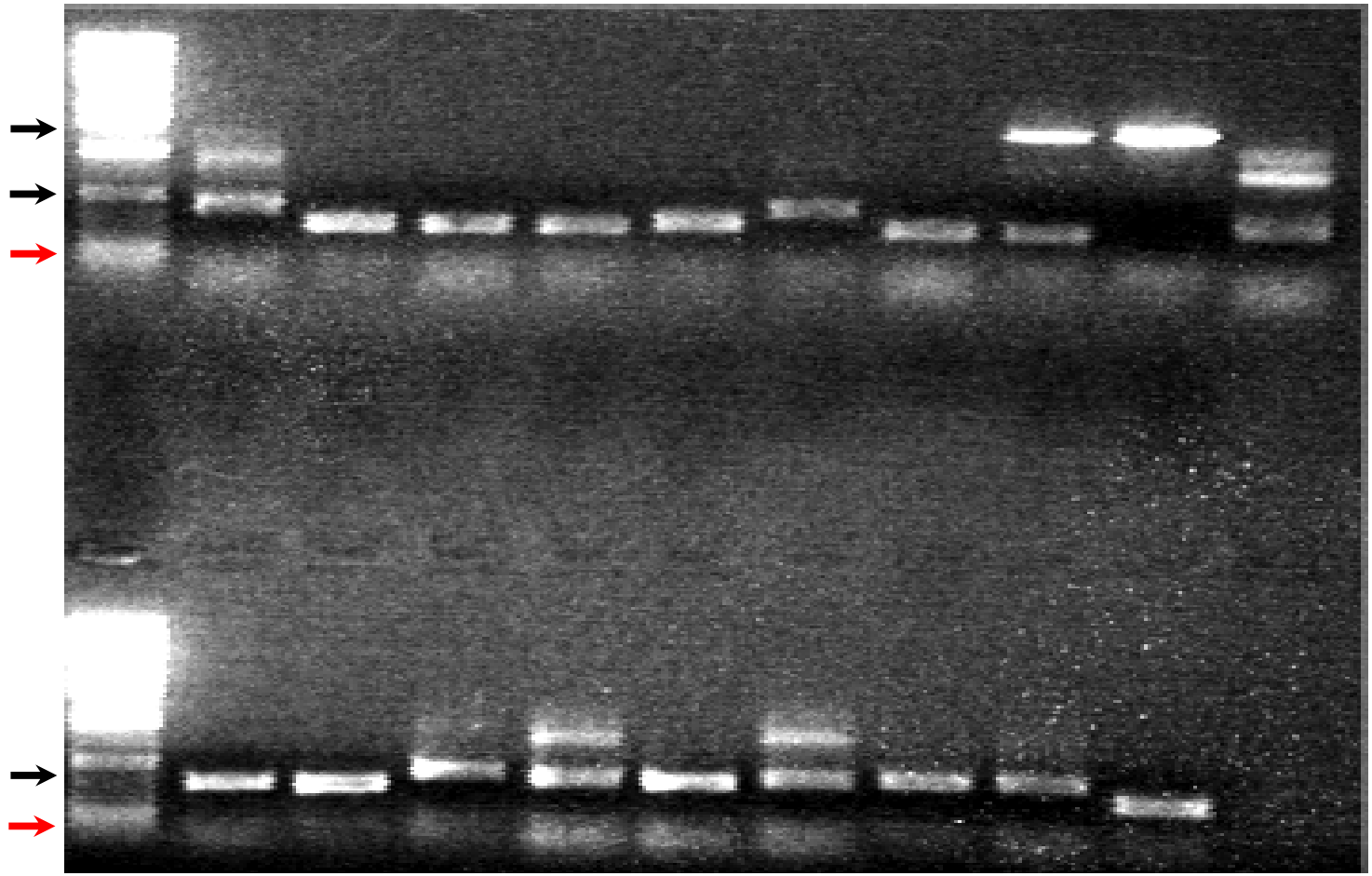

Figure 3.7

Table 3.1:

Bioinformatics study performed on Lamin A/C interacting colony:

The sequences were imported into Vector NTI software. Using the contig Express feature, the unreadable sequences were excluded. 366 sequences remained out of ~1000 positive colonies sent for DNA sequencing. Ambiguous nucleotides (N) were corrected by using the chromatographs of the sequence data. 11 contigs and 263 individual sequences resulted from the assembly. This table shows only the blast results of selected contigs. Contig 5 gave the highest score to Cytochrome c Oxidase subunit II (Cox2).

Table 3-1. Bioinformatics result of Lamin A mating to cDNA-library cells.

Contig			*Blast 2.0*					
Contig	No. of Assembled sequences / contig	Length (bp)	Hit count	Score (Bit)	Molecule Name	Accession #	Position	Server
1	3	349	97	39 (77.8)	Clone DKFZp686C06106	HSM807040	120-159	NCBI-Blast
2	19	239	102	39 (77.8)	Clone DKFZp686C06106	HSM807040	120-159	NCBI-Blast
3	19	227	113	39 (77.8)	Clone DKFZp686C06106	HSM807040	121-160	NCBI-Blast
4	3	221	114	39 (77.8)	Clone DKFZp686C06106	HSM807040	121-160	NCBI-Blast
5	6	600	500	448 (888.6)	Cytochrome c Oxidase II	EU935845.1	152-600	NCBI-Blast
6	2	336	93	36 (77.8)	Clone DKFZp686C06106	HSM807040	118-154	NCBI-Blast
7	5	1522	93	39 (77.8)	Clone DKFZp686C06106	HSM807040	86-125	NCBI-Blast
8	2	429	76	36 (71.8)	Clone DKFZp686C06106	HSM807040	120-156	NCBI-Blast
9	23	308	100	39 (77.8)	Clone DKFZp686C06106	HSM807040	102-141	NCBI-Blast
10	16	1634	113	41 (81.8)	Clone DKFZp686C06106	HSM807040	100-141	NCBI-Blast
11	5	1371	500	34 (67.8)	Clone DKFZp686C06106	HSM807040	124-158	NCBI-Blast

Table 3.2:

Bioinformatics study performed on LAP2α interacting colony:

The sequences were imported into Vector NTI software. Using the contig Express feature, the unreadable sequences were excluded. 37 sequences resulted out of ~42 positive colonies sent for DNA sequencing. Ambiguous nucleotides (N) were corrected using the chromatographs of the sequence data. This table shows the result of a BLAST search of 3 contigs and 3 individual sequences. Sequence 8 (Seq8) shows a good match match to Cytochrome c Oxidase subunit II (Cox2).

Table 3-2. Bioinformatics result of LAP2α mating to cDNA-library cells.

Contig			*Blast 2.0*					
Contig	**No. of Assembled sequences / contig**	**Length (bp)**	**Hit count**	**Score (Bit)**	**Molecule Name**	**Accession #**	**Position**	**Server**
1	20	313	76	39 (77.8)	Clone DKFZp686C06106	HSM807040	117-156	NCBI-Blast
2	9	292	87	39 (77.8)	Clone DKFZp686C06106	HSM807040	106-145	NCBI-Blast
3	5	293	73	36 (71.8)	Clone DKFZp686C06106	HSM807040	113-149	NCBI-Blast
Seq 8	1	521	500	496 (983.7)	Cytochrome c Oxidase II	EU443512.1	1-496	NCBI-Blast
Seq L34	1	832	92	303 (601.1)	Mediator complex subunit 16	NM_005481.2	103-406	NCBI-Blast
Seq L43	1	809	84	368 (730)	Thyroid hormone receptor-associated protein complex	AF121228	118-154	NCBI-Blast

Chapter 4: In-Vitro conformation of the putative binding of Cox2 with Lamin A/C and LAP2α.

4.1 Introduction.

4.1.1 Lamin A/C function in health and disease.

To understand the function of lamin A/C, we need to determine the interactions of Lamin A/C with other proteins in vivo. Over a decade of work on lamins by many investigators has focused on this problem.

4.1.1.1 Lamin A/C function in health.

As described in chapter 1 Lamin A/C participates with other lamins to build up the lamina structure underneath the inner nuclear membrane (INM) (Moir *et al.*, 2000; Hutchison, 2002; Herrmann and Foisner, 2003; Hutchison and Worman, 2004). These studies also showed that A-type lamins are involved in several different cell activities, such as the cell cycle, cell signaling and the maintenance of the size and shape of the nucleus.

4.1.1.2 Lamin A/C function in diseases.

Since 1999 mutations in LMNA have been shown to cause several different inherited diseases affecting muscle, fat, bone, skin and nerves. In the gene expression hypotheses, A-type lamins are considered to be essential for the correct tissue-specific expression of certain genes. Thus, a pathogenic mechanism for certain diseases might be a change in gene expression patterns caused by mutations in lamin A and C (Worman and Courvalin, 2002). In the mechanical stress hypotheses, mutations in lamins A and C are thought to weaken the structural integrity of an integrated nucleocytoplasmic skeletal network (Worman and Courvalin, 2002). However, A-type lamin mutations were implicated in cell stress and reactive oxygen species (ROS) (Caron *et al.*, 2007). Familial partial lipodystrophy of Dunnigan type 2 (FPLD2) was caused by mutations in LMNA. Belonging to these are R482W and R439C that are associated with a significant increase in ROS upon induction of oxidative stress by H_2O_2 (Verstraeten *et al.*, 2009).

4.1.2 LAP2α function.

LAP2α is one of the binding partners for nucleoskeletal Lamin A/C. When LAP2α was immunoprecipitated from nuclear fractions, lamins A/C and hypophosphorylated Retinoblastoma (Rb) were co-precipitated efficiently (Markiewicz *et al.*, 2002). This study also showed that LAP2α bound strongly to pocket C and weakly to pocket B of Rb. This study suggested that lamin A/C and

LAP2α complex is important in tethering Rb protein inside the nucleus. Another study showed the function of LAP2α on cell cycle progression and differentiation. Several studies have shown the involvement of LAP2α in the cell cycle and nuclear envelope (NE) assembly. Studies have shown that LAP2α assembled around chromosomes earlier than LAP2β, suggesting that it is one of the first proteins among the NE/nucleoskeleton components to associate with chromosomes during NE assembly (Foisner, 2003).

When LAP2α expression is decreased it has a negative effect on the growth arrest response to serum starvation. When its expression is increased it delays the transition from G_0 to S phase (Dorner *et al.*, 2006).

4.1.3 Mitochondrial Respiratory Chain (MRC).

The mitochondrial respiratory chain (MRC) composes of five multiple subunit complexes embedded in the mitochondrial inner membrane (MIM). These complexes are; complex I (NADH dehydrogenase), II (succinate-ubiquinone oxidoreductase), III (ubiquinol-cytochrome oxidoreductase), IV (cytochrome c oxidase (COX)) and V (ATP synthase). Electron transfer in cell respiration is coupled with proton translocation across the mitochondrial membrane, which is a primary event in energy production (Belevich *et al.*, 2006). Under physiological conditions, electron donations from NADH or $FADH_2$ enter the MRC either through Complex I or II respectively. Variety of carriers; such as haeme-containing cytochrome, iron-sulfur proteins, and ubiquinone (coenzyme Q) are associated in

MRC structure and are implicated in transferring electrons from one complex to another (Kristal and Krasnikov, 2003) .

Complex I is a 1 MDa complex comprising 45 polypeptides. It is the entry point for electrons donated from NADH into the MRC. The structure of the water soluble arm of complex I was studied in *Thermus thermophilus* which are most similar to the mammalian homologues and contains the FMN (Flavin Mono-Nucleotide) and the FeS (iron-sulfur) centers (Sazanov and Hinchliffe, 2006; Sazanov, 2007). The study illustrated that complex I has seven FeS centers in both the hydrophilic arms. They are involved in passing the electron from FMN centre through CoQ to O_2 and to donate an electron from the FMN centre or CoQ to O_2 (Sazanov, 2007).

Complex II is also known as succinate dehydrogenase or succinate-ubiquinone oxidoreductase. Succinate-ubiquinone oxidoreductase (SQR) of *Escherichia coli*, is often referred to as homologous to Complex II. It is also the entry point of electrons donated from $FADH_2$ to MRC. It comprises of two homologous integral membrane proteins, Succinate-quinone oxidoreductase (SQR) or succinate dehydrogenase (SDH) and quinol-fumarate oxidoreductase (QFR) or fumarate reductase. SQR/SDH is involved in the Krebs cycle and aerobic respiratory chain coupling the oxidation of succinate to fumarate with the reduction of quinine (Q) to quinol (QH_2). QFR/fumarate reductase is involved in catalyzing the reverse reaction to SQR during anaerobic respiration. SDH is composed of four subunits two of them hydrophilic and two hydrophobic, hydrophilic ones are a flavoprotein (SdhA) and an ironsulfur (SdhB), while the hydrophobic subunits are SdhC and SdhD. The SdhAB are involved in catalyzing the coupling reactions of the oxidation of succinate to

furmarate with the reduction of quinone to quinol. SdhAB are anchored to the membrane by the hydrophobic subunits SdhCD (Horsefield *et al.*, 2006).

Complex III is a monomer of ~240 KDa and compose of 11 polypeptides, three haeme and an FeS centre, and it interacts transiently with CoQ during the Q-cycle at the Q_i and Q_o sites (Iwata *et al.*, 1998).

Complex IV, Cytochrome c Oxidase (COX) is the terminal electron acceptor enzyme complex of the mitochondrial respiratory chain. It is important in transferring electrons from reduced cytochrome c to molecular oxygen to form water (Capaldi, 1990). COX is a complex of thirteen subunits, three of which are encoded by MtDNA. The remaining subunits are encoded by nuclear DNA and imported into the mitochondrial matrix. It has a Y shape structure made of three domains. The two arms of the Y span the lipid bilayer of the inner mitochondrial membrane while the third arm extends outside the membrane into the intermembrane space (Henderson *et al.*, 1977; Fuller *et al.*, 1979).

Complex V is also known as ATP-synthase. In mitochondria complex V is composed of three parts; membrane sub-complex F_0 that comprises three polypeptide subunits through which protons flow; stator stalk that consists of four polypeptide subunits, which connect F_0 to F_1; and the peripheral catalytic sub-complex F_1 that consists of five polypeptide subunits and carries the nucleotide binding sites (Belogrudov *et al.*, 1995; Weber, 2006).

4.1.4 ROS production by MRC.

MRC is the main source of ROS production during ATP generation or pathogenesis. This ROS production is important in cell signaling in health and pathology. Studies were focused on how mitochondria produce ROS; isolated mitochondria were performed in the lab. Scientist noticed that ROS was produced from complex I, III and IV of MRC. The mechanisms of producing ROS from complex I were summarized into two mechanisms: when the amount of NADH/NAD+ is high, leading to a reduced FMN site on complex I, and when electrons donated to CoQ pool is associated with a high protonmotive force leading to RET (reverse electron transport) (Murphy, 2009).

It was shown that when complex III was inhibited by antimycin, accumulation of large amounts of superoxide was associated. It was summarized that the amount of ROS produced from complex III under physiological conditions is negligible compared with the amount that was produced from complex I (Murphy, 2009).

Cox2 is the smallest enzyme of complex IV (COX) of the mitochondrial respiratory chain encoded by MtDNA. COX is the terminal electron acceptor enzyme complex of the mitochondrial respiratory chain. It is important in transferring electrons from reduced cytochrome c to molecular oxygen to form water (Capaldi, 1990).

Mitochondrial dysfunction was associated with Alzheimer disease (AD) and COX deficiency (Ojaimi and Byrne, 2001). Reduction in COX activity causes an elevation of reactive oxygen species (ROS) and a reduction in ATP production in

mitochondria from AD derived cells (Cardoso *et al.*, 2004). Cox2 is one of the mitochondrial apoptotic proteins including Apaf-1 and caspase-9 (Mazzanti *et al.*, 2006).

4.2 The aim of this study.

As described above the function of lamin A/C and LAP2α is complex. Therefore it is important to look for novel protein interactions to lamin A/C and/or LAP2α. In the previous chapter we have shown that Cox2 is one of the putative proteins that bind to Lamin A/C and LAP2α. However, the yeast 2-hybrid system may result in false positives even with all of the controls provided. So, it is important to use alternative methods to confirm the interactions. Because, lamin A/C and LAP2α are nuclear proteins and Cox2 is a mitochondrial protein. First, western blots of cell fractions were done on HT29 cells to investigate the localization of these proteins. Second, co-immunoprecipitation on mitochondrial or nuclear fractions was also provided to investigate the in vivo interactions between these proteins.

4.3 Results.

4.3.1 RT-PCR.

In the previous chapter Cox2 was identified as a putative lamin A/C and LAP2α binding protein. It is important to confirm that this protein is expressed and found in the original cDNA library. PCR primers were designed to Cox2 **(Table 2.2**). RT-PCR was performed using 1^{ss} cDNA generated (**section 2.6)** from colon epithelial RNA (**section 2.3.a) (samples 1 and 2 Figure 4.1)** and by using 1^{ss} cDNA generated from HT29 cell line RNA **(samples 3 and 4 Figure 4.1)**.

4.3.2 Western Blot.

Western blots were used to investigate the expression of Lamin A/C, LAP2 α and Cox2 in the cytosol, mitochondrial and nuclear fractions. Protein was extracted (**section 2.13.1)** from the HT29 cell line. Protein concentration was determined as described in **section 2.13.3**. Proteins were separated using 10% SDS-PAGE (**section 2.13.4)** followed by immunobloting (**section 2.13.5).** Four independent protein extractions were blotted with Jol2 (lamin A/C antibody) which showed the expression of lamin A/C in both the mitochondrial and nuclear fractions but not in the cytosolic fraction **(Figure 4.2)**. The same samples were blotted with LAP2α antibody which also showed the expression of LAP2α in the mitochondrial and nuclear fractions but not in the cytosolic fraction **(Figure 4.3)**. The same samples

were further blotted with Cox2 antibody which showed the expression of Cox2 in the mitochondrial fraction but not in the cytosolic and nuclear fractions **(Figure 4.4)**. To show that the fractions were clear of cross contamination, two different antibodies were used for all of the samples. Retinoblastoma (Rb) antibody showed expression of Rb in the cytosolic and nuclear fractions but not in the mitochondrial fraction **(Figure 4.5)**. LAP2β antibody showed expression of LAP2β in the nuclear fraction but not in the cytosolic and mitochondrial fractions **(Figure 4.6)**. These experiments show the presence of both lamin A/C and LAP2α in mitochondria as well as Cox2. The controls showed us that the fractions were cleared of cross contamination between each other.

The same blots were subjected to probe by anti-lamin B antibody that recognizes both lamin B1 and B2. The lamin B antibody showed expression of lamin B in the nuclear fraction but not in the cytosolic or mitochondrial fractions **(Figure 4.7)**. This result will confirm that the cell fractions were cleared of cross contamination and confirm the distribution of lamin A/C and LAP2α in mitochondria and nucleus.

Because of the dilution factors between the original sample of nuclear, cytosolic and mitochondrial fractions were 2.5 (**section 2.13.5)**. The histograms represent two bars of each fraction; blue bar for the band density in the loaded sample, red bar for the band density in the total sample after it was multiplied by 2.5.

4.3.3 Co-Immunoprecipitation.

Having shown interactions between Cox2 and lamin A/C and LAP2α using yeast 2-hybrid system **(Chapter 3)** and that these proteins are co-located as determined by cell fractionation followed by immunoblotting, it was important to show direct protein-protein interactions using another method. The method employed here was co-immunoprecipitation. Because, Cox2 is a mitochondrial protein and Lamin A/C and LAP2α are nuclear proteins. Immunoprecipitation on protein extracts of mitochondrial and nuclear fractions from HT29 cell lines were performed. Five co-immunoprecipitations tubes were set as described in **section 2.13.2**. Tubes 1 and 2 are mitochondrial fractions; tubes 3, 4 and 5 are nuclear fractions. Tubes 2 and 3 were precipitated using Cox2 antibody, while tubes 1 and 4 were the serum control. Tube 5 was precipitated by lamin A/C (Jol2) antibody. The supernatant (S) and immunoprecipitate (IP) of each sample was resolved using 10% SDS-PAGE. After transfer of proteins, the membrane was blotted with Jol2 which detected lamin A/C in IP fractions 2 and 5 and S fractions 1, 3, 4 and 5. This result detects the presence of lamin A/C in mitochondria which is precipitated by anti-Cox2 **(Figure 4.8a)**. The same samples were resolved again using 10% SDS-PAGE and after transfer of proteins, the membrane was blotted with anti-LAP2α antibody which detected the precipitation of LAP2α in samples 2 and 5 but not in samples 1, 3 and 4. This again shows the interaction of LAP2α with Cox2 in sample 2 and lamin A/C in sample 5 **(Figure 4.8-1b)**. The membranes were blotted by anti-Cox2 antibody which detected Cox2 only sample 1 as expected **(Figure 4.8-1c)**.

This experiment was repeated two more times on mitochondrial fraction of HT29 cell lines as follow. Two co-immunoprecipitation tubes were set as described in **section 2.13.2**. Tube 1 was precipitated using serum, while tube 2 was using anti-Cox2 antibody. The samples were resolved using 10% SDS-PAGE. The transmembranes were blotted with antibody to; lamin A/C (Jol2), LAP2α and Cox2 respectively. Lamin A/C was detected in IP of sample 2 and S of sample 1 **(Figure 4.8 d&e)**. LAP2α was detected in IP of sample 2 and S of samples 1 & 2 **(Figure 4.8 f&g)** and Cox2 was detected in IP of sample 2 and S of samples 1& 2 **(Figure 4.8 h&i)** as well.

4.4 Discussion.

From chapter 3, it was shown that Cox2 is one of the proteins that interact with lamin A/C and LAP2α. Further experiments needed to be used to confirm this interaction and answer the questions that this initial observation raises.

First of all, RT-PCR shows that Cox2 is expressed in the original tissue that was used to generate the cDNA library. Secondly, western blots of cell fractions show that the lamin A/C is detected in mitochondrial and nuclear fractions but not in the cytosolic fraction. The same samples were blotted with LAP2α antibody which also shows that LAP2α is detected in mitochondrial and nuclear fractions but not in the cytosolic fraction. By way of contrast, Cox2 was detected only in the mitochondrial fraction but not in the cytosolic or nuclear fractions. These blots have been subjected to control by probing with different antibodies that show the individual cell fractions are clear of cross contamination. Retinoblastoma (Rb) antibody was

used for this and showed that Rb is detected in cytosolic and nuclear fractions but not the mitochondrial fraction. LAP2β antibody was used as a second control on these blots. Again, LAP2β was detected in the nuclear fraction but not in the cytosolic and mitochondrial fractions.

From above experiments, we can conclude that lamin A/C and LAP2α localize in the mitochondria as well as the nucleus. However, Cox2 localizes only in mitochondria.

Does Cox2 interact with lamin A/C and/or LAP2α as it was suggested in the yeast 2-hybrid experiments? To answer this, co-immunoprecipitation was performed on mitochondrial and nuclear fractions. It was shown by using Cox2 or lamin A/C antibodies on the mitochondrial fraction, lamin A/C, Cox2 and LAP2α were co-precipitated. These experiments confirmed the yeast 2-hybrid result in the previous chapter and also the localization of lamin A/C and LAP2α in mitochondria.

These results raise a question. Is there lamina cage structure underneath of the mitochondrial inner membrane like the one in the nuclear envelope? To answer this question, anti-lamin B antibody that recognizes both lamin B1 and B2 was used on all of the samples. The lamin B antibody showed expression of lamin B in the nuclear fraction but not in the cytosolic or mitochondrial fractions **(Figure 4.7)**. This result will confirm there is no lamina structure in mitochondria and would be good control to show that there were no cross contamination between the cell fraction that used in these experiments.

Further studies need to be performed to confirm this interaction and suggest the functions of lamin A/C and/or LAP2α in mitochondria.

4.5 Figures.

Figure 4.1: Cytochrome c Oxidase subunit II (COX2):

Rt-PCR of Cox2 using cDNA generated from normal colon RNA (lanes 1&2) and cDNA generated from HT29 cells (lanes 3&4).

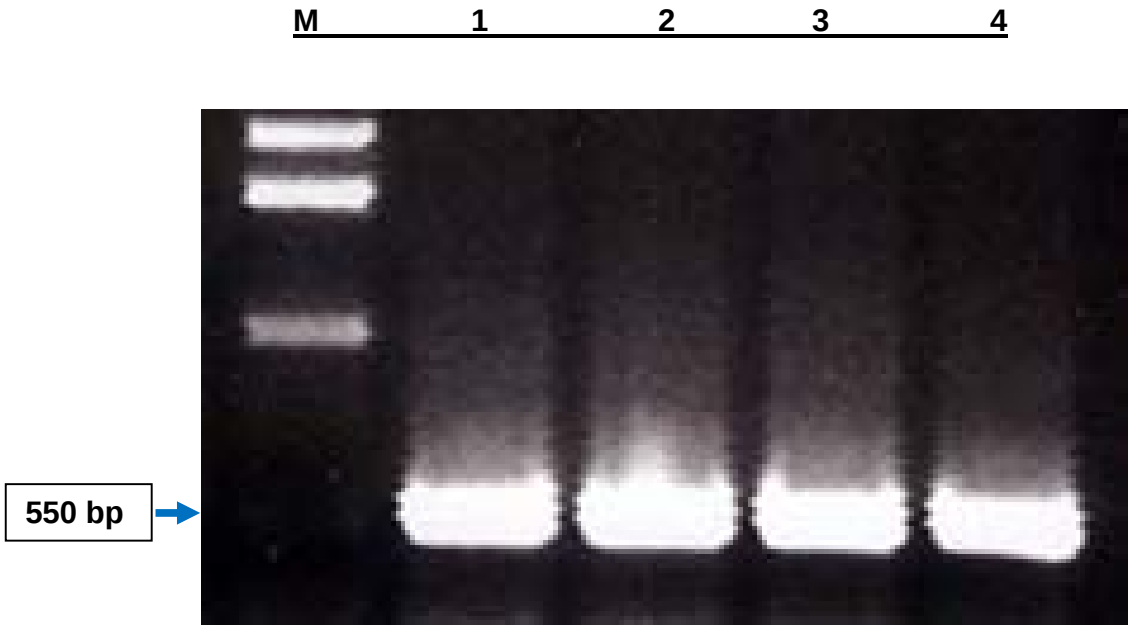

Figure 4-1

Figure 4.2: Western Blot of cell fractions with Lamin A/C antibody.

(A) Four independent extractions from cytosol (C), mitochondrial (M) and nuclear (N) fractions were resolved using 10% SDS-PAGE and blotted with Jol2 antibody. Double bands of Lamin A (~69KDa) and C (~65KDa) is detected in mitochondrial and nuclear fractions but not in cytosolic fraction. **(B)** Histogram shows the density of both bands. Data are expressed as the mean of at least four independent determinations. Blue bar represents the protein expression level per band. Red bar represents the expecting protein expression level per sample, after multiply the histogram mean of the band by the dilution factor between nuclear fraction and other fractions which are (2.5) see section **(2.13.5)**.

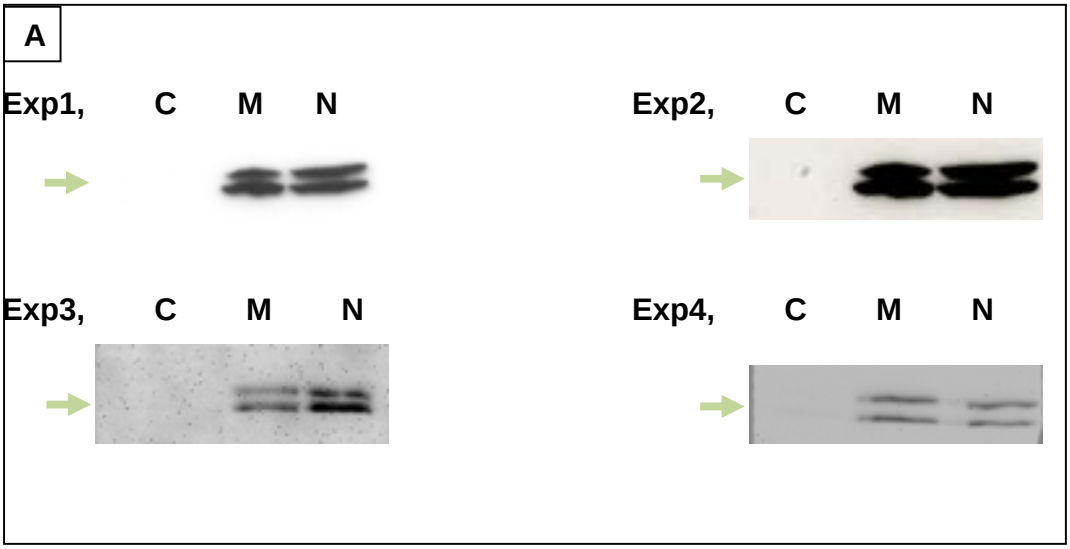
A
Exp1, C M N
Exp2, C M N
Exp3, C M N
Exp4, C M N

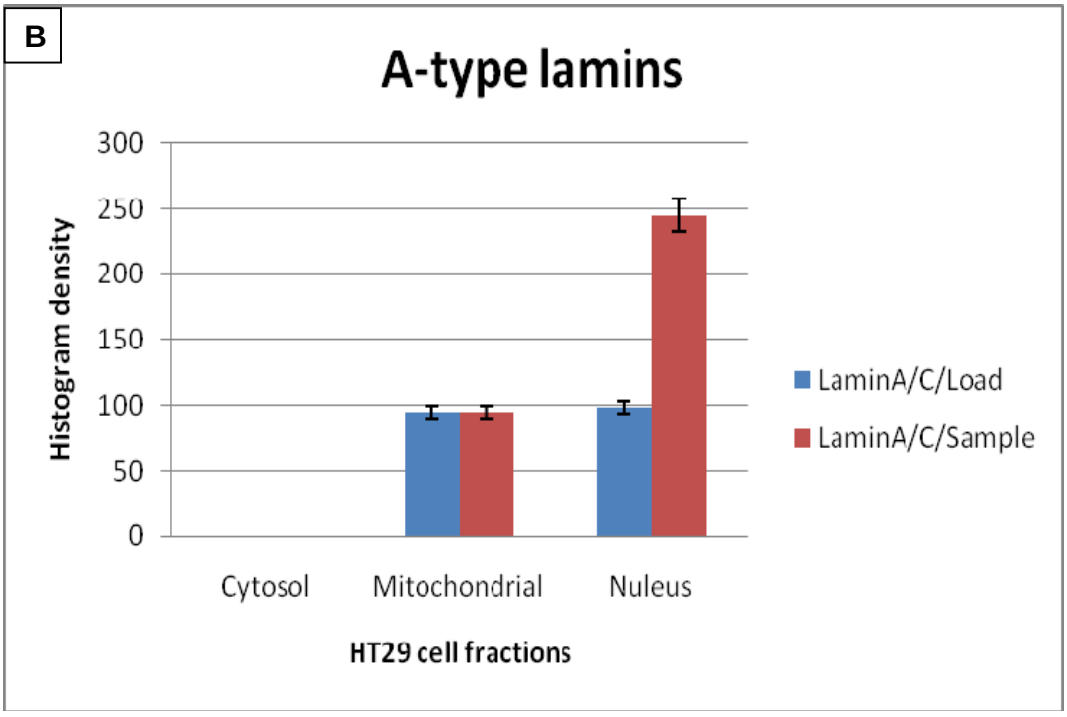
B
A-type lamins
Histogram density
300
250
200
150
100
50
0
Cytosol
Mitochondrial
Nuleus
HT29 cell fractions
LaminA/C/Load
LaminA/C/Sample

Figure 4-2

Figure 4.3: Western Blot of cell fractions with LAP2α antibody.

(A) Four independent extractions from cytosol (C), mitochondrial (M) and nuclear (N) fractions were resolved using 10% SDS-PAGE and blotted with LAP2α antibody. LAP2α is detected in mitochondrial and nuclear fractions but not in cytosolic fraction. **(B)** Histogram shows the density of the bands. Data are expressed as the mean of at least four independent determinations. Blue bar represents the protein expression level per band. Red bar represents the expecting protein expression level per sample, after multiply the histogram mean of the band by the dilution factor between nuclear fraction and other fractions which are (2.5) see section **(2.13.5)**.

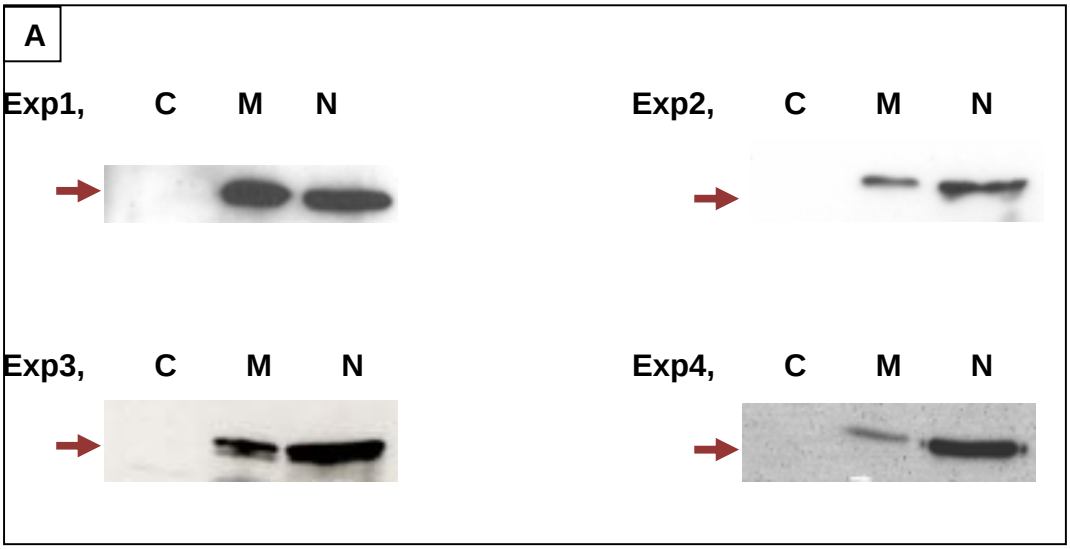
A
Exp1, C M N
Exp2, C M N
Exp3, C M N
Exp4, C M N

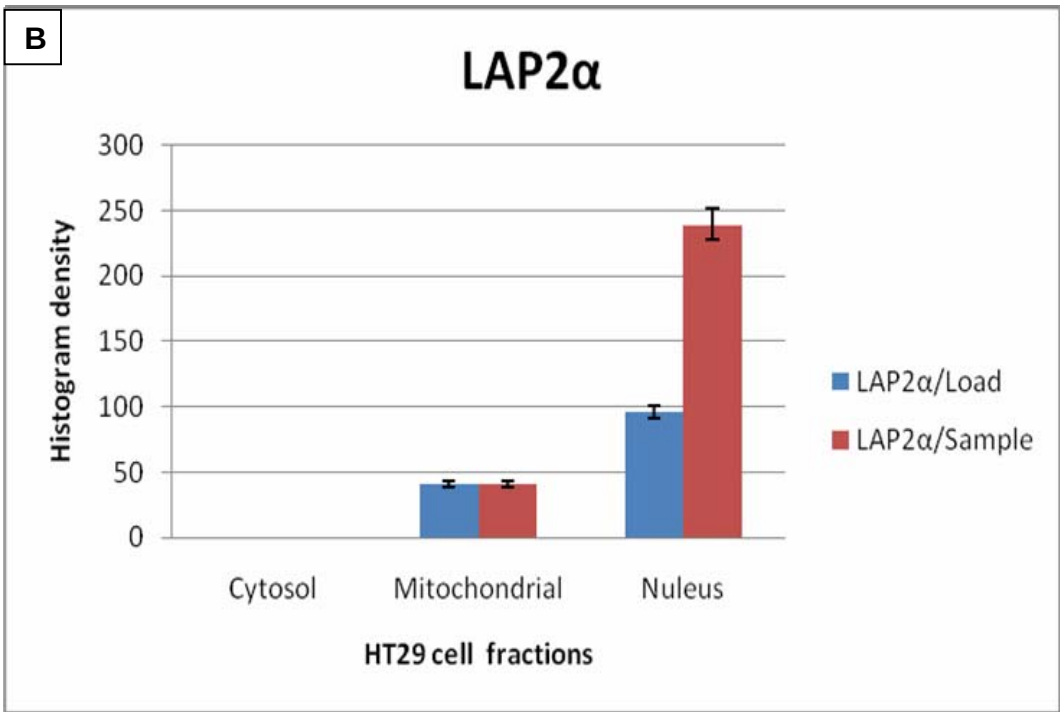
B
LAP2α
300
250
200
150
100
50
0
Histogram density
Cytosol
Mitochondrial
Nuleus
HT29 cell fractions
LAP2α/Load
LAP2α/Sample

Figure 4-3

Figure 4.4: Western Blot of cell fractions labeled with Cox2 antibody.

(A) Four independent extractions from cytosol (C), mitochondrial (M) and nuclear (N) fractions were resolved using 10% SDS-PAGE and blotted with Cox2 antibody. Cox2 is detected in mitochondrial fraction but not in nuclear and cytosolic fractions. **(B)** Histogram shows the density of the bands. Data are expressed as the mean of at least four independent determinations. Blue bar represents the protein expression level per band. Red bar represents the expecting protein expression level per sample, after multiply the histogram mean of the band by the dilution factor between nuclear fraction and other fractions which are (2.5) see section **(2.13.5)**.

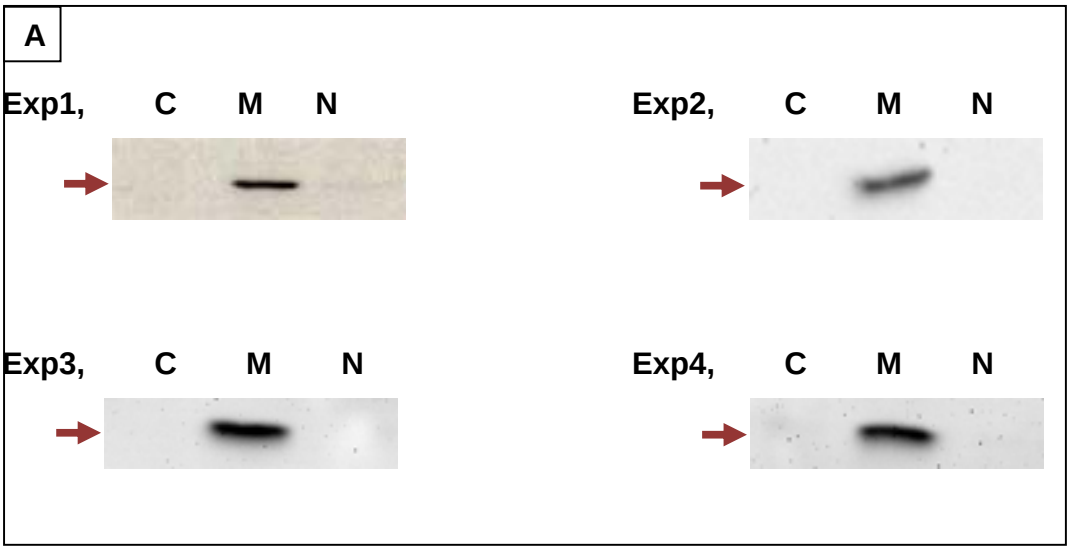
A
Exp1, C M N
Exp2, C M N
Exp3, C M N
Exp4, C M N

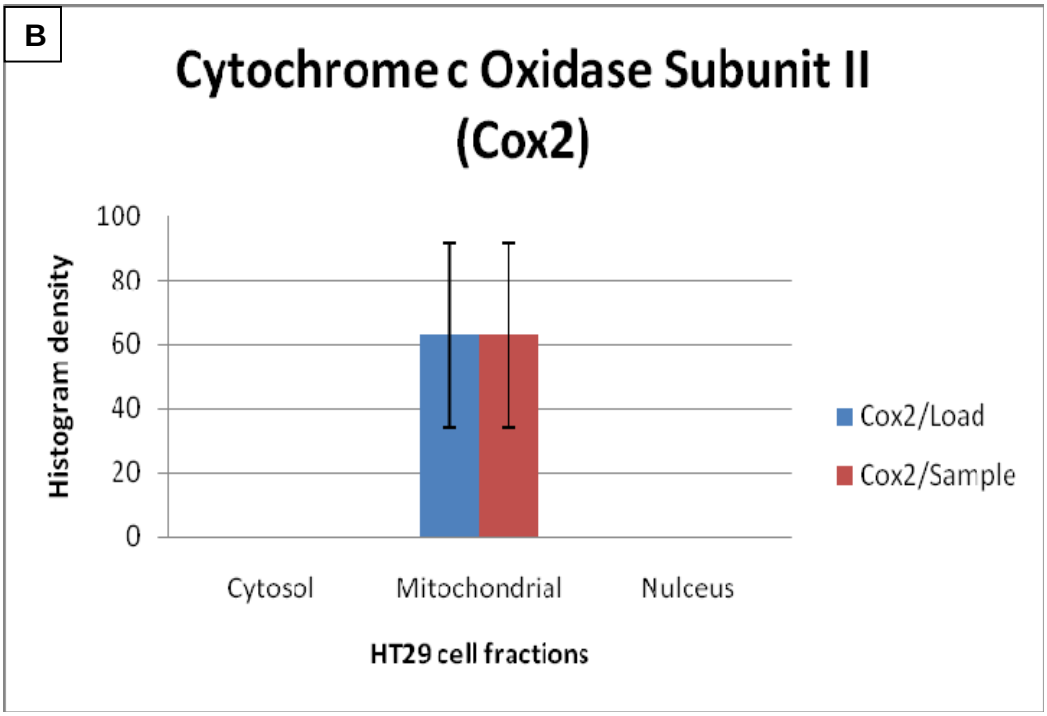
B
Cytochrome c Oxidase Subunit II (Cox2)
Histogram density
100
80
60
40
20
0
Cytosol
Mitochondrial
Nulceus
HT29 cell fractions
Cox2/Load
Cox2/Sample

Figure 4-4

Figure 4.5: Western Blot of cell fractions with Retinoblastoma (Rb) antibody.

(A) Four independent extractions from cytosol (C), mitochondrial (M) and nuclear (N) fractions were resolved using 10% SDS-PAGE and blotted with Rb antibody. Rb is detected in nuclear and cytosolic fractions but not in mitochondria fraction. **(B)** Histogram shows the density of the bands. Data are expressed as the mean of at least four independent determinations. Blue bar represents the protein expression level per band. Red bar represents the expecting protein expression level per sample, after multiply the histogram mean of the band by the dilution factor between nuclear fraction and other fractions which are (2.5) see section **(2.13.5)**.

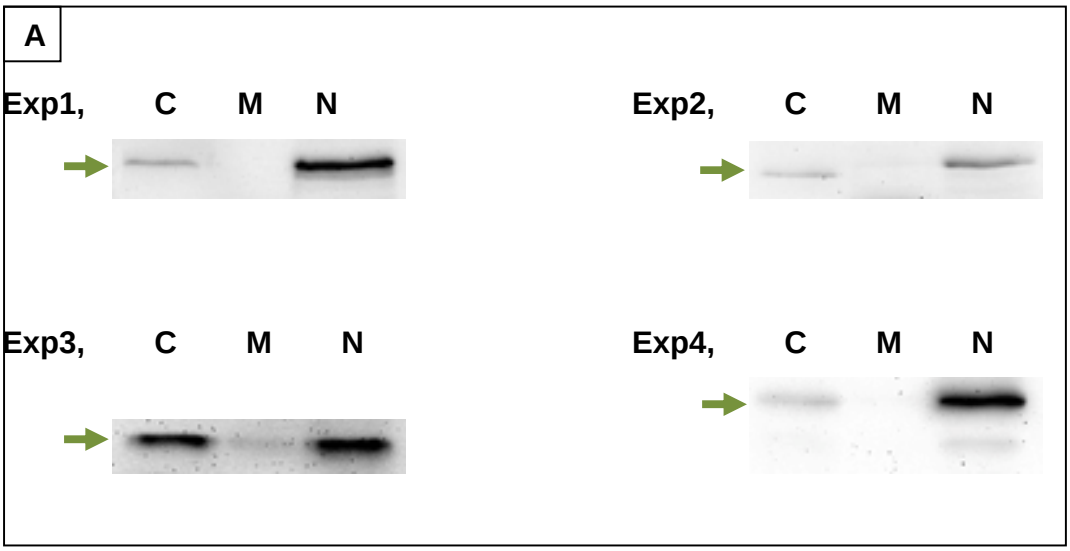
A
Exp1, C M N
Exp2, C M N
Exp3, C M N
Exp4, C M N

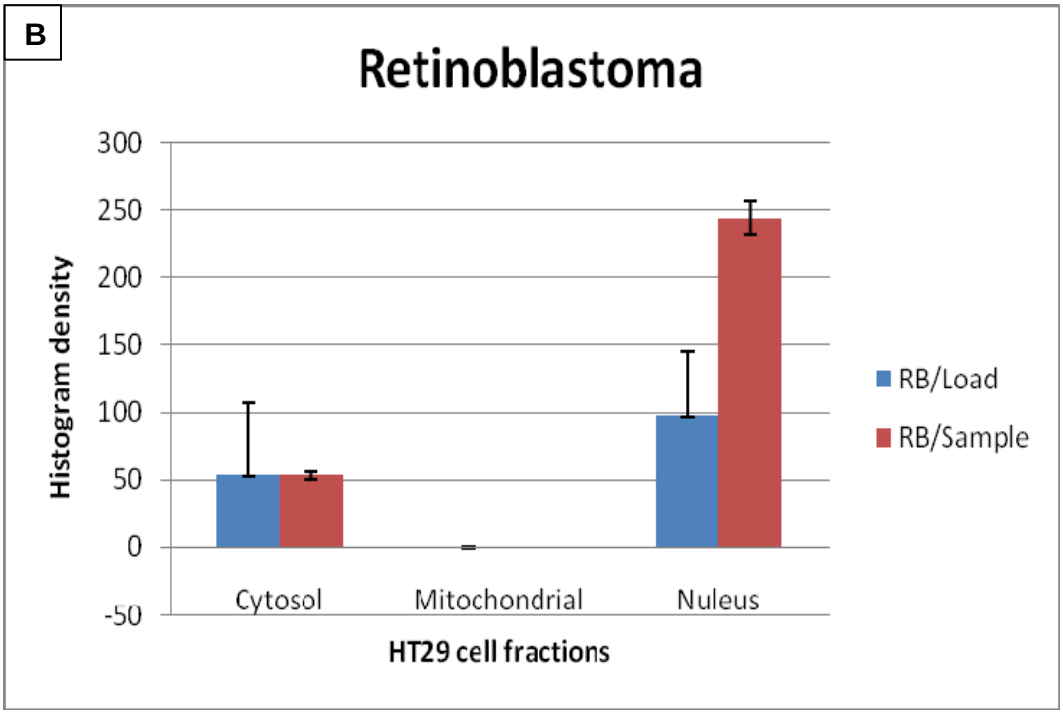
B
Retinoblastoma
300
250
200
150
100
50
0
-50
Histogram density
Cytosol
Mitochondrial
Nuleus
HT29 cell fractions
RB/Load
RB/Sample

Figure 4-5

Figure 4.6: Western Blot of cell fractions with LAP2β antibody.

(A) Four independent extractions from cytosol (C), mitochondrial (M) and nuclear (N) fractions were resolved using 10% SDS-PAGE and blotted with LAP2β antibody. LAP2β is detected in nuclear fraction but not in cytosolic and mitochondria fractions. **(B)** Histogram shows the density of the bands. Data are expressed as the mean of at least four independent determinations. Blue bar represents the protein expression level per band. Red bar represents the expecting protein expression level per sample, after multiply the histogram mean of the band by the dilution factor between nuclear fraction and other fractions which are (2.5) see section **(2.13.5)**.

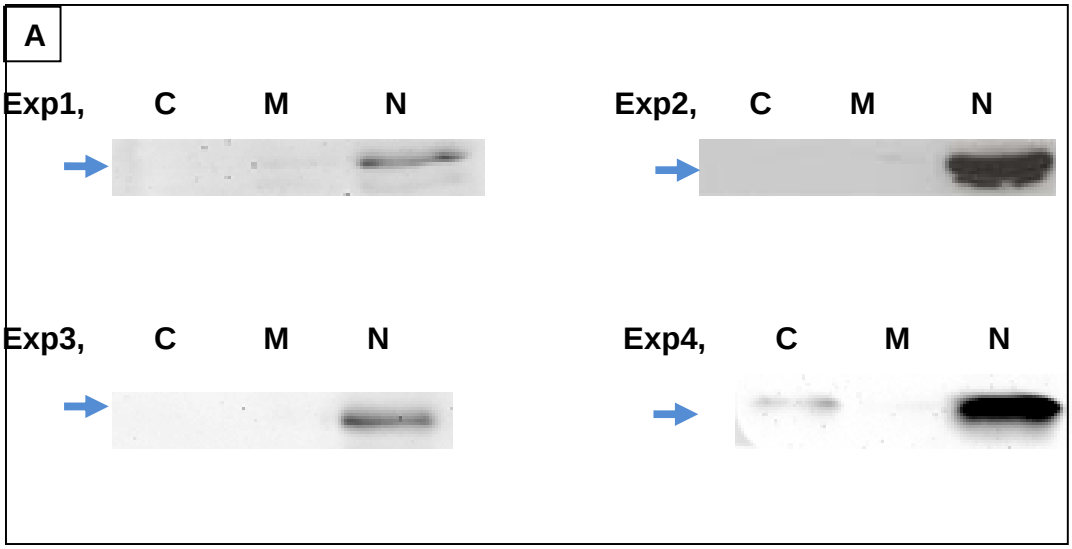
A
Exp1, C M N
Exp2, C M N
Exp3, C M N
Exp4, C M N

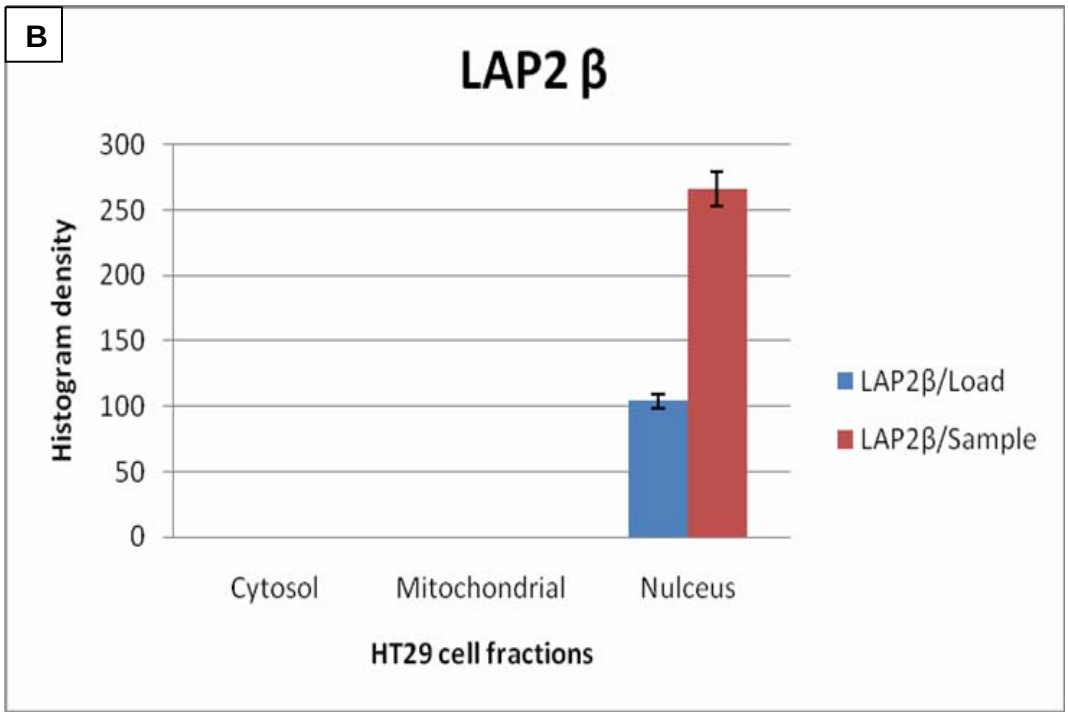
B
LAP2 β
Histogram density
300
250
200
150
100
50
0
Cytosol
Mitochondrial
Nulceus
HT29 cell fractions
LAP2β/Load
LAP2β/Sample

Figure 4-6

Figure 4.7: Western Blot of cell fractions with Lamin B antibody.

(A) Four independent extractions from cytosol (C), mitochondrial (M) and nuclear (N) fractions were resolved using 10% SDS-PAGE and blotted with antibody to lamin B1 and B2. Lamin B is detected in nuclear fraction but not in cytosolic and mitochondria fractions. **(B)** Histogram shows the density of the bands. Data are expressed as the mean of at least four independent determinations. Blue bar represents the protein expression level per band. Red bar represents the expecting protein expression level per sample, after multiply the histogram mean of the band by the dilution factor between nuclear fraction and other fractions which are (2.5) see section **(2.13.5)**.

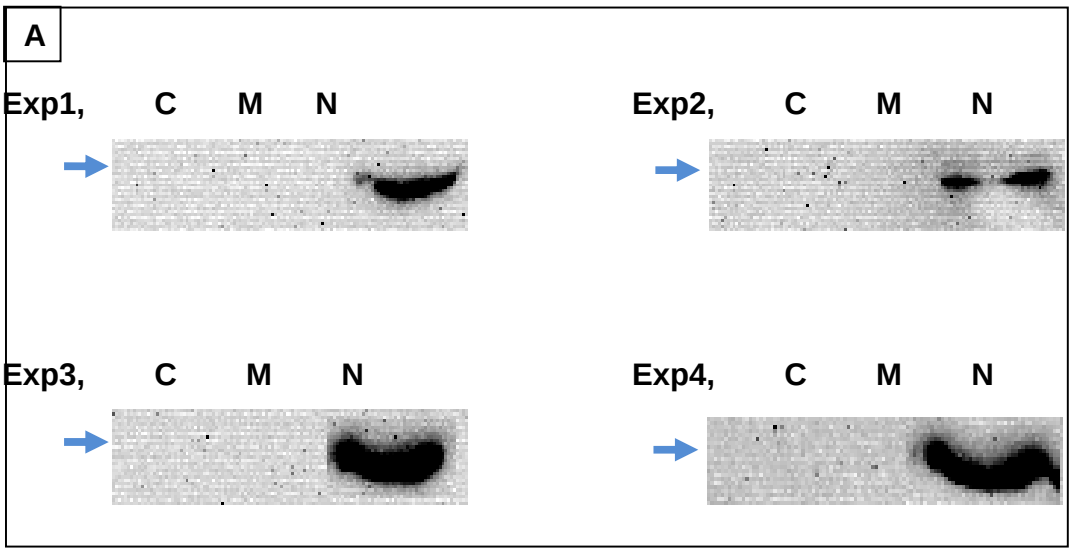
A
Exp1, C M N
Exp2, C M N
Exp3, C M N
Exp4, C M N

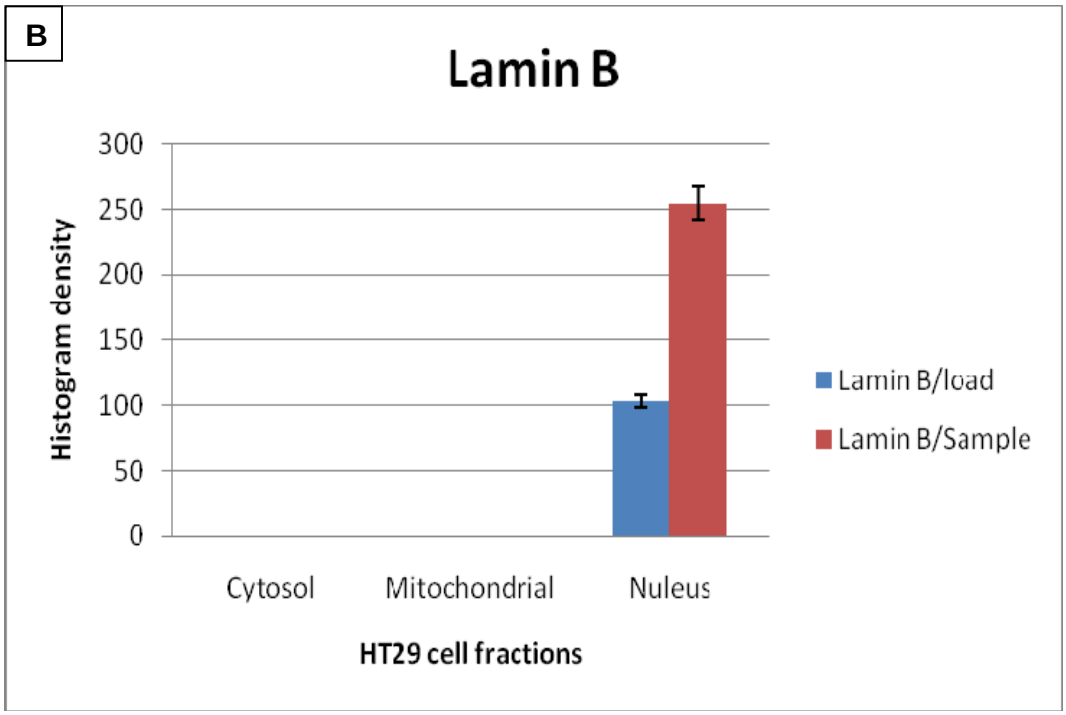
B
Lamin B
300
250
200
150
100
50
0
Histogram density
Cytosol
Mitochondrial
Nuleus
HT29 cell fractions
Lamin B/load
Lamin B/Sample

Figure 4-7

Figure 4.8: Immunopreciptation (IP) of mitochondrial and nuclear fractions.

Experiment # 1: Western blots of immunoprecipitation experiments on cell fractions. Sample 1 and 2 are the mitochondrial extract, samples 3,4 and 5 are nuclear extracts. Samples 2 and 3 were immunoprecipitated with anti-Cox2 antibody. Sample 1 and 4 were immunoprecipitated with serum control. Sample 5 was immunoprecipitated with anti-lamin A/C antibody (Jol2). Immunoprecipitate (IP), supernatant (S).
(A) Samples transferred membrane probed with anti-lamin A/C antibody (Jol2). **(B)** Samples transferred membrane probed with anti-LAP2α antibody. **(C)** Samples transferred membrane probed with anti-Cox2 antibody.

Experiment # 2 & 3: Western blots of immunoprecipitation experiments on mitochondrial fractions of HT29. Sample 1 was immunoprecipitated with serum control. Samples 2 was immunoprecipitated with anti-Cox2 antibody. Immunoprecipitate (IP), supernatant (S).
(D & E) Samples transferred membrane probed with anti-lamin A/C antibody (Jol2). **(F & G)** Samples transferred membrane probed with anti-LAP2α antibody. **(H & I)** Samples transferred membrane probed with anti-Cox2 antibody.

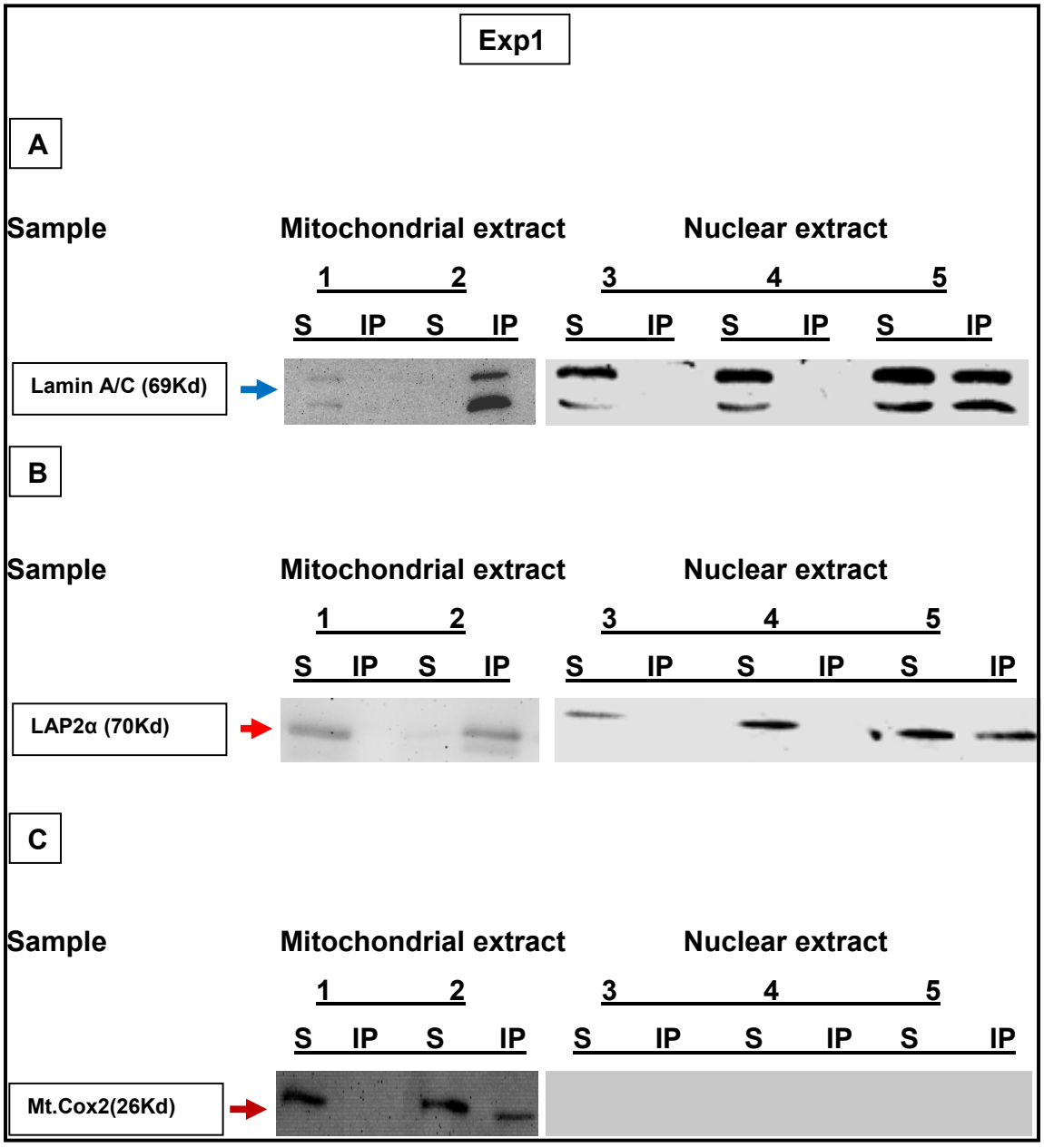
Exp1
A
Sample
Mitochondrial extract
Nuclear extract
1
2
3
4
5
S
IP
S
IP
S
IP
S
IP
S
IP
Lamin A/C (69Kd)
B
Sample
Mitochondrial extract
Nuclear extract
1
2
3
4
5
S
IP
S
IP
S
IP
S
IP
S
IP
LAP2α (70Kd)
C
Sample
Mitochondrial extract
Nuclear extract
1
2
3
4
5
S
IP
S
IP
S
IP
S
IP
S
IP
Mt.Cox2(26Kd)

Figure 4-8

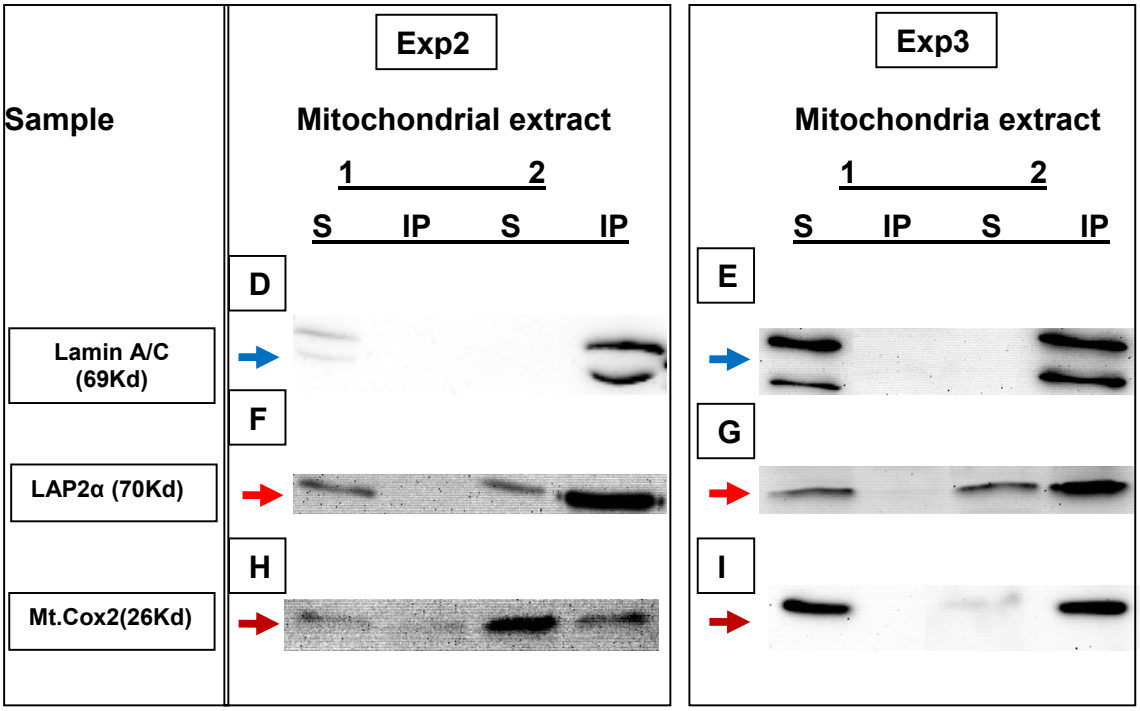
Sample
Exp2
Mitochondrial extract
1
2
S
IP
S
IP
D
Lamin A/C
(69Kd)
F
LAP2α (70Kd)
H
Mt.Cox2(26Kd)
Exp3
Mitochondria extract
1
2
S
IP
S
IP
E
G
I

Figure 4.8

Chapter 5: Localization and functional assay of lamin A/C and LAP2α in mitochondria.

5.1 Introduction:

5.1.1 Cytochrome c Oxidase (Complex IV, COX) structure and function.

Cytochrome c oxidase (COX) which is the terminal enzyme of MRC, it has a unique function in energy metabolism. COX is a heterooligomeric complex of approximately 200 KDa. It is complicated by its dual genetic origin of thirteen subunits (Taanman, 1997) of which the three largest which are Cox1, Cox2 and Cox3 are encoded by mtDNA and form the catalytic core of the enzyme. The remaining ten subunits such as Cox4, Cox5a, and Cox6a are encoded by nuclear DNA and involved in assembly and regulation of the enzyme (Kadenbach *et al.*, 1991). Up to date, mutations in nuclear encoded proteins such as Surf1, Sco1, Sco2, Cox10, Cox15 and LRPPRC have been identified in humans and implicated in the assembly of functional COX (Stiburek *et al.*, 2006). Cox1 is highly hydrophobic protein composed of twelve transmembrane helices extended by short extramembrane loops. It consists Haem a, a3 and Cu_B that coordinates the catalytic site of the enzyme and constitutes the two proton translocation pathways (D- and K-pathway) (Wikstrom, 2000). Cox2 is the smallest enzyme of COX anchored to the inner membrane of mitochondria with an N-terminal α-helical hairpin, whereas it's large C-terminal hydrophilic domain protrudes into the

intermembrane space. Cox2's C-terminal domain is composed of ten stranded β barrel, coordinates the Cu_A center and serves as a docking site for cytochrome c (Capaldi, 1990; Tsukihara *et al.*, 1996). Cox3 is highly hydrophobic protein spanning the inner membrane with seven transmembrane helices (Tsukihara *et al.*, 1996). Investigation in *Rhodobacter sphaeroides aa3*-type implicated Cox3 in maintaining rapid proton uptake through the D-pathway at physiological pH (Gilderson *et al.*, 2003).

The remaining 10 nuclear encoded subunits associated on the surface of the enzyme. Subunits Cox5a, Cox5b and Cox6b are hydrophilic extramembrane proteins, while the rest are hydrophobic proteins, spanning the inner membrane once. The small polypeptides were implicated in the stability/assembly of the holoenzyme (Ludwig *et al.*, 2001). In addition to the constituent proteins, COX contains several metal centers like haeme a, haeme a3, Cu_A and Cu_B implicated in electron transfer (Taanman, 1997). It also contains cofactors like Zn_2, Mg_2, Ca_2 and Na ion (Tsukihara *et al.*, 1996). However, their function and import/insertion pathways remain unknown. The mechanism of coupling of electron transfer with proton translocation toward intermediate space was illustrated (Belevich *et al.*, 2006).

5.1.2 Synthesis and insertion of haeme moieties and copper ions in COX.

The redox centers involved in electron transfer are composed of two haeme (a and a_3) and two copper centers (Cu_A and Cu_B). This metal center has a critical function in COX subunit assembly and catalysis. Defects in the synthesis of the metal center often cause a marked reduction in fully assembled COX subunits. The low-spin haeme a is a six-coordinate haem responsible for transfer of electrons to the a_3-Cu_B centre. The high-spin haeme a_3 is a five-coordinate haeme that forms a heterobimetallic site with Cu_B where the O_2, CO or NO binds (Michel *et al.*, 1998; Brunori *et al.*, 2005). Both metal centers haeme a-a3 are enfolded within the hydrophobic interior of Cox1 (Carr and Winge, 2003). Surf1 is a 30 KDa protein embedded in the mitochondrial inner membrane, composed of two transmembrane domains and central loop region facing the intermembrane space (Yao and Shoubridge, 1999). Recent evidence from *R.sphaeroides* implicates Surf1 protein in inserting haeme a3 into COX (Smith *et al.*, 2005). Copper ions are important in mitochondria for the formation of Cu_A and Cu_B centers associated in MRC and for incorporation of superoxide dismutase (Cobine *et al.*, 2006). The small proteins such as Cox17 and Cox19 were implicated in copper transfer from the cytoplasm to mitochondria. Both of them have a copper binding site and dual localization in cytoplasm and mitochondria which implicated them to act as a copper shuttle (Beers *et al.*, 1997; Nobrega *et al.*, 2002). However, deletion of Cox17 or Cox19 has no affect on the mitochondrial copper level (Cobine *et al.*, 2004; Cobine *et al.*, 2006). Sco protein family was implicated in the formation of COX. Sco protein family composes of two proteins; Sco1 and Sco2. Sco1 is a copper-binding protein member which has the ability to act downstream of Cox17 to deliver Cu_A to Cox2

(Buchwald *et al.*, 1991). Sco2 is a second member of the Sco protein family, also containing a copper-binding domain that are implicated in the delivery of Cu_A to Cox2 (Cobine *et al.*, 2006). COX deficiency was identified in either Sco1 or Sco2 deficient fibroblasts. Over-expression of the mutant Sco proteins in Sco deficient fibroblasts fail to rescue COX deficiency (Horng *et al.*, 2005).

5.1.3 Assembly of COX in mitochondrial inner membrane.

The assembly of the COX holoenzyme is not fully understood. However, there is evidence to show that Cox2 and Cox3 are both required in the assembled holoenzyme COX. This suggests that any pathogenic mutation in these proteins will affect the assembly of COX decrease overall COX activity (Wielburski *et al.*, 1982; Wielburski and Nelson, 1983). The half life of the holoenzyme is thought to be around three days (Leary *et al.*, 2002). Because, of rapid proteolytic degradation is difficult to imagine how the subassemblies of COX are formed. Two studies suggest that insertion of Heme a occurs on unassembled Cox1 or during formation of Cox1, Cox4 and Cox5 (Tsukihara *et al.*, 1996). Recent findings also suggested that insertion of haeme a within Cox1 stabilizes the binding of Cox1 to Cox4-Cox5a heterodimer (Stiburek *et al.*, 2005). Investigations implicated Cox11 in the formation of CuB site in Cox1 (Carr *et al.*, 2002). Formation of the CuA site in Cox2 is believed to be formed before the association of Cox2 with Cox1-Cox4-Cox5a sub-complex (Williams *et al.*, 2004; Stiburek *et al.*, 2005). The maturation step in forming the COX holoenzyme is by forming a covalent bond on Cox1

bridging His240, one of the three histidine ligand of CuB, with conserved Tyr244 located at the end of the proton translocation K-channel (Yoshikawa *et al.*, 1998).

5.1.4 COX in disease.

Cox2 is one of the mitochondrial pro-apoptotic proteins including Apaf-1 and caspase-9 (Mazzanti *et al.*, 2006). A putative interaction between Cox2 and epidermal growth factor receptor (EGFR) was confirmed in biochemical and immunoflurescence experiments. That interaction may play an important role in the regulation of apoptosis, but the exact mechanism of translocation of plasma membrane bound EGFR to mitochondria is not understood (Boerner *et al.*, 2004). EGFR has a critical role in the regulation of cellular processes including cell proliferation, differentiation and survival. It's over expression is associated with oncogenesis and cancer development (Biscardi *et al.*, 2000).

Evidence suggests that mitochondrial dysfunction in Alzheimer disease (AD) is also linked to COX deficiency (Ojaimi and Byrne, 2001). Reduction in COX activity causes an elevation of reactive oxygen species (ROS) and a reduction in ATP production in mitochondria from AD derived cells (Cardoso *et al.*, 2004). Mutation in Surf1 is associated in COX deficient Leigh syndrome, a subacute necrotizing encephalomyopath (Shoubridge, 2001; Pecina *et al.*, 2004). Sco2 mutation is also implicated in COX deficiency and associated with encephalopathy and hypertropic cardiomyopathy (Papadopoulou *et al.*, 1999).

5.2 The aim of this study.

In chapter 3 and 4, the interaction of both Lamin A/C and LAP2α with Cox2 was showed by yeast 2-hybrid screen and confirmed by co-immunoprecipitation. It was also showed that both Lamin A/C and LAP2α are localized in the mitochondria as well as in the nucleus. Alternative methods were necessary to confirm these results. Firstly, quantitative immunogold labeling of lamin A/C, LAP2α and Cox2 in cryo-sections from HT29 colon carcinoma cell line was suggested to investigate co-localization of all three proteins in mitochondria.

Secondly, the cDNA library was generated from colon tissue and used in the yeast 2-hybrid study. Most of the confirmation methods that were used were on the HT29 cells. In this study, the phenomena of localization of lamin A in mitochondria and interaction with Cox2 were selected for further studies. To investigate whether this phenomena is specific to colon or is more general. It was suggested to use quantitative immunogold labeling of lamin A on different cell lines; such as fibroblast, fibrosarcoma and brain cancer.

Thirdly, it was also important to investigate why lamin A/C or LAP2α might interact with Cox2 in mitochondria. In this study, lamin A was selected for further study. Cox2 is the smallest subunit that is encoded by mtDNA and localized in COX. COX deficiency was implicated in neurodegenerative diseases such as Alzheimer (AD). COX deficiency was also associated with ROS production and ATP reduction. Recently, LMNA mutations were also implicated in ROS production and oxidative stress. Increase mitochondrial mass were implicated in mitochondrial myopathy

mice. Increase in mitochondrial mass was associated with reduction in ATP generation and mitochondrial abnormality (Wredenberg *et al.*, 2002). Because of that, different functional assays were suggested such as; ROS production, mitochondrial mass and expression of Cox2. LMNA null cells were compared verses, Lamin B receptor null, Emerin null and fibroblast wild type.

5.3 Results

5.3.1 Immunofluorescence (Confocal).

In previous chapters interactions between lamin A/C to Cox2 have been demonstrated. Co-immunoprecipitation confirmed the putative interaction of lamin A/C and/or LAP2α with Cox2. Western blot identified the expression of lamin A/C and LAP2α in the mitochondrial and in the nuclear fractions but not in the cytosolic fraction. Alternative methods are necessary to confirm this finding. Immunofluorescent (IF) staining was suggested.

HT29 colon cancer cells were grown on cover slips and prepared for IF as described in section **(2.18)**. The analysis showed the localization of lamin A and LAP2α in the nucleus and nothing in the mitochondria or the cytoplasm. However, the analysis showed the localization of Cox2 in mitochondria alone. When compare this result with biochemicals, it has different explanations, it may the fixation and permeabilization steps need more modification or the antibody cannot enter the

mitochondria inner membrane and matrix. However, the case in Cox2 is different, because the C-terminus is more accessible and localizes at the intermediate space. So, an alternative quantitative immunogold staining was suggested to confirm the biochemical's finding.

5.3.2 Immunogold staining.

5.3.2.1 Lamin A/C.

HT29 colon cancer cells were fixed and prepared for transmission electron microscopy (TEM). To investigate the specificity of the immunogold particles that distributed in mitochondria for lamin A, cryo-sections were stained with a range of lamin A antibodies from different sources. All of them identify lamin A (C-terminal). Jol2 recognizes the same epitope of lamin A/C corresponding to amino acid 464-572 and raised in mouse **(Table 5.1)**. Two of which recognize the same epitope of lamin A corresponding to amino acid residues 598-611, but one of them is raised in rabbit and the second one is raised in mouse **(Table 5.1)**. The forth one recognizes the epitope of lamin A corresponding to amino acid 636-650 and raised in mouse **(Table 5.1)**. The primary antibodies were followed by secondary antibodies as described in section **2.14.** Analysis of at least thirty TEM images **(**section **2.15)** shows a distribution of gold particles in both mitochondria and the nucleus for all anti-lamin A antibodies used in this study **(Figure 5.1, 5.2 & 5.3)** except Jol2 didn't show gold particles in mitochondria but showed in the NE (data

not show). This has one explanation which is the epitope that Jol2 recognizes is not accessible in mitochondria as in the nucleus.

From the previous experiments above, all antibodies that worked gave similar results. However, rabbit-anti lamin A antibody was more efficient. Because of that this antibody was used in further experiments. The phenomena of localization of lamin A/C in mitochondria and its putative interaction with Cox2 were examined in colon tissue. To investigate whether this phenomena is specific for colon or it is general. Cryo-sections of normal human fibroblast cells (NHF), fibro sarcoma cells (US913T) and brain cancer cells (U373) were prepared and stained with rabbit anti-lamin A antibody. At least thirty images of each cell line were analyzed. In each cell line lamin A was detected in mitochondria and nuclei but not in the cytosol **(Figures 5.4, 5.5 & 5.6)**. As a negative control sections were probed with secondary antibodies alone. No gold particles were detected under these conditions **(Appendix V)**.

As a further control for specificity to show that the antibody used in this study did not cross-react with unknown proteins in mitochondria which contain of the same epitope recognized by anti-lamin A/C. Lamin $A/C^{-/-}$ fibroblast were investigated (Muchir *et al.*, 2003). Cryo-sections were prepared and probed with rabbit anti-lamin A antibody as described in section **2.14.** At least thirty images were analyzed. The results showed an absence of gold particles in mitochondria, nuclei and cytosol **(Figures 5.7)**. This result suggested that the localization of anti-lamin A antibody specifically detected lamin A in mitochondria.

5.3.2.2 LAP2α.

In previous chapters, similar to lamin A/C, it has shown that LAP2α interacts with Cox2 and is also localized in mitochondria as well as the nucleus as determined by western blots.

HT29 cryo-sections were prepared and stained with rabbit anti-LAP2α antibody as before**.** Analysis of thirty TEM images showed that LAP2α was detected in the cytosol, mitochondria and nucleus. The staining of the mitochondria was more intense than in both the nucleus and the cytoplasm **(Figure 5.8).** This is could be because the gold particles were counted per um^2 where the surface area of both nucleus and cytoplasm are much more compared to mitochondrial surface area. Whereas the image showed part of these cell compartments. Localization of LAP2α in cytoplasm could be a background or a third place of localization**.**

5.3.2.3 Cox2.

The western blots of cell fractions showed the expression of Cox2 in the mitochondrial fraction only. To confirm this finding cryo-section of HT29 were prepared and probed with mouse anti-Cox2 antibody. At least thirty TEM images showed that Cox2 was only detected in mitochondria **(Figure 5.9)**.

5.3.2.4 B-type lamins.

A long time ago, it was found that B-type lamins are specifically associated with inner nuclear membrane proteins and implicated in forming lamina structure. Last chapter, it was shown by using immunoblotting that B-type lamins are only expressed in the nuclear fraction. As an additional control mouse anti-lamin B antibody that recognizes lamin B2 was used to probe HT29 cryo-sections. TEM images showed that lamin B is only detected in the nucleus **(Figure 5.10)**. However, the labeling was all over the nucleus which is unexpected.

5.3.2.5 Co-localization and conclusion.

TEM double labeling was suggested for further investigations. Cryo-sections of HT29 were subjected to double labeling with rabbit anti-lamin A antibody and mouse anti-Cox2 antibody. Three different cell pellets were fixed, embedded and sectioned. Then two groups of sections were probed by primary antibodies. Group 1 was using 10nm and 20nm of gold particles to determine lamin A and Cox2 respectively (**Figure 5.11.1).** Group 2 was using 20nm and 10nm of gold particles to determine lamin A and Cox2 respectively **(Figure 5.11.2).** Analysis of images on both groups demonstrated the distribution and localization of lamin A and Cox2 in mitochondria and lamin A alone in the nucleus.

Table 5.1: The selected antibodies were used in TEM.

Primary Antibodies	Target	hype	Reference	Catalog #	EM
M-Lamin A/C	Lamin A/C	Mouse-M	In house	In house	1:10
R-Lamin A	Lamin A	Rabbit-R	Sigma	L1293	1:600
M-Lamin A	Lamin A	Mouse-M	Santa Cruz	Sc-7292	1:10
M-Lamin A	Lamin A	Mouse-M	Novus	NB 100-674	1:5
R-LAP2α	LAP2α	Rabbit-R	ImmuQuest	IQ175	1:300
Mt.COX2	Cytochrom C Oxidase	Mouse- M	Invitrogen	A6404	1:50
Lamin B2 (LN43)	B2	Mouse-M	Abcam	Ab8983	1:50
Secondary Antibodies	Target	Type	Reference	-	EM
Goat anti-mouse IgG	Mouse primary antibodies	Gold 5, 10 or 20 nm	British Biocell International	-	1:20
Goat anti-Rabbit IgG	Rabbit primary antibodies	Gold 5, 10 or 20 nm	British Biocell International	-	1:20

5.3.3 ROS production and measurement.

Further investigations were carried out to determine if lamin A has a role in mitochondrial function. As explained in the introduction above, Cox2 is a mtDNA encoded protein that is a component of COX. COX deficiency was implicated in different diseases. COX was also associated with ROS production and ATP reduction. Recent studies implicated LMNA mutations in ROS productions and oxidative stress (Caron *et al.*, 2007). Because of this the link between ROS production in LMNA mutants with the localization of lamin A in mitochondria was investigated. Five different cell lines were used; NHF, Lamin A/C$^{-/-}$, LBR$^{-/+}$, LBR$^{-/-}$ and emerin$^{-/-}$. LBR and emerin are nuclear integral membrane proteins (Ye and Worman, 1994; Clements *et al.*, 2000). They have been implicated in anchoring

lamina to the NE (Duband-Goulet *et al.*, 1998; Haraguchi *et al.*, 2000). Whereas, different studies showed that emerin null cell lines were implicated in miss-localization of lamin A into the NE (Capanni *et al.*, 2009). So, if the ROS are detected in these entire cell lines, this will implicate the miss-localization of A-type lamin in NE with regulating specific genes that are involved in ROS production. However, if the ROS level is not detected in these entire cell lines but is only detected in lamin null cells, this may illustrate the role of lamin A in mitochondria. For instant, it may implicate lamin A in the mitochondrial inner membrane structure or in assembling a particular protein in the MRC.

Next the levels of ROS were evaluated by measuring the oxidation status of permeant derivative CM-H_2DCFDA in these cell lines as described in section **2.16**. The experiments were repeated at least three times. The median of the FL1 green fluorescence of wild-type was made 100% as basal level. Then the median of each cell lines including the controls were calculated based on that. Lamin $A^{-/-}$ cells showed 10 times fold induction of ROS. LBR mutant cells showed 25-35% induction of ROS. Whereas emerin null cell doesn't produce ROS **(Figure 5.12)**. As there is no significant increase of ROS in any of nuclear protein mutant cell lines except in Lamin $A^{-/-}$ cells. This result may implicate lamin A directly in mitochondrial function.

5.3.4 Does Lamin A/C regulate Cox2 gene expression?

The question remains as to how lamin A/C is involved in ROS production. One study showed striking decrease in the expression of Cox2 in fibroblasts with LMNA mutations. This study was also able to observe low expression in Cox2 in adipose tissue sample (Caron *et al.*, 2007). It was thought that Lamin A/C may regulate Cox2 gene expression. Thus, western blots were used to quantify the expression level of Cox2 in NHF, emerin$^{-/-}$, LBR$^{-/+}$, LBR$^{-/-}$ and Lamin A/C$^{-/-}$ cell lines. Total cell extracts were resolved using 10 or 12 % one dimensional SDS-PAGE and probed with anti-lamin A/C, β-actin and Cox2 antibodies as described in sections **2.13.1-2.13.5**. The blots showed the expression of Cox2 was even in all of the cell lines that were used, the blots were normalized using β-actin. This result illustrate that lamin A/C doesn't regulate the expression of Cox2 **(Figure 5.13)**. However, the presence of lamin A/C in mitochondria may have an important role in the assembly of Cox2 into the COX holoenzyme.

5.3.5 Mitochondria mass measurement.

Mitochondrial mass was implicated in mitochondrial abnormality and associated with reduction in ATP generation. It was also implicated in myopathy disease (Wredenberg *et al.*, 2002). To answer the question of how lamin A/C is involved in ROS production, a second suggestion was to measure mitochondria mass in NHF, emerin$^{-/-}$, LBR$^{-/+}$, LBR$^{-/-}$ and Lamin A/C$^{-/-}$ cell lines. To monitor the mitochondrial mass of specific cells, fluorescent dye 10-*n*-nonyl-acridine orange (NAO) was

used. This dye binds specifically to the negatively charged cardiolipin (diphosphatidylglycerol) in the mitochondrial inner membrane independently of the membrane potential. Cell lines were stained by NAO as described in section **(2.17).** This experiment was repeated at least three times. Then the median of FL1 of wild-type was made 100% as a basal level. The median of all cell lines were calculated base on that**.** The chart showed that mitochondrial mass was even between the entire cells lines used in this study under these conditions **(Figure 5.14).** The conclusion is: first Lamin A/C has no effect on the mitochondria mass. Second the increase of ROS in lamin null cell lines was not because of change in mitochondria mass between the cell lines that used in this study under this condition.

5.4 Discussion.

The previous chapters have suggested that Cox2 protein putatively interacts with Lamin A/C and LAP2α. This was shown in yeast 2-hybrid studies and confirmed by co-immunoprecipitation. It was also demonstrated that Lamin A/C and LAP2α are found in the mitochondria as well as the nucleus but never seen in the cytosol. Cox2 is localized only in the mitochondria.

The localization of lamin A/C and LAP2α in mitochondria as well as the nucleus was also demonstrated by an alternative method. HT29 cryo-sections and TEM images showed the localization of lamin A/C in the matrix of mitochondria and the nuclear envelope. This finding was confirmed using three different antibodies against lamin A/C. All of them showed significant labeling of lamin A/C in the matrix

of mitochondria. These TEM images support my finding in the previous chapters that lamin A/C is located in both the mitochondria and nucleus.

To demonstrate that the anti-lamin A antibody did not cross react to other protein localized in the mitochondria. Lamin $A/C^{-/-}$ fibroblasts were used to prepare cryo-sections. All images showed that there is no lamin A gold particles in these sections.

HT29 cryo-sections were also prepared for immunogold labeling with antibodies to LAP2α and Cox2. Again, as it was suggested in western blots, LAP2α is distributed in mitochondria and the nucleus but not in the cytosol. However, the cryo-sections that were stained with anti-Cox2 didn't show significant labeling in the nucleus or cytosol but was significant in mitochondria. This result illustrated that LAP2α is presented everywhere inside the cell including mitochondria. Whereas, Cox2 is localized only in mitochondria.

It was confirmed that B-type lamins are associated in the lamina structure at NE. To investigate if lamina-like structure may form in the mitochondria, western blots, cryo-sections of HT29 were suggested by probing with anti-lamin B antibody. There was no lamin B expression in either cytosol or mitochondria. Moreover, there was no significant gold labeling in either mitochondria or cytosol. The labeling was all over the nucleus which is unexpected. However this result confirms there is no lamina-like structure at mitochondria and supports that the fractions were used were cleared of cross contamination.

The initial investigation in this study was performed using a cDNA library generated from normal human colon tissue and all of the confirmation experiments were performed on a single colon cancer derived cell line (HT29). Therefore, I need to investigate the possibility that this phenomenon is peculiar to colon cell. To answer this question, TEM experiments were performed on a range cell lines from different tissue. The cell lines used were normal human fibroblast (NHF), Fibro sarcoma (US913T) and brain cancer (U373). The data shows that lamin A/C is distributed in mitochondria as well as the nucleus in all cell types, indicating that this is a general property of lamin A/C.

To demonstrate that lamin A/C has a functional role in mitochondria, ROS production was measured in different cell lines. ROS was significantly elevated in Lamin A/C$^{-/-}$ cell lines compared to other cell lines used in this study. This result demonstrates the link between the localization of lamin A/C in mitochondria with ROS production.

The question as to how lamin A/C is involved in ROS production was addressed next. One suggestion was that Lamin A/C regulates Cox2 protein levels (Caron *et al.*, 2007). Western blots of NHF, emerin$^{-/-}$, LBR$^{-/+}$, LBR$^{-/-}$ and Lamin A/C$^{-/-}$ cell lines showed even in the expression levels of Cox2 protein. This result illustrate that lamin A/C doesn't regulate the expression of Cox2.

A second possibility is that lamin A/C is involved in mitochondria division. Alteration in mitochondrial mass was implicated in different diseases (PD), mitochondrial abnormality and reduction of ATP generation (Wredenberg *et al.*, 2002).

Measurement of mitochondrial mass on NHF, emerin$^{-/-}$, LBR$^{-/+}$, LBR$^{-/-}$ and Lamin A/C$^{-/-}$ cell lines was suggested. The results showed no difference in mitochondrial mass resulting from loss of expression of lamin A/C or other NE proteins.

In summary these results indicate that lamin A/C and LAP2α are localized in the mitochondria and in the nuclei. The localization of A-type lamins in mitochondria may implicate in regulating ROS production. From the experiments above A-type lamins do not regulate the expression of Cox2 or affect mitochondrial mass. This may illustrate that A-type lamins have critical role in assembling Cox2 protein to the holoenzyme structure of COX.

The localization and interaction of A-type lamins and LAP2α with Cox2 at mitochondria requires more experiments to be done. First, by generating different domain of GFP-Lamins or GFP-LAP2α constructs and transforms them in lamin A/C null or LAP2α null cell lines respectively. This will allow us to study the localization of these proteins in mitochondria. Secondly, in vitro overlay assay from those constructs may help us to define the binding entire domain on each of which to Cox2 recombinant protein.

5.5 Figures.

Figure 5-1: Immunogold labelling of HT29 cell lines using Rabbit anti-Lamin A antibody (Sigma).

HT29 were fixed, embedded and sectioned. Sections were prepared from at least three different blocks. The distribution of gold particles between cytosol, mitochondria and nuclei was quantified. At least ten images per cell compartments were analyzed. The average of the gold particles was divided by the average of the surface area. The density of gold labeling was evaluated by calculating the gold particles/um^2.

A, B, and C represent selected images from each cell pellet. Red and blue arrows represent gold labeling of the nucleus and mitochondria respectively. Secondary antibody alone was used as a negative control image in **(Appendix V)**.

D. Bar chart representing the value of the density of gold labeling expressed in the cytosol, mitochondria and nuclear envelope (NE), as the mean $\pm$ SD (n= 30 images, 10 images of each cell pellet). Significance was calculated using the Student *t*-test. $P < 0.005$. Comparing mitochondria or nucleus to cytosol.

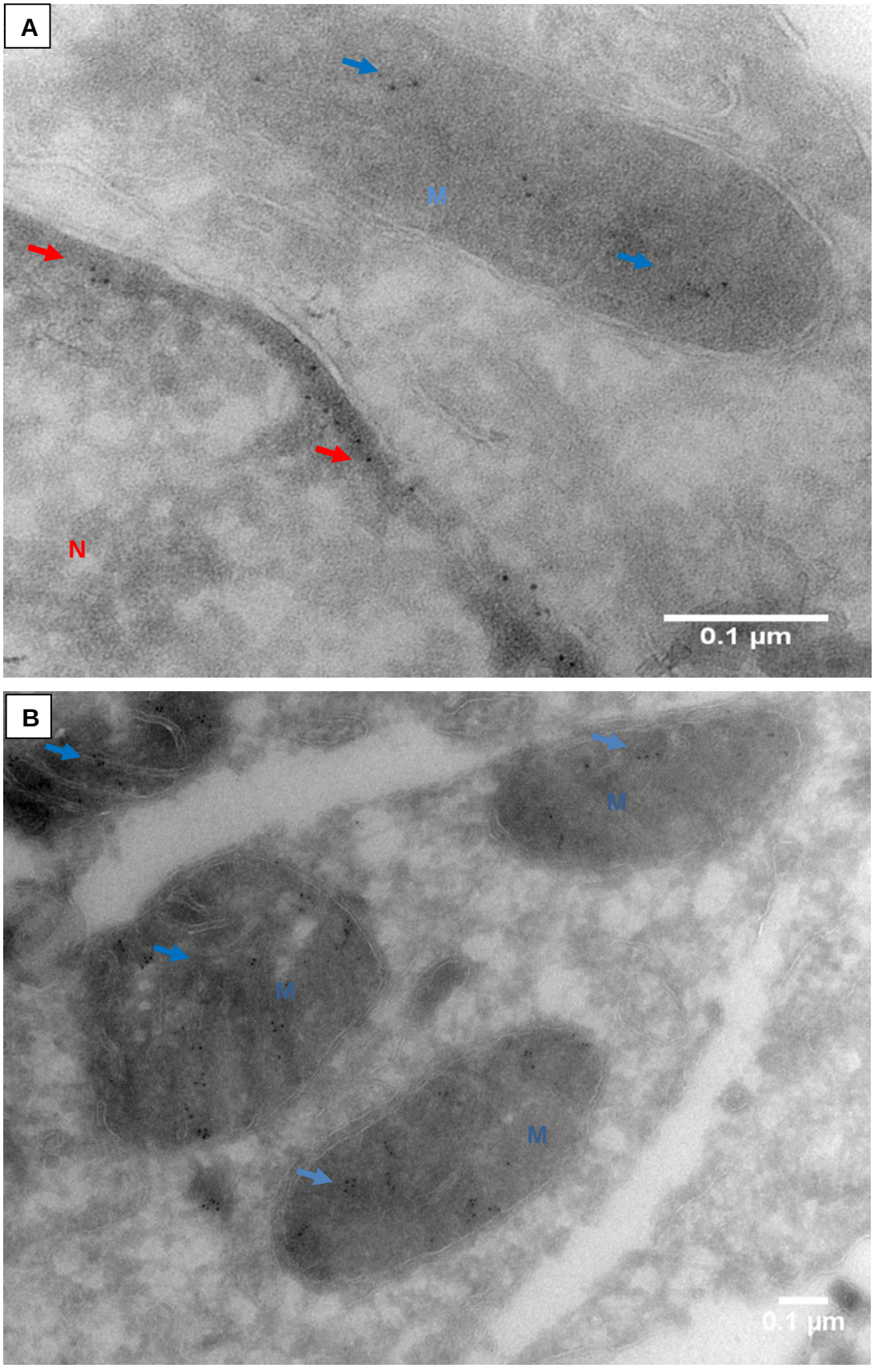
A
M
N
0.1 μm
B
M
M
M
0.1 μm

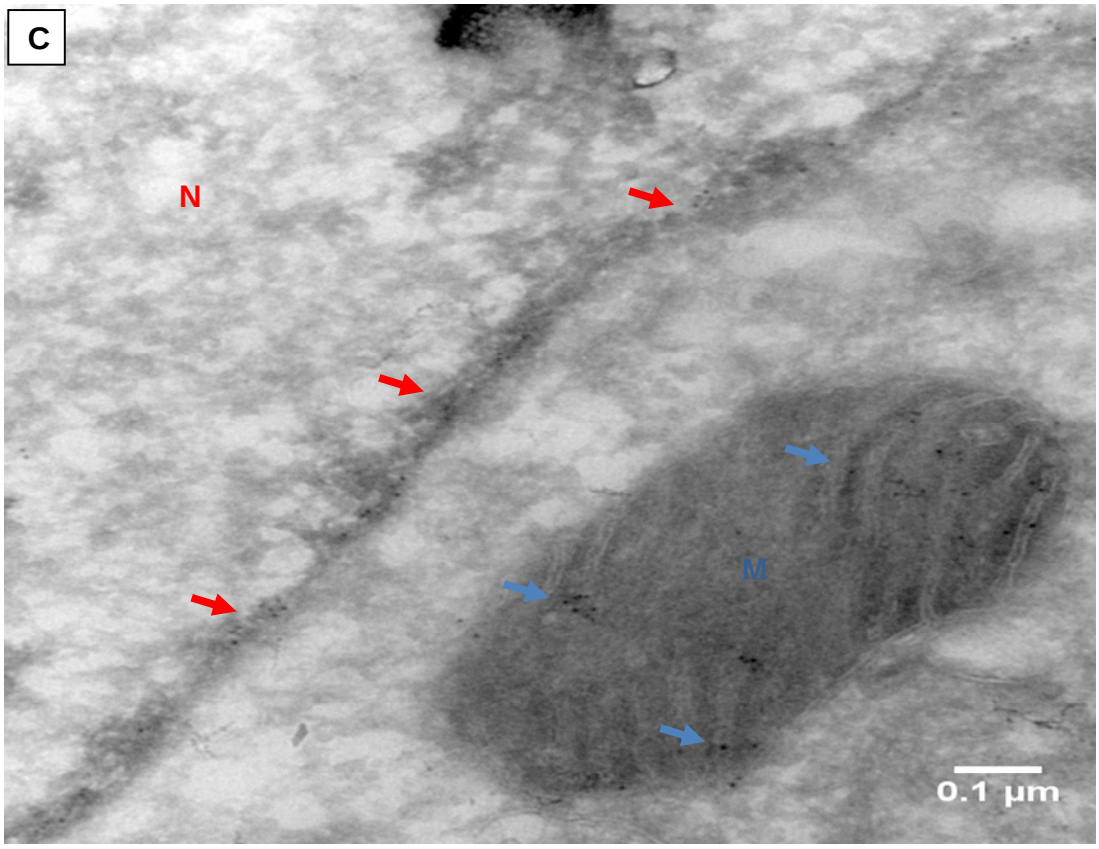
C
N
M
0.1 µm

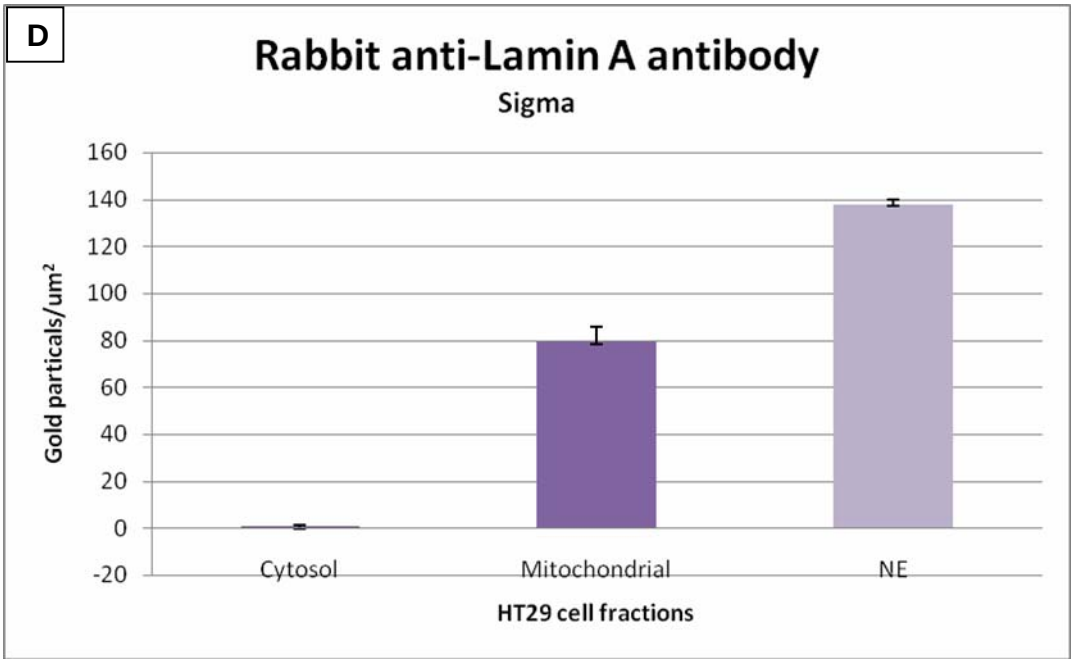
D
Rabbit anti-Lamin A antibody
Sigma
Gold particals/um²
160
140
120
100
80
60
40
20
0
-20
Cytosol
Mitochondrial
NE
HT29 cell fractions

Figure 5-1

Figure 5-2: Immunogold labelling of HT29 cell lines using mouse anti-Lamin A/C antibody (Santa Cruz Biotechnology, INC.).

HT29 were fixed, embedded and sectioned. Sections were prepared from at least three different blocks. The distribution of gold particles between cytosol, mitochondria and nuclei was quantified. At least ten images per cell compartments were analyzed. The average of the gold particles was divided by the average of the surface area. The density of gold labeling was evaluated by calculating the gold particles/um^2.

A, B, and C represent selected images from each cell pellet. Red and blue arrows represent gold labeling of the nucleus and mitochondria respectively. Secondary antibody alone was used as a negative control image in **(Appendix V)**.

D. Bar chart representing the value of the density of gold labeling expressed in the cytosol, mitochondria and nuclear envelope (NE), as the mean $\pm$ SD (n= 30 images, 10 images of each cell pellet). Significance was calculated using the Student *t*-test. $P < 0.005$. Comparing mitochondria or nucleus to cytosol.

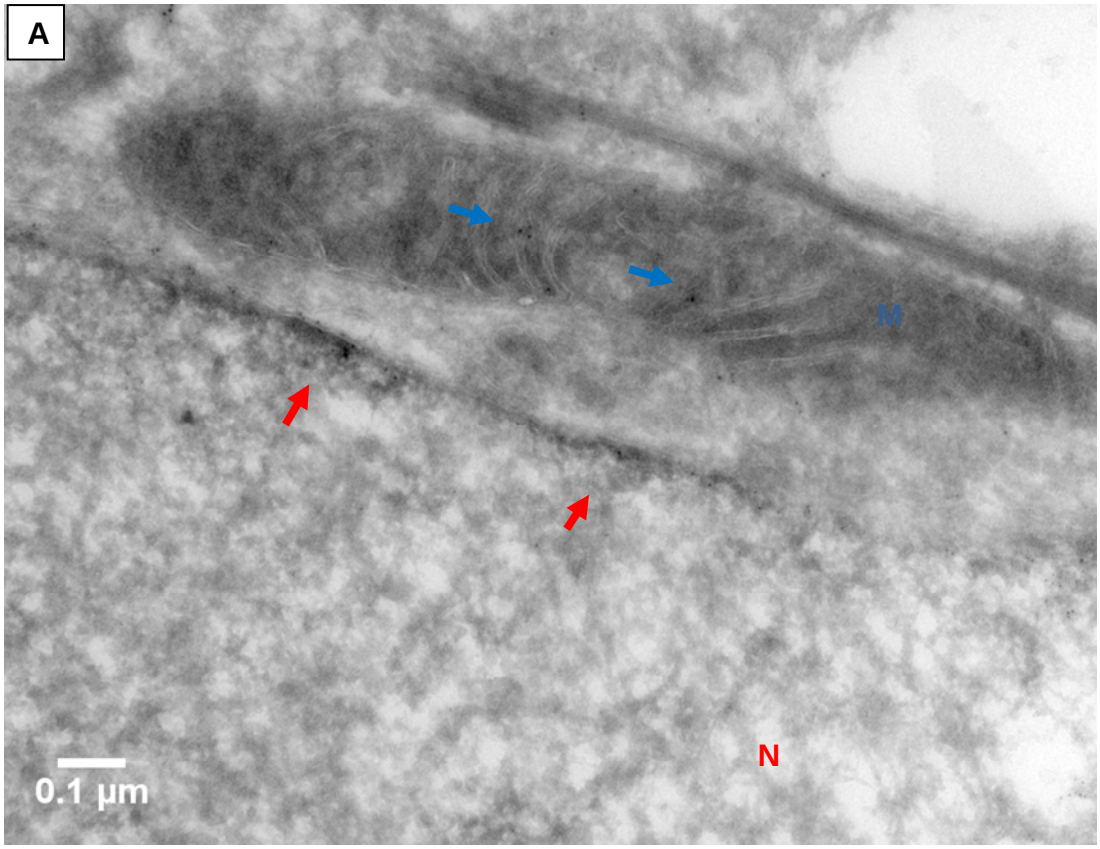
A
M
N
0.1 μm

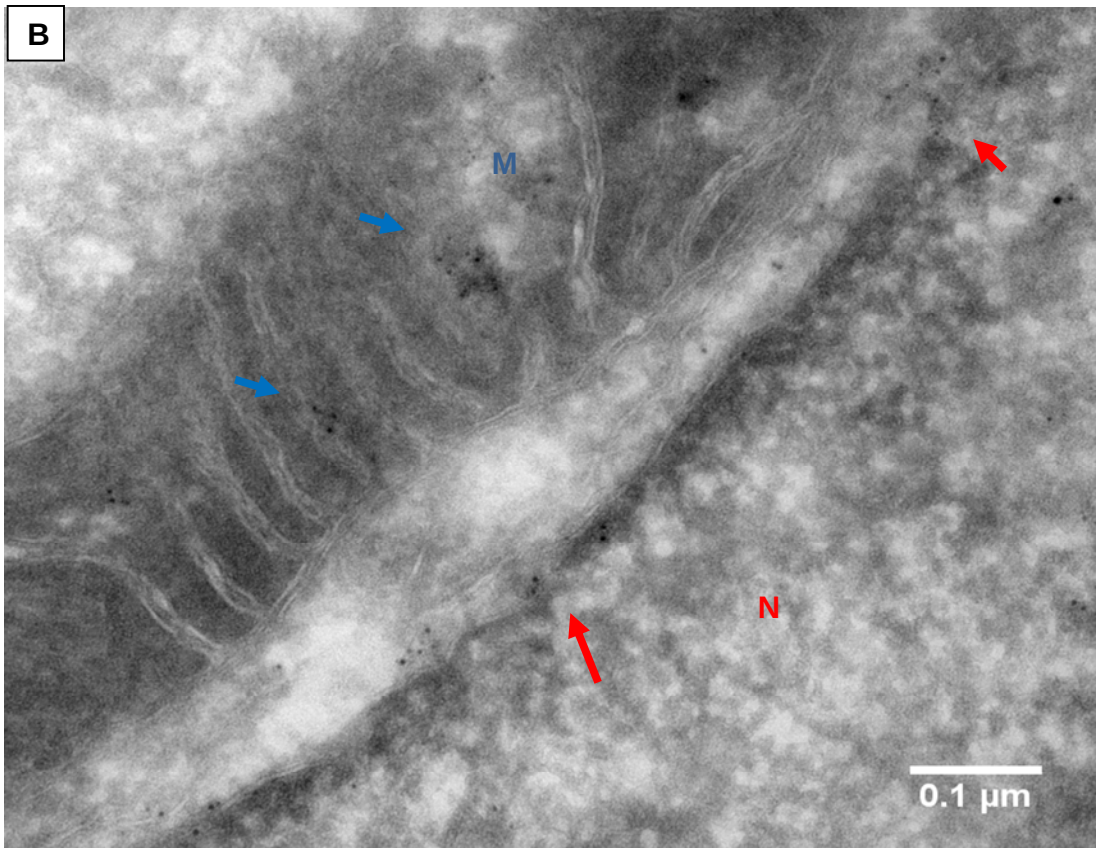
B
M
N
0.1 μm

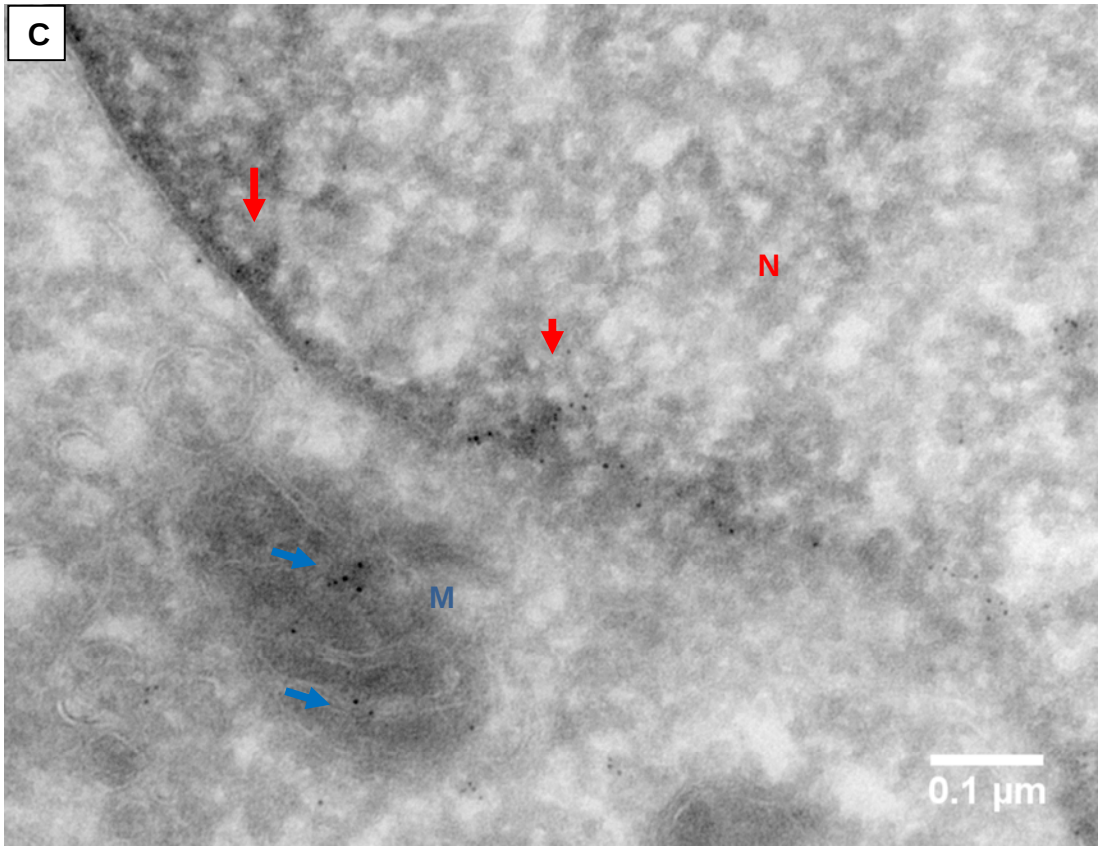
C
N
M
0.1 µm

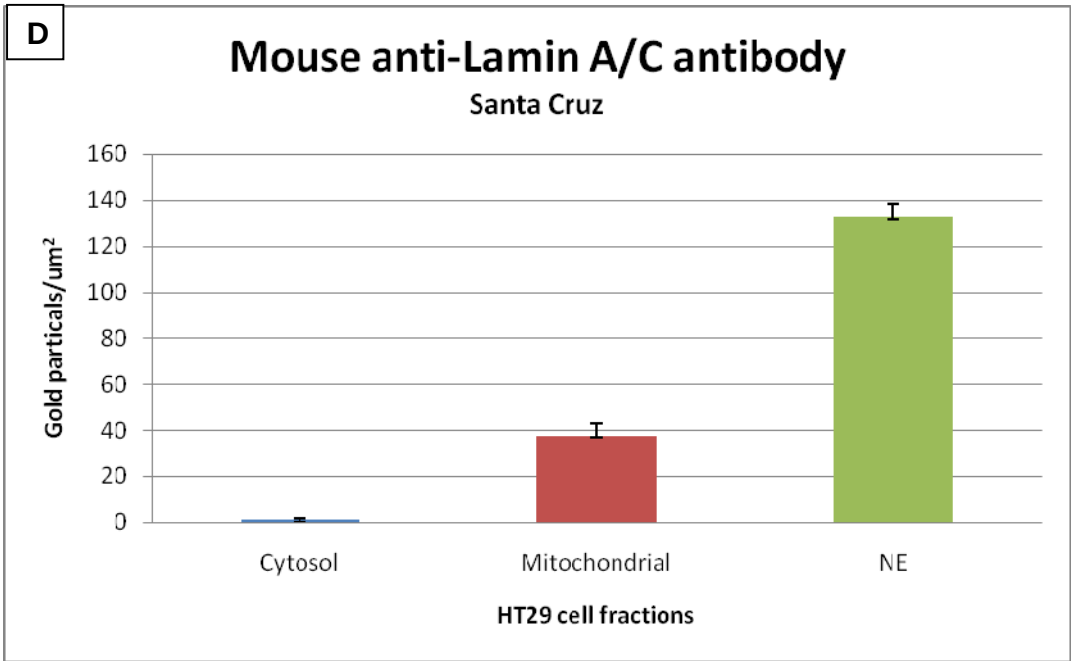
D
Mouse anti-Lamin A/C antibody
Santa Cruz
Gold particals/um²
160
140
120
100
80
60
40
20
0
Cytosol
Mitochondrial
NE
HT29 cell fractions

Figure 5-2

Figure 5-3: Immunogold labelling of HT29 cell lines using mouse anti-Lamin A antibody (Novus Biologicals).

HT29 were fixed, embedded and sectioned. Sections were prepared from at least three different blocks. The distribution of gold particles between cytosol, mitochondria and nuclei was quantified. At least ten images per cell compartments were analyzed. The average of the gold particles was divided by the average of the surface area. The density of gold labeling was evaluated by calculating the gold particles/um^2.

A, B, and C represent selected images from each cell pellet. Red and blue arrows represent gold labeling of the nucleus and mitochondria respectively. Secondary antibody alone was used as a negative control image in **(Appendix V)**.

D. Bar chart representing the value of the density of gold labeling expressed in the cytosol, mitochondria and nuclear envelope (NE), as the mean $\pm$ SD (n= 30 images, 10 images of each cell pellet). Significance was calculated using the Student *t*-test. $P < 0.005$. Comparing mitochondria or nucleus to cytosol.

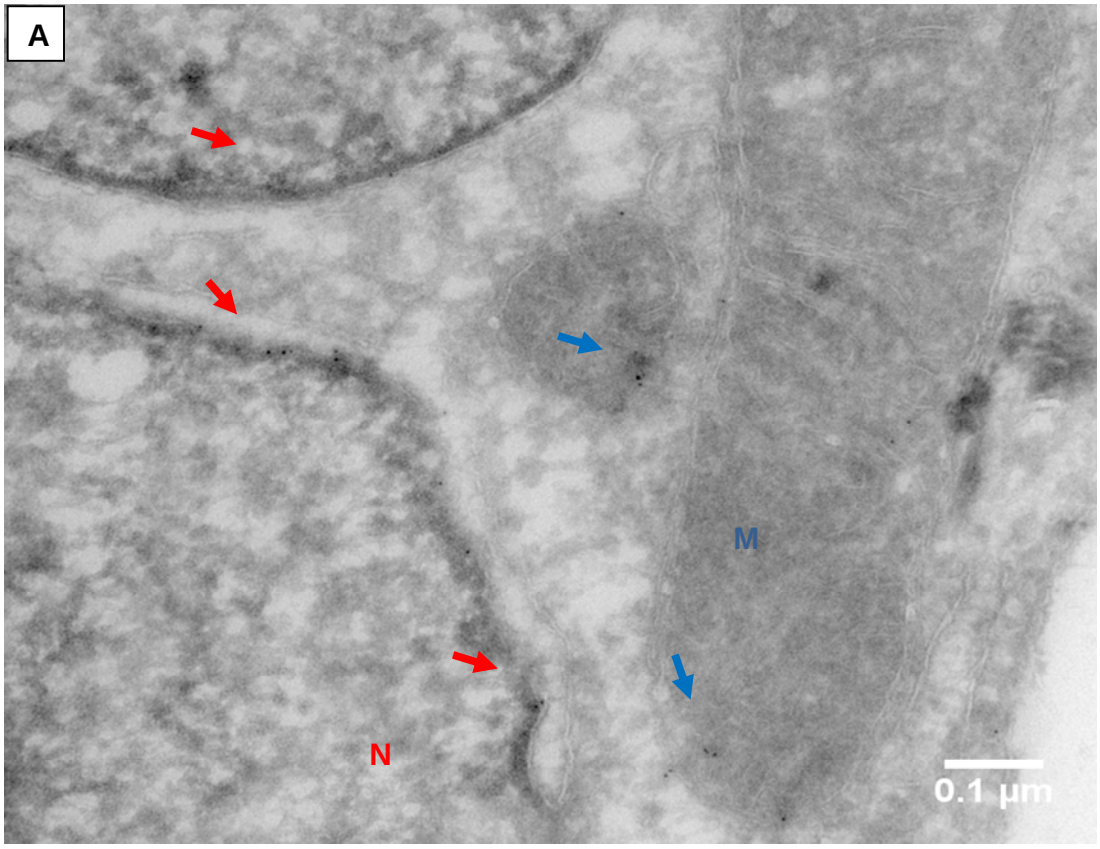
A
M
N
0.1 µm

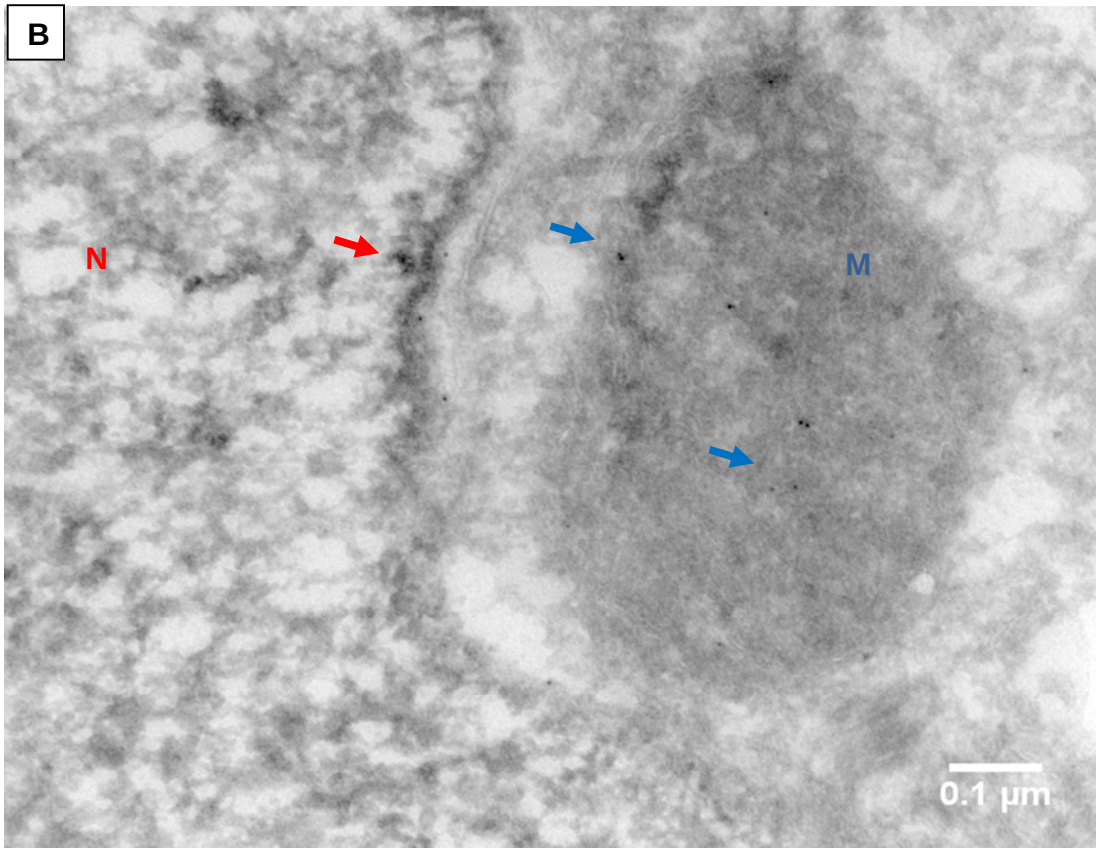
B
N
M
0.1 µm

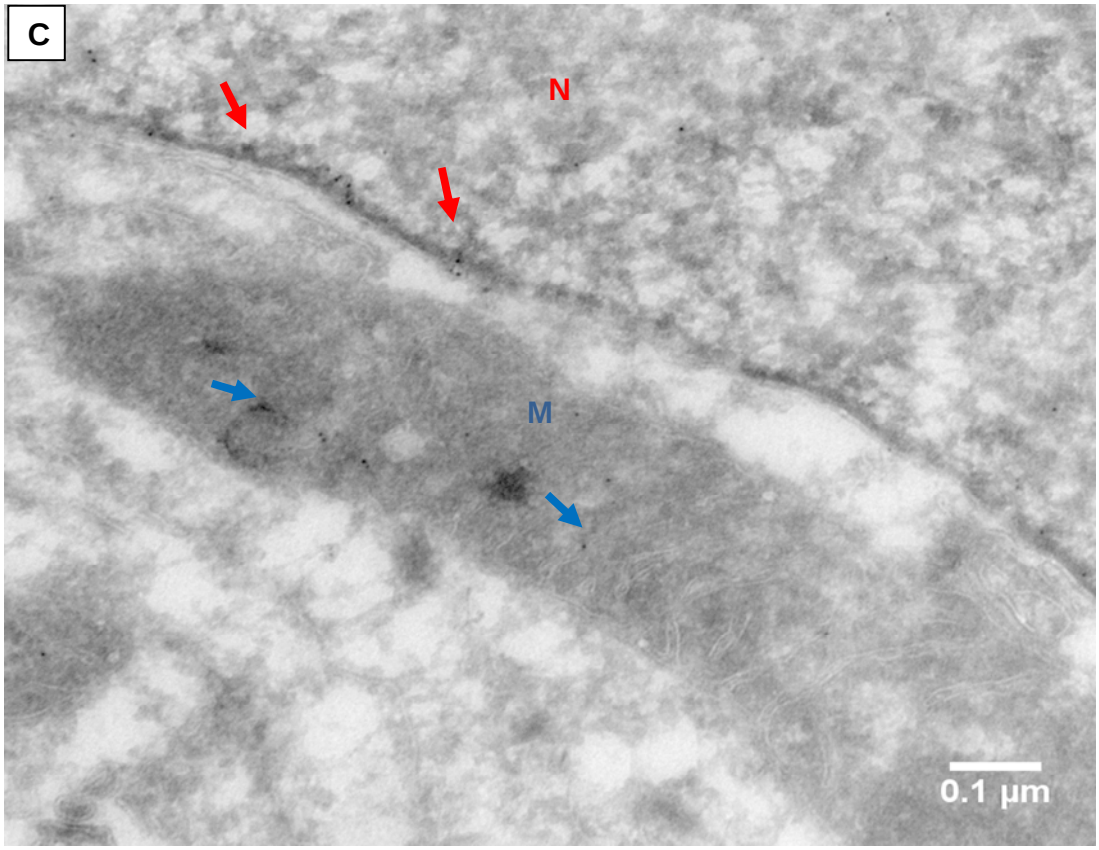
C
N
M
0.1 µm

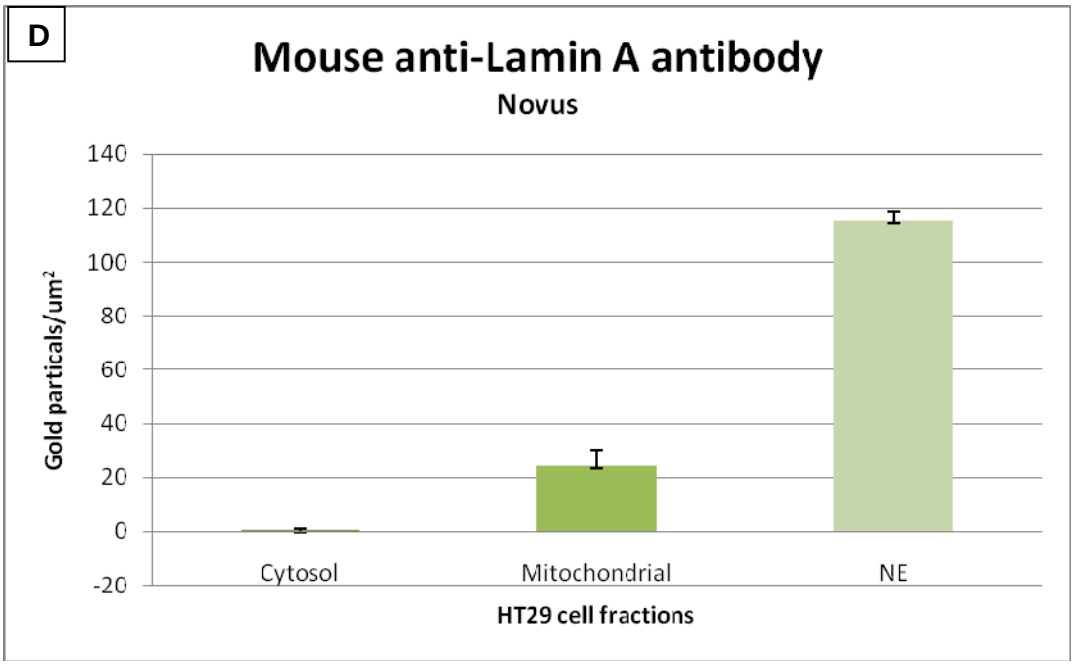
D
Mouse anti-Lamin A antibody
Novus
Gold particals/um²
140
120
100
80
60
40
20
0
-20
Cytosol
Mitochondrial
NE
HT29 cell fractions

Figure 5-3

Figure 5-4: Immunogold labelling of Normal Human Fibroblast cell lines using Rabbit anti-Lamin A antibody.

NHF were fixed, embedded and sectioned. Sections were prepared from at least three different blocks. The distribution of gold particles between cytosol, mitochondria and nuclei was quantified. At least ten images per cell compartments were analyzed. The average of the gold particles was divided by the average of the surface area. The density of gold labeling was evaluated by calculating the gold particles/um^2.

A, B, and C represent selected images from each cell pellet. Red, dark orange and blue arrows represent gold labeling of the nucleus, cytosol and mitochondria respectively. Secondary antibody alone was used as a negative control image in **(Appendix V)**.

D. Bar chart representing the value of the density of gold labeling expressed in the cytosol, mitochondria and nuclear envelope (NE), as the mean $\pm$ SD (n= 30 images, 10 images of each cell pellet). Significance was calculated using the Student *t*-test. $P < 0.005$. Comparing mitochondria or nucleus to cytosol.

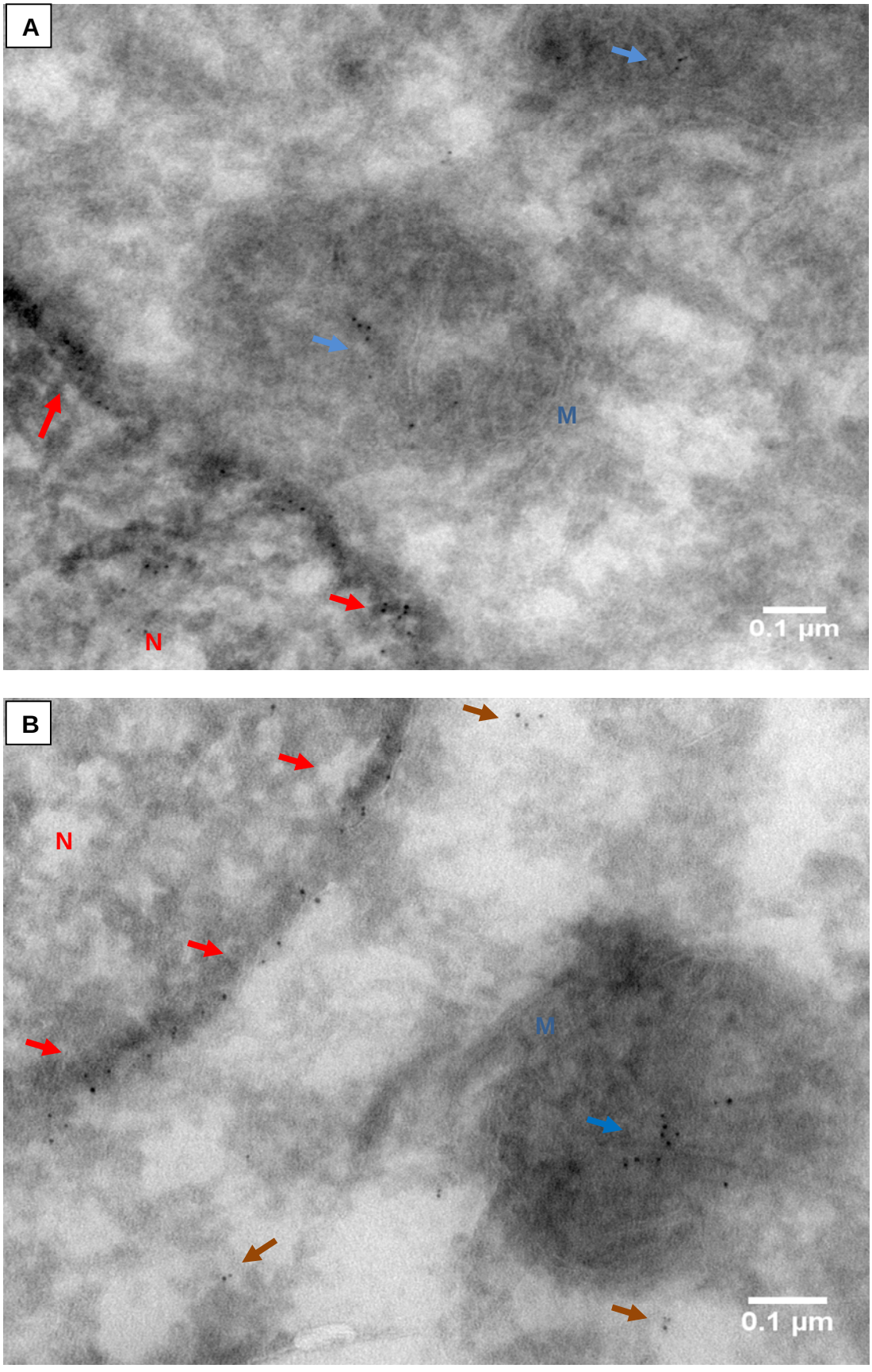
A
M
N
0.1 μm
B
N
M
0.1 μm

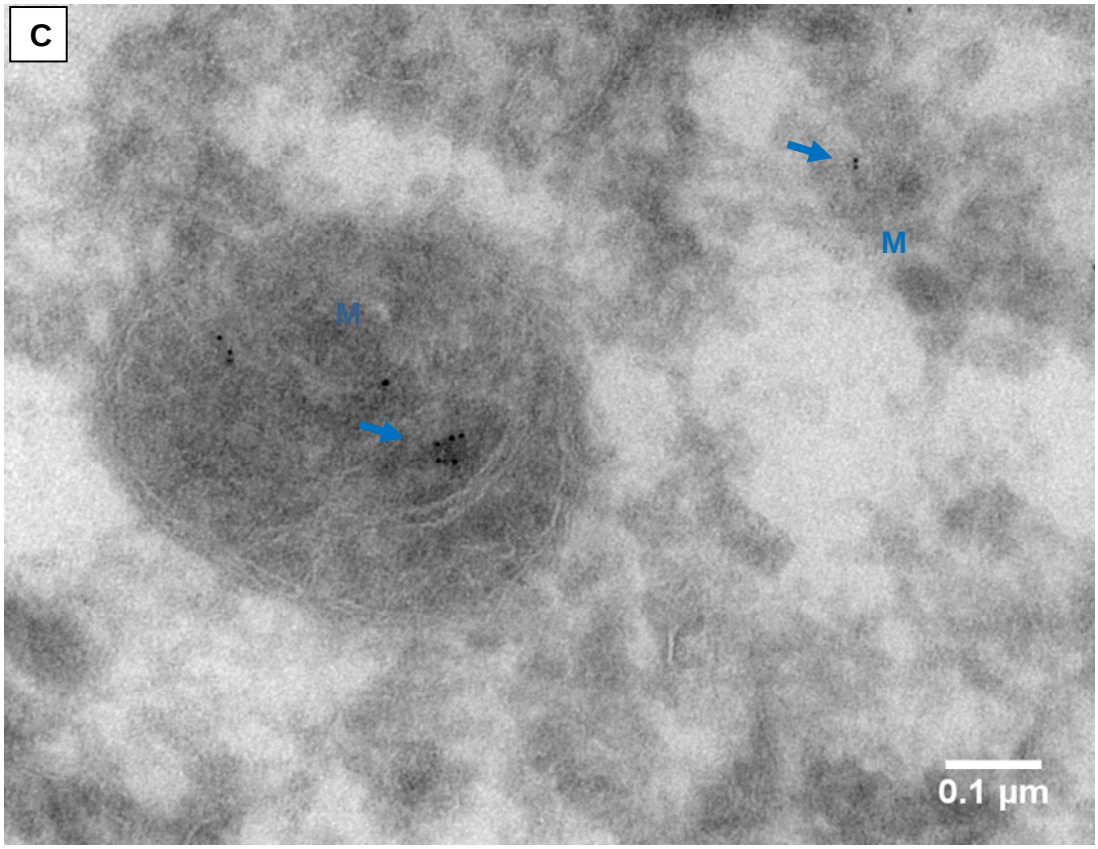
C
M
M
0.1 µm

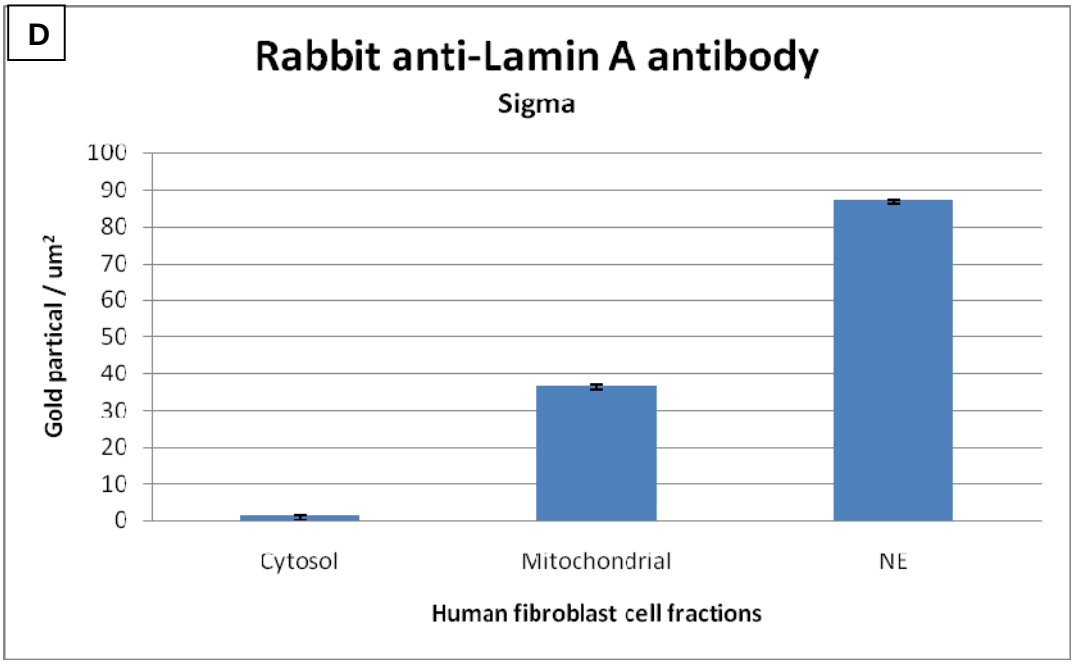
D
Rabbit anti-Lamin A antibody
Sigma
Gold partical / um²
100
90
80
70
60
50
40
30
20
10
0
Cytosol
Mitochondrial
NE
Human fibroblast cell fractions

Figure 5-4

Figure 5-5: Immunogold labelling of Human Fibro-sarcoma (US913T) cell lines using Rabbit anti-Lamin A antibody.

Fibrosarcoma were fixed, embedded and sectioned. Sections were prepared from at least three different blocks. The distribution of gold particles between cytosol, mitochondria and nuclei was quantified. At least ten images per cell compartments were analyzed. The average of the gold particles was divided by the average of the surface area. The density of gold labeling was evaluated by calculating the gold particles/um^2.

A, B, and C represent selected images from each cell pellet. Red, dark orange and blue arrows represent gold labeling of the nucleus, cytosol and mitochondria respectively. Secondary antibody alone was used as a negative control image in **(Appendix V)**.

D. Bar chart representing the value of the density of gold labeling expressed in the cytosol, mitochondria and nuclear envelope (NE), as the mean $\pm$ SD (n= 30 images, 10 images of each cell pellet). Significance was calculated using the Student *t*-test. $P < 0.005$. Comparing mitochondria or nucleus to cytosol.

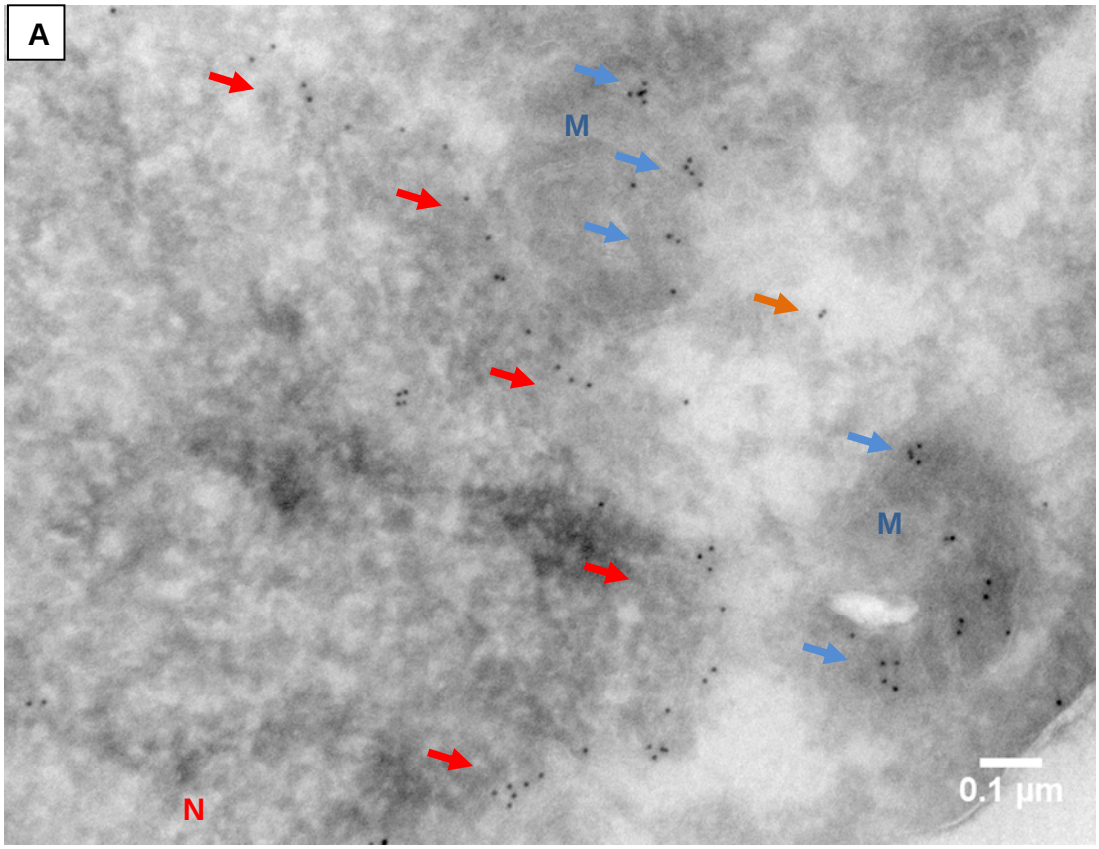
A
M
M
N
0.1 µm

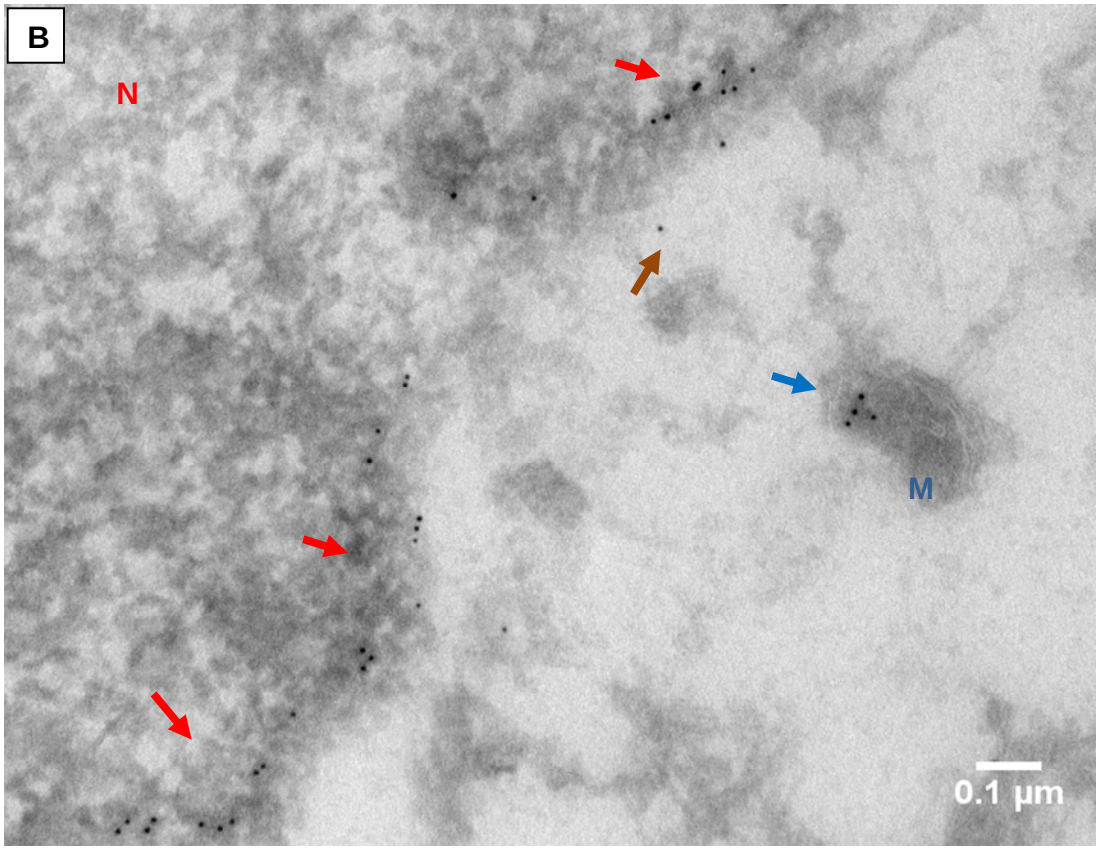
B
N
M
0.1 µm

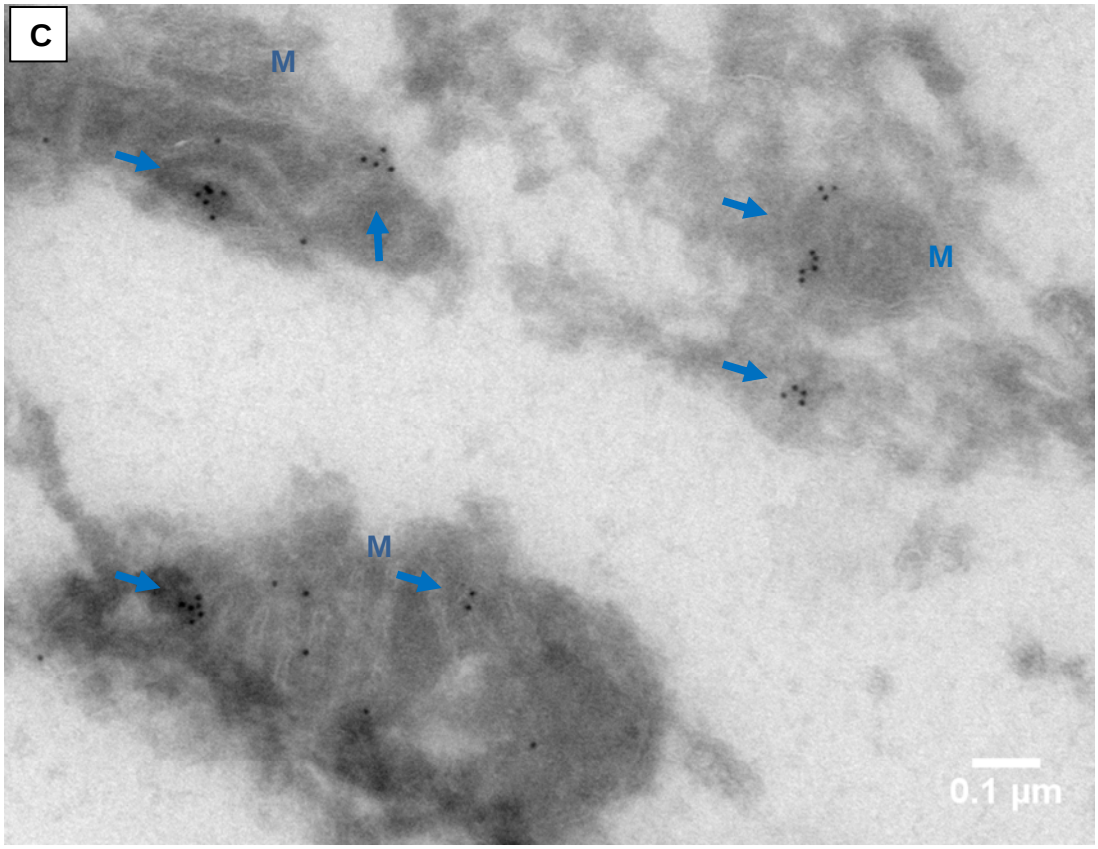
C
M
M
M
0.1 µm

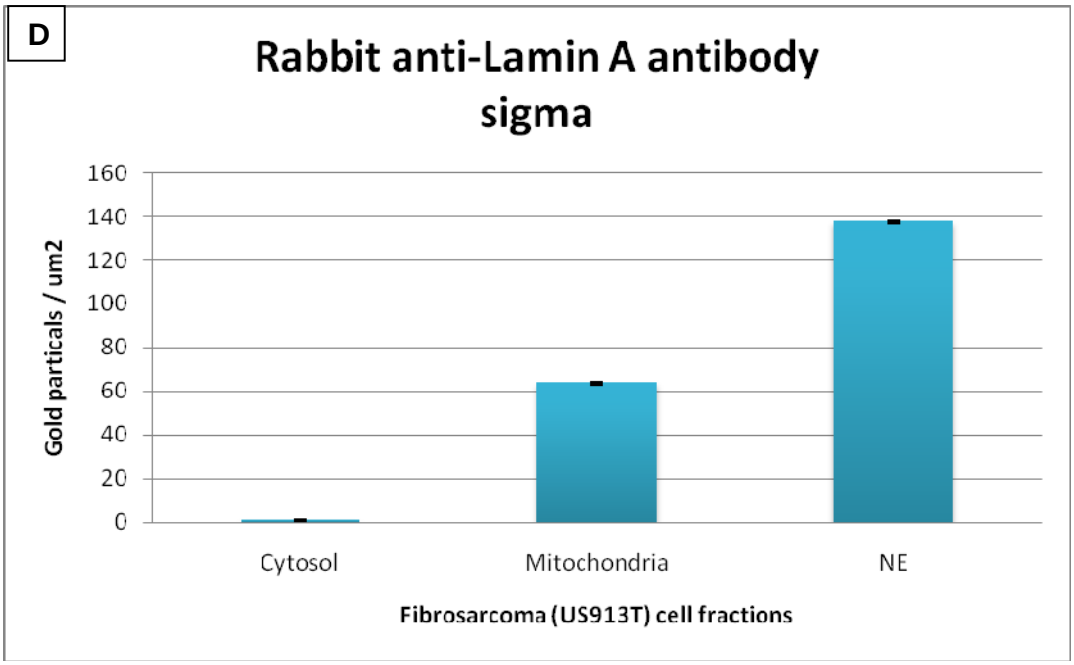
D
Rabbit anti-Lamin A antibody sigma
Gold particals / um2
160
140
120
100
80
60
40
20
0
Cytosol
Mitochondria
NE
Fibrosarcoma (US913T) cell fractions

Figure 5-5

Figure 5-6: Immunogold labelling of Human Brain cancer cells (U373) using Rabbit anti-Lamin A antibody.

Brain cancer cell were fixed, embedded and sectioned. Sections were prepared from at least three different blocks. The distribution of gold particles between cytosol, mitochondria and nuclei was quantified. At least ten images per cell compartments were analyzed. The average of the gold particles was divided by the average of the surface area. The density of gold labeling was evaluated by calculating the gold particles/um^2.

A, B, and C represent selected images from each cell pellet. Red, dark orange and blue arrows represent gold labeling of the nucleus, cytosol and mitochondria respectively. Secondary antibody alone was used as a negative control image in **(Appendix V)**.

D. Bar chart representing the value of the density of gold labeling expressed in the cytosol, mitochondria and nuclear envelope (NE), as the mean $\pm$ SD (n= 30 images, 10 images of each cell pellet). Significance was calculated using the Student *t*-test. $P < 0.005$. Comparing mitochondria or nucleus to cytosol.

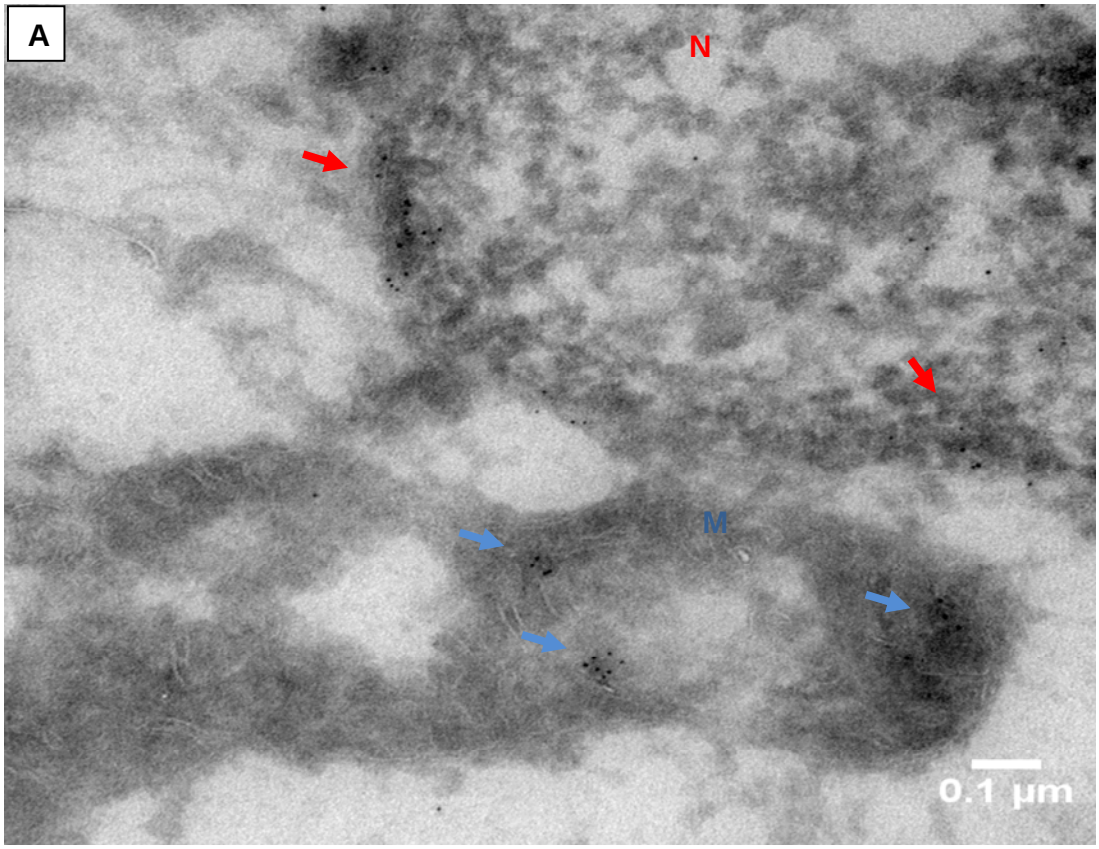
A
N
M
0.1 μm

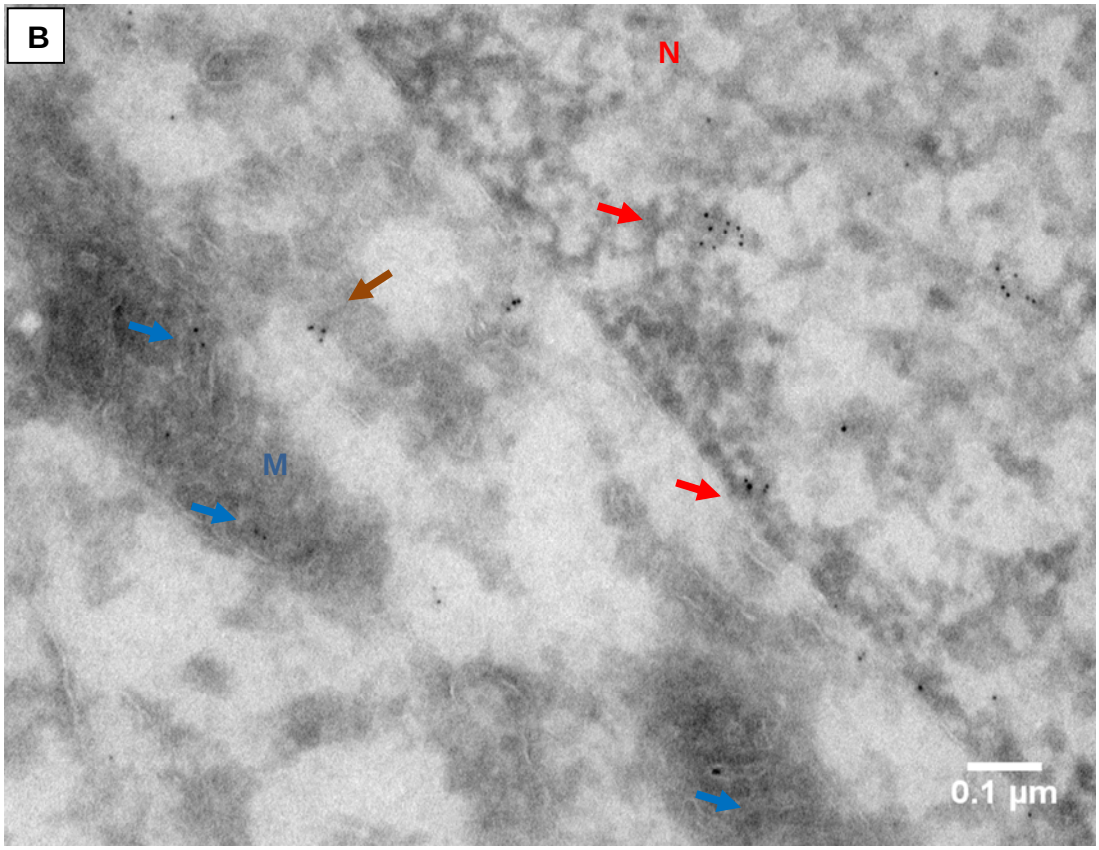
B
N
M
0.1 μm

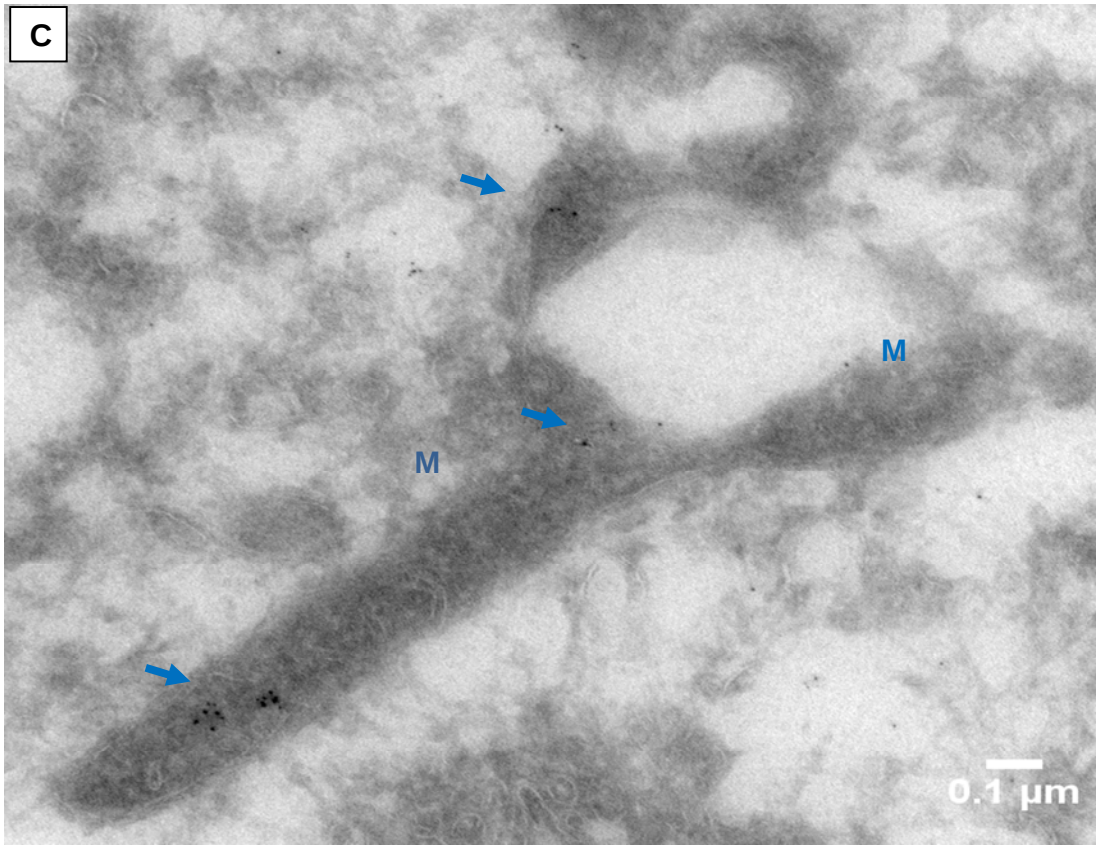
C
M
M
0.1 µm

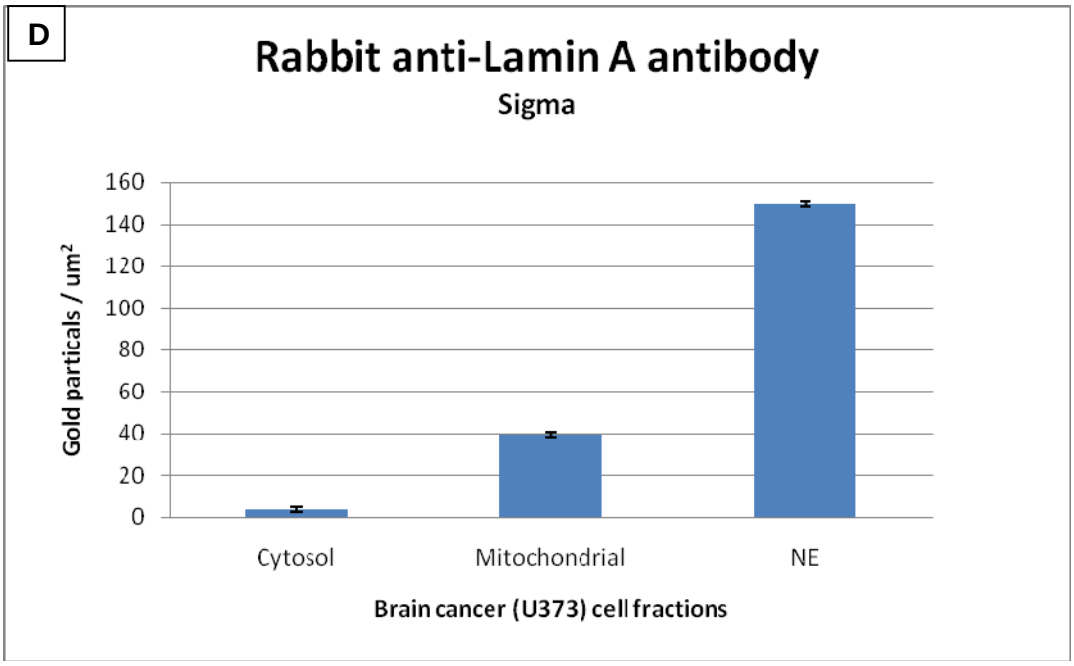
D
Rabbit anti-Lamin A antibody
Sigma
Gold particals / um²
160
140
120
100
80
60
40
20
0
Cytosol
Mitochondrial
NE
Brain cancer (U373) cell fractions

Figure 5-6

Figure 5-7: Immunogold labelling of Lamin A/C$^{-/-}$ cell lines using different antibodies.

Lamin A/C$^{-/-}$ were fixed, embedded and sectioned. Sections were prepared from at least three different blocks. A, B, C and D represent selected images. Red, and blue arrows represent gold labeling of the nucleus and mitochondria respectively. Secondary antibody alone was used as a negative control image in **(Appendix V)**.

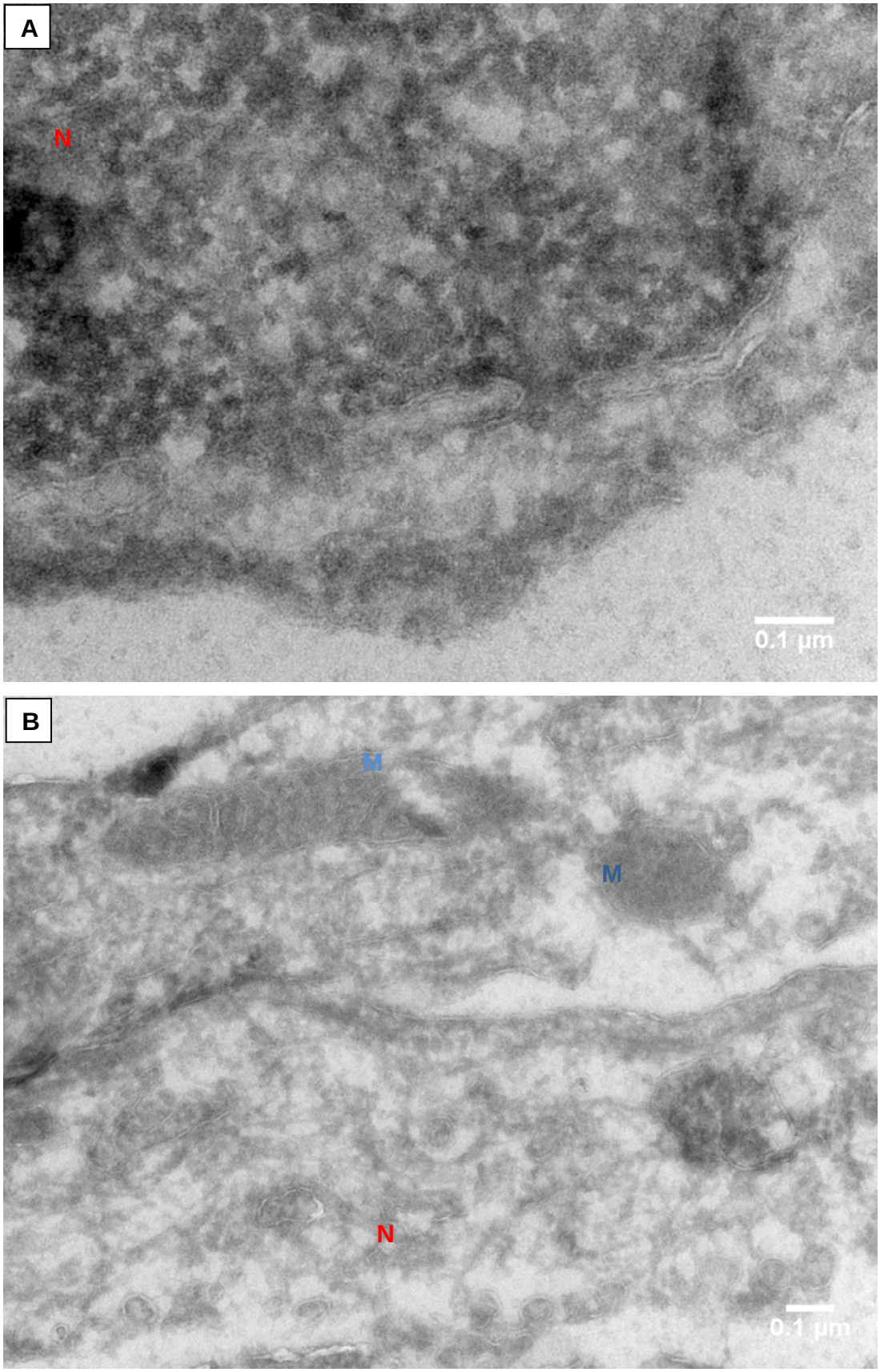
A
N
0.1 µm
B
M
M
N
0.1 µm

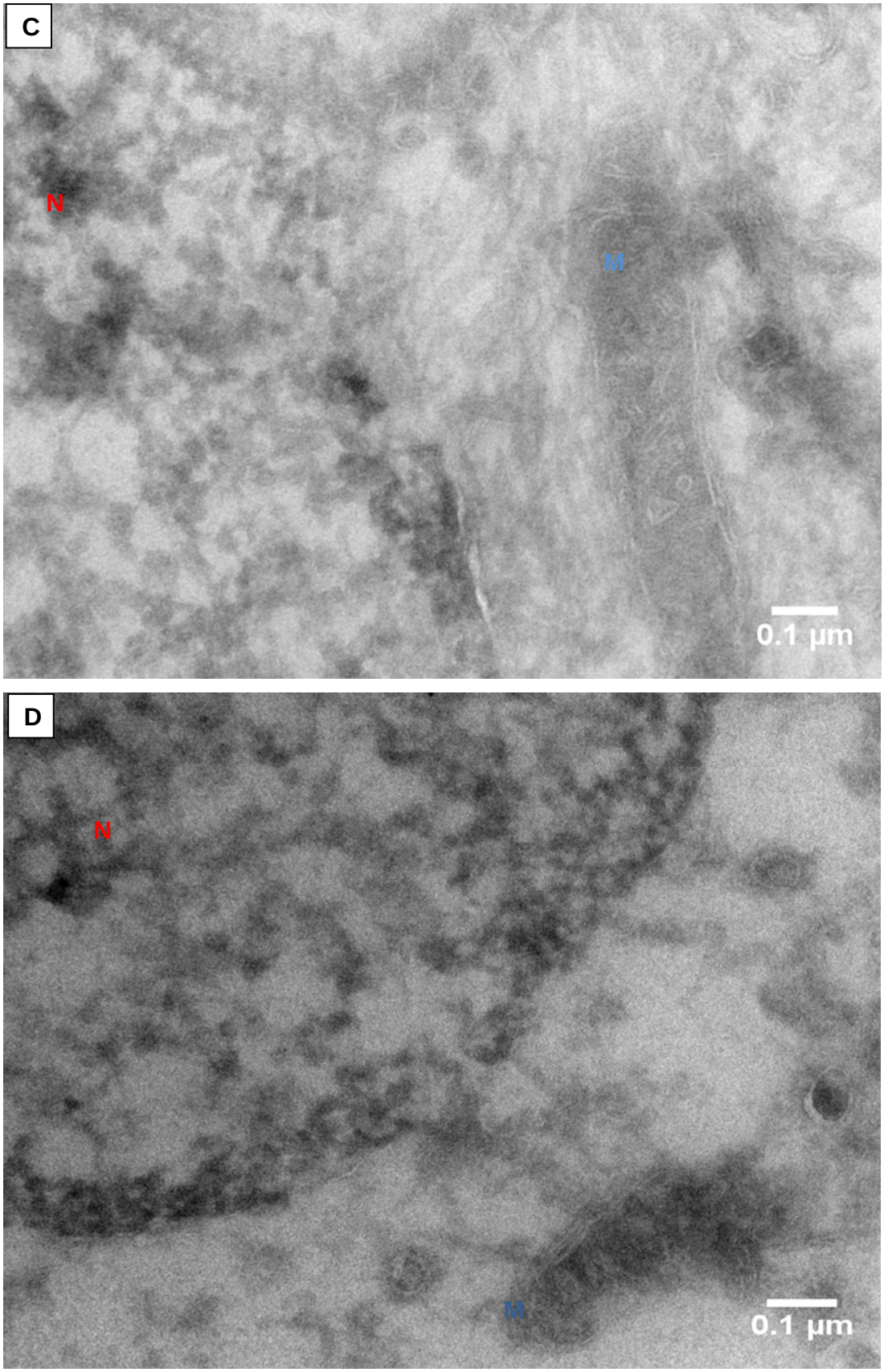

Figure 5-7

Figure 5-8: Immunogold labelling of HT29 cell lines using Rabbit anti-LAP2 alpha antibody (ImmuQuest).

HT29 were fixed, embedded and sectioned. Sections were prepared from at least three different blocks. The distribution of gold particles between cytosol, mitochondria and nuclei was quantified. At least ten images per cell compartments were analyzed. The average of the gold particles was divided by the average of the surface area. The density of gold labeling was evaluated by calculating the gold particles/um^2.

A, B, and C represent selected images from each cell pellet. Red, dark orange and blue arrows represent gold labeling of the nucleus, cytosol and mitochondria respectively. Secondary antibody alone was used as a negative control image in **(Appendix V)**.

D. Bar chart representing the value of the density of gold labeling expressed in the cytosol, mitochondria and nucleus, as the mean $\pm$ SD (n= 30 images, 10 images of each cell pellet). Significance was calculated using the Student *t*-test. $P < 0.005$. Comparing mitochondria or nucleus to cytosol.

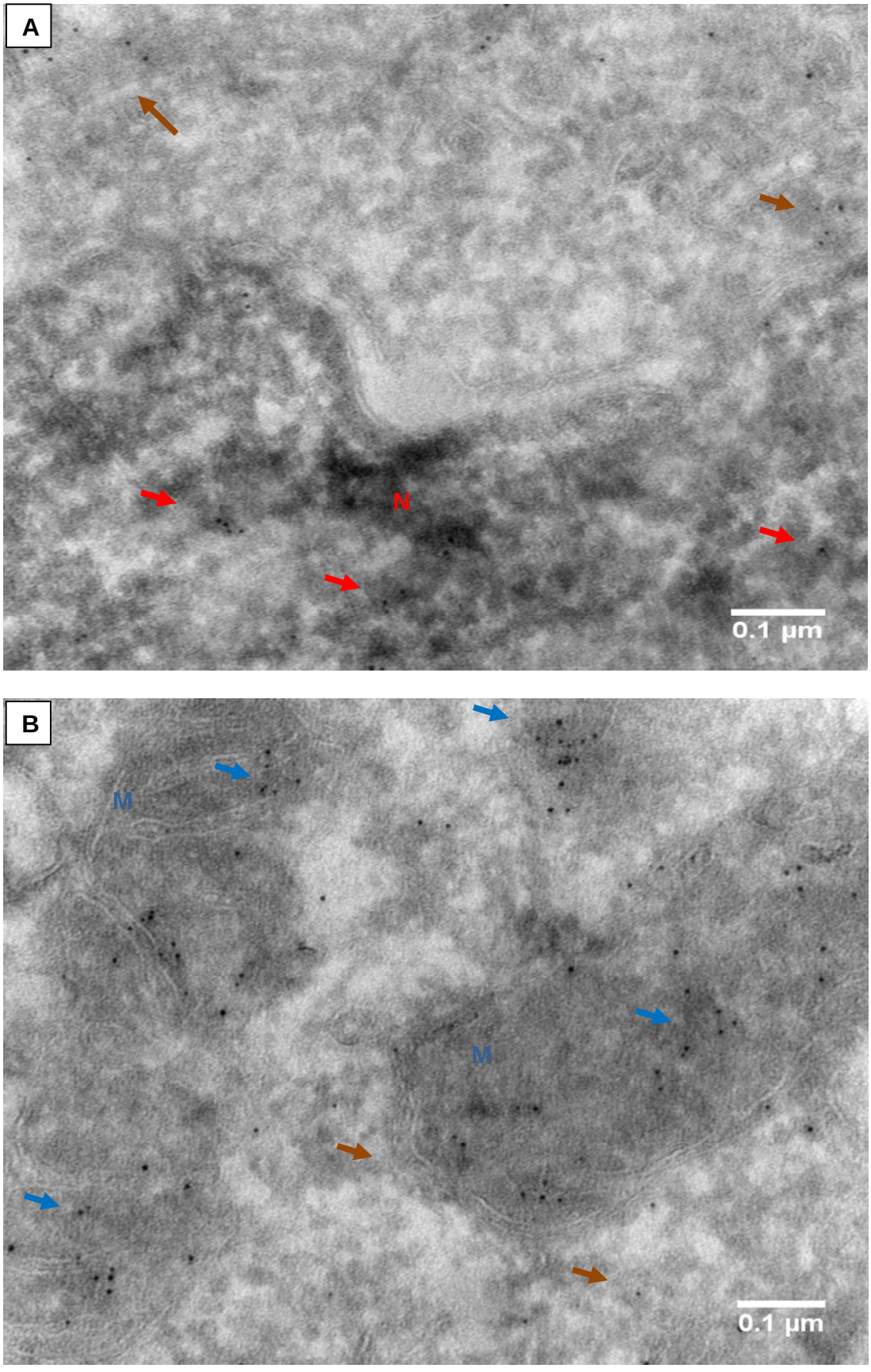
A
N
0.1 µm
B
M
M
0.1 µm

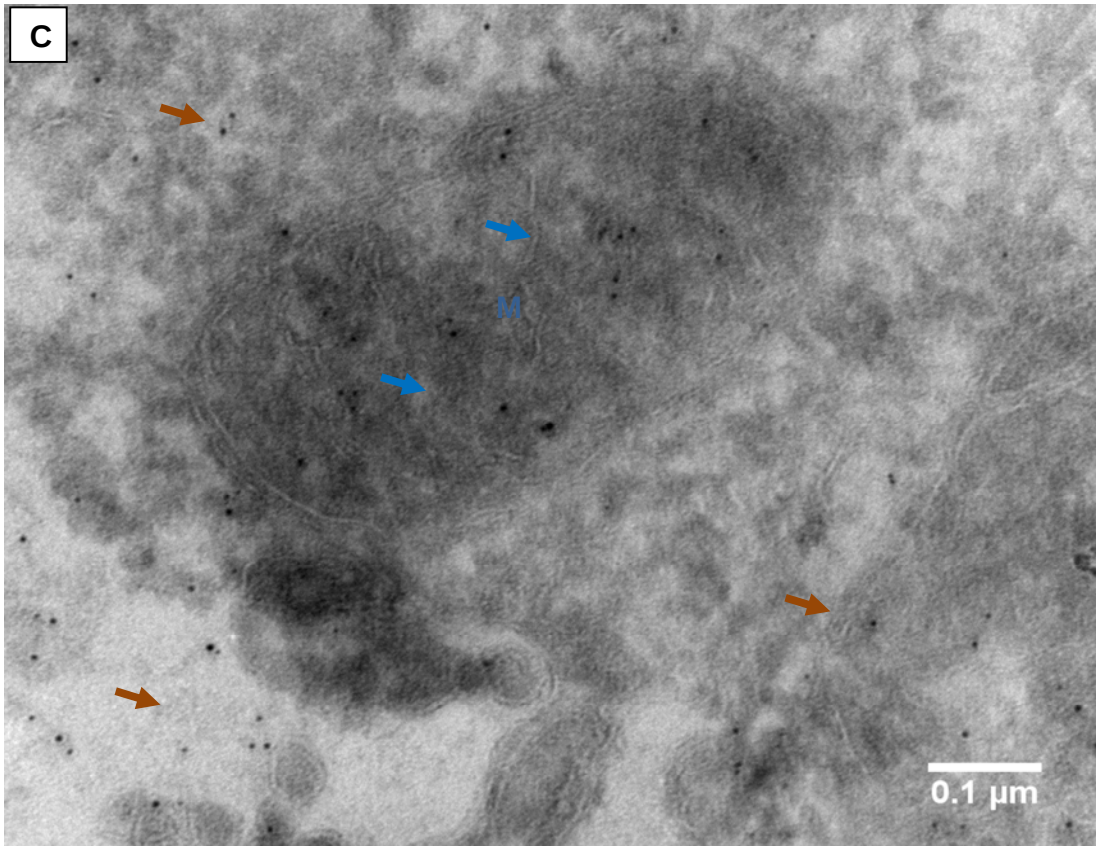
C
M
0.1 µm

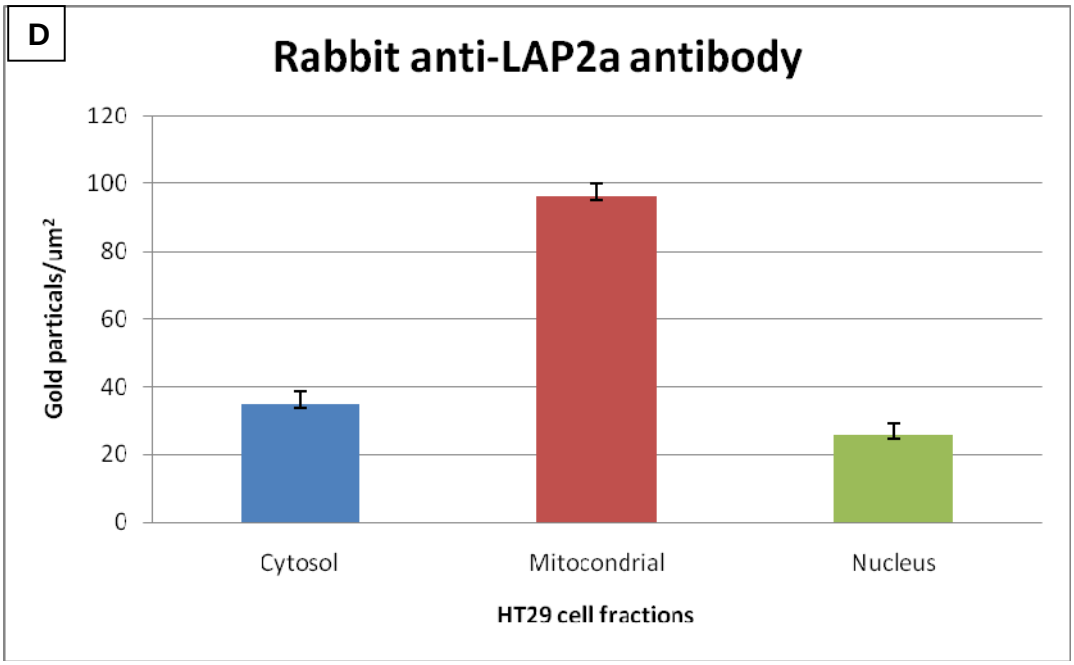
D
Rabbit anti-LAP2a antibody
120
100
80
60
40
20
0
Gold particals/um²
Cytosol
Mitocondrial
Nucleus
HT29 cell fractions

Figure 5-8

Figure 5-9: Immunogold labelling of HT29 cell lines using mouse anti-Cox2 antibody (Invitrogen).

HT29 were fixed, embedded and sectioned. Sections were prepared from at least three different blocks. The distribution of gold particles between cytosol, mitochondria and nuclei was quantified. At least ten images per cell compartments were analyzed. The average of the gold particles was divided by the average of the surface area. The density of gold labeling was evaluated by calculating the gold particles/um^2.

A, B, and C represent selected images from each cell pellet. Red, dark orange and blue arrows represent gold labeling of the nucleus, cytosol and mitochondria respectively. Secondary antibody alone was used as a negative control image in **(Appendix V)**.

D. Bar chart representing the value of the density of gold labeling expressed in the cytosol, mitochondria and nucleus, as the mean $\pm$ SD (n= 30 images, 10 images of each cell pellet). Significance was calculated using the Student *t*-test. $P < 0.005$. Comparing mitochondria or nucleus to cytosol.

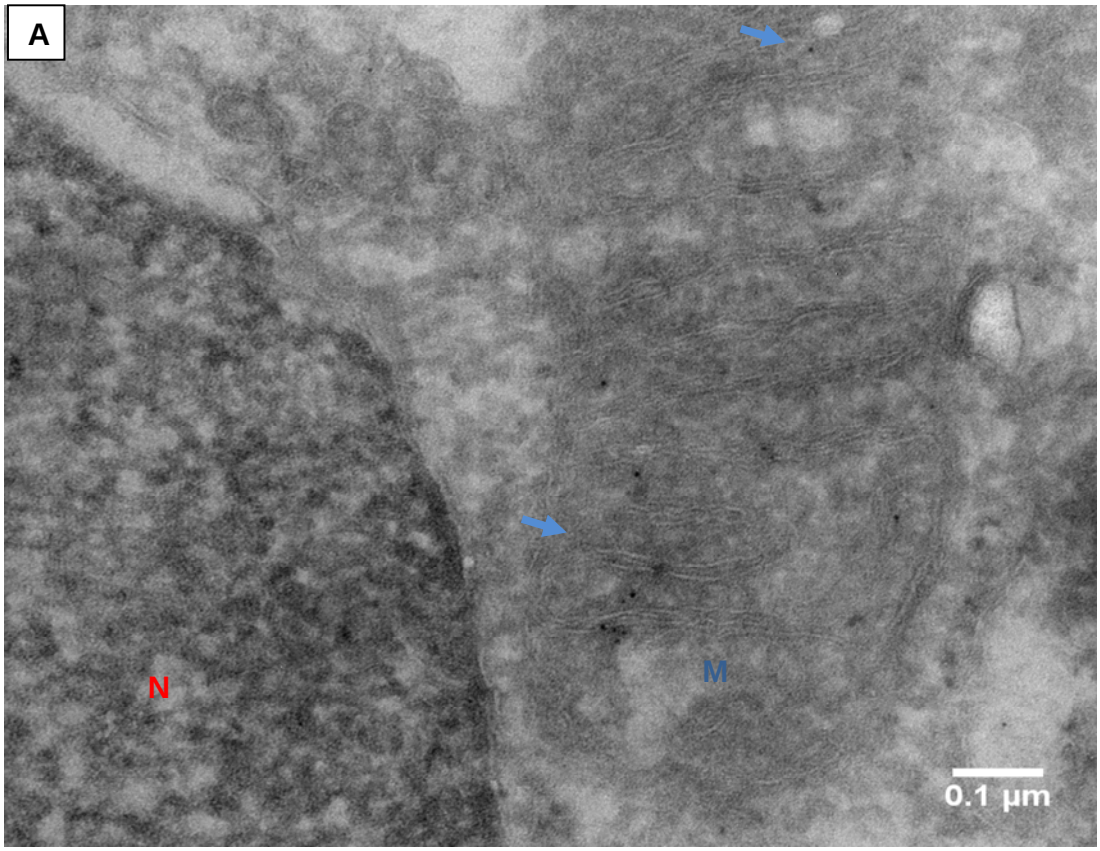
A
N
M
0.1 μm

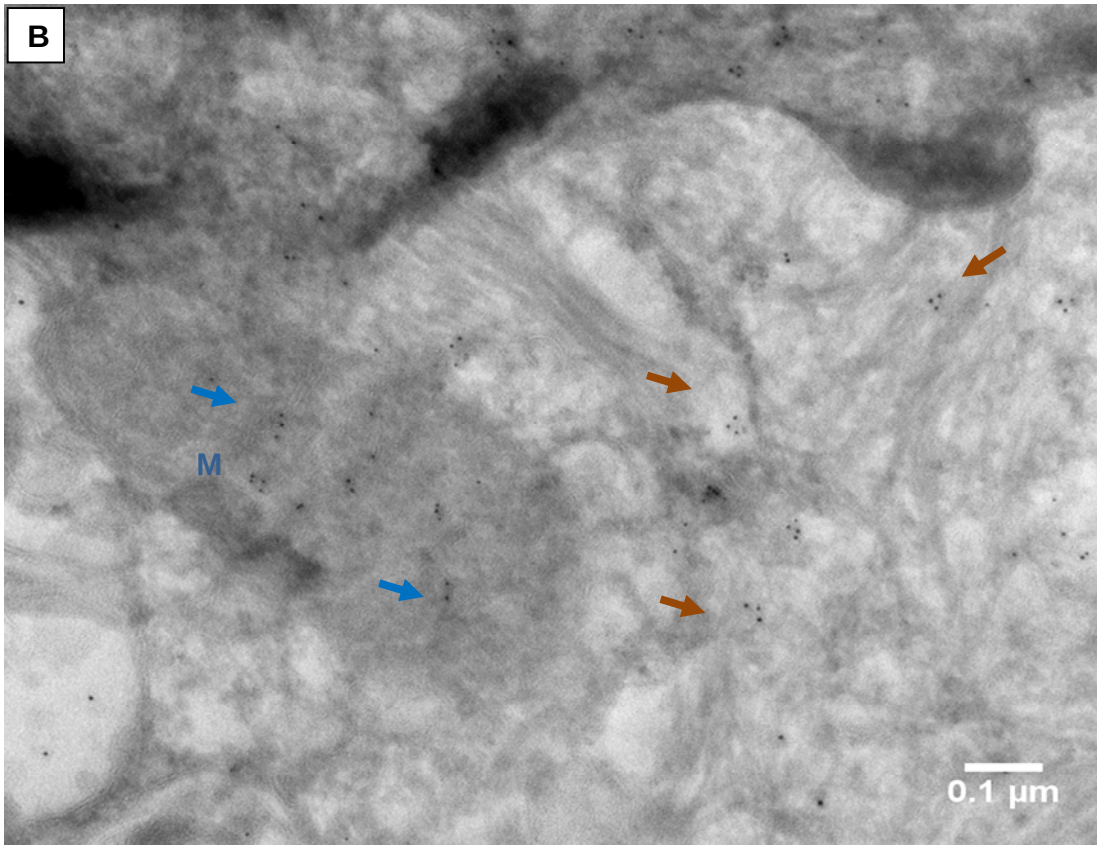
B
M
0.1 μm

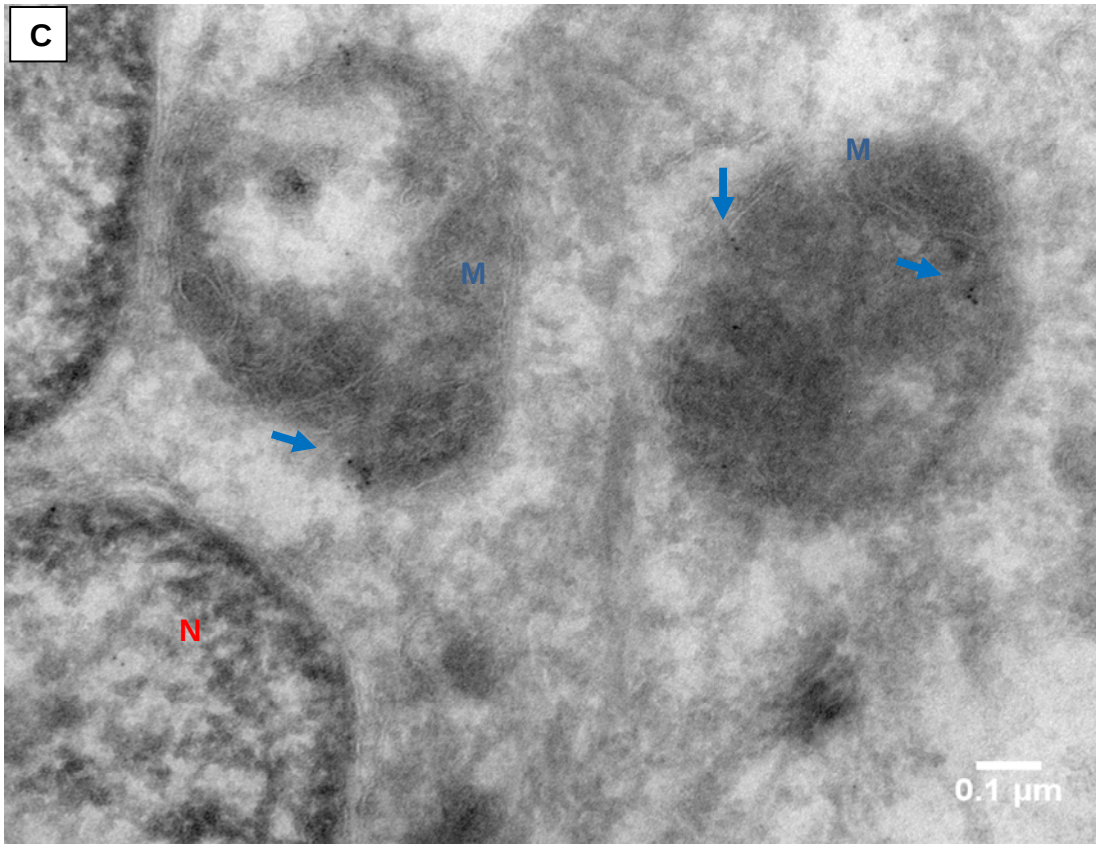
C
M
M
N
0.1 µm

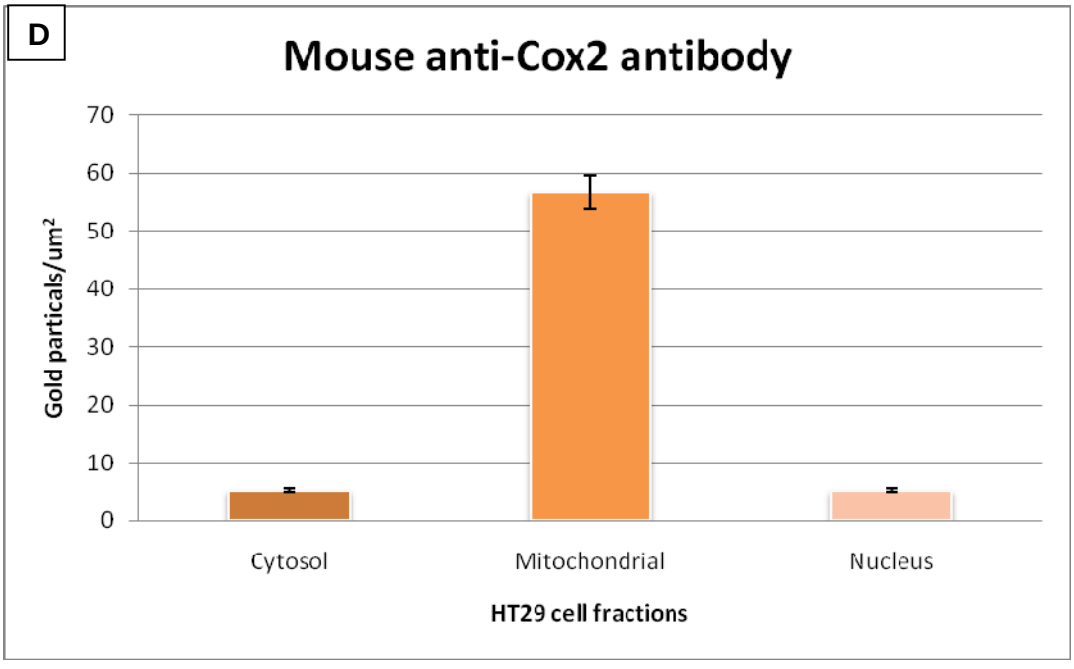
D
Mouse anti-Cox2 antibody
Gold particals/um²
70
60
50
40
30
20
10
0
Cytosol
Mitochondrial
Nucleus
HT29 cell fractions

Figure 5-9

Figure 5-10: Immunogold labelling of HT29 cell lines using mouse anti-Lamin B antibody (Abcam).

HT29 cell were fixed, embedded and sectioned. Sections were prepared from at least three different blocks. The distribution of gold particles between cytosol, mitochondria and nuclei was quantified. At least ten images per cell compartments were analyzed. The average of the gold particles was divided by the average of the surface area. The density of gold labeling was evaluated by calculating the gold particles/um^2.

A, B, and C represent selected images from each cell pellet. Red and blue arrows represent gold labeling of the nucleus and mitochondria respectively. Secondary antibody alone was used as a negative control image in **(Appendix V)**.

D. Bar chart representing the value of the density of gold labeling expressed in the cytosol, mitochondria and nucleus, as the mean $\pm$ SD (n= 30 images, 10 images of each cell pellet). Significance was calculated using the Student *t*-test. $P < 0.005$. Comparing mitochondria or nucleus to cytosol.

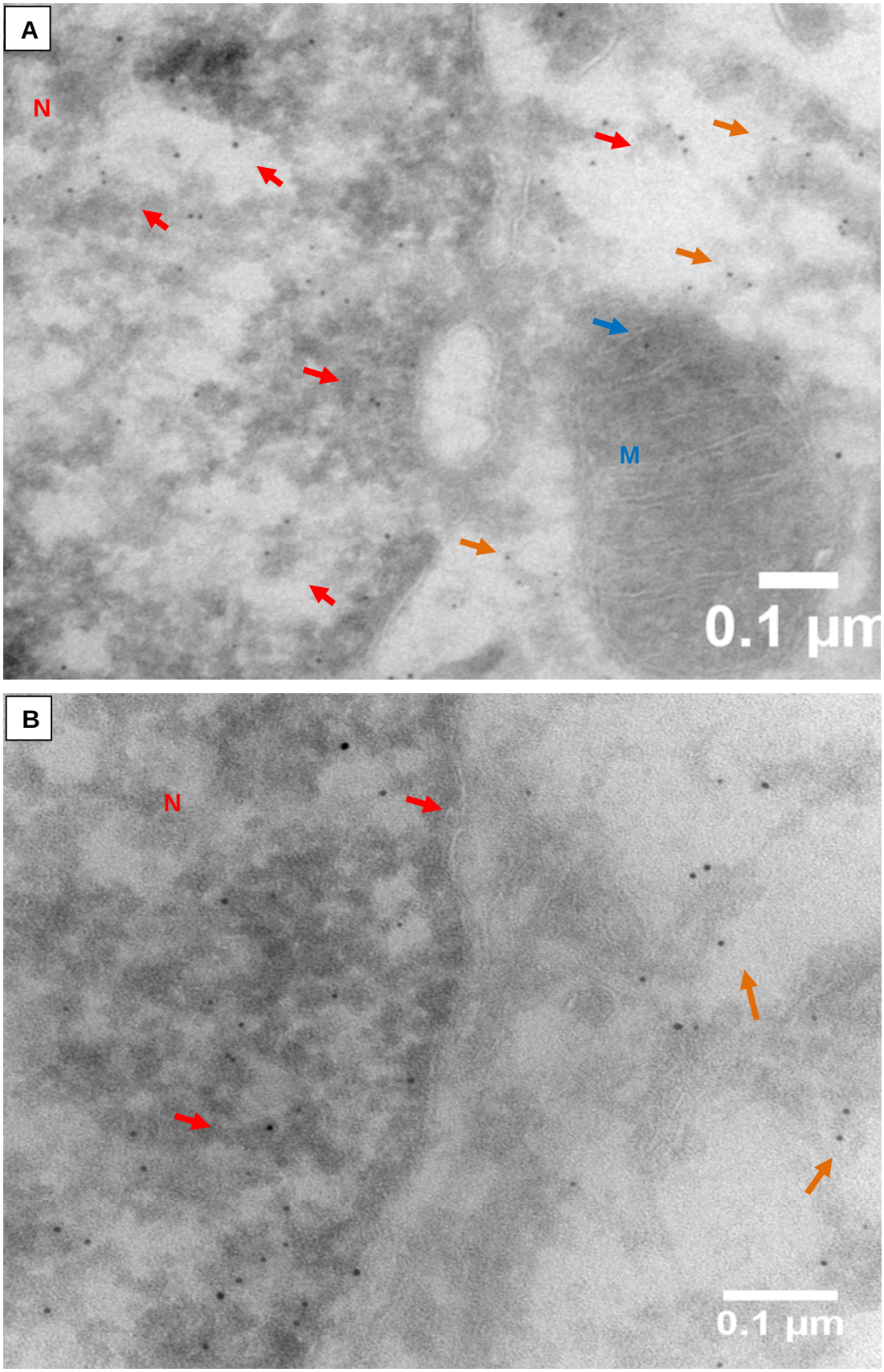
A
N
M
0.1 µm
B
N
0.1 µm

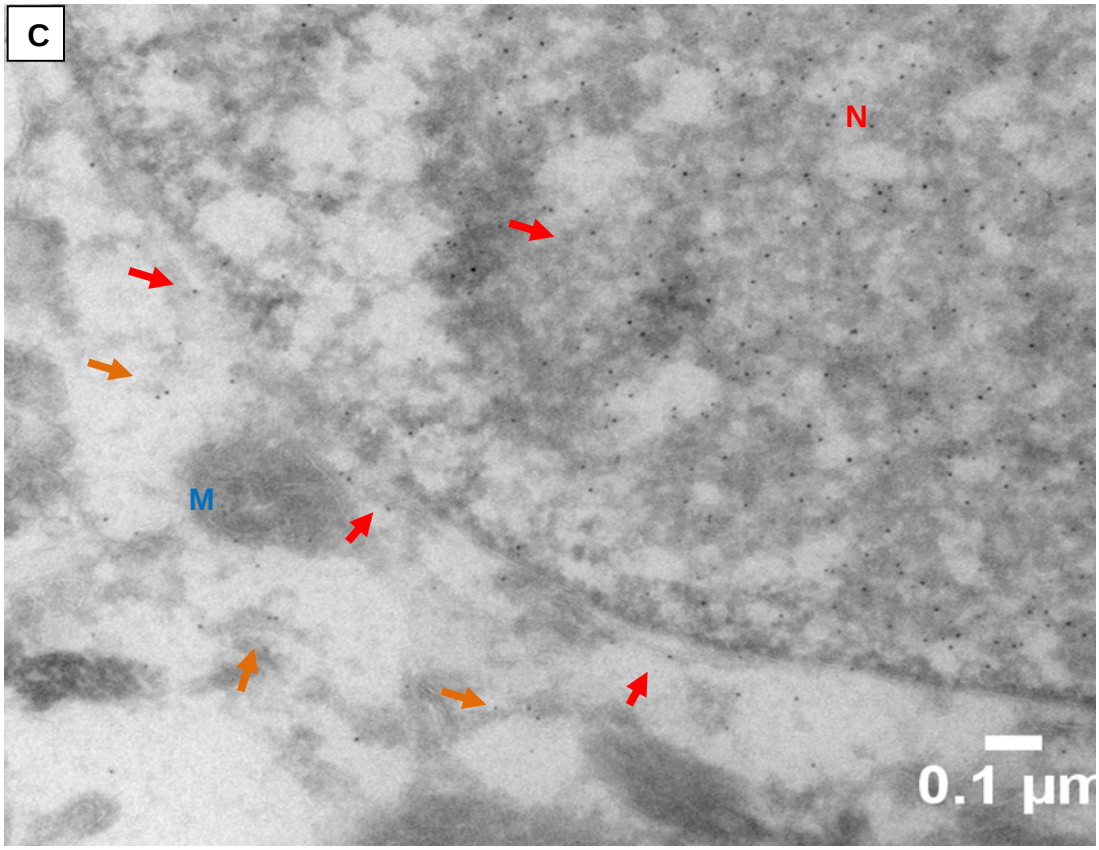
C
N
M
0.1 µm

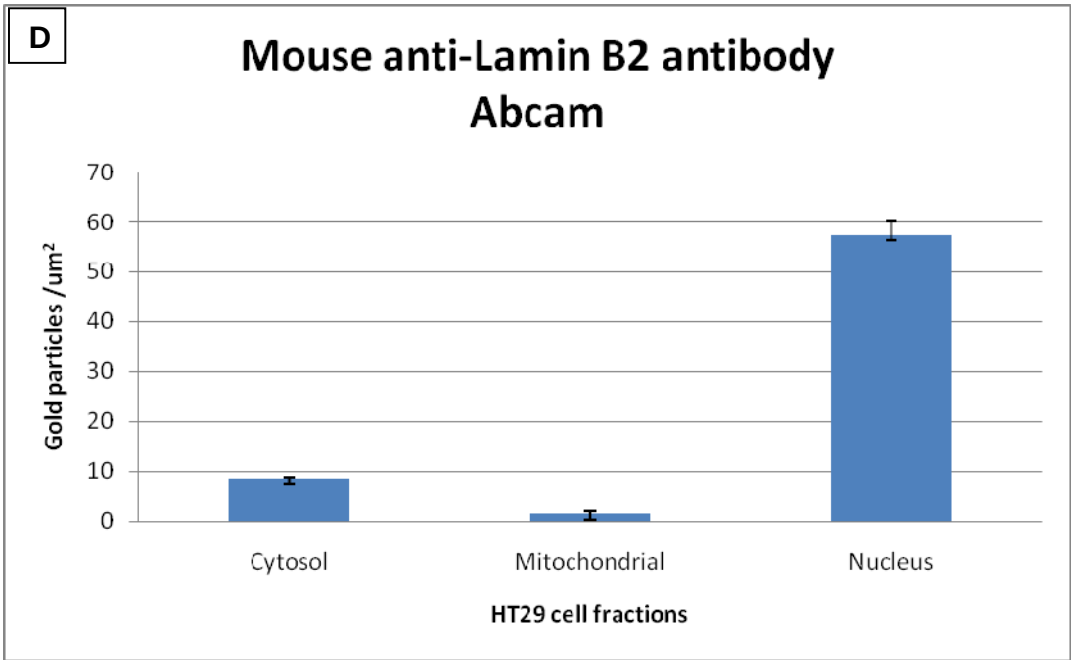
D
Mouse anti-Lamin B2 antibody
Abcam
Gold particles /um²
70
60
50
40
30
20
10
0
Cytosol
Mitochondrial
Nucleus
HT29 cell fractions

Figure 5-10

Figure 5-11-1: Immunogold double labelling of HT29 cell lines using Rabbit anti-Lamin A antibody and mouse anti-Cox2 antibody.

HT29 cell were fixed, embedded and sectioned. Sections were prepared from at least three different blocks. 10 and 20nm of gold particles were used to determine lamin A and Cox2 respectively.

A, B, C and D represent selected images from each cell pellet. Red and blue arrows represent gold labeling of the nucleus and mitochondria respectively. Secondary antibody alone was used as a negative control image in **(Appendix V)**.

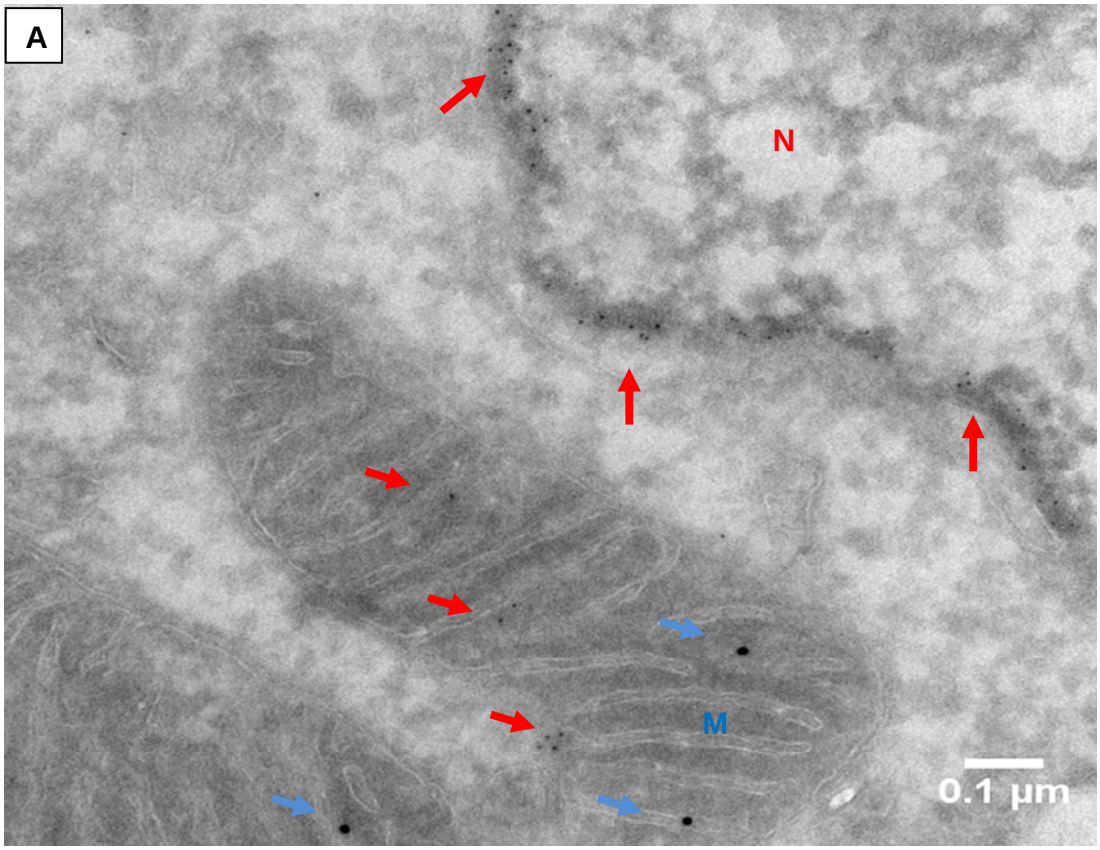
A
N
M
0.1 μm

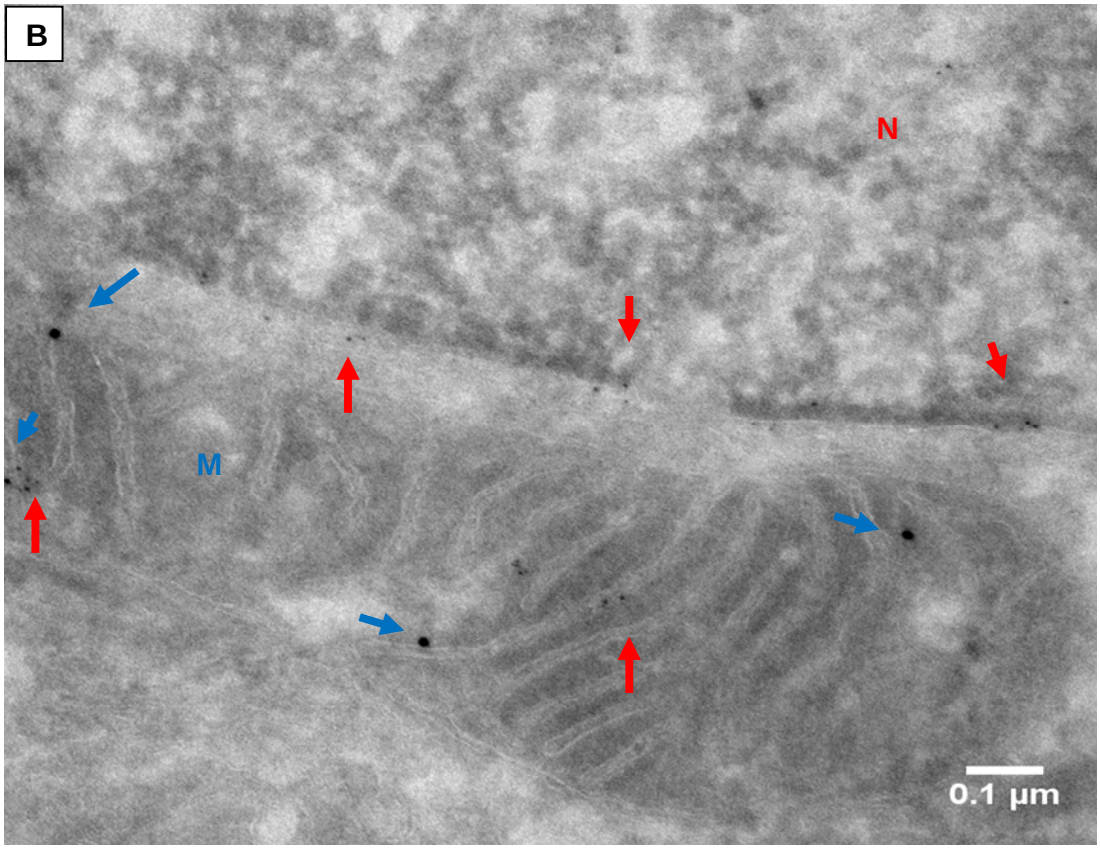
B
N
M
0.1 μm

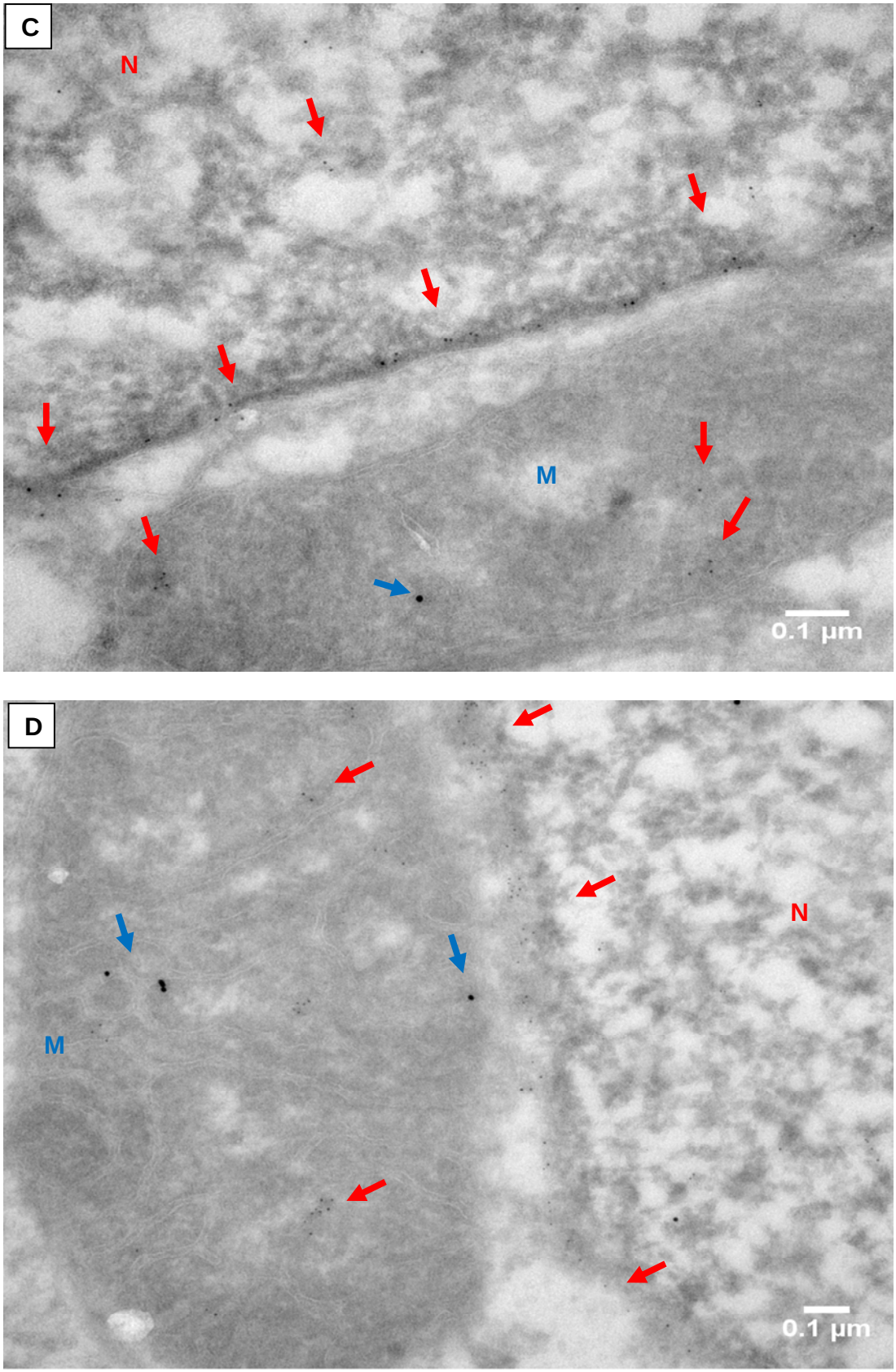

Figure 5.11.1

Figure 5-11-2: Immunogold double labelling on HT29 cell lines using Rabbit anti-Lamin A antibody and mouse anti-Cox2 antibody.

HT29 cell were fixed, embedded and sectioned. Sections were prepared from at least three different blocks. 20 and 10nm of gold particles were used to determine lamin A and Cox2 respectively.

A, B, C and D represent selected images from each cell pellet. Red and blue arrows represent gold labeling of the nucleus and mitochondria respectively. Secondary antibody alone was used as a negative control image in **(Appendix V)**.

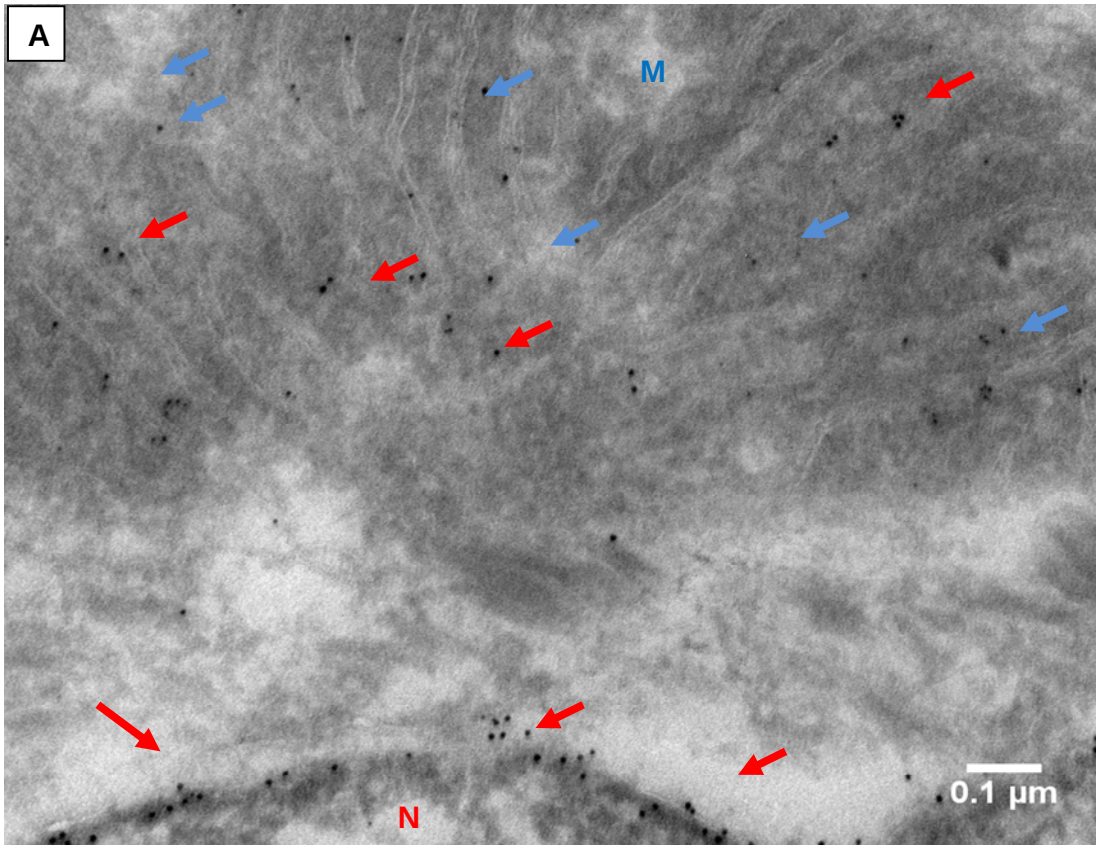
A
M
N
0.1 µm

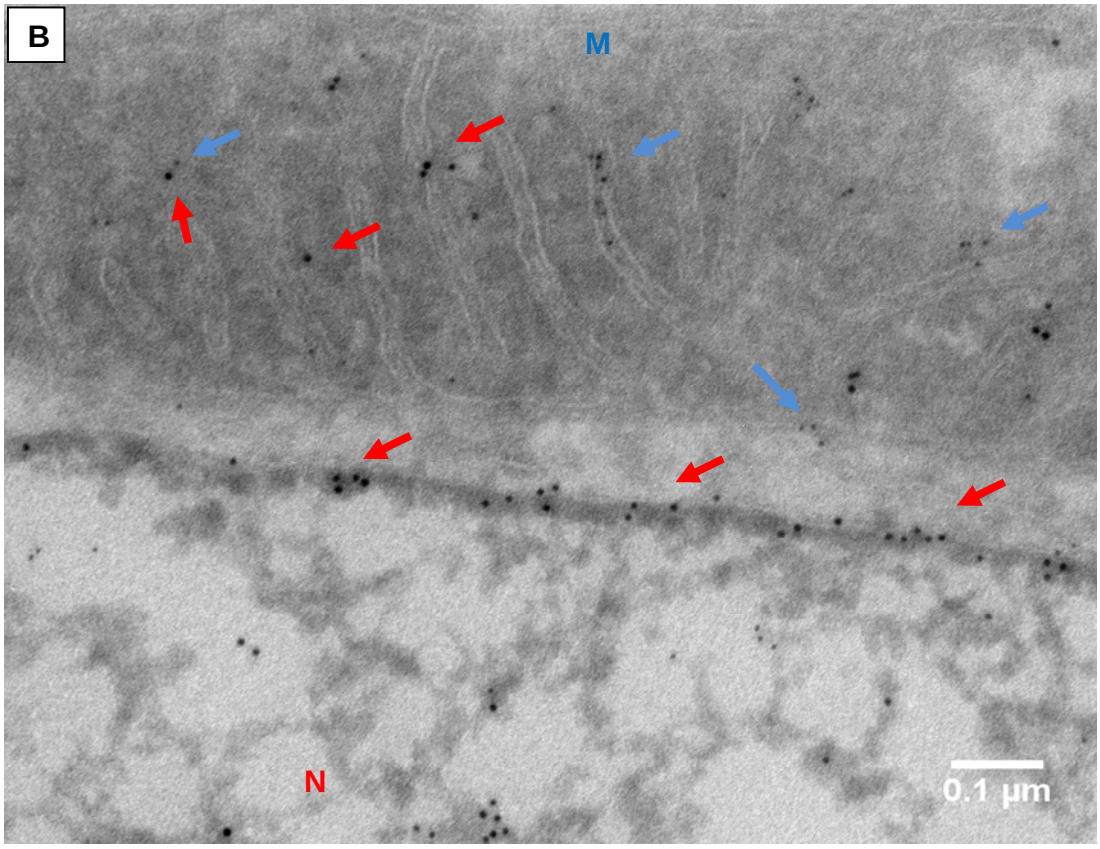
B
M
N
0.1 µm

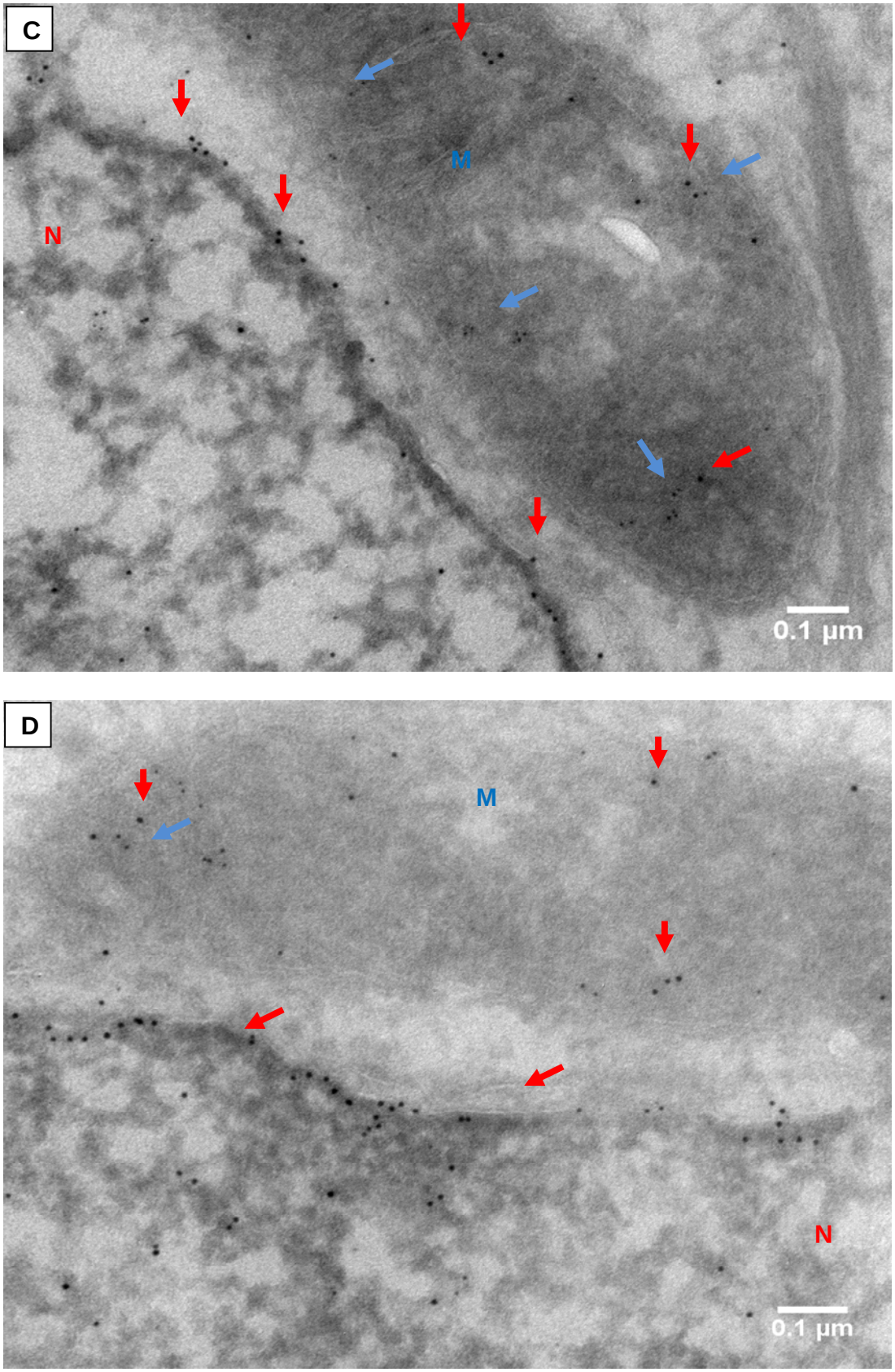

Figure 5.11.2

Figure 5.12: Lamin A/C functional assay in mitochondria.

Reactive Oxygen Species (ROS) production was measured in terms of the oxidation of CM-H_2DCFDA and normalized to 10,000 events/ sample. Sample was run in FACS-calibre by using filter 1 (green).

A. NHF solid red was used as cell control or treated with 1% DMSO gray or 5uM Valinomycine yellow for 12hrs as a negative control or ROS production positive control respectively.

B, C, D, E. Lamin $A^{-/-}$ violet, $LBR^{-/+}$ (Heterozygote) blue, $LBR^{-/-}$ (Homozygote) green and $Emerin^{-/-}$ (KK) brown, used to measure ROS production respectively.

F. The overlays of the FACS result from all cell lines used in this study excluding the treatments.

G. Bar chart representing the percentage of ROS level. The median of the FL1 FACS data were analyzed. The cell control was made 100%, and all cell types were analysis based on that. The mean $\pm$ SD (n= 3 individual experiments).

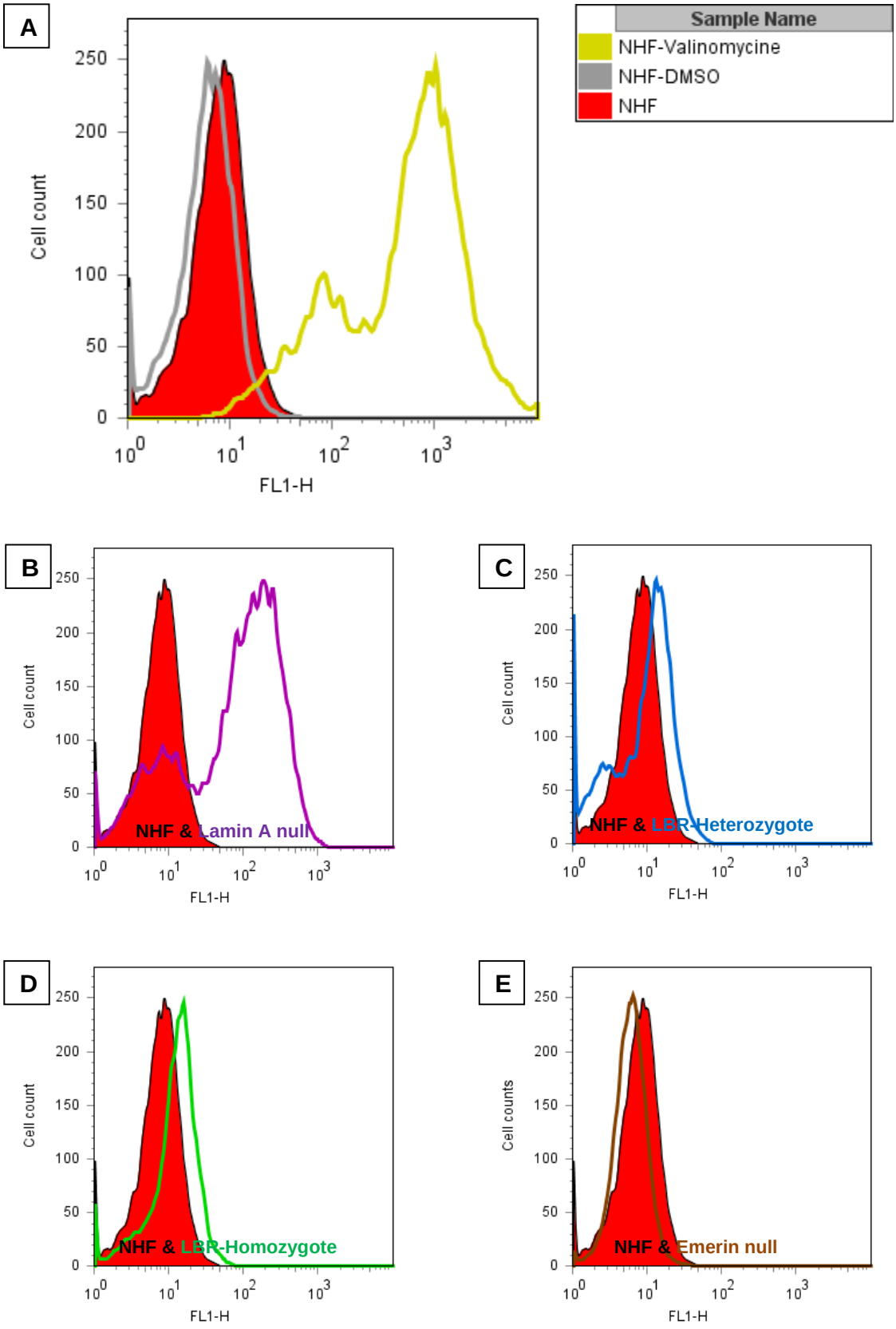
A
Sample Name
NHF-Valinomycine
NHF-DMSO
NHF
Cell count
FL1-H
B
NHF & Lamin A null
C
NHF & LBR-Heterozygote
D
NHF & LBR-Homozygote
E
Cell counts
NHF & Emerin null

Figure 5-12a

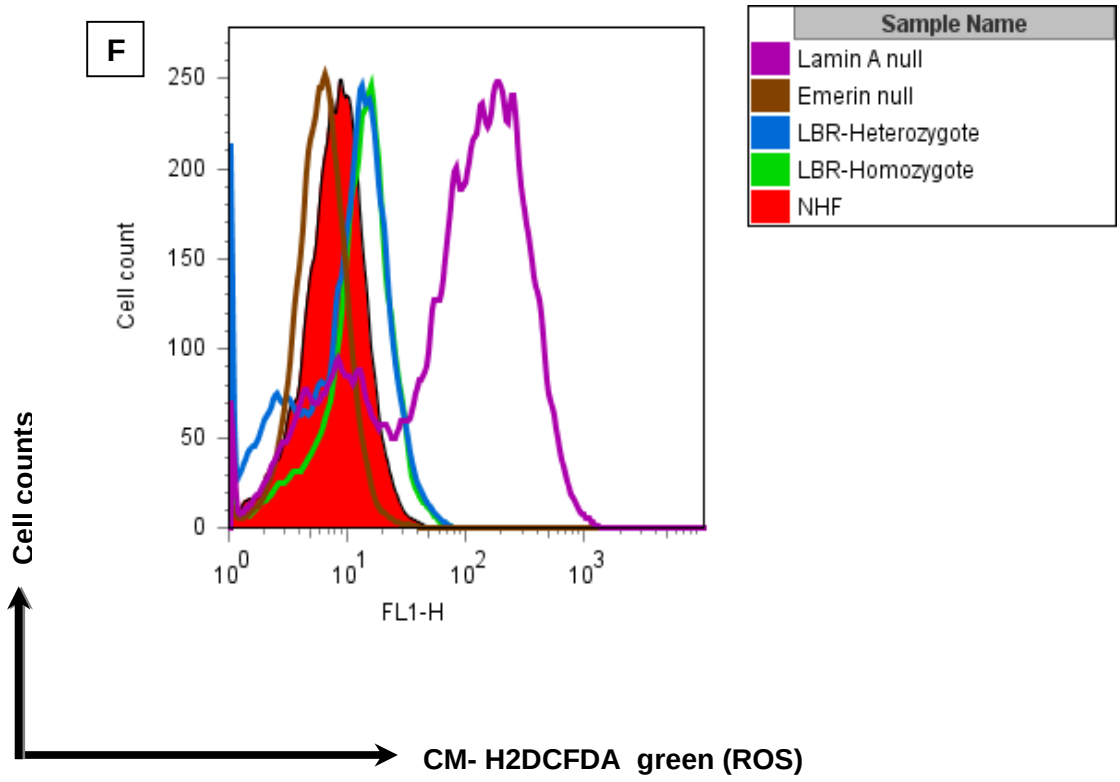
F
Sample Name
Lamin A null
Emerin null
LBR-Heterozygote
LBR-Homozygote
NHF
Cell count
250
200
150
100
50
0
10^0
10^1
10^2
10^3
FL1-H
Cell counts
CM- H2DCFDA green (ROS)

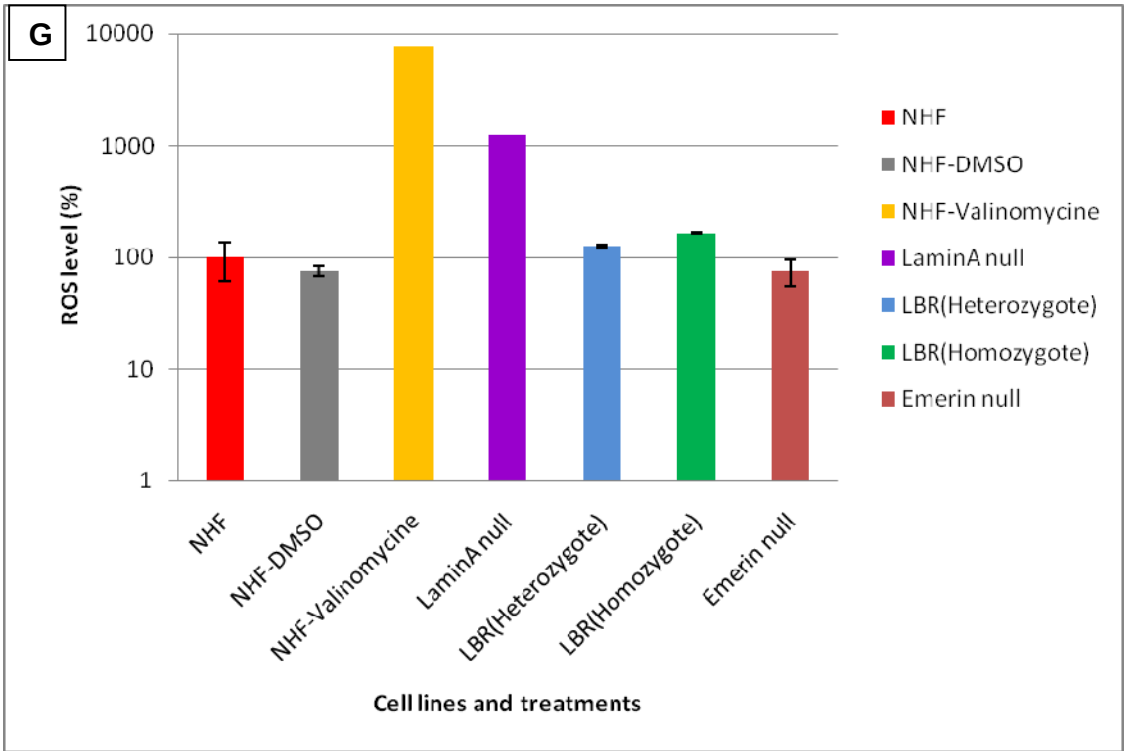
G
10000
1000
100
10
1
ROS level (%)
NHF
NHF-DMSO
NHF-Valinomycine
LaminA null
LBR(Heterozygote)
LBR(Homozygote)
Emerin null
Cell lines and treatments

Figure 5-12b

Figure 5.13: Cox2 gene expression.

Western blot of cell total extracts of NHF, Emerin$^{-/-}$, LBR$^{-/+}$, LBR$^{-/-}$ and LaminA/C$^{-/-}$ cell lines were performed. Trans-membrane probed with antibody to lamin A/C, β.actin and Cox2 antibodies. The expression of lamin A/C loss in lamin A/C$^{-/-}$ compare to other cell lines. The expression of Cox2 was identical in all cell type used in this experiment.

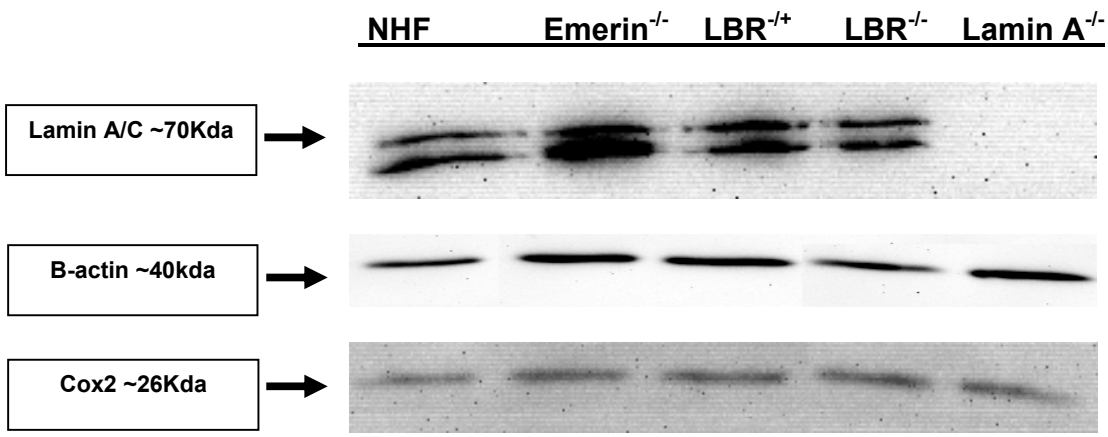
NHF
Emerin-/-
LBR-/+
LBR-/-
Lamin A-/-
Lamin A/C ~70Kda
B-actin ~40kda
Cox2 ~26Kda

Figure 5-13

Figure 5.14: Mitochondria mass.

Mitochondria mass was measured using 10-*n*-nonyl-acridine orange (NAO) followed by FACS. Samples were run in FACS-calibre and normalized to 10,000 events/sample

A. NHF was used as cell control without dye (NHF –NAO) solid light blue or NHF with die as basal level (NHF +NAO) red.

B. NHF treated with 5uM Valinomycine (yellow) for 12hrs was used as a dye sensitivity and stability when mitochondrial outer membrane potential are changed by ROS production.

C, D, E and F. Lamin $A^{-/-}$ violet, $LBR^{-/+}$ (Heterozygote) blue, $LBR^{-/-}$ (Homozygote) green and $Emerin^{-/-}$ (KK) brown used to measure mitochondria mass respectively versus NHF -NAO.

G. Bar chart representing the percentage of the mitochondria mass. The median of the FL1 FACS data were analyzed. The cell control was made 100%, and all cell types were analysis based on that. The mean $\pm$ SD (n= 3 individual experiments).

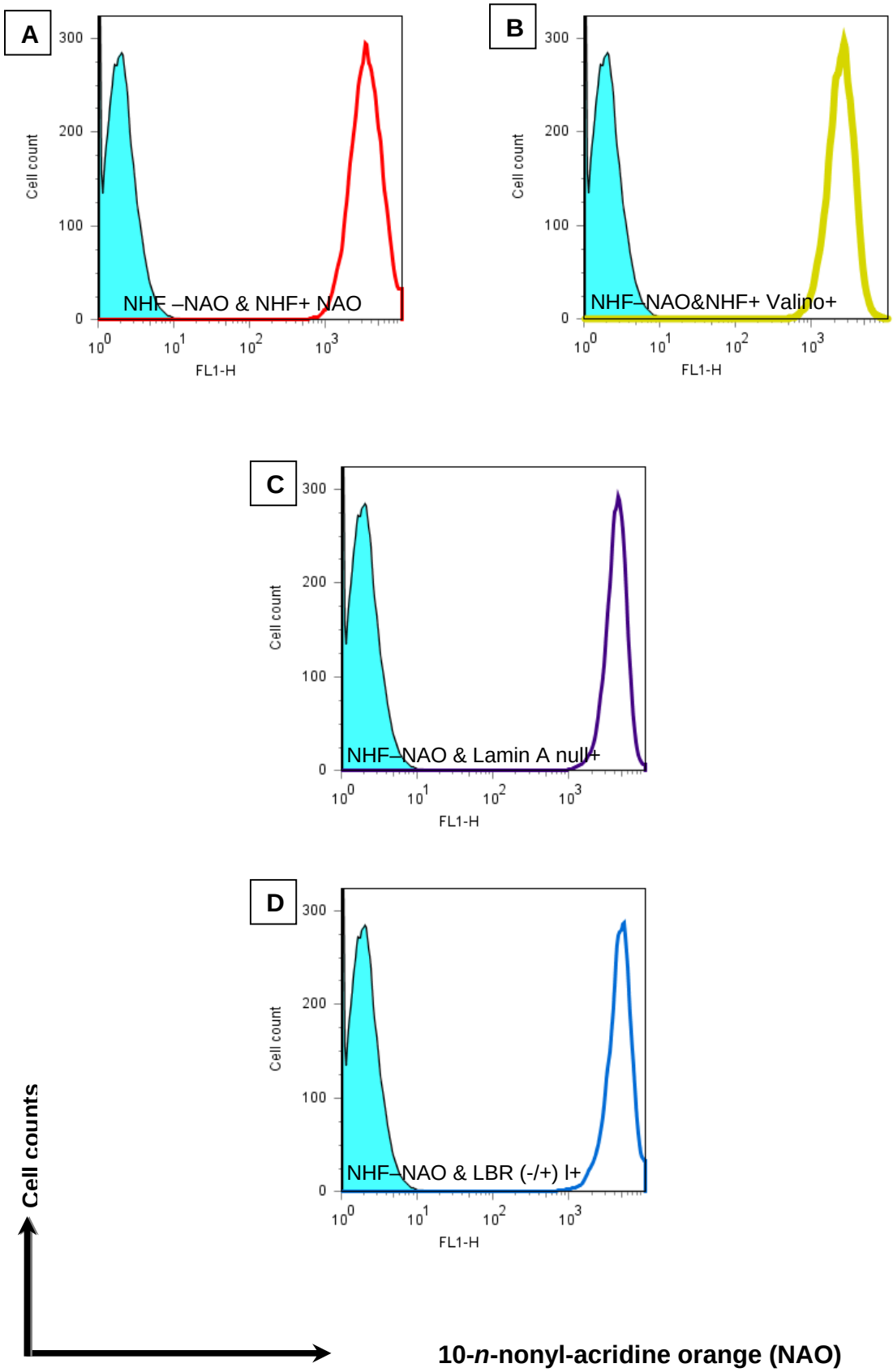
A
B
C
D
Cell count
FL1-H
NHF –NAO & NHF+ NAO
NHF–NAO&NHF+ Valino+
NHF–NAO & Lamin A null+
NHF–NAO & LBR (-/+) I+
Cell counts
10-*n*-nonyl-acridine orange (NAO)

Figure 5-14a

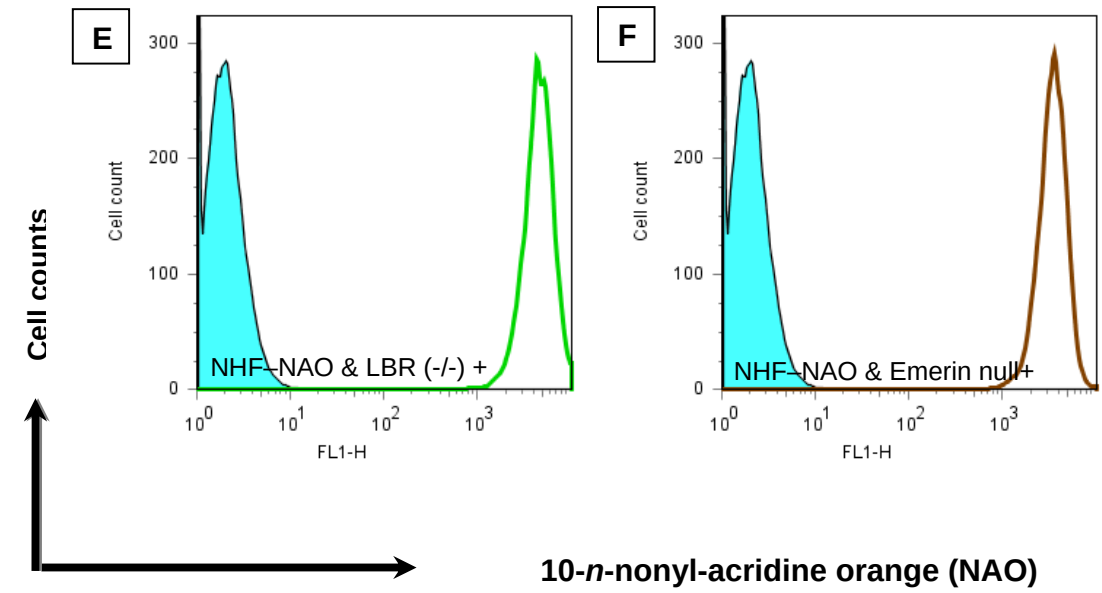
E
F
Cell counts
Cell count
300
200
100
0
NHF–NAO & LBR (-/-) +
NHF–NAO & Emerin null+
10^0
10^1
10^2
10^3
FL1-H
10-*n*-nonyl-acridine orange (NAO)

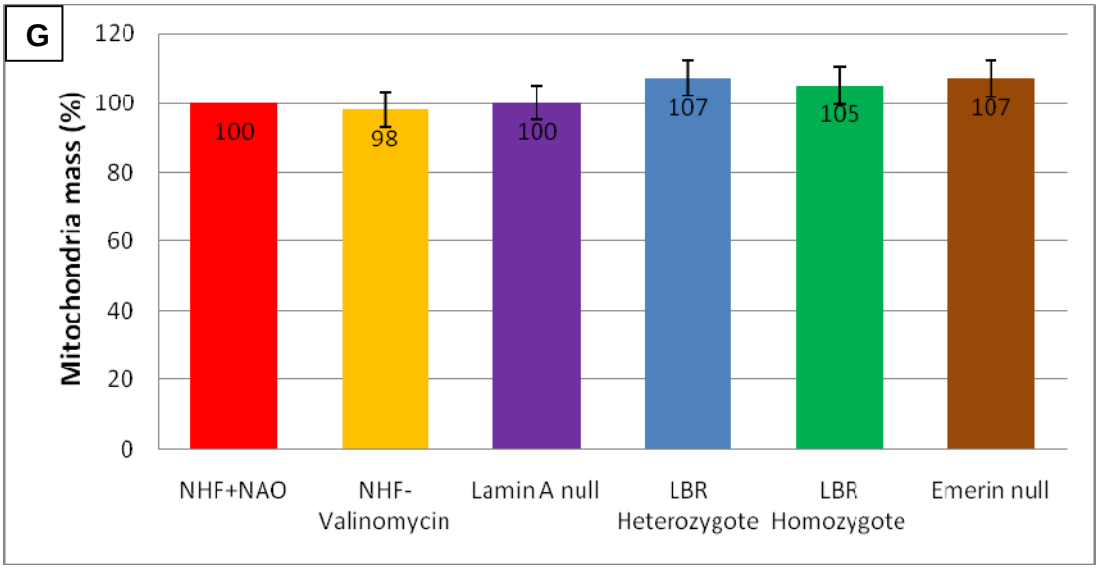
G
Mitochondria mass (%)
120
100
80
60
40
20
0
100
98
100
107
105
107
NHF+NAO
NHF-
Valinomycin
Lamin A null
LBR
Heterozygote
LBR
Homozygote
Emerin null

Figure 5-14b

Chapter 6: Discussion:

Changed expression of lamin A/C has been associated with different cancers, such as lymphoma and leukemia (Agrelo *et al.*, 2005), lung cancer (Kaufmann *et al.*, 1991) and colon cancer which suggested that changed lamin expression in colon cancer could be a biological marker of malignancy (Moss *et al.*, 1999). One study in colorectal cancer showed that the expression of A-type lamin in tumors leads to a more aggressive-form. This study also demonstrated that lamin A expression was associated with high cell motility, loss of cell adhesion and invasiveness (Willis *et al.*, 2008). In other studies down regulated expression of lamin A was correlated to rapid growth within basal cell carcinomas, while down regulated expression of lamin C was correlated with slow growth within similar tumors. These finding suggest that lamin A has a negative influence on cell proliferation (Venables *et al.*, 2001; Tilli *et al.*, 2003). Nucleoplasmic complexes of Lamin A/C/LAP2α interact with the tumor suppressor retinoblastoma (Rb) has been reported (Markiewicz *et al.*, 2002). This interaction may help in regulating the expression of Rb-E2F-dependent target genes and in cell differentiation (Dorner *et al.*, 2006). It has also been reported that three different transcription regulators bind strongly to A-type lamins: the kruppel-like protein (MOK2), the sterol response element-binding protein (SREBP1) and c-Fos (Ozaki *et al.*, 1994; Dreuillet *et al.*, 2002; Lloyd *et al.*, 2002; Ivorra *et al.*, 2006). Therefore, the aim of this research was to understand more about the function of Lamin A/C and LAP2α in colon epithelial cells, and their role in colorectal carcinoma. To achieve this, I wished to identify novel proteins that bind to Lamin A/C and/or LAP2α in colon tissue using a yeast 2-hybrid system.

Mitochondrial cytochrome c oxidase subunit II (Cox2) was the protein found to interact most frequently with lamin A/C and LAP2α in the yeast 2-hybrid screen. To confirm this finding, a second independent experimental technique was used to directly demonstrate the interaction between lamin A/C, LAP2α and Cox2. Co-immunoprecipitation from mitochondrial fractions showed an in-vitro interaction between lamin A/C and LAP2α and Cox2.

Given the different reported cellular locations of lamin A/C, LAP2α (Nucleus) and Cox2 (mitochondria) this result was surprising (Taanman, 1997; Dechat *et al.*, 1998; Hutchison, 2002). Thus, additional experiments were needed to determine if the proteins could co-localize in cells. Therefore, biochemical assays of cell fractions were performed. HT29 cells were fractionated into cytosol, mitochondrial and nuclear cell fractions. Lamin A/C and LAP2α were shown to be localized in the mitochondrial as well as the nuclear fractions but not in the cytosol. When these fractions were subjected to blotting with anti-LAP2β and anti-Rb antibodies, the results confirmed that the fractions were not cross contaminated. When the same blots were probed with anti-Cox2 antibody, Cox2 was only found in the mitochondria. These data suggest that both lamin A/C and LAP2α are localized in mitochondria as well as the nucleus. This finding raised a question as to whether a lamina-like structure exists in mitochondria. To address this question samples were blotted with antibody against lamin B1 and B2. Neither B-type lamin blotted was found in mitochondria.

To confirm the localization of both lamin A/C and LAP2α in mitochondria, HT29 cells were subjected to fixation and cryo-sectioning for TEM analysis using immunogold labeling with different antibodies. Different anti-lamin A/C antibodies showed a localization of Lamin A/C in nuclei and mitochondria. Anti-LAP2α antibody was used, LAP2α was found in nuclei and mitochondria. The phenomena of localization of lamin A/C in mitochondria and its putative interaction with Cox2 were issued in colon tissue. To investigate whether this phenomena is specific for colon or colon cancer or it is general in normal tissue or different cancer. Cryo-sections of normal human fibroblast cells (NHF), fibro sarcoma cells (US913T) and brain cancer cells (U373) were prepared and stained with rabbit anti-lamin A antibody. In each cell line lamin A was detected in mitochondria and nuclei but not in the cytosol. As a further control for specificity to show that the anti-lamin A antibody used in this study did not cross-react with unknown proteins in mitochondria which contain of the same epitope recognized by anti-lamin A/C. Lamin $A/C^{-/-}$ fibroblast were investigated (Muchir *et al.*, 2003). Cryo-sections were prepared and probed with rabbit anti-lamin A antibody. The results showed an absence of gold particles in mitochondria, nuclei and cytosol. This result suggested that the localization of anti-lamin A antibody specifically detected lamin A in mitochondria. As a negative control sections were always probed with secondary antibodies alone. No gold particles were detected under these conditions.

Most mitochondrial proteins are encoded by nuclear DNA and translated in the cytosol. A specific pathway exists for these proteins to enter mitochondria. Three characteristics are important for this import into mitochondria: (1) An N-terminal

mitochondrial-targeting sequence, (2) un-folded proteins are imported into mitochondria so all of these proteins should interact with one of the chaperone proteins found in the cytosol (cytosolic Hsc 70 or MSF), and (3) translocation of proteins to the mitochondrial matrix happens only at rare sites where the outer and the inner mitochondrial membrane are juxtaposed. One of these criteria was investigated for both lamin A/C and LAP2α by constructing a helical-wheel of the first 18 amino acids the amphipathic nature of the Lamin A/C and LAP2α N-terminal domains in silico **(Figure 6.1 and 6.2).** The result show the possibility of both lamin A/C and LAP2α contain of MTS on their N-terminus.

The interactions of lamin A with chaperones such as Hsp70 have been investigated (Willsie and Clegg, 2002). It was also suggested that chaperones such as Hsp25 and Hsp70 may have a role in stabilizing lamins network (Adhikari *et al.*, 2004). These finding in addition to the data shows in this study illustrate how lamin A/C may be imported into mitochondria. It was shown that lamin assembly in-vitro involve lateral interaction via coiled-coil associations of α-helical rod domains of two lamin chains to form homodimers (Stuurman *et al.*, 1998). This raises several questions need to be demonstrated; how a homodimer of lamin A imported to mitochondria and does lamin A make a filament. To address these questions further investigation are required. Further studies need to investigate the importance of LAP2α into mitochondria.

This study shows; 1) the complex of lamin A/C and LAP2α with Cox2 and 2) the co-localization of lamin A/C and LAP2α in mitochondria and nuclei. However, the

function of lamin A/C and/or LAP2α in mitochondria needs further investigation. A main function of mitochondria is to make a balance in utilization and releasing of NO, H_2O_2, O^-_2 through ATP generation and the redox system responding to the needs to cell proliferation, differentiation and apoptosis pathways in health and diseases (Huang *et al.*, 2000; Wang *et al.*, 2000). Since, both lamin A/C and Cox2 have been implicated in ROS production. The measurements of ROS level in presence and absence of A-type lamin was suggested. Therefore, lamin $A/C^{-/-}$ (Y259X) and normal human fibroblast (NHF) cells were then used. Y259X is a fibroblast with a homozygous nonsense mutation in LMNA which does not express A-type lamins and has a slow growth rate (Muchir *et al.*, 2003). ROS levels were very high compared to NHF. To investigate whether increased ROS levels are linked to the localization of lamin A in mitochondria. Three more cell lines were selected $LBR^{-/-}$ homozygous, $LBR^{-/+}$ heterozygous, emerin null. In the study ROS production was always higher in the Lamin $A/C^{-/-}$ cells compared to other nuclear envelope knock out cell lines or control cells treated with 1% DMSO or 5uM Valinomycin. This experiment suggests that the localization of lamin A/C in mitochondria might be important in regulating ROS levels.

Increases of ROS in LMNA null cells were raised a question as how lamin A/C is involved in ROS production. A recent study demonstrated that in Lamin A/C mutant cells prelamin A accumulated, ROS production increased and Cox2 levels strikingly decreased (Caron *et al.*, 2007). In my study, it was confirmed that lamin A/C interacts with Cox2 and localizes in mitochondria. So, two things may explain the importance of this finding. The first one is to look for the expression of Cox2

protein in the presence or absence of lamin A/C. Therefore, NHF, $LBR^{-/+}$, $LBR^{-/-}$, $emerin^{-/-}$ and Lamin $A/C^{-/-}$ cell lines were selected for western blot experiments. The results showed the expression of Cox2 was even in all of the cell lines that were used.

Mitochondrial mass has been implicated in mitochondrial abnormalities and associated with reduction in ATP generation. It was also implicated in myopathy disease (Wredenberg *et al.*, 2002). So, the second one is to look for mitochondrial mass in the presence or absence lamin A/C. The same selection of cell lines was used. The experiments showed there was no change in mitochondrial mass in all the cell lines that were used in this study.

From the study above, the localization of lamin A/C in the mitochondria and it is interaction with Cox2 was implicated in ROS production. However, lamin A/C has no effect on the expression level of Cox2 or on the mitochondrial mass. These findings may implicate lamin A/C in the assembly process of COX by anchoring Cox2 to the right position. It may have special role in forming the mitochondrial unique cristae structure which may have important role in mitochondrial functions. These things need further study.

Mitochondria play an important role in both cell life and death. Mitochondria are essential for the production of ATP, through oxidative phosphorylation. Mitochondria regulate intracellular Ca^{2+} levels and generate reactive oxygen species (ROS). ROS function as cellular switches for signaling pathways involved

in cell growth, cell death, mitogenesis, angiogenesis and carcinogenesis (Desouki *et al.*, 2005). Recent evidence has shown that ROS are implicated in inducing premature senescence through prolonged oxidative DNA-damage in bone marrow (BM) cells enriched for hematopoietic stem cells (HSCs) and progenitor cells (Zhang *et al.*, 2007). Inhibition of one of the mitochondrial respiratory complexes will reduce the complex activity which increases ROS production and reduces cell viability.

Cytochrome c oxidase (COX) also known as complex IV which is the terminal enzyme of MRC, has a unique function in energy metabolism. COX has a critical role in the consumption of molecular oxygen involved in the aerobic part of the energy production of the cell. Because the activity level of COX is low in cancer cells (Chen and Pervaiz, 2009), the cell switches to glycolysis to produce ATP (Marin-Hernandez *et al.*, 2009). Reduction in COX activity causes an elevation of reactive oxygen species (ROS) and a reduction in ATP production in mitochondria from AD derived cells (Cardoso *et al.*, 2004). COX deficiency is involved in Leigh syndrome and fatal and benign infantile myopathies (DiMauro *et al.*, 1983; Rahman *et al.*, 1996). Mutations in the SURF-1 gene on chromosome 9 have been identified in patients with Leigh syndrome. It was suggested that SURF-1 may have an important role in COX assembly (Tiranti *et al.*, 1998; Zhu *et al.*, 1998). Investigations have shown that by using siRNA to subunit Cox Vb of COX holoenzyme (MRC-complex IV) activity was low, mitochondrial ROS was high and cell viability reduced (Campian *et al.*, 2007). Mutations in nuclear genes that encode COX proteins have been reported in Cox10, and Cox15 which are

associated with leukodystrophy, Leigh syndrome, sensorineural deafness and fatal infantile hypertrophic cardiomyopathy (Valnot *et al.*, 2000b; Antonicka *et al.*, 2003a; Antonicka *et al.*, 2003b).

Cox2 is the smallest subunit encoded by mtDNA and assembled to COX. It contains Cu_A center and serves as a docking site for cytochrome c (Capaldi, 1990; Tsukihara *et al.*, 1996). Cox2 is one of the mitochondrial pro-apoptotic proteins including Apaf-1 and caspase-9 (Mazzanti *et al.*, 2006). A putative interaction between Cox2 and epidermal growth factor receptor (EGFR) was confirmed in biochemical and immunoflurescence experiments. This interaction may illustrate the role of Cox2 in apoptosis (Boerner *et al.*, 2004). The expression of nuclear encoded NADPH-oxidase 1 (Nox1) and localized in mitochondria is controlled by Cox2 and this control is mediated by ROS production (Desouki *et al.*, 2005). The p53 gene is commonly mutated in cancer cells. It has been shown that the expression of Cox2 is increased in wild-type but not in mutant p53 colon cancer cells. This shows that p53 regulates Cox2 expression (Yu *et al.*, 1999). In $p53^{-/-}$ mice the mitochondrial respiratory process are reduced because p53 modulates the balance between the utilization of aerobic and glycolytic pathways by regulating the expression of Cox2 (Matoba *et al.*, 2006). It was suggested that p53 is involved in the regulation of Cox2 protein levels.

There is increasing evidence that implicates mtDNA in different diseases. Mutations in the Co I and Co II genes, which encode Cox1 and Cox2 respectively, were reported diseases, such as neonatal-onset hepatic failure, encephalopathy,

fatal infantile hypertrophic cardiomyopathy and spinal muscular atrophy (Jaksch *et al.*, 2000; Valnot *et al.*, 2000a; Salviati *et al.*, 2002). Missense mutations in CO II have been identified in a 14-years old boy with proximal myopathy and lactic acidosis. A thymine to adenine transversion at nucleotide position 7671 in CO II (T7671A) changes a methionine to lysine residue in the middle of the N-terminal region of Cox2. This mutation is a heteroplasmic and has a high level of mutant load (90%) in the skeletal muscle. This result in a dramatic decrease in Cox1 associated with haeme $a_{3,}$ a reduction in cross reactivity of Cox3 and the nuclear encoded subunits of complex IV Vb, VIa, VIb, and VIc. This observation suggests that the structural associations of Cox2 and Cox1 are important in the stable binding of heme a_3 to Cox1 (Rahman *et al.*, 1999). A novel mutation T7587C, in CO II was also found in a patient with Cox deficiency. This mutation changes methionine to threonine with a mutant load of 67% in muscle biopsies and increase ROS level (Clark *et al.*, 1999).

Low levels of mitochondrial activity are associated with high cell proliferation rate (Nisoli *et al.*, 2003; Navarro *et al.*, 2005). Proliferating, embryonic and tumor cells are low in mitochondrial number, Nitric oxide (NO), which also results in low H_2O_2 production (Simonnet *et al.*, 2002)**.** Colon epithelial cells show not only abnormal proliferation, differentiation and apoptosis processes (Bedi *et al.*, 1995), but also is associated with a significantly depressed steady state mitochondrial mRNA (Augenlicht *et al.*, 1991), mitochondrial enzymatic activity (Sun *et al.*, 1981) and alterations in mitochondrial membrane potential (Summerhayes *et al.*, 1982). However, cancer cells over expressing Bcl-2 shows an increase in COX activity,

oxygen consumption and mitochondrial respiration (Desouki *et al.*, 2005; Chen and Pervaiz, 2007). This suggests that Bcl-2 may be able to create an environment in the cancer cell suited for survival by regulating mitochondrial respiration and keeping ROS levels under control.

Lamin A/C mutations and a lack of Lamin A function have been implicated in a wide range of different diseases such as skeletal and cardiac muscular dystrophies and premature aging (Donadille *et al.*, 2005). A lack of lamin A activity in cardiomyocyte nuclei results in altered nuclear shape, a distorted nuclear envelope, severe heterochromatin reorganization and nuclear interior remodeling (Fidzianska *et al.*, 2008). A mutation in the lamin A/C gene (LMNA) has been reported to be the cause of dilated cardiomyopathy (DCM) (Fujimori *et al.*, 2008). A subject with familial dilated cardiomyopathy has lamin A mutations E203G, E203K and K201R. All are associated with increased cell death and decreased lamin A sumoylation, which may demonstrate the importance of SUMO modification in normal lamin A function (Zhang and Sarge, 2008). However, a recent study demonstrated that in Lamin A/C mutant cells prelamin A accumulated, ROS production increased and Cox2 levels strikingly decreased (Caron *et al.*, 2007). Familial partial lipodystrophy of Dunnigan type 2 (FPLD2) was caused by mutations in LMNA. Belong of those R482W and R439C that associated with significant increase in ROS upon induction of oxidative stress by H_2O_2 (Verstraeten *et al.*, 2009). These findings implicate lamin A/C in ROS production within the cell. This led to the link between lamin A/C and mitochondrial function as the main source of ROS production in cells.

The above evidence implicates lamin A/C in the apoptotic pathway and ROS productions as well as the more well known roles in nuclear structure and function. The new findings in this study demonstrate the localization of lamin A/C and LAP2α in mitochondria and their interaction to Cox2. The interaction with Cox2 may be helps us understand the link between lamin A/C, ROS production and the apoptosis pathway. It becomes obvious that A-type lamins have no effects on the expression level of Cox2 and on the mitochondrial mass. Missense mutation in Co II have been implicated in a dramatic change in COX structure, decrease Cox1 associated with haeme a_3 and reduction in cross reactivity of Cox3 (Rahman *et al.*, 1999). This may suggest the importance of localization of A-type lamins in mitochondria and it is interaction to Cox2, which may implicate A-type lamins in the assembling of Cox2 into COX.

It was demonstrated a long time ago that Lamin A/C contains a specific chromatin binding site which may be important in interacting with other cellular structures (Glass *et al.*, 1993). Recently, it was found that lamin A/C is required for a reduction of heterochromatin in viral promoters during lytic infection. This result shows that lamin A/C can serve as a molecular scaffold for DNA and the protein complexes that regulate both euchromatin and heterochromatin modification (Silva *et al.*, 2008). It was also shown that disruption of lamin A/C prevents plasmid DNA transport through the nuclear envelope (Ondrej *et al.*, 2008). In conclusion, it is important to note that lamin A/C is localized in compartments of the cell that contain DNA, which may link the importance of lamin A/C in regulating DNA structure and function. If this exists it may implicates lamin A/C in two major roles.

One links with the nucleus and the other to the mitochondria. The localization of lamin A is associated with localization of other proteins like lamin C and LAP2α. Further experiments need to be done to investigate more about the function of lamin A/C and LAP2α in mitochondria. Lamin A/C and LAP2α are implicated in binding to nuclear chromatin. Therefore the structure and function of mtDNA or mtDNA damage need to be investigated in lamin A/C$^{-/-}$ or LAP2α$^{-/-}$ cell lines. Because the expression of Cox2 was normal in lamin A/C$^{-/-}$ cells while ROS production was high and mitochondrial mass was similar, the localization of Cox2 in COX holoenzyme in lamin A/C$^{-/-}$ cells needs to be investigated. It may also be interesting to look for the expression and function of the redox proteins in lamin A/C$^{-/-}$ verses wild-type. Lamins have direct role in supporting the nucleus shape, it will be interesting to check the shape of mitochondria in lamin A/C$^{-/-}$ verses wild-type. Because it is difficult to use antibodies to identify a protein localize in the mitochondrial matrix, I could not demonstrate immunoflurescence of lamin A/C or LAP2α. To address this full length of lamin A/C and LAP2α with GFP at C-terminal need to be constructed and used for studying the importing and localization of A-type lamin inside mitochondria.

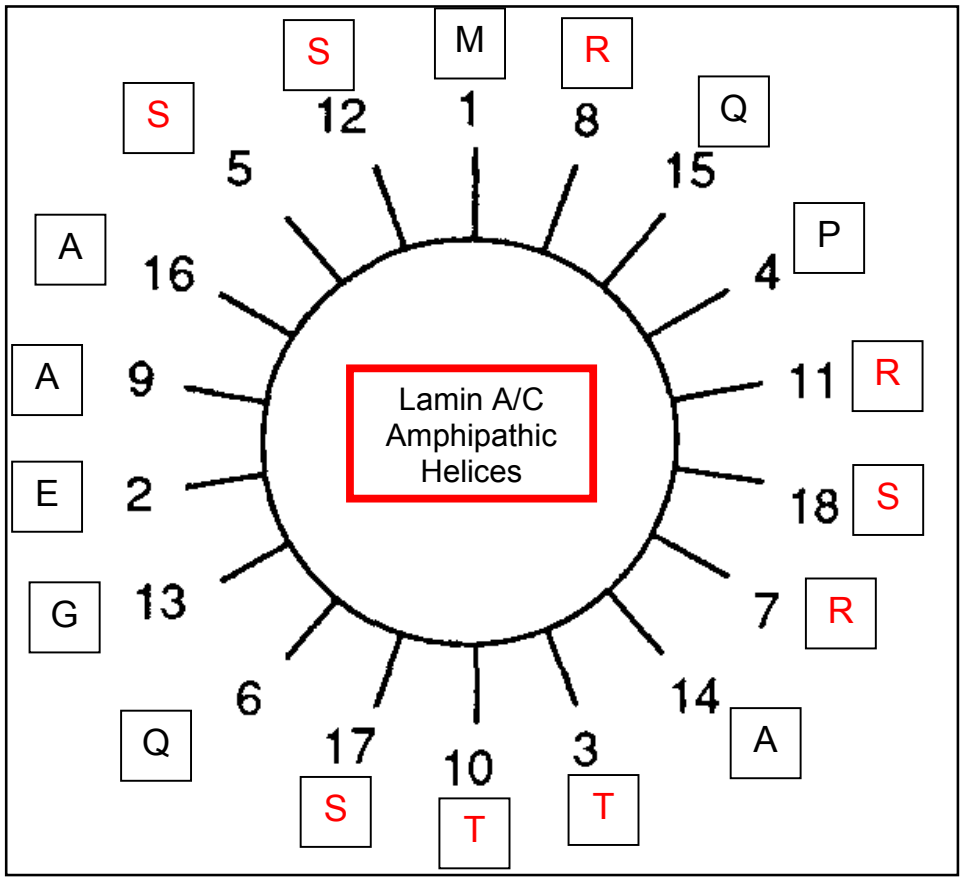

This is the distribution of the first 18 amino acids of the lamin A/C protein sequence according to gene bank data accession no. NM_170707. It shows the positive charged amino acids (red) are distributed approximately on one side of the helical wheel. This may present an amphipathic helix that forms a mitochondrial targeting sequence (MTS).

Figure 6.1

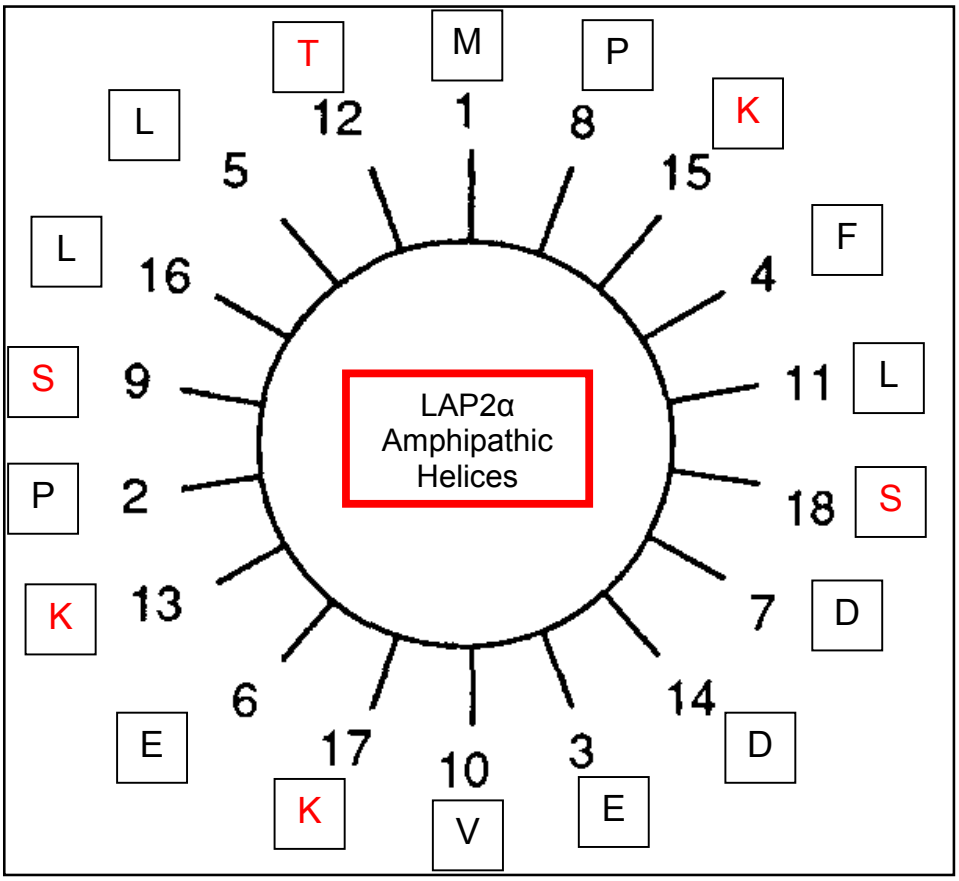

This is the distribution of the first 18 amino acids of the LAP2α protein sequence according to gene bank data accession no. U09086. It shows the positive charged amino acids (red) are distributed approximately on one side of the helical wheel. This may present an amphipathic helix that forms a mitochondrial targeting sequence (MTS).

Figure 6.2

Appendix I: Stock Solutions.

1. DEPC-DD Water

1000 ml of	Double Dionized water
200 ul of	Diethyl Pyrocarbonate DEPC (Sigma)

Stir over night.

Autoclave cycle is 121^{o}C, 15 psig (1bar) for 20 minutes.

2. 1X PBS RNAse free.

- One tablet of PBS (sigma) was dissolved in 200ml DEPC-DD Water.
- Correct pH to 7.2.
- Filtered through 0.2um syringe.

3. 10X TAE (Tris-Acetate EDTA).

48.4g	Tris-Base (Sigma)
11.4ml	Glacial Acetic acid
20ml	0.5M EDTA (pH 8.0)

Made up to 1 liter with DD-water.

4. 50% PEG solution.

167.55g Polyethylene glycol, PEG3350 (Sigma)
Made up to 100 ml with DD-water.
Autoclave cycle is 121^{o}C, 15 psig (1bar) for 20 minutes.

5. 10X TE Buffer.

4.8g	Tris-Base (Sigma)
2ml	0.5M EDTA (pH 8.0)
90mls	DD-water

pH adjusted to 8.0 with 1NHcl.
Made up to 100ml with DD-water.
Autoclave cycle is 121^{o}C, 15 psig (1bar) for 20 minutes.

6. 10X LiAc solution.

1 M lithium acetate (Sigma)
Adjust pH to 7.5 with acetic acid.
Autoclave cycle is 121^{o}C, 15 psig (1bar) for 20 minutes.

7. PEG/LiAc solution.

In the day of transformation mix this in 15 ml falcon tube.

8mls	50% PEG.
1ml	10X TE.
1ml	10X LiAc.

8. 20 X TBST (Tris Buffer Saline Plus Tween).

Tris- Base	24.2 g
NaCl	174.4 g

Made up to 1 liter with DD-water.

Adjust pH to 7.4 with 1 N Hcl .

Tween	2.5 ml/L (0.25%)

To make 2 X TBST:

20 X TBST	100 ml

Made up to 1 liter with DD-Water.

9. 10 X Transfer Buffer.

Tris-Base	30.2	g
Glycine	144	g
SDS (Solid)	0.2	g (0.02%), or 2ml of 10% SDS solution.

Made up to 1 liter with DD-water.

To make 1 X Transfer Buffer.

10 X Transfer Buffer	100 ml
Methanol	200 ml

Made up to 1 liter with DD-water.

10. 10 X Running Buffer.

Tris-Base	30.2	g
Glycine	144	g
SDS (Solid)	10	g (1%), or 100ml of 10% SDS solution.

Made up to 1 liter with DD-water.

To make 1X Running Buffer:

10 X Running Buffer	100 ml

Made up to 1 liter with DD-water.

11. Sample Buffer.

	2 X	4X	5 X	Final Concentration
1 M- Tris pH 6.8	1 ml	2 ml	2.5 ml	50 mM
DTT	0.31 g	0.62 g	0.78 g	100 mM
SDS	0.4 g	0.8 g	1 g	2 %
Bromphenol Blue	0.02 g	0.04 g	0.05 g	0.1%
Glycerol	2 ml	4 ml	5 ml	10 %

Made up to 10ml with DD-water.

Filter through whatman paper.

Aliquot in small volume and store at -20^{o}c.

12. Hypotonic solution.

KCL	10 mM
HEPES-KOH	10 Mm
pH adjusted	7.4
$MgCL_2$	1.5 Mm
Triton X-100	0.1 %
DTT*	1 mM
Protease Inhibitor*	1 X

Made up to 50ml with DD-water. Store at 4^{o}c.

13. Hypertonic solution.

NaCl	0.5 mM
KCL	10 mM
HEPES-KOH	10 mM
pH adjusted	7.4
$MgCL_2$	1.5 mM
Triton X-100	0.1 %
DTT*	1 mM
Protease Inhibitor*	1 X

Made up to 50ml with DD-water. Store at 4^{o}c.

14. NP40.

Tris- HCL	50 mM
Na CL	150 mM
NP-40	1 %

pH adjusted to 8.0 with 1 N Hcl.

15. 4 X Laemmli Sample Buffer (LSB).

Tris-HCl pH 6.8 0.25 M	5	ml
SDS 0.6%	0.6	g
Sucrose 40%	4	g

Made up to 10ml with DD-Water.

16 Fixation Buffers.

- **Double strength fixation buffer.**
  8% paraformuldehyde fresh made in 0.1M PBS.

- **Single strength fixation buffer.**
  4% paraformuldehyde fresh made in 0.1M PBS.

Appendix II: Medium Preparation.

1. YPDA (Yeast Peptone Dextrose Adenine):

20g Peptone (DIFCO)

10g Yeast Extract (DIFCO)

935ml DD-water

Autoclave cycle is 121^{o}C, 15 psig (1bar) for 20 minutes.

Cool down the medium at 55^{o}c water bath, then add:

50ml 50% Glucose (BDH)

15ml 0.2% Adenine (Sigma)

2. YPDA Agar:

20g Peptone (DIFCO)

10g Yeast Extract (DIFCO)

20g Agar (DIFCI)

935ml DD-water

Autoclave cycle is 121^{o}C, 15 psig (1bar) for 20 minutes.

Cool down the medium at 55^{o}c water bath, then add:

50ml 50% Glucose (BDH)

15ml 0.2% Adenine (Sigma)

Pour 25ml/100mm diameter plate or 60ml/150mm diameter plate.

3. SD medium (Synthetic Defined Medium):

6.7g yeast Nitrogen Base 9 (DIFCO)

What ever says in DO supplements amino acid (BD Bioscience)

950ml DD-water

Autoclave cycle is 121^{o}C, 15 psig (1bar) for 20 minutes.

Cool down the medium at 55^{o}c water bath, then add:

50ml 50% Glucose (BDH)

4. SD Agar:

20g Agar (DIFCO)

6.7g yeast Nitrogen Base 9 (DIFCO)

What ever says in DO supplements amino acid (BD Bioscience)

950ml DD-water

Autoclave cycle is 121^{o}C, 15 psig (1bar) for 20 minutes.

Cool down the medium at 55^{o}c water bath, and then add:

50ml 50% Glucose (BDH)

Pour 25ml/100mm diameter plate or 60ml/150mm diameter plate.

5. LB medium (Luria-Bertani Medium):

25g Nutrient Broth (LAB M)

Made up to 1 liter with DD-water

Autoclave cycle is 121^{o}C, 15 psig (1bar) for 20 minutes.

6. LB Agar:

28g Nutrient Agar (LAB M)

Made up to 1 liter with DD-water.

Autoclave cycle is 121^{o}C, 15 psig (1bar) for 20 minutes.

Pour 25ml/100mm diameter plate or 60ml/150mm diameter plate.

7. S.O.C:

20g	Peptone (DIFCO)
5g	Yeast Extract (DIFCO)
0.5g	$Nacl_2$
950ml	DD-water
10ml	Kcl (1.8g of kcl dissolved in 100ml DD-water)

Adjust pH to 7.0 with 5 N NaoH.

Made up to 1 liter with DD-water.

Autoclave cycle is 121^{o}C, 15 psig (1bar) for 20 minutes.

Cool down the media at 55^{o}C water bath, and then add:

20ml	Glucose (1M)

Aliquot them in 50ml tube and keep at –20^{o}c.

8. SDS-Page gel preparation.

I) Preparation of 10 ml of Resolving Gel.

	10%	12%	
DD-H20	5.3	4.9	ml
ProSieve® 50 gel solution	2.0	2.4	ml
1.5 M Tris- HCL, pH 8.8	2.5	2.5	ml
10% SDS solution	100	100	ul
10% APS*	100	100	ul
TEMED	4.0	4.0	ul

*Ammonium per sulfate (APS) prepared freshly just prior to use.

II) Preparation of 5 % of Stacking Buffer.

	3 ml	5 ml	
DD-H20	2.25	3.75	ml
ProSieve® 50 gel solution	0.5	0.3	ml
1.5 M Tris- HCL, pH 6.8	0.4	0.65	ml
10% SDS solution	30	50	ul
10% APS*	30	50	ul
TEMED	5.0	5.0	ul

*Ammonium per sulfate (APS) prepared freshly just prior to use.

Appendix III: Competent cells preparation.

1. **DH5α E. Coli chemical competent cells:**
   a) 20ul of glycerol stock of DH5α was spread on new LB agar plate no antibiotics.
   b) Next day, one nice big colony was inoculated in 10ml LB media no antibiotics shaking overnight at 225-rpm and 37^{o}C.
   c) 25ml of LB media with no antibiotics was added in each 4 of 100ml flasks. 250ul of overnight culture was mixed to each flask, shaking at 225 rpm and 37^{o}C. Every 30min the cell growth was measured by using spectrophotometer OD_{600}, until it gave reading between 0.25-0.5 OD.
   d) Cells were transferred into 2 of 50ml falcon tubes and chill on ice for 10mins.
   e) The tubes were centrifuge at 2500rpm for 10mins at 4^{o}C.
   f) The cell pellet was resuspended in 20ml of Buffer I and incubated on ice for 30mins (Resuspend the cells in 1/5 of original volume).
   g) The tubes were centrifuge at 2500rpm for 10mins at 4^{o}C.
   h) The cell pellet was resuspended in 4mls of Buffer II and incubated on ice for 15mins (Resuspend the cell pellets in 1/25 of the original volume).
   i) The cells aliquot in 50ul/vial and freeze at –80^{o}C.

Competency Buffer I (200ml):	Competency Buffer II (200ml):
20mls of 1M KCl	2mls of 1 M KCL
12mls of 1M CaCL2	15mls of 1M CaCL2
30mls of Glycerol.	30mls of Glycerol.
1.2ml of 5 M K acetate.	4mls of 5 M K acetate.
118ml DD-water	133ml DD-water
PH 5.8 with 0.2M acetic acid.	PH 6.8 with 10M NaoH
. Made up to 200ml of DD-water.	Made up to 200ml of DD-water.

2. **Yeast Strain Competent cells:**

These competent cells should be freshly made on the day of the transformation.

a) 20ul of glycerol stock of yeast strain AH109 or Y187 were spread on YPDA agar plate.
b) One colony of 2mm in diameter was inoculated in 2ml of YPDA and vortex vigorously for 5 mins to disperse the clumps.
c) The cell mixture was inoculated in a flask contains 50mls of YPDA medium. Overnight shaking at 225rpm in 30^{o}C. Next day, the cell density were measured at OD_{600} it should >1.5.
d) 30mls of the culture were transferred into 300ml of YPDA medium. The cell growth was measured at OD_{600} every 30mins until it gives OD_{600} 0.4-0.6.
e) The cells were spin down at 1000g for 5mins at room temperature.
f) The supernatant were discarded and the cell pellet were resuspend in 5ml of 1X TE buffer.
g) Step f was repeated.
h) Then the cells pellet were suspended in 1.5ml of freshly prepared sterile 1X TE/1X LiAc (See Appendix 1). Keep these cells on ice until use.

3. Yeast Strain Transformations:

At the day of transformation when the competent cells are ready for using the transformation step is as follow:

a) 0.1ug of plasmid and 0.1mg of denatured herring testes carrier DNA was mixed in 1.5 ml sterile eppendorf tube.
b) 100ul of the competent yeast cells (above) was added to each transformation tube.
c) 600ul of sterile fresh mixture of PEG/LiAc (see appendix1) was added. The whole mixture was vortex well and incubated at 30^{o}C for 30mins with shaking at 220rpm.
d) Then 70ul of DMSO was added and mix well by gently inversion.
e) The tube were heat shock for 15mins in 42^{o}C water bath. Chill on ice for 2mins.
f) The it spin down for 30 seconds at 14000rpm at room temperature. The supernatant were discarded and the cells were resuspended in 500ul of 1X TE.
g) Then, 100ul were spread on each selective plate of 100mm or 200ul of 150mm. Incubate at 30^{o}C incubator until the colonies will appear.

Appendix IV: Gene accession and DNA sequencing.

Appendix IV-1a: Lamin A/C gene bank.

Homo sapiens lamin A/C (LMNA), transcript variant 1, mRNA. Accession no. NM_170707. The full length gene bank mRNA of lamin A/C that used to design PCR primer to generate bait construct.

```
LOCUS       NM_170707               3181 bp    mRNA    linear   PRI 24-SEP-2005
DEFINITION  Homo sapiens lamin A/C (LMNA), transcript variant 1, mRNA.
ACCESSION   NM_170707
VERSION     NM_170707.1  GI:27436945
KEYWORDS    .
SOURCE      Homo sapiens (human)
  ORGANISM  Homo sapiens
            Eukaryota; Metazoa; Chordata; Craniata; Vertebrata; Euteleostomi;
            Mammalia; Eutheria; Euarchontoglires; Primates; Catarrhini;
            Hominidae; Homo.
REFERENCE   1  (bases 1 to 3181)
  AUTHORS   Sylvius,N., Bilinska,Z.T., Veinot,J.P., Fidzianska,A.,
            Bolongo,P.M., Poon,S., McKeown,P., Davies,R.A., Chan,K.L.,
            Tang,A.S., Dyack,S., Grzybowski,J., Ruzyllo,W., McBride,H. and
            Tesson,F.
  TITLE     In vivo and in vitro examination of the functional significances of
            novel lamin gene mutations in heart failure patients
  JOURNAL   J. Med. Genet. 42 (8), 639-647 (2005)
   PUBMED   16061563
REFERENCE   2  (bases 1 to 3181)
  AUTHORS   Young,J., Morbois-Trabut,L., Couzinet,B., Lascols,O., Dion,E.,
            Bereziat,V., Feve,B., Richard,I., Capeau,J., Chanson,P. and
            Vigouroux,C.
  TITLE     Type A insulin resistance syndrome revealing a novel lamin A
            mutation
  JOURNAL   Diabetes 54 (6), 1873-1878 (2005)
   PUBMED   15919811
  REMARK    GeneRIF: This study further extends the vast range of diseases
            linked to LMNA mutations and identifies another genetic cause for
            the type A insulin resistance syndrome.
REFERENCE   3  (bases 1 to 3181)
  AUTHORS   Broers,J.L., Kuijpers,H.J., Ostlund,C., Worman,H.J., Endert,J. and
            Ramaekers,F.C.
  TITLE     Both lamin A and lamin C mutations cause lamina instability as well
            as loss of internal nuclear lamin organization
  JOURNAL   Exp. Cell Res. 304 (2), 582-592 (2005)
   PUBMED   15748902
  REMARK    GeneRIF: Our findings suggest a loss of function of A-type lamin
            mutant proteins in the organization of intranuclear chromatin and
            predict the loss of gene regulatory function in laminopathies.
REFERENCE   4  (bases 1 to 3181)
  AUTHORS   Walter,M.C., Witt,T.N., Weigel,B.S., Reilich,P., Richard,P.,
            Pongratz,D., Bonne,G., Wehnert,M.S. and Lochmuller,H.
  TITLE     Deletion of the LMNA initiator codon leading to a neurogenic
            variant of autosomal dominant Emery-Dreifuss muscular dystrophy
  JOURNAL   Neuromuscul. Disord. 15 (1), 40-44 (2005)
   PUBMED   15639119
  REMARK    GeneRIF: This study identified a novel mutation in the 5' region of
            the LMNA gene -3del15, resulting in the loss of 15 nucleotides from
            -3 to +12, including the translation ATG initiator codon.
REFERENCE   5  (bases 1 to 3181)
  AUTHORS   Kirschner,J., Brune,T., Wehnert,M., Denecke,J., Wasner,C.,
            Feuer,A., Marquardt,T., Ketelsen,U.P., Wieacker,P., Bonnemann,C.G.
            and Korinthenberg,R.
  TITLE     p.S143F mutation in lamin A/C: a new phenotype combining myopathy
            and progeria
  JOURNAL   Ann. Neurol. 57 (1), 148-151 (2005)
   PUBMED   15622532
  REMARK    GeneRIF: this is the first report of a patient combining features
            of these two phenotypes because of a single mutation(S143F)
            mutation in LMNA.
REFERENCE   6  (bases 1 to 3181)
  AUTHORS   Navarro,C.L., De Sandre-Giovannoli,A., Bernard,R., Boccaccio,I.,
            Boyer,A., Genevieve,D., Hadj-Rabia,S., Gaudy-Marqueste,C.,
            Smitt,H.S., Vabres,P., Faivre,L., Verloes,A., Van Essen,T.,
            Flori,E., Hennekam,R., Beemer,F.A., Laurent,N., Le Merrer,M.,
            Cau,P. and Levy,N.
  TITLE     Lamin A and ZMPSTE24 (FACE-1) defects cause nuclear disorganization
            and identify restrictive dermopathy as a lethal neonatal
            laminopathy
  JOURNAL   Hum. Mol. Genet. 13 (20), 2493-2503 (2004)
   PUBMED   15317753
  REMARK    GeneRIF: Heterozygous splicing mutation in the LMNA gene, leading
            to the complete or partial loss of exon 11 in mRNAs encoding Lamin
            A in restrictive dermopathy was found.
REFERENCE   7  (bases 1 to 3181)
  AUTHORS   Schirmer,E.C. and Gerace,L.
  TITLE     The stability of the nuclear lamina polymer changes with the
            composition of lamin subtypes according to their individual binding
            strengths
```

Appendix IV-1b: Lamin A/C-pGBKT7 bait construction.

The sequence of the open reading frame of lamin A/C-pGBKT7 constructs. An alternative method used to double check the orientation of the construct. PCR was performed on one of the miniprep that showed the right orientation by using restriction enzyme and colony PCR. The PCR was performed by using T7-promoter PCR primer and gene specific downstream PCR primer. Then, DNA sequencing applied by using T7-promoter PCR primer. As we see in the sequence there is no stop codon generated inside the sequence that may affect the fusion of Gal4-DNA Binding domain to the gene sequence.

Applied Biosystems

Signal G:309 A:167 T:114 C:272 AvSig:215
Basecaller-3730POP7SR.bcp
ABI 1.6.0 Cap:36

E10_270808
F_LaminAK-pGBKT7
DT3730POP7{BDv3}.mob
Pts 1883 to 14000 Pk1 Loc:1883
Version 5.1.1 HiSQV Bases: 0 Primer T7 Promoter

Inst Model/Name 3730/DNA3730-16111-007
Aug 27,2008 05:40PM, BST
Spacing:13.64 Pts/Panel2000
Plate Name: 270808

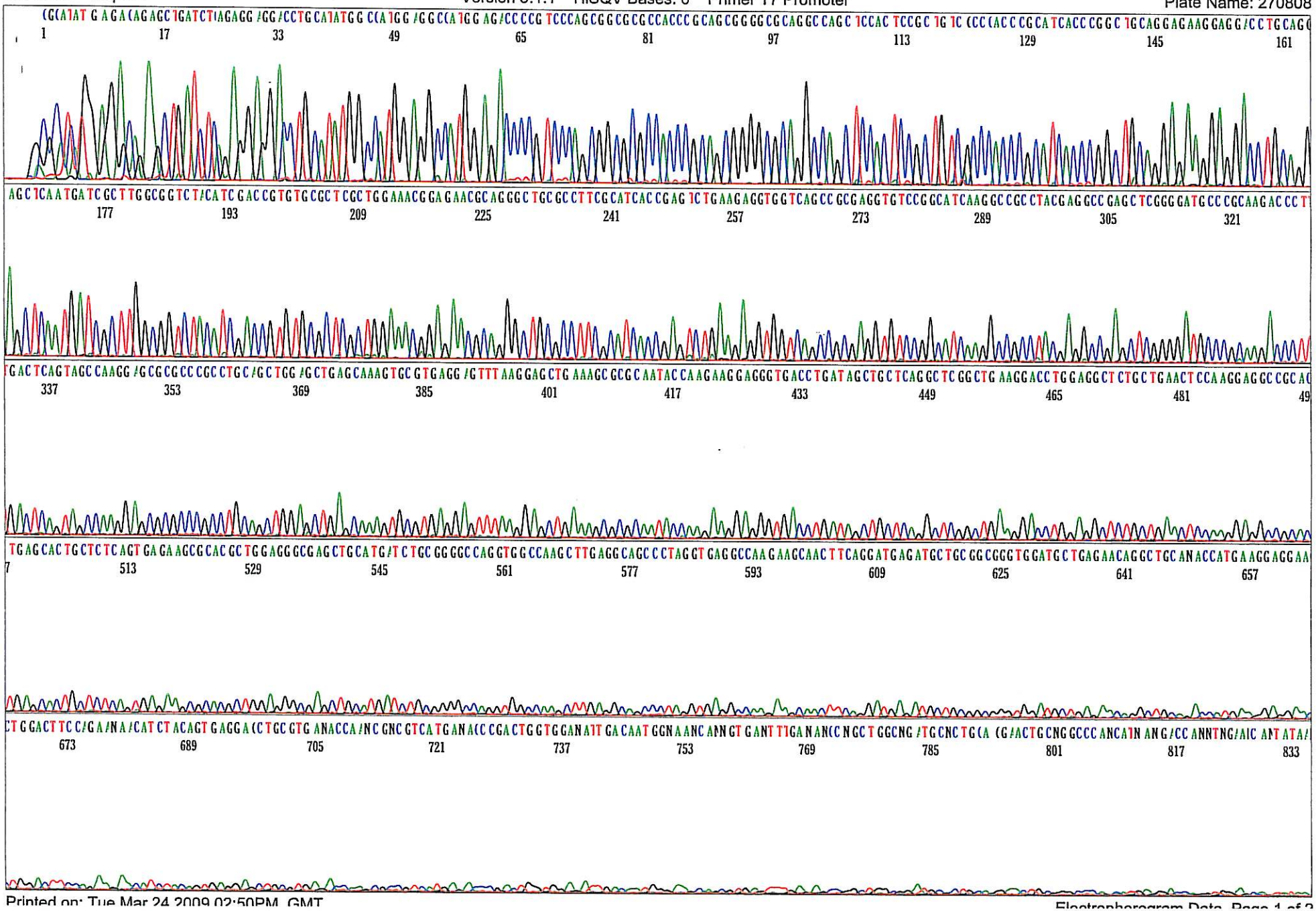

Appendix IV-2a: LAP2α gene bank.

Human thymopoietin alpha mRNA (LAP2α) complete cds. Accession no. U09086. The full length gene bank mRNA of LAP2α that used to design PCR primer to generate bait constructs.

NCBI | Nucleotide banner | My NCBI [Sign In] [Register]

PubMed Nucleotide Protein Genome Structure PMC Taxonomy OMIM Books

Search Nucleotide for Go Clear

Limits Preview/Index History Clipboard Details

Display GenBank Show 20 Send to

Range: from begin to end Reverse complemented strand Features: SNP CDD MGC HPRD STS tRNA Refresh

1: U09086. Reports Human thymopoieti...[gi:508724] Links

```
LOCUS       HSU09086                2490 bp    mRNA    linear   PRI 09-JUL-1994
DEFINITION  Human thymopoietin alpha mRNA, complete cds.
ACCESSION   U09086
VERSION     U09086.1  GI:508724
KEYWORDS    .
SOURCE      Homo sapiens (human)
  ORGANISM  Homo sapiens
            Eukaryota; Metazoa; Chordata; Craniata; Vertebrata; Euteleostomi;
            Mammalia; Eutheria; Euarchontoglires; Primates; Catarrhini;
            Hominidae; Homo.
REFERENCE   1  (bases 1 to 2490)
  AUTHORS   Harris,C.A., Andryuk,P.J., Cline,S., Chan,H.K., Natarajan,A.,
            Siekierka,J.J. and Goldstein,G.
  TITLE     Three distinct human thymopoietins are derived from alternatively
            spliced mRNAs
  JOURNAL   Proc. Natl. Acad. Sci. U.S.A. 91 (14), 6283-6287 (1994)
   PUBMED   7517549
REFERENCE   2  (bases 1 to 2490)
  AUTHORS   Harris,C.A.
  TITLE     Direct Submission
  JOURNAL   Submitted (20-APR-1994) Crafford A. Harris, Immunobiology Research
            Institute, Route 22 East, Annandale, NJ 08801-0999, USA
FEATURES             Location/Qualifiers
     source          1..2490
                     /organism="Homo sapiens"
                     /mol_type="mRNA"
                     /db_xref="taxon:9606"
                     /tissue_type="thymus"
     CDS             205..2289
                     /codon_start=1
                     /product="thymopoietin alpha"
                     /protein_id="AAB60329.1"
                     /db_xref="GI:508725"
                     /translation="MPEFLEDPSVLTKDKLKSELVANNVTLPAGEQRKDVYVQLYLQH
                     LTARNRPPLPAGTNSKGPPDFSSDEEREPTPVLGSGAAAAGRSRAAVGRKATKKTDKP
                     RQEDKDDLDVTELTNEDLLDQLVKYGVNPGPIVGTTRKLYEKKLLKLREQGTESRSST
                     PLPTISSSAENTRQNGSNDSDRYSDNEEGKKKEHKKVKSTRDIVPFSELGTTPSGGGF
                     FQGISFPEISTRPPLGSTELQAAKKVHTSKGDLPREPLVATNLPGRGQLQKLASERNL
                     FISCKSSHDRCLEKSSSSSSQPEHSAMLVSTAASPSLIKETTTGYYKDIVENICGREK
                     SGIQPLCPERSHISDQSPLSSKRKALEESESSQLISPPLAQAIRDYVNSLLVQGGVGS
                     LPGTSNSMPPLDVENIQKRIDQSKFQETEFLSPPRKVPRLSEKSVEERDSGSFVAFQN
                     IPGSELMSSFAKTVVSHSLTTLGLEVAKQSQHDKIDASELSFPFHESILKVIEEEWQQ
                     VDRQLPSLACKYPVSSREATQILSVPKVDDEILGFISEATPLGGIQAASTESCNQQLD
                     LALCRAYEAAASALQIATHTAFVAKAMQADISQAAQILSSDPSRTHQALGILSKTYDA
                     ASYICEAAFDEVKMAAHTMGNATVGRRYLWLKDCKINLASKNKLASTPFKGGTLFGGE
                     VCKVIKKRGNKH"
     variation       1999
                     /replace="g"
ORIGIN
        1 gttcgtagtt cggctctggg gtcttttgtg tccgggtctg gcttggcttt gtgtccgcga
       61 gtttttgttc cgctccgcag cgctcttccc gggcaggagc cgtgaggctc ggaggcggca
      121 gcgcggtccc cggccaggag caagcgcgcc ggcgtgagcg gcggcggcaa aggctgtggg
      181 gagggggctt cgcagatccc cgagatgccg gagttcctgg aagacccctc ggtcctgaca
      241 aaagacaagt tgaagagtga gttggtcgcc aacaatgtga cgctgccggc cggggagcag
      301 cgcaaagacg tgtacgtcca gctctacctg cagcacctca cggctcgcaa ccggccgccg
      361 ctccccgccg gcaccaacag caaggggccc ccggacttct ccagtgacga agagcgcgag
      421 cccaccccgg tcctcggctc tggggccgcc gccgcgggcc ggagccgagc agccgtcggc
      481 aggaaagcca caaaaaaaac tgataaaccc agacaagaag ataaagatga tctagatgta
      541 acagagctca ctaatgaaga tcttttggat cagcttgtga aatacggagt gaatcctggt
      601 cctattgtgg gaacaaccag gaagctatat gagaaaaagc ttttgaaact gagggaacaa
      661 ggaacagaat caagatcttc tactcctctg ccaacaattt cttcttcagc agaaaataca
      721 aggcagaatg gaagtaatga ttctgacaga tacagtgaca atgaagaagg aaagaagaaa
      781 gaacacaaga aagtgaagtc cactagggat attgttcctt tttctgaact tggaactact
      841 ccctctggtg gtggattttt tcagggtatt tcttttcctg aaatctccac ccgtcctcct
      901 ttgggcagta ccgaactaca ggcagctaag aaagtacata cttctaaggg agacctacct
      961 agggagcctc ttgttgccac aaacttgcct ggcaggggac agttgcagaa gttagcctct
     1021 gaaaggaatt tgtttatttc atgcaagtct agccatgata ggtgtttaga gaaaagttct
     1081 tcgtcatctt ctcagcctga acacagtgcc atgttggtct ctactgcagc ttctccttca
     1141 ctgattaaag aaaccaccac tggttactat aaagacatag tagaaaatat ttgcggtaga
     1201 gagaaaagtg gaattcaacc attatgtcct gagaggtccc atatttcaga tcaatcgcct
     1261 ctctccagta aaaggaaagc actagaagag tctgagagct cacaactaat ttctccgcca
     1321 cttgcccagg caatcagaga ttatgtcaat tctctgttgg tccagggtgg ggtaggtagt
     1381 ttgcctggaa cttctaactc tatgccccca ctggatgtag aaaacataca gaagagaatt
     1441 gatcagtcta agtttcaaga aactgaattc ctgtctcctc caagaaaagt ccctagactg
     1501 agtgagaagt cagtggagga aagggattca ggttccttta tggcatttca gaacatacct
     1561 ggatccgaac tgatgtcttc ttttgccaaa actgttgtct ctcattcact cactacctta
     1621 ggtctagaag tggctaagca atcacagcat gataaaatag atgcctcaga actatctttt
     1681 cccttccatg aatctatttt aaaagtaatt gaagaagaat ggcagcaagt tgacaggcag
     1741 ctgccttcac tggcatgcaa atatccagtt tcttccaggg aggcaacaca gatattatca
     1801 gttccaaaag tagatgatga aatcctaggg tttatttctg aagccactcc actaggaggt
```

```
    1861 attcaagcag cctccactga gtcttgcaat cagcagttgg acttagcact ctgtagagca
    1921 tatgaagctg cagcatcagc attgcagatt gcaactcaca ctgcctttgt agctaaggct
    1981 atgcaggcag acattagtca agctgcacag attcttagct cagatcctag tcgtacccac
    2041 caagcgcttg ggattctgag caaaacatat gatgcagcct catatatttg tgaagctgca
    2101 tttgatgaag tgaagatggc tgcccatacc atgggaaatg ccactgtagg tcgtcgatac
    2161 ctctggctga aggattgcaa aattaattta gcttctaaga ataagctggc ttccactccc
    2221 tttaaaggtg gaacattatt tggaggagaa gtatgcaaag taattaaaaa gcgtggaaat
    2281 aaacactagt aaaattaagg acaaaaagac atctatctta tctttcaggt actttatgcc
    2341 aacattttct tttctgttaa ggttgtttta gtttccagat agggctaatt acaaaatgtt
    2401 aagcttctac ccatcaaatt acagtataaa agtaattgcc tgtgtagaac tacttgtctt
    2461 ttctaaagat ttgcgtagat aggaagcctg
//
```

Appendix IV-2b: LAP2α-pGBKT7 bait construction.

The sequence of the open reading frame of LAP2α-pGBKT7 constructs. An alternative method used to double check the orientation of the construct. PCR was performed on one of the miniprep that showed the right orientation by using restriction enzyme and colony PCR. The PCR was performed by using T7-promoter PCR primer and gene specific downstream PCR primer. Then, DNA sequencing applied by using T7-promoter PCR primer. As we see in the sequence there is no stop codon generated inside the sequence that may affect the fusion of Gal4-DNA Binding domain to the gene sequence.

Applied Biosystems

Signal G:457 A:377 T:297 C:474 AvSig:401
Basecaller-3730POP7SR.bcp
ABI 1.6.0 Cap:35

F10_270808
F_Lap2-pGBKT7
DT3730POP7{BDv3}.mob
Pts 1895 to 18760 Pk1 Loc:1895
Version 5.1.1 HiSQV Bases: 0 Primer T7 Promoter

Inst Model/Name 3730/DNA3730-16111-007
Aug 27,2008 05:40PM, BST
Spacing:13.29 Pts/Panel2000
Plate Name: 270808

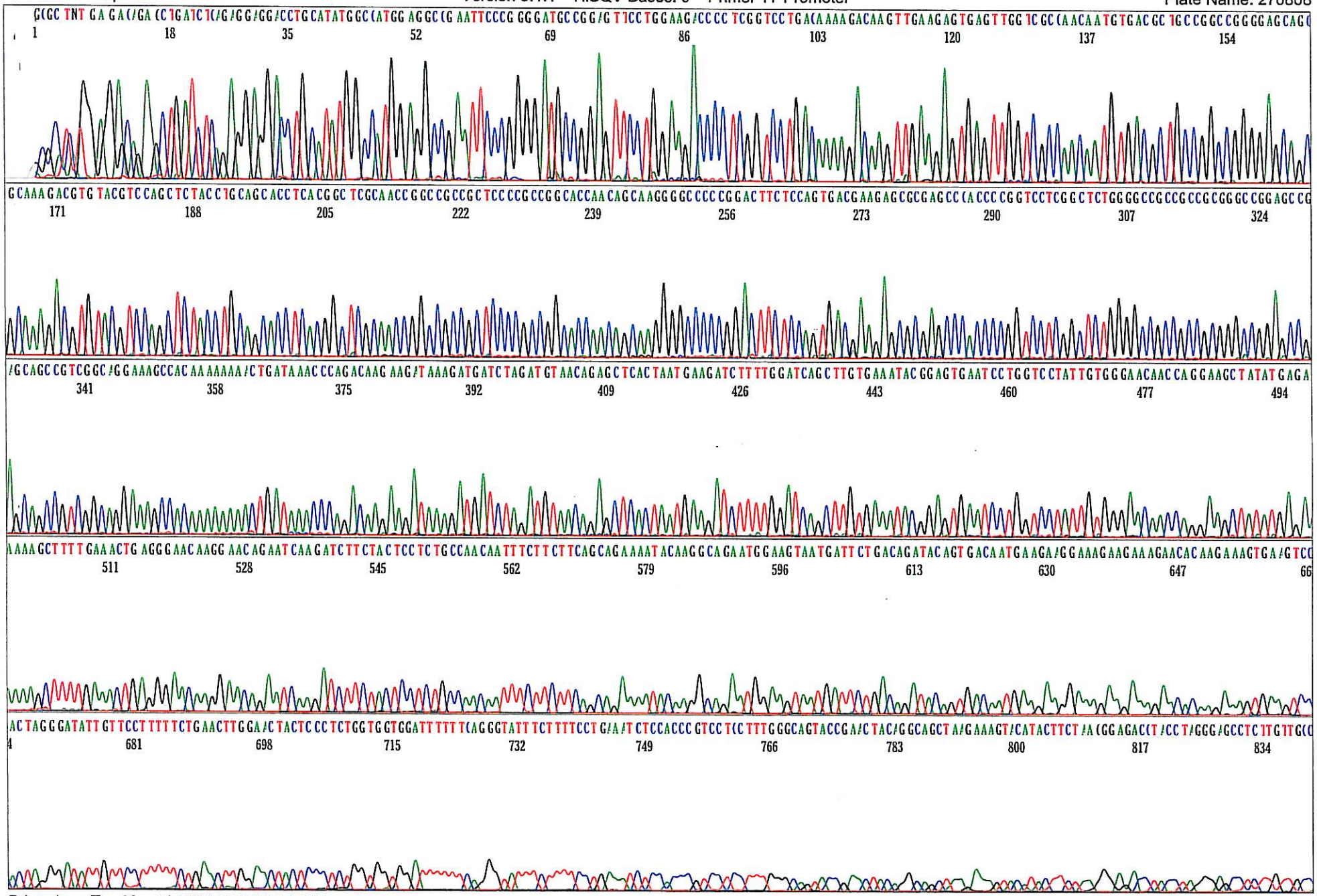

Printed on: Tue Mar 24 2009 02:50PM GMT

Appendix IV-3a: Conig 5 result of mating Lamin A/C-bait construct to cDNA-library construct cells.

The sequence of contig5 resulted of bioinformatics analysis for the positive colonies that resulted from mating lamin A/C-bait construct cell to cDNA-library construct cells.

Applied Biosystems

A01_111006
FA_1-cox2
DT3730POP7{BDv3}.mob
Pts 1879 to 10760 Pk1 Loc:1879
Version 5.1.1 HiSQV Bases: 0 Primer UP

Inst Model/Name 3730/DNA3730-16111-007

Signal G:1044 A:2231 T:2424 C:3469 AvSig:2292
Basecaller-3730POP7SR.bcp
ABI 1.6.0 Cap:8

Oct 11,2006 05:20PM, BST
Spacing:15.05 Pts/Panel2000
Plate Name: 111006

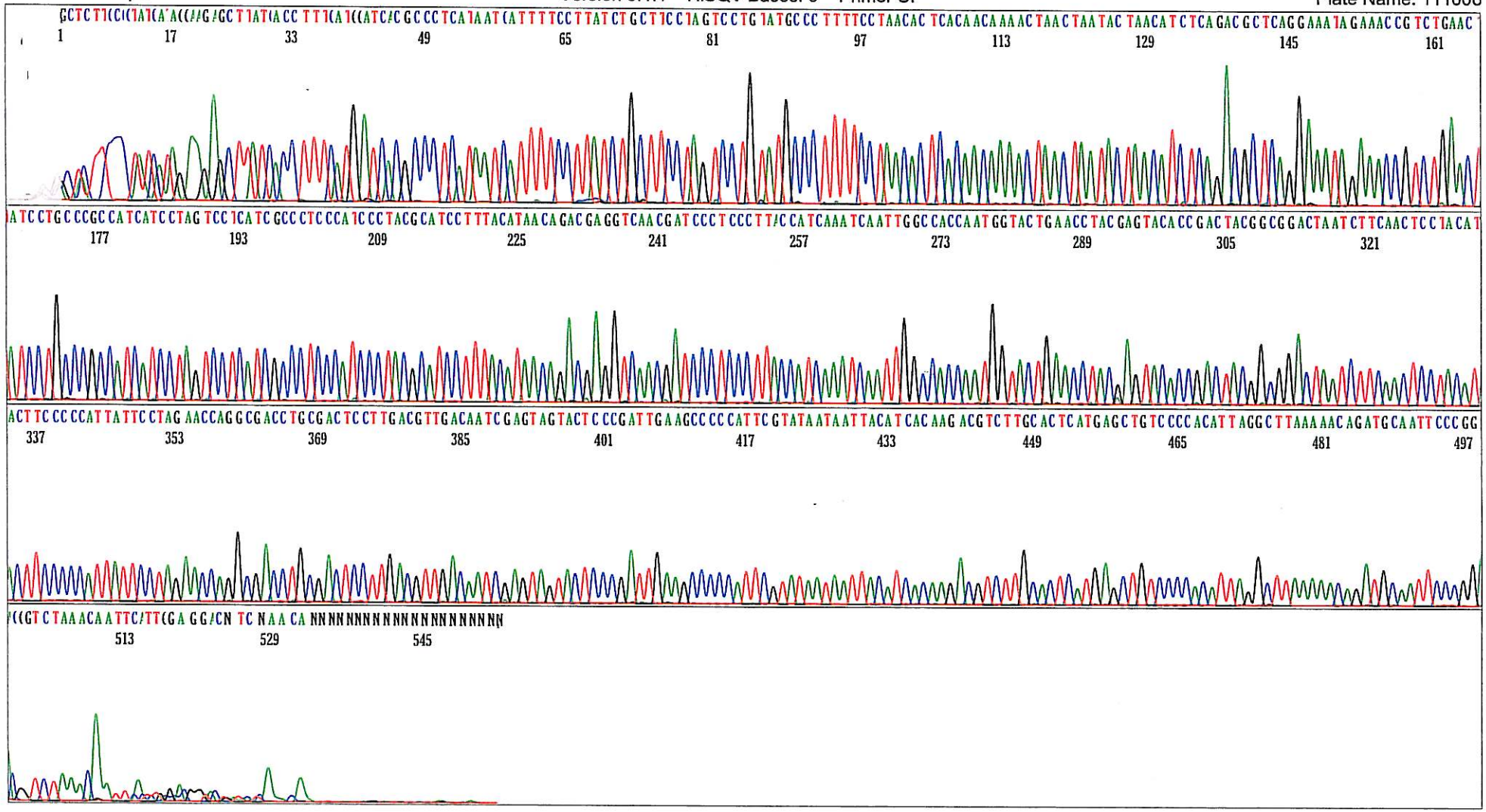

Appendix IV-3b: Seq8 result of mating LAP2α-bait construct to cDNA-library construct cells.

The sequence of seq8 (colony # 8) resulted of bioinformatics analysis for the positive colonies that resulted from mating LAP2α-bait construct cell to cDNA-library construct cells.

Applied Biosystems

A01_181006
FA_Seq8
DT3730POP7{BDv3}.mob
Pts 1990 to 8800 Pk1 Loc:1990
Version 5.1.1 HiSQV Bases: 0 Primer UP2

Inst Model/Name 3730/DNA3730-16111-007

Signal G:165 A:116 T:116 C:91 AvSig:122
Basecaller-3730POP7SR.bcp
ABI 1.6.0 Cap:8

Oct 18,2006 05:16PM, BST
Spacing:15.05 Pts/Panel2000
Plate Name: 181006

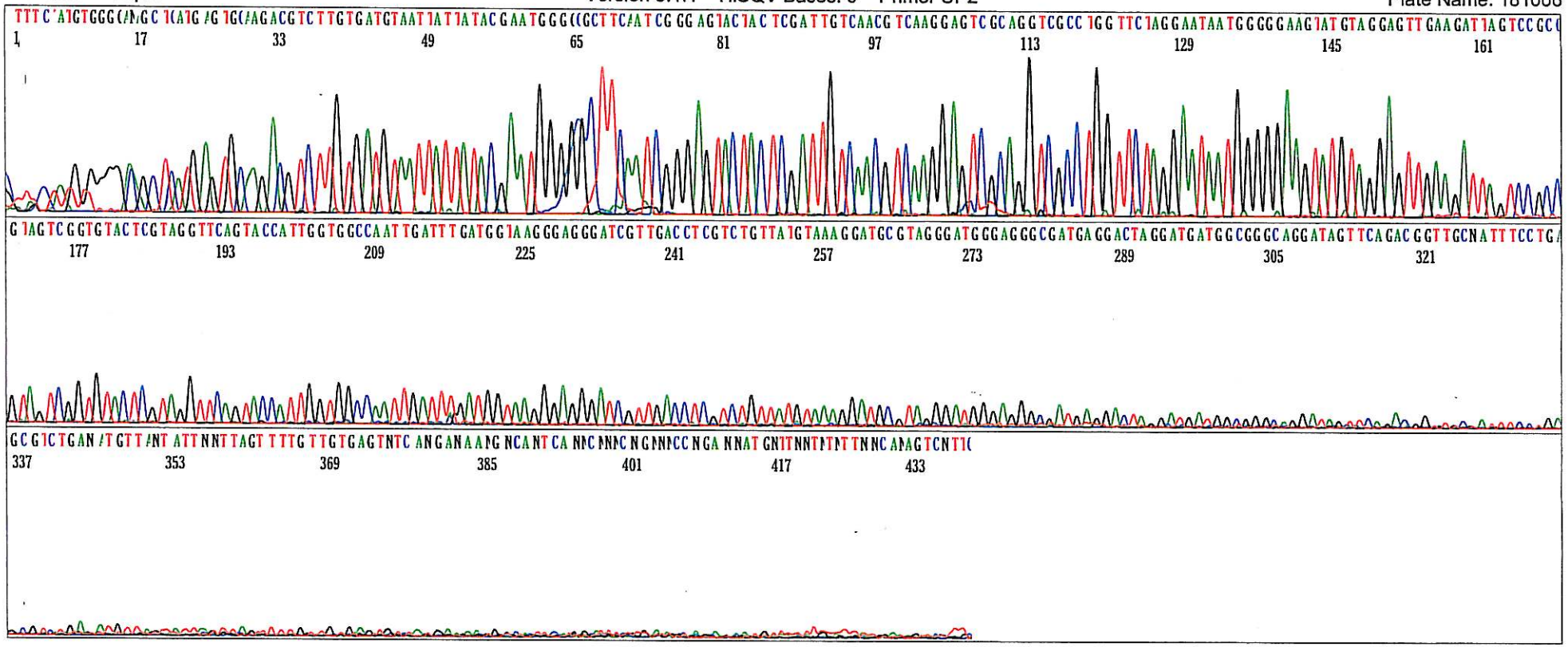

Appendix IV-3c: Cox2 gene bank.

Human mitochondrial mRNA cytochrome c oxidase subunit II (Cox2) complete cds. Accession no. X15759. The full length gene bank mRNA of Cox2 that resulted from yeast 2-hybrid screen.

GenBank: X15759.1

H.sapiens mitochondrial mRNA for cytochrome c oxidase subunit II

Comment Features Sequence

```
LOCUS       X15759                  708 bp    mRNA    linear   PRI 18-APR-
2005
DEFINITION  H.sapiens mitochondrial mRNA for cytochrome c oxidase subunit II.
ACCESSION   X15759
VERSION     X15759.1  GI:12583
KEYWORDS    cytochrome c oxidase subunit II.
SOURCE      mitochondrion Homo sapiens (human)
  ORGANISM  Homo sapiens
            Eukaryota; Metazoa; Chordata; Craniata; Vertebrata; Euteleostomi;
            Mammalia; Eutheria; Euarchontoglires; Primates; Haplorrhini;
            Catarrhini; Hominidae; Homo.
REFERENCE   1  (bases 1 to 708)
  AUTHORS   Power,M.D., Kiefer,M.C., Barr,P.J. and Reeves,R.
  TITLE     Nucleotide sequence of human mitochondrial cytochrome c oxidase
II
            cDNA
  JOURNAL   Nucleic Acids Res. 17 (16), 6734 (1989)
   PUBMED   2550900
REFERENCE   2  (bases 1 to 708)
  AUTHORS   Power,M.D.
  TITLE     Direct Submission
  JOURNAL   Submitted (07-JUL-1989) Power M.D., Athena Neurosciences Inc,
800-F
            Gateway Blvd, South San Francisco CA 94080, U S A
COMMENT     Related entries J01415 & J01416
            Data kindly reviewed (20-Sep-1989) by Power M.D.
FEATURES             Location/Qualifiers
     source          1..708
                     /organism="Homo sapiens"
                     /organelle="mitochondrion"
                     /mol_type="mRNA"
                     /db_xref="taxon:9606"
                     /cell_line="BC-10"
                     /cell_type="stimulated lymphocyte"
                     /clone_lib="lambda ZAP"
     CDS             2..685
                     /codon_start=1
                     /transl_table=2
                     /product="cytochrome c oxidase subunit II"
                     /protein_id="CAA33766.1"
                     /db_xref="GI:12584"
                     /db_xref="GDB:118901"
                     /db_xref="GOA:P00403"
                     /db_xref="HGNC:7421"
                     /db_xref="InterPro:IPR001505"
                     /db_xref="InterPro:IPR002429"
                     /db_xref="InterPro:IPR008972"
                     /db_xref="InterPro:IPR011759"
                     /db_xref="UniProtKB/Swiss-Prot:P00403"
                     /translation="MAHAAQVGLQDATSPIMEELITFHDHALMIIFLICFLVLYAL
FL

TLTTKLTNTNISDAQEMETVWTILPAIILVLIALPSLRILYMTDEVNDPSLTIKSIGH

QWYWTYEYTDYGGLIFNSYMLPPLFLEPGDLRLLDVDNRVVLPIEAPIRMMITSQDVL

HSWAVPTLGLKTDAIPGRLNQTTFTATRPGVYYGQCSEICGANHSFMPIVLELIPLKI
                     FEMGPVFTL"
     polyA_site      708
ORIGIN
        1 tatggcacat gcagcgcaag taggtctaca agacgctact tcccctatca tagaagagct
       61 tatcaccttt catgatcacg ccctcataat cattttcctt atctgcttcc tagtcctgta
      121 tgccctttc ctaacactca caacaaaact aactaatact aacatctcag acgctcagga
      181 aatagaaacc gtctgaacta tcctgcccgc catcatccta gtcctcatcg ccctcccatc
      241 cctacgcatc ctttacataa cagacgaggt caacgatccc tcccttacca tcaaatcaat
      301 tggccaccaa tggtactgaa cctacgagta caccgactac ggcggactaa tcttcaactc
      361 ctacatactt cccccattat tcctagaacc aggcgacctg cgactccttg acgttgacaa
      421 tcgagtagta ctcccgattg aagcccccat tcgtataata attacatcac aagacgtctt
      481 gcactcatga gctgtcccca cattaggctt aaaaacagat gcaattcccg gacgtctaaa
```

```
      541 ccaaaccact ttcaccgcta cacgaccggg ggtatactac ggtcaatgct ctgaaatctg
      601 tggagcaaac cacagtttca tgcccatcgt cctagaatta attcccctaa aaatctttga
      661 aatagggccc gtatttaccc tatagcaccc cctctacccc ctctagag
//
```

Appendix V: TEM negative control.

Appendix V: TEM negative control.

As a negative control, sections were prepared and stained with secondary antibody alone. No gold particles were detected under these conditions. It was run in parallel at each time to the actual experiment.

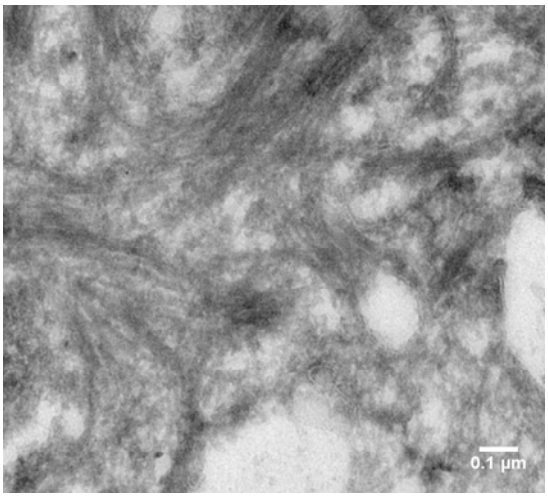

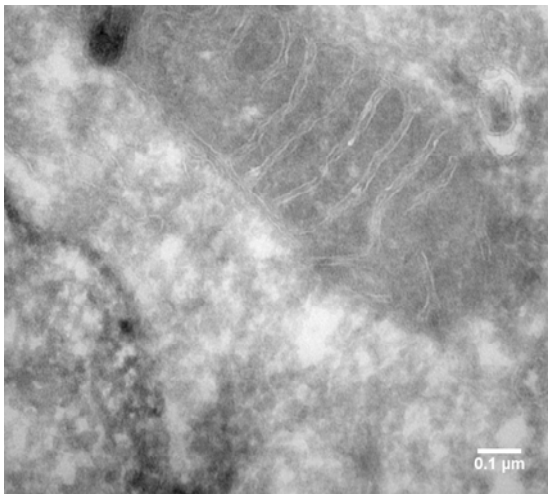

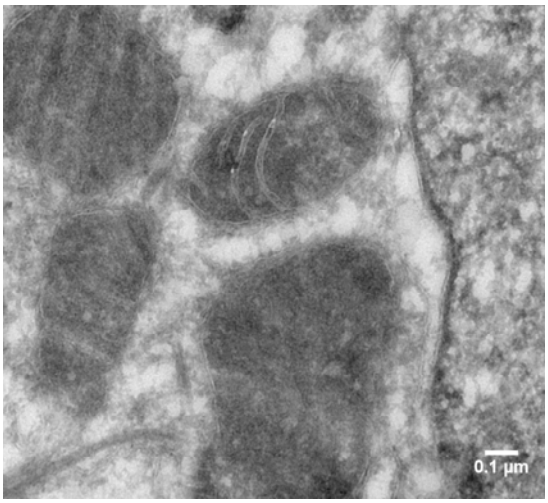

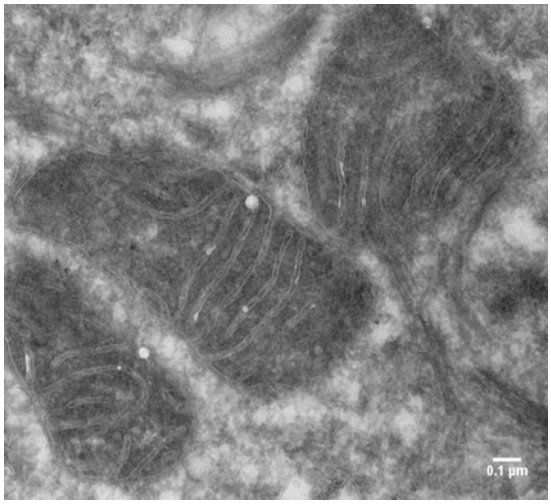

Appendix V

REFERENCES

- Abramov, A.Y., Canevari, L., and Duchen, M.R. (2004). Beta-amyloid peptides induce mitochondrial dysfunction and oxidative stress in astrocytes and death of neurons through activation of NADPH oxidase. J Neurosci *24*, 565-575.
- Adhikari, A.S., Sridhar Rao, K., Rangaraj, N., Parnaik, V.K., and Mohan Rao, C. (2004). Heat stress-induced localization of small heat shock proteins in mouse myoblasts: intranuclear lamin A/C speckles as target for alphaB-crystallin and Hsp25. Exp Cell Res *299*, 393-403.
- Aebi, U., Cohn, J., Buhle, L., and Gerace, L. (1986). The nuclear lamina is a meshwork of intermediate-type filaments. Nature *323*, 560-564.
- Agrelo, R., Setien, F., Espada, J., Artiga, M.J., Rodriguez, M., Perez-Rosado, A., Sanchez-Aguilera, A., Fraga, M.F., Piris, M.A., and Esteller, M. (2005). Inactivation of the lamin A/C gene by CpG island promoter hypermethylation in hematologic malignancies, and its association with poor survival in nodal diffuse large B-cell lymphoma. J Clin Oncol *23*, 3940-3947.
- Alavi, A., Clark, C., and Fazekas, F. (1998). Cerebral ischemia and Alzheimer's disease: critical role of PET and implications for therapeutic intervention. J Nucl Med *39*, 1363-1365.
- Alcouffe, J., Caspar-Bauguil, S., Garcia, V., Salvayre, R., Thomsen, M., and Benoist, H. (1999). Oxidized low density lipoproteins induce apoptosis in PHA-activated peripheral blood mononuclear cells and in the Jurkat T-cell line. J Lipid Res *40*, 1200-1210.
- Alderton, W.K., Cooper, C.E., and Knowles, R.G. (2001). Nitric oxide synthases: structure, function and inhibition. Biochem J *357*, 593-615.
- Ames, B.N., and Liu, J. (2004). Delaying the mitochondrial decay of aging with acetylcarnitine. Ann N Y Acad Sci *1033*, 108-116.
- Antonicka, H., Leary, S.C., Guercin, G.H., Agar, J.N., Horvath, R., Kennaway, N.G., Harding, C.O., Jaksch, M., and Shoubridge, E.A. (2003a). Mutations in COX10 result in a defect in mitochondrial heme A biosynthesis and account for multiple, early-onset clinical phenotypes associated with isolated COX deficiency. Hum Mol Genet *12*, 2693-2702.
- Antonicka, H., Mattman, A., Carlson, C.G., Glerum, D.M., Hoffbuhr, K.C., Leary, S.C., Kennaway, N.G., and Shoubridge, E.A. (2003b). Mutations in COX15 produce a defect in the mitochondrial heme biosynthetic pathway, causing early-onset fatal hypertrophic cardiomyopathy. Am J Hum Genet *72*, 101-114.
- Araujo-Vilar, D., Lado-Abeal, J., Palos-Paz, F., Lattanzi, G., Bandin, M.A., Bellido, D., Dominguez-Gerpe, L., Calvo, C., Perez, O., Ramazanova, A., Martinez-Sanchez, N., Victoria, B., and Costa-Freitas, A.T. (2008). A novel phenotypic expression associated with a new mutation in LMNA gene, characterized by partial lipodystrophy, insulin resistance, aortic stenosis and hypertrophic cardiomyopathy. Clin Endocrinol (Oxf) *69*, 61-68.
- Attardi, G., and Schatz, G. (1988). Biogenesis of mitochondria. Annu Rev Cell Biol *4*, 289-333.

- Augenlicht, L.H., Taylor, J., Anderson, L., and Lipkin, M. (1991). Patterns of gene expression that characterize the colonic mucosa in patients at genetic risk for colonic cancer. Proc Natl Acad Sci U S A *88*, 3286-3289.
- Autere, J., Moilanen, J.S., Finnila, S., Soininen, H., Mannermaa, A., Hartikainen, P., Hallikainen, M., and Majamaa, K. (2004). Mitochondrial DNA polymorphisms as risk factors for Parkinson's disease and Parkinson's disease dementia. Hum Genet *115*, 29-35.
- Beaudouin, J., Gerlich, D., Daigle, N., Eils, R., and Ellenberg, J. (2002). Nuclear envelope breakdown proceeds by microtubule-induced tearing of the lamina. Cell *108*, 83-96.
- Bedi, A., Pasricha, P.J., Akhtar, A.J., Barber, J.P., Bedi, G.C., Giardiello, F.M., Zehnbauer, B.A., Hamilton, S.R., and Jones, R.J. (1995). Inhibition of apoptosis during development of colorectal cancer. Cancer Res *55*, 1811-1816.
- Belevich, I., Verkhovsky, M.I., and Wikstrom, M. (2006). Proton-coupled electron transfer drives the proton pump of cytochrome c oxidase. Nature *440*, 829-832.
- Bell, E.L., Emerling, B.M., and Chandel, N.S. (2005). Mitochondrial regulation of oxygen sensing. Mitochondrion *5*, 322-332.
- Belogrudov, G.I., Tomich, J.M., and Hatefi, Y. (1995). ATP synthase complex. Proximities of subunits in bovine submitochondrial particles. J Biol Chem *270*, 2053-2060.
- Bengtsson, L. (2007). What MAN1 does to the Smads. TGFbeta/BMP signaling and the nuclear envelope. Febs J *274*, 1374-1382.
- Berger, R., Theodor, L., Shoham, J., Gokkel, E., Brok-Simoni, F., Avraham, K.B., Copeland, N.G., Jenkins, N.A., Rechavi, G., and Simon, A.J. (1996). The characterization and localization of the mouse thymopoietin/lamina-associated polypeptide 2 gene and its alternatively spliced products. Genome Res *6*, 361-370.
- Biscardi, J.S., Ishizawar, R.C., Silva, C.M., and Parsons, S.J. (2000). Tyrosine kinase signalling in breast cancer: epidermal growth factor receptor and c-Src interactions in breast cancer. Breast Cancer Res *2*, 203-210.
- Biswas, S., Chida, A.S., and Rahman, I. (2006). Redox modifications of protein-thiols: emerging roles in cell signaling. Biochem Pharmacol *71*, 551-564.
- Boerner, J.L., Demory, M.L., Silva, C., and Parsons, S.J. (2004). Phosphorylation of Y845 on the epidermal growth factor receptor mediates binding to the mitochondrial protein cytochrome c oxidase subunit II. Mol Cell Biol *24*, 7059-7071.
- Bogenhagen, D., and Clayton, D.A. (1977). Mouse L cell mitochondrial DNA molecules are selected randomly for replication throughout the cell cycle. Cell *11*, 719-727.
- Bonne, G., Di Barletta, M.R., Varnous, S., Becane, H.M., Hammouda, E.H., Merlini, L., Muntoni, F., Greenberg, C.R., Gary, F., Urtizberea, J.A., Duboc, D., Fardeau, M., Toniolo, D., and Schwartz, K. (1999). Mutations in the gene encoding lamin A/C cause autosomal dominant Emery-Dreifuss muscular dystrophy. Nat Genet *21*, 285-288.

- Bonora, E., Kiechl, S., Willeit, J., Oberhollenzer, F., Egger, G., Targher, G., Alberiche, M., Bonadonna, R.C., and Muggeo, M. (1998). Prevalence of insulin resistance in metabolic disorders: the Bruneck Study. Diabetes *47*, 1643-1649.
- Bourdel-Marchasson, I., Delmas-Beauvieux, M.C., Peuchant, E., Richard-Harston, S., Decamps, A., Reignier, B., Emeriau, J.P., and Rainfray, M. (2001). Antioxidant defences and oxidative stress markers in erythrocytes and plasma from normally nourished elderly Alzheimer patients. Age Ageing *30*, 235-241.
- Boveris, A., Costa, L.E., Cadenas, E., and Poderoso, J.J. (1999). Regulation of mitochondrial respiration by adenosine diphosphate, oxygen, and nitric oxide. Methods Enzymol *301*, 188-198.
- Bridger, J.M., Foeger, N., Kill, I.R., and Herrmann, H. (2007). The nuclear lamina. Both a structural framework and a platform for genome organization. Febs J *274*, 1354-1361.
- Broers, J.L., Raymond, Y., Rot, M.K., Kuijpers, H., Wagenaar, S.S., and Ramaekers, F.C. (1993). Nuclear A-type lamins are differentially expressed in human lung cancer subtypes. Am J Pathol *143*, 211-220.
- Broers, J.L., Machiels, B.M., Kuijpers, H.J., Smedts, F., van den Kieboom, R., Raymond, Y., and Ramaekers, F.C. (1997). A- and B-type lamins are differentially expressed in normal human tissues. Histochem Cell Biol *107*, 505-517.
- Broers, J.L., Ramaekers, F.C., Bonne, G., Yaou, R.B., and Hutchison, C.J. (2006). Nuclear lamins: laminopathies and their role in premature ageing. Physiol Rev *86*, 967-1008.
- Brookes, P.S., and Darley-Usmar, V.M. (2004). Role of calcium and superoxide dismutase in sensitizing mitochondria to peroxynitrite-induced permeability transition. Am J Physiol Heart Circ Physiol *286*, H39-46.
- Brown, G.C. (1995). Nitric oxide regulates mitochondrial respiration and cell functions by inhibiting cytochrome oxidase. FEBS Lett *369*, 136-139.
- Brunori, M., Giuffre, A., and Sarti, P. (2005). Cytochrome c oxidase, ligands and electrons. J Inorg Biochem *99*, 324-336.
- Buchwald, P., Krummeck, G., and Rodel, G. (1991). Immunological identification of yeast SCO1 protein as a component of the inner mitochondrial membrane. Mol Gen Genet *229*, 413-420.
- Busson, S., Dujardin, D., Moreau, A., Dompierre, J., and De Mey, J.R. (1998). Dynein and dynactin are localized to astral microtubules and at cortical sites in mitotic epithelial cells. Curr Biol *8*, 541-544.
- Cadenas, E., Poderoso, J.J., Antunes, F., and Boveris, A. (2000). Analysis of the pathways of nitric oxide utilization in mitochondria. Free Radic Res *33*, 747-756.
- Campian, J.L., Gao, X., Qian, M., and Eaton, J.W. (2007). Cytochrome C oxidase activity and oxygen tolerance. J Biol Chem *282*, 12430-12438.
- Capaldi, R.A. (1990). Structure and function of cytochrome c oxidase. Annu Rev Biochem *59*, 569-596.
- Cardoso, S.M., Santana, I., Swerdlow, R.H., and Oliveira, C.R. (2004). Mitochondria dysfunction of Alzheimer's disease cybrids enhances Abeta toxicity. J Neurochem *89*, 1417-1426.

- Caron, M., Auclair, M., Donadille, B., Bereziat, V., Guerci, B., Laville, M., Narbonne, H., Bodemer, C., Lascols, O., Capeau, J., and Vigouroux, C. (2007). Human lipodystrophies linked to mutations in A-type lamins and to HIV protease inhibitor therapy are both associated with prelamin A accumulation, oxidative stress and premature cellular senescence. Cell Death Differ *14*, 1759-1767.
- Carr, H.S., George, G.N., and Winge, D.R. (2002). Yeast Cox11, a protein essential for cytochrome c oxidase assembly, is a Cu(I)-binding protein. J Biol Chem *277*, 31237-31242.
- Carr, H.S., and Winge, D.R. (2003). Assembly of cytochrome c oxidase within the mitochondrion. Acc Chem Res *36*, 309-316.
- Cobine, P.A., Ojeda, L.D., Rigby, K.M., and Winge, D.R. (2004). Yeast contain a non-proteinaceous pool of copper in the mitochondrial matrix. J Biol Chem *279*, 14447-14455.
- Carreras, M.C., and Poderoso, J.J. (2007). Mitochondrial nitric oxide in the signaling of cell integrated responses. Am J Physiol Cell Physiol *292*, C1569-1580.
- Casley, C.S., Land, J.M., Sharpe, M.A., Clark, J.B., Duchen, M.R., and Canevari, L. (2002). Beta-amyloid fragment 25-35 causes mitochondrial dysfunction in primary cortical neurons. Neurobiol Dis *10*, 258-267.
- Cereghetti, G.M., and Scorrano, L. (2006). The many shapes of mitochondrial death. Oncogene *25*, 4717-4724.
- Chan, D.C. (2006). Mitochondrial fusion and fission in mammals. Annu Rev Cell Dev Biol *22*, 79-99.
- Chen, Z.X., and Pervaiz, S. (2007). Bcl-2 induces pro-oxidant state by engaging mitochondrial respiration in tumor cells. Cell Death Differ *14*, 1617-1627.
- Cobine, P.A., Pierrel, F., and Winge, D.R. (2006). Copper trafficking to the mitochondrion and assembly of copper metalloenzymes. Biochim Biophys Acta *1763*, 759-772.
- Chinnaiyan, A.M., O'Rourke, K., Yu, G.L., Lyons, R.H., Garg, M., Duan, D.R., Xing, L., Gentz, R., Ni, J., and Dixit, V.M. (1996a). Signal transduction by DR3, a death domain-containing receptor related to TNFR-1 and CD95. Science *274*, 990-992.
- Chinnaiyan, A.M., Orth, K., O'Rourke, K., Duan, H., Poirier, G.G., and Dixit, V.M. (1996b). Molecular ordering of the cell death pathway. Bcl-2 and Bcl-xL function upstream of the CED-3-like apoptotic proteases. J Biol Chem *271*, 4573-4576.
- Christopherson, K.S., and Bredt, D.S. (1997). Nitric oxide in excitable tissues: physiological roles and disease. J Clin Invest *100*, 2424-2429.
- Ciechanover, A. (1998). The ubiquitin-proteasome pathway: on protein death and cell life. Embo J *17*, 7151-7160.
- Cipolat, S., Martins de Brito, O., Dal Zilio, B., and Scorrano, L. (2004). OPA1 requires mitofusin 1 to promote mitochondrial fusion. Proc Natl Acad Sci U S A *101*, 15927-15932.
- Clark, K.M., Taylor, R.W., Johnson, M.A., Chinnery, P.F., Chrzanowska-Lightowlers, Z.M., Andrews, R.M., Nelson, I.P., Wood, N.W., Lamont, P.J., Hanna, M.G., Lightowlers, R.N., and Turnbull, D.M. (1999). An mtDNA

mutation in the initiation codon of the cytochrome C oxidase subunit II gene results in lower levels of the protein and a mitochondrial encephalomyopathy. Am J Hum Genet *64*, 1330-1339.

- Clayton, D.A., Doda, J.N., and Friedberg, E.C. (1974). The absence of a pyrimidine dimer repair mechanism in mammalian mitochondria. Proc Natl Acad Sci U S A *71*, 2777-2781.
- Cleeter, M.W., Cooper, J.M., Darley-Usmar, V.M., Moncada, S., and Schapira, A.H. (1994). Reversible inhibition of cytochrome c oxidase, the terminal enzyme of the mitochondrial respiratory chain, by nitric oxide. Implications for neurodegenerative diseases. FEBS Lett *345*, 50-54.
- Clements, L., Manilal, S., Love, D.R., and Morris, G.E. (2000). Direct interaction between emerin and lamin A. Biochem Biophys Res Commun *267*, 709-714.
- Cohen, T.V., Kosti, O., and Stewart, C.L. (2007). The nuclear envelope protein MAN1 regulates TGFbeta signaling and vasculogenesis in the embryonic yolk sac. Development *134*, 1385-1395.
- Collas, P. (1998). Nuclear envelope disassembly in mitotic extract requires functional nuclear pores and a nuclear lamina. J Cell Sci *111 (Pt 9)*, 1293-1303.
- Collas, P., Thompson, L., Fields, A.P., Poccia, D.L., and Courvalin, J.C. (1997). Protein kinase C-mediated interphase lamin B phosphorylation and solubilization. J Biol Chem *272*, 21274-21280.
- Colurso, G.J., Nilson, J.E., and Vervoort, L.G. (2003). Quantitative assessment of DNA fragmentation and beta-amyloid deposition in insular cortex and midfrontal gyrus from patients with Alzheimer's disease. Life Sci *73*, 1795-1803.
- Cortopassi, G.A., Shibata, D., Soong, N.W., and Arnheim, N. (1992). A pattern of accumulation of a somatic deletion of mitochondrial DNA in aging human tissues. Proc Natl Acad Sci U S A *89*, 7370-7374.
- Crisp, M., Liu, Q., Roux, K., Rattner, J.B., Shanahan, C., Burke, B., Stahl, P.D., and Hodzic, D. (2006). Coupling of the nucleus and cytoplasm: role of the LINC complex. J Cell Biol *172*, 41-53.
- Daigle, N., Beaudouin, J., Hartnell, L., Imreh, G., Hallberg, E., Lippincott-Schwartz, J., and Ellenberg, J. (2001). Nuclear pore complexes form immobile networks and have a very low turnover in live mammalian cells. J Cell Biol *154*, 71-84.
- De Sandre-Giovannoli, A., Chaouch, M., Kozlov, S., Vallat, J.M., Tazir, M., Kassouri, N., Szepetowski, P., Hammadouche, T., Vandenberghe, A., Stewart, C.L., Grid, D., and Levy, N. (2002). Homozygous defects in LMNA, encoding lamin A/C nuclear-envelope proteins, cause autosomal recessive axonal neuropathy in human (Charcot-Marie-Tooth disorder type 2) and mouse. Am J Hum Genet *70*, 726-736.
- Dechat, T., Gotzmann, J., Stockinger, A., Harris, C.A., Talle, M.A., Siekierka, J.J., and Foisner, R. (1998). Detergent-salt resistance of LAP2alpha in interphase nuclei and phosphorylation-dependent association with chromosomes early in nuclear assembly implies functions in nuclear structure dynamics. Embo J *17*, 4887-4902.

- Dechat, T., Vlcek, S., and Foisner, R. (2000). Review: lamina-associated polypeptide 2 isoforms and related proteins in cell cycle-dependent nuclear structure dynamics. J Struct Biol *129*, 335-345.
- DeFronzo, R.A., Ferrannini, E., and Simonson, D.C. (1989). Fasting hyperglycemia in non-insulin-dependent diabetes mellitus: contributions of excessive hepatic glucose production and impaired tissue glucose uptake. Metabolism *38*, 387-395.
- Delettre, C., Lenaers, G., Griffoin, J.M., Gigarel, N., Lorenzo, C., Belenguer, P., Pelloquin, L., Grosgeorge, J., Turc-Carel, C., Perret, E., Astarie-Dequeker, C., Lasquellec, L., Arnaud, B., Ducommun, B., Kaplan, J., and Hamel, C.P. (2000). Nuclear gene OPA1, encoding a mitochondrial dynamin-related protein, is mutated in dominant optic atrophy. Nat Genet *26*, 207-210.
- Desouki, M.M., Kulawiec, M., Bansal, S., Das, G.M., and Singh, K.K. (2005). Cross talk between mitochondria and superoxide generating NADPH oxidase in breast and ovarian tumors. Cancer Biol Ther *4*, 1367-1373.
- DiMauro, S., Nicholson, J.F., Hays, A.P., Eastwood, A.B., Papadimitriou, A., Koenigsberger, R., and DeVivo, D.C. (1983). Benign infantile mitochondrial myopathy due to reversible cytochrome c oxidase deficiency. Ann Neurol *14*, 226-234.
- Dohm, J.A., Lee, S.J., Hardwick, J.M., Hill, R.B., and Gittis, A.G. (2004). Cytosolic domain of the human mitochondrial fission protein fis1 adopts a TPR fold. Proteins *54*, 153-156.
- Donadille, B., Lascols, O., Capeau, J., and Vigouroux, C. (2005). Etiological investigations in apparent type 2 diabetes: when to search for lamin A/C mutations? Diabetes Metab *31*, 527-532.
- Dorner, D., Vlcek, S., Foeger, N., Gajewski, A., Makolm, C., Gotzmann, J., Hutchison, C.J., and Foisner, R. (2006). Lamina-associated polypeptide 2alpha regulates cell cycle progression and differentiation via the retinoblastoma-E2F pathway. J Cell Biol *173*, 83-93.
- Dreuillet, C., Tillit, J., Kress, M., and Ernoult-Lange, M. (2002). In vivo and in vitro interaction between human transcription factor MOK2 and nuclear lamin A/C. Nucleic Acids Res *30*, 4634-4642.
- Du, C., Fang, M., Li, Y., Li, L., and Wang, X. (2000). Smac, a mitochondrial protein that promotes cytochrome c-dependent caspase activation by eliminating IAP inhibition. Cell *102*, 33-42.
- Du, X., Matsumura, T., Edelstein, D., Rossetti, L., Zsengeller, Z., Szabo, C., and Brownlee, M. (2003). Inhibition of GAPDH activity by poly(ADP-ribose) polymerase activates three major pathways of hyperglycemic damage in endothelial cells. J Clin Invest *112*, 1049-1057.
- Dyer, J.A., Lane, B.E., and Hutchison, C.J. (1999). Investigations of the pathway of incorporation and function of lamin A in the nuclear lamina. Microsc Res Tech *45*, 1-12.
- Ellenberg, J., Siggia, E.D., Moreira, J.E., Smith, C.L., Presley, J.F., Worman, H.J., and Lippincott-Schwartz, J. (1997). Nuclear membrane dynamics and reassembly in living cells: targeting of an inner nuclear membrane protein in interphase and mitosis. J Cell Biol *138*, 1193-1206.

- Ellis, D.J., Jenkins, H., Whitfield, W.G., and Hutchison, C.J. (1997). GST-lamin fusion proteins act as dominant negative mutants in Xenopus egg extract and reveal the function of the lamina in DNA replication. J Cell Sci *110 (Pt 20)*, 2507-2518.
- Fadeel, B., and Orrenius, S. (2005). Apoptosis: a basic biological phenomenon with wide-ranging implications in human disease. J Intern Med *258*, 479-517.
- Fairley, E.A., Kendrick-Jones, J., and Ellis, J.A. (1999). The Emery-Dreifuss muscular dystrophy phenotype arises from aberrant targeting and binding of emerin at the inner nuclear membrane. J Cell Sci *112 (Pt 15)*, 2571-2582.
- Fan, A.C., Bhangoo, M.K., and Young, J.C. (2006). Hsp90 functions in the targeting and outer membrane translocation steps of Tom70-mediated mitochondrial import. J Biol Chem *281*, 33313-33324.
- Faraci, F.M., and Heistad, D.D. (1998). Regulation of the cerebral circulation: role of endothelium and potassium channels. Physiol Rev *78*, 53-97.
- Fatkin, D., MacRae, C., Sasaki, T., Wolff, M.R., Porcu, M., Frenneaux, M., Atherton, J., Vidaillet, H.J., Jr., Spudich, S., De Girolami, U., Seidman, J.G., Seidman, C., Muntoni, F., Muehle, G., Johnson, W., and McDonough, B. (1999). Missense mutations in the rod domain of the lamin A/C gene as causes of dilated cardiomyopathy and conduction-system disease. N Engl J Med *341*, 1715-1724.
- Fink, S.L., and Cookson, B.T. (2005). Apoptosis, pyroptosis, and necrosis: mechanistic description of dead and dying eukaryotic cells. Infect Immun *73*, 1907-1916.
- Fidzianska, A., Walczak, E., Glinka, Z., and Religa, G. (2008). Nuclear architecture remodelling in cardiomyocytes with lamin A deficiency. Folia Neuropathol *46*, 196-203.
- Foisner, R. (2003). Cell cycle dynamics of the nuclear envelope. ScientificWorldJournal *3*, 1-20.
- Foisner, R., and Gerace, L. (1993). Integral membrane proteins of the nuclear envelope interact with lamins and chromosomes, and binding is modulated by mitotic phosphorylation. Cell *73*, 1267-1279.
- Fox, T.D. (1979). Five TGA "stop" codons occur within the translated sequence of the yeast mitochondrial gene for cytochrome c oxidase subunit II. Proc Natl Acad Sci U S A *76*, 6534-6538.
- Franco, M.C., Arciuch, V.G., Peralta, J.G., Galli, S., Levisman, D., Lopez, L.M., Romorini, L., Poderoso, J.J., and Carreras, M.C. (2006). Hypothyroid phenotype is contributed by mitochondrial complex I inactivation due to translocated neuronal nitric-oxide synthase. J Biol Chem *281*, 4779-4786.
- Fruehauf, J.P., and Meyskens, F.L., Jr. (2007). Reactive oxygen species: a breath of life or death? Clin Cancer Res *13*, 789-794.
- Fujimori, Y., Okimatsu, H., Kashiwagi, T., Sanda, N., Okumura, K., Takagi, A., Nagata, K., Murate, T., Uchida, A., Node, K., Saito, H., and Kojima, T. (2008). Molecular defects associated with antithrombin deficiency and dilated cardiomyopathy in a Japanese patient. Intern Med *47*, 925-931.

- Fuller, S.D., Capaldi, R.A., and Henderson, R. (1979). Structure of cytochrome c oxidase in deoxycholate-drived two-dimensional crystals. J Mol Biol *134*, 305-327.
- Furukawa, K., and Kondo, T. (1998). Identification of the lamina-associated-polypeptide-2-binding domain of B-type lamin. Eur J Biochem *251*, 729-733.
- Galli, S., Labato, M.I., Bal de Kier Joffe, E., Carreras, M.C., and Poderoso, J.J. (2003). Decreased mitochondrial nitric oxide synthase activity and hydrogen peroxide relate persistent tumoral proliferation to embryonic behavior. Cancer Res *63*, 6370-6377.
- Gant, T.M., Harris, C.A., and Wilson, K.L. (1999). Roles of LAP2 proteins in nuclear assembly and DNA replication: truncated LAP2beta proteins alter lamina assembly, envelope formation, nuclear size, and DNA replication efficiency in Xenopus laevis extracts. J Cell Biol *144*, 1083-1096.
- Gant, T.M., and Wilson, K.L. (1997). Nuclear assembly. Annu Rev Cell Dev Biol *13*, 669-695.
- Garlid, K.D., Dos Santos, P., Xie, Z.J., Costa, A.D., and Paucek, P. (2003). Mitochondrial potassium transport: the role of the mitochondrial ATP-sensitive K(+) channel in cardiac function and cardioprotection. Biochim Biophys Acta *1606*, 1-21.
- Georgatos, S.D., Pyrpasopoulou, A., and Theodoropoulos, P.A. (1997). Nuclear envelope breakdown in mammalian cells involves stepwise lamina disassembly and microtubule-drive deformation of the nuclear membrane. J Cell Sci *110 (Pt 17)*, 2129-2140.
- Gerace, L., and Blobel, G. (1980). The nuclear envelope lamina is reversibly depolymerized during mitosis. Cell *19*, 277-287.
- Ghafourifar, P., and Richter, C. (1997). Nitric oxide synthase activity in mitochondria. FEBS Lett *418*, 291-296.
- Ghafourifar, P., and Richter, C. (1999). Mitochondrial nitric oxide synthase regulates mitochondrial matrix pH. Biol Chem *380*, 1025-1028.
- Gilderson, G., Salomonsson, L., Aagaard, A., Gray, J., Brzezinski, P., and Hosler, J. (2003). Subunit III of cytochrome c oxidase of Rhodobacter sphaeroides is required to maintain rapid proton uptake through the D pathway at physiologic pH. Biochemistry *42*, 7400-7409.
- Giulivi, C., Poderoso, J.J., and Boveris, A. (1998). Production of nitric oxide by mitochondria. J Biol Chem *273*, 11038-11043.
- Glass, C.A., Glass, J.R., Taniura, H., Hasel, K.W., Blevitt, J.M., and Gerace, L. (1993). The alpha-helical rod domain of human lamins A and C contains a chromatin binding site. Embo J *12*, 4413-4424.
- Gogvadze, V., Robertson, J.D., Enoksson, M., Zhivotovsky, B., and Orrenius, S. (2004). Mitochondrial cytochrome c release may occur by volume-dependent mechanisms not involving permeability transition. Biochem J *378*, 213-217.
- Goldberg, M. (2004). Import and export at the nuclear envelope. Symp Soc Exp Biol, 115-133.
- Goldberg, M., Jenkins, H., Allen, T., Whitfield, W.G., and Hutchison, C.J. (1995). Xenopus lamin B3 has a direct role in the assembly of a replication competent nucleus: evidence from cell-free egg extracts. J Cell Sci *108 (Pt 11)*, 3451-3461.

- Goldberg, M.S., Fleming, S.M., Palacino, J.J., Cepeda, C., Lam, H.A., Bhatnagar, A., Meloni, E.G., Wu, N., Ackerson, L.C., Klapstein, G.J., Gajendiran, M., Roth, B.L., Chesselet, M.F., Maidment, N.T., Levine, M.S., and Shen, J. (2003). Parkin-deficient mice exhibit nigrostriatal deficits but not loss of dopaminergic neurons. J Biol Chem *278*, 43628-43635.
- Goldberg, M.W., Fiserova, J., Huttenlauch, I., and Stick, R. (2008a). A new model for nuclear lamina organization. Biochem Soc Trans *36*, 1339-1343.
- Goldberg, M.W., Huttenlauch, I., Hutchison, C.J., and Stick, R. (2008b). Filaments made from A- and B-type lamins differ in structure and organization. J Cell Sci *121*, 215-225.
- Goodell, S., and Cortopassi, G. (1998). Analysis of oxygen consumption and mitochondrial permeability with age in mice. Mech Ageing Dev *101*, 245-256.
- Gozuacik, D., and Kimchi, A. (2004). Autophagy as a cell death and tumor suppressor mechanism. Oncogene *23*, 2891-2906.
- Green, D.R., and Kroemer, G. (2004). The pathophysiology of mitochondrial cell death. Science *305*, 626-629.
- Greene, J.C., Whitworth, A.J., Kuo, I., Andrews, L.A., Feany, M.B., and Pallanck, L.J. (2003). Mitochondrial pathology and apoptotic muscle degeneration in Drosophila parkin mutants. Proc Natl Acad Sci U S A *100*, 4078-4083.
- Gruenbaum, Y., Margalit, A., Goldman, R.D., Shumaker, D.K., and Wilson, K.L. (2005). The nuclear lamina comes of age. Nat Rev Mol Cell Biol *6*, 21-31.
- Guo, X., Macleod, G.T., Wellington, A., Hu, F., Panchumarthi, S., Schoenfield, M., Marin, L., Charlton, M.P., Atwood, H.L., and Zinsmaier, K.E. (2005). The GTPase dMiro is required for axonal transport of mitochondria to Drosophila synapses. Neuron *47*, 379-393.
- Halestrap, A.P. (1989). The regulation of the matrix volume of mammalian mitochondria in vivo and in vitro and its role in the control of mitochondrial metabolism. Biochim Biophys Acta *973*, 355-382.
- Halliwell, B. (1991). Reactive oxygen species in living systems: source, biochemistry, and role in human disease. Am J Med *91*, 14S-22S.
- Haraguchi, T., Koujin, T., Osakada, H., Kojidani, T., Mori, C., Masuda, H., and Hiraoka, Y. (2007). Nuclear localization of barrier-to-autointegration factor is correlated with progression of S phase in human cells. J Cell Sci *120*, 1967-1977.
- Harborth, J., Elbashir, S.M., Bechert, K., Tuschl, T., and Weber, K. (2001). Identification of essential genes in cultured mammalian cells using small interfering RNAs. J Cell Sci *114*, 4557-4565.
- Harman, D. (1972). The biologic clock: the mitochondria? J Am Geriatr Soc *20*, 145-147.
- Harris, C.A., Andryuk, P.J., Cline, S., Chan, H.K., Natarajan, A., Siekierka, J.J., and Goldstein, G. (1994). Three distinct human thymopoietins are derived from alternatively spliced mRNAs. Proc Natl Acad Sci U S A *91*, 6283-6287.
- Heessen, S., and Fornerod, M. (2007). The inner nuclear envelope as a transcription factor resting place. EMBO Rep *8*, 914-919.

- Hegele, R.A., Cao, H., Liu, D.M., Costain, G.A., Charlton-Menys, V., Rodger, N.W., and Durrington, P.N. (2006). Sequencing of the reannotated LMNB2 gene reveals novel mutations in patients with acquired partial lipodystrophy. Am J Hum Genet *79*, 383-389.
- Heitlinger, E., Peter, M., Haner, M., Lustig, A., Aebi, U., and Nigg, E.A. (1991). Expression of chicken lamin B2 in Escherichia coli: characterization of its structure, assembly, and molecular interactions. J Cell Biol *113*, 485-495.
- Henderson, R., Capaldi, R.A., and Leigh, J.S. (1977). Arrangement of cytochrome oxidase molecules in two-dimensional vesicle crystals. J Mol Biol *112*, 631-648.
- Hennekes, H., Peter, M., Weber, K., and Nigg, E.A. (1993). Phosphorylation on protein kinase C sites inhibits nuclear import of lamin B2. J Cell Biol *120*, 1293-1304.
- Hensley, K., Carney, J.M., Mattson, M.P., Aksenova, M., Harris, M., Wu, J.F., Floyd, R.A., and Butterfield, D.A. (1994). A model for beta-amyloid aggregation and neurotoxicity based on free radical generation by the peptide: relevance to Alzheimer disease. Proc Natl Acad Sci U S A *91*, 3270-3274.
- Herrmann, H., and Foisner, R. (2003). Intermediate filaments: novel assembly models and exciting new functions for nuclear lamins. Cell Mol Life Sci *60*, 1607-1612.
- Herrmann, H., Bar, H., Kreplak, L., Strelkov, S.V., and Aebi, U. (2007). Intermediate filaments: from cell architecture to nanomechanics. Nat Rev Mol Cell Biol *8*, 562-573.
- Hessler, J.R., Robertson, A.L., Jr., and Chisolm, G.M., 3rd. (1979). LDL-induced cytotoxicity and its inhibition by HDL in human vascular smooth muscle and endothelial cells in culture. Atherosclerosis *32*, 213-229.
- Hoepken, H.H., Gispert, S., Morales, B., Wingerter, O., Del Turco, D., Mulsch, A., Nussbaum, R.L., Muller, K., Drose, S., Brandt, U., Deller, T., Wirth, B., Kudin, A.P., Kunz, W.S., and Auburger, G. (2007). Mitochondrial dysfunction, peroxidation damage and changes in glutathione metabolism in PARK6. Neurobiol Dis *25*, 401-411.
- Hoffmann, K., Sperling, K., Olins, A.L., and Olins, D.E. (2007). The granulocyte nucleus and lamin B receptor: avoiding the ovoid. Chromosoma *116*, 227-235.
- Horng, Y.C., Leary, S.C., Cobine, P.A., Young, F.B., George, G.N., Shoubridge, E.A., and Winge, D.R. (2005). Human Sco1 and Sco2 function as copper-binding proteins. J Biol Chem *280*, 34113-34122.
- Holmuhamedov, E.L., Jovanovic, S., Dzeja, P.P., Jovanovic, A., and Terzic, A. (1998). Mitochondrial ATP-sensitive K+ channels modulate cardiac mitochondrial function. Am J Physiol *275*, H1567-1576.
- Horsefield, R., Yankovskaya, V., Sexton, G., Whittingham, W., Shiomi, K., Omura, S., Byrne, B., Cecchini, G., and Iwata, S. (2006). Structural and computational analysis of the quinone-binding site of complex II (succinate-ubiquinone oxidoreductase): a mechanism of electron transfer and proton conduction during ubiquinone reduction. J Biol Chem *281*, 7309-7316.

- Hsieh, R.H., Hou, J.H., Hsu, H.S., and Wei, Y.H. (1994). Age-dependent respiratory function decline and DNA deletions in human muscle mitochondria. Biochem Mol Biol Int *32*, 1009-1022.
- Huang, L.E., Gu, J., Schau, M., and Bunn, H.F. (1998). Regulation of hypoxia-inducible factor 1alpha is mediated by an O2-dependent degradation domain via the ubiquitin-proteasome pathway. Proc Natl Acad Sci U S A *95*, 7987-7992.
- Huang, P., Feng, L., Oldham, E.A., Keating, M.J., and Plunkett, W. (2000). Superoxide dismutase as a target for the selective killing of cancer cells. Nature *407*, 390-395.
- Hutchison, C.J. (2002). Lamins: building blocks or regulators of gene expression? Nat Rev Mol Cell Biol *3*, 848-858.
- Hutchison, C.J., Alvarez-Reyes, M., and Vaughan, O.A. (2001). Lamins in disease: why do ubiquitously expressed nuclear envelope proteins give rise to tissue-specific disease phenotypes? J Cell Sci *114*, 9-19.
- Hutchison, C.J., and Worman, H.J. (2004). A-type lamins: guardians of the soma? Nat Cell Biol *6*, 1062-1067.
- Inoue, M., Sato, E.F., Nishikawa, M., Park, A.M., Kira, Y., Imada, I., and Utsumi, K. (2003). Mitochondrial generation of reactive oxygen species and its role in aerobic life. Curr Med Chem *10*, 2495-2505.
- Ivorra, C., Kubicek, M., Gonzalez, J.M., Sanz-Gonzalez, S.M., Alvarez-Barrientos, A., O'Connor, J.E., Burke, B., and Andres, V. (2006). A mechanism of AP-1 suppression through interaction of c-Fos with lamin A/C. Genes Dev *20*, 307-320.
- Iwata, S., Lee, J.W., Okada, K., Lee, J.K., Iwata, M., Rasmussen, B., Link, T.A., Ramaswamy, S., and Jap, B.K. (1998). Complete structure of the 11-subunit bovine mitochondrial cytochrome bc1 complex. Science *281*, 64-71.
- Izumi, M., Vaughan, O.A., Hutchison, C.J., and Gilbert, D.M. (2000). Head and/or CaaX domain deletions of lamin proteins disrupt preformed lamin A and C but not lamin B structure in mammalian cells. Mol Biol Cell *11*, 4323-4337.
- Jagatheesan, G., Thanumalayan, S., Muralikrishna, B., Rangaraj, N., Karande, A.A., and Parnaik, V.K. (1999). Colocalization of intranuclear lamin foci with RNA splicing factors. J Cell Sci *112 (Pt 24)*, 4651-4661.
- Jaksch, M., Ogilvie, I., Yao, J., Kortenhaus, G., Bresser, H.G., Gerbitz, K.D., and Shoubridge, E.A. (2000). Mutations in SCO2 are associated with a distinct form of hypertrophic cardiomyopathy and cytochrome c oxidase deficiency. Hum Mol Genet *9*, 795-801.
- Jeronimo, C., Nomoto, S., Caballero, O.L., Usadel, H., Henrique, R., Varzim, G., Oliveira, J., Lopes, C., Fliss, M.S., and Sidransky, D. (2001). Mitochondrial mutations in early stage prostate cancer and bodily fluids. Oncogene *20*, 5195-5198.
- Ji, J.Y., Lee, R.T., Vergnes, L., Fong, L.G., Stewart, C.L., Reue, K., Young, S.G., Zhang, Q., Shanahan, C.M., and Lammerding, J. (2007). Cell nuclei spin in the absence of lamin b1. J Biol Chem *282*, 20015-20026.
- Jiang, B.H., Semenza, G.L., Bauer, C., and Marti, H.H. (1996). Hypoxia-inducible factor 1 levels vary exponentially over a physiologically relevant range of O2 tension. Am J Physiol *271*, C1172-1180.

- Johnson, B.R., Nitta, R.T., Frock, R.L., Mounkes, L., Barbie, D.A., Stewart, C.L., Harlow, E., and Kennedy, B.K. (2004). A-type lamins regulate retinoblastoma protein function by promoting subnuclear localization and preventing proteasomal degradation. Proc Natl Acad Sci U S A *101*, 9677-9682.
- Kadenbach, B., Schneyder, B., Mell, O., Stroh, S., and Reimann, A. (1991). Respiratory chain proteins. Rev Neurol (Paris) *147*, 436-442.
- Kagan, J., and Srivastava, S. (2005). Mitochondria as a target for early detection and diagnosis of cancer. Crit Rev Clin Lab Sci *42*, 453-472.
- Kaguni, L.S. (2004). DNA polymerase gamma, the mitochondrial replicase. Annu Rev Biochem *73*, 293-320.
- Kalaria, R.N. (1999). The blood-brain barrier and cerebrovascular pathology in Alzheimer's disease. Ann N Y Acad Sci *893*, 113-125.
- Kaufmann, S.H., Mabry, M., Jasti, R., and Shaper, J.H. (1991). Differential expression of nuclear envelope lamins A and C in human lung cancer cell lines. Cancer Res *51*, 581-586.
- Kawai, M., Kalaria, R.N., Harik, S.I., and Perry, G. (1990). The relationship of amyloid plaques to cerebral capillaries in Alzheimer's disease. Am J Pathol *137*, 1435-1446.
- Kirchhoff, P., and Geibel, J. P. (2006). Role of calcium and other trace elements in the gastrointestinal physiology. World J Gastroenterol *12*, 3229-3236.
- Kischkel, F.C., Lawrence, D.A., Tinel, A., LeBlanc, H., Virmani, A., Schow, P., Gazdar, A., Blenis, J., Arnott, D., and Ashkenazi, A. (2001). Death receptor recruitment of endogenous caspase-10 and apoptosis initiation in the absence of caspase-8. J Biol Chem *276*, 46639-46646.
- Klener, P., Jr., Andera, L., Klener, P., Necas, E., and Zivny, J. (2006). Cell death signalling pathways in the pathogenesis and therapy of haematologic malignancies: overview of therapeutic approaches. Folia Biol (Praha) *52*, 119-136.
- Komiya, T., Rospert, S., Schatz, G., and Mihara, K. (1997). Binding of mitochondrial precursor proteins to the cytoplasmic domains of the import receptors Tom70 and Tom20 is determined by cytoplasmic chaperones. Embo J *16*, 4267-4275.
- Koshiba, T., Detmer, S.A., Kaiser, J.T., Chen, H., McCaffery, J.M., and Chan, D.C. (2004). Structural basis of mitochondrial tethering by mitofusin complexes. Science *305*, 858-862.
- Kristal, B.S., and Krasnikov, B.F. (2003). Structure-(Dys)function relationships in mitochondrial electron transport chain complex II? Sci Aging Knowledge Environ *2003*, PE3.
- Lamas, S., Marsden, P.A., Li, G.K., Tempst, P., and Michel, T. (1992). Endothelial nitric oxide synthase: molecular cloning and characterization of a distinct constitutive enzyme isoform. Proc Natl Acad Sci U S A *89*, 6348-6352.
- Lamb, N.J., Cavadore, J.C., Labbe, J.C., Maurer, R.A., and Fernandez, A. (1991). Inhibition of cAMP-dependent protein kinase plays a key role in the induction of mitosis and nuclear envelope breakdown in mammalian cells. Embo J *10*, 1523-1533.

- Langston, J.W., Ballard, P., Tetrud, J.W., and Irwin, I. (1983). Chronic Parkinsonism in humans due to a product of meperidine-analog synthesis. Science *219*, 979-980.
- Lattanzi, G., Cenni, V., Marmiroli, S., Capanni, C., Mattioli, E., Merlini, L., Squarzoni, S., and Maraldi, N.M. (2003). Association of emerin with nuclear and cytoplasmic actin is regulated in differentiating myoblasts. Biochem Biophys Res Commun *303*, 764-770.
- Leary, S.C., Hill, B.C., Lyons, C.N., Carlson, C.G., Michaud, D., Kraft, C.S., Ko, K., Glerum, D.M., and Moyes, C.D. (2002). Chronic treatment with azide in situ leads to an irreversible loss of cytochrome c oxidase activity via holoenzyme dissociation. J Biol Chem *277*, 11321-11328.
- Lee, J.S., Hale, C.M., Panorchan, P., Khatau, S.B., George, J.P., Tseng, Y., Stewart, C.L., Hodzic, D., and Wirtz, D. (2007). Nuclear lamin A/C deficiency induces defects in cell mechanics, polarization, and migration. Biophys J *93*, 2542-2552.
- Lee, K.K., Haraguchi, T., Lee, R.S., Koujin, T., Hiraoka, Y., and Wilson, K.L. (2001). Distinct functional domains in emerin bind lamin A and DNA-bridging protein BAF. J Cell Sci *114*, 4567-4573.
- Lee, K.K., Starr, D., Cohen, M., Liu, J., Han, M., Wilson, K.L., and Gruenbaum, Y. (2002). Lamin-dependent localization of UNC-84, a protein required for nuclear migration in Caenorhabditis elegans. Mol Biol Cell *13*, 892-901.
- Lehner, C.F., Kurer, V., Eppenberger, H.M., and Nigg, E.A. (1986). The nuclear lamin protein family in higher vertebrates. Identification of quantitatively minor lamin proteins by monoclonal antibodies. J Biol Chem *261*, 13293-13301.
- Li, Z., Okamoto, K., Hayashi, Y., and Sheng, M. (2004). The importance of dendritic mitochondria in the morphogenesis and plasticity of spines and synapses. Cell *119*, 873-887.
- Libotte, T., Zaim, H., Abraham, S., Padmakumar, V.C., Schneider, M., Lu, W., Munck, M., Hutchison, C., Wehnert, M., Fahrenkrog, B., Sauder, U., Aebi, U., Noegel, A.A., and Karakesisoglou, I. (2005). Lamin A/C-dependent localization of Nesprin-2, a giant scaffolder at the nuclear envelope. Mol Biol Cell *16*, 3411-3424.
- Lim, K.H., Javadov, S.A., Das, M., Clarke, S.J., Suleiman, M.S., and Halestrap, A.P. (2002). The effects of ischaemic preconditioning, diazoxide and 5-hydroxydecanoate on rat heart mitochondrial volume and respiration. J Physiol *545*, 961-974.
- Lin, F., Blake, D.L., Callebaut, I., Skerjanc, I.S., Holmer, L., McBurney, M.W., Paulin-Levasseur, M., and Worman, H.J. (2000). MAN1, an inner nuclear membrane protein that shares the LEM domain with lamina-associated polypeptide 2 and emerin. J Biol Chem *275*, 4840-4847.
- Lin, F., and Worman, H.J. (1993). Structural organization of the human gene encoding nuclear lamin A and nuclear lamin C. J Biol Chem *268*, 16321-16326.

- Liu, J., Rolef Ben-Shahar, T., Riemer, D., Treinin, M., Spann, P., Weber, K., Fire, A., and Gruenbaum, Y. (2000). Essential roles for Caenorhabditis elegans lamin gene in nuclear organization, cell cycle progression, and spatial organization of nuclear pore complexes. Mol Biol Cell *11*, 3937-3947.
- Lloyd, D.J., Trembath, R.C., and Shackleton, S. (2002). A novel interaction between lamin A and SREBP1: implications for partial lipodystrophy and other laminopathies. Hum Mol Genet *11*, 769-777.
- Longley, M.J., Ropp, P.A., Lim, S.E., and Copeland, W.C. (1998). Characterization of the native and recombinant catalytic subunit of human DNA polymerase gamma: identification of residues critical for exonuclease activity and dideoxynucleotide sensitivity. Biochemistry *37*, 10529-10539.
- Lovell, M.A., Xie, C., and Markesbery, W.R. (1998). Decreased glutathione transferase activity in brain and ventricular fluid in Alzheimer's disease. Neurology *51*, 1562-1566.
- Ludwig, B., Bender, E., Arnold, S., Huttemann, M., Lee, I., and Kadenbach, B. (2001). Cytochrome C oxidase and the regulation of oxidative phosphorylation. Chembiochem *2*, 392-403.
- Lum, H., and Roebuck, K.A. (2001). Oxidant stress and endothelial cell dysfunction. Am J Physiol Cell Physiol *280*, C719-741.
- Luoma, P., Melberg, A., Rinne, J.O., Kaukonen, J.A., Nupponen, N.N., Chalmers, R.M., Oldfors, A., Rautakorpi, I., Peltonen, L., Majamaa, K., Somer, H., and Suomalainen, A. (2004). Parkinsonism, premature menopause, and mitochondrial DNA polymerase gamma mutations: clinical and molecular genetic study. Lancet *364*, 875-882.
- Machiels, B.M., Zorenc, A.H., Endert, J.M., Kuijpers, H.J., van Eys, G.J., Ramaekers, F.C., and Broers, J.L. (1996). An alternative splicing product of the lamin A/C gene lacks exon 10. J Biol Chem *271*, 9249-9253.
- Madamanchi, N.R., and Runge, M.S. (2007). Mitochondrial dysfunction in atherosclerosis. Circ Res *100*, 460-473.
- Malone, C.J., Fixsen, W.D., Horvitz, H.R., and Han, M. (1999). UNC-84 localizes to the nuclear envelope and is required for nuclear migration and anchoring during C. elegans development. Development *126*, 3171-3181.
- Malone, C.J., Misner, L., Le Bot, N., Tsai, M.C., Campbell, J.M., Ahringer, J., and White, J.G. (2003). The C. elegans hook protein, ZYG-12, mediates the essential attachment between the centrosome and nucleus. Cell *115*, 825-836.
- Mandemakers, W., Morais, V.A., and De Strooper, B. (2007). A cell biological perspective on mitochondrial dysfunction in Parkinson disease and other neurodegenerative diseases. J Cell Sci *120*, 1707-1716.
- Markiewicz, E., Dechat, T., Foisner, R., Quinlan, R.A., and Hutchison, C.J. (2002). Lamin A/C binding protein LAP2alpha is required for nuclear anchorage of retinoblastoma protein. Mol Biol Cell *13*, 4401-4413.
- Markiewicz, E., Venables, R., Mauricio Alvarez, R., Quinlan, R., Dorobek, M., Hausmanowa-Petrucewicz, I., and Hutchison, C. (2002). Increased solubility of lamins and redistribution of lamin C in X-linked Emery-Dreifuss muscular dystrophy fibroblasts. J Struct Biol *140*, 241-253.

- Markiewicz, E., Tilgner, K., Barker, N., van de Wetering, M., Clevers, H., Dorobek, M., Hausmanowa-Petrusewicz, I., Ramaekers, F.C., Broers, J.L., Blankesteijn, W.M., Salpingidou, G., Wilson, R.G., Ellis, J.A., and Hutchison, C.J. (2006). The inner nuclear membrane protein emerin regulates beta-catenin activity by restricting its accumulation in the nucleus. Embo J *25*, 3275-3285.
- Martins, S., Eikvar, S., Furukawa, K., and Collas, P. (2003). HA95 and LAP2 beta mediate a novel chromatin-nuclear envelope interaction implicated in initiation of DNA replication. J Cell Biol *160*, 177-188.
- Matoba, S., Kang, J.G., Patino, W.D., Wragg, A., Boehm, M., Gavrilova, O., Hurley, P.J., Bunz, F., and Hwang, P.M. (2006). p53 regulates mitochondrial respiration. Science *312*, 1650-1653.
- Mattson, M.P. (2004). Pathways towards and away from Alzheimer's disease. Nature *430*, 631-639.
- Maxwell, P.H., Wiesener, M.S., Chang, G.W., Clifford, S.C., Vaux, E.C., Cockman, M.E., Wykoff, C.C., Pugh, C.W., Maher, E.R., and Ratcliffe, P.J. (1999). The tumour suppressor protein VHL targets hypoxia-inducible factors for oxygen-dependent proteolysis. Nature *399*, 271-275.
- Mazzanti, R., Solazzo, M., Fantappie, O., Elfering, S., Pantaleo, P., Bechi, P., Cianchi, F., Ettl, A., and Giulivi, C. (2006). Differential expression proteomics of human colon cancer. Am J Physiol Gastrointest Liver Physiol *290*, G1329-1338.
- Mecocci, P., MacGarvey, U., and Beal, M.F. (1994). Oxidative damage to mitochondrial DNA is increased in Alzheimer's disease. Ann Neurol *36*, 747-751.
- Meier, J., Campbell, K.H., Ford, C.C., Stick, R., and Hutchison, C.J. (1991). The role of lamin LIII in nuclear assembly and DNA replication, in cell-free extracts of Xenopus eggs. J Cell Sci *98 (Pt 3)*, 271-279.
- Metzen, E., Zhou, J., Jelkmann, W., Fandrey, J., and Brune, B. (2003). Nitric oxide impairs normoxic degradation of HIF-1alpha by inhibition of prolyl hydroxylases. Mol Biol Cell *14*, 3470-3481.
- Michel, H., Behr, J., Harrenga, A., and Kannt, A. (1998). Cytochrome c oxidase: structure and spectroscopy. Annu Rev Biophys Biomol Struct *27*, 329-356.
- Miselli, F., Negri, T., Gronchi, A., Losa, M., Conca, E., Brich, S., Fumagalli, E., Fiore, M., Casali, P.G., Pierotti, M.A., Tamborini, E., and Pilotti, S. (2008). Is autophagy rather than apoptosis the regression driver in imatinib-treated gastrointestinal stromal tumors? Transl Oncol *1*, 177-186.
- Mislow, J.M., Holaska, J.M., Kim, M.S., Lee, K.K., Segura-Totten, M., Wilson, K.L., and McNally, E.M. (2002). Nesprin-1alpha self-associates and binds directly to emerin and lamin A in vitro. FEBS Lett *525*, 135-140.
- Moir, R.D., Donaldson, A.D., and Stewart, M. (1991). Expression in Escherichia coli of human lamins A and C: influence of head and tail domains on assembly properties and paracrystal formation. J Cell Sci *99 (Pt 2)*, 363-372.

- Moir, R.D., Spann, T.P., Lopez-Soler, R.I., Yoon, M., Goldman, A.E., Khuon, S., and Goldman, R.D. (2000a). Review: the dynamics of the nuclear lamins during the cell cycle-- relationship between structure and function. J Struct Biol *129*, 324-334.
- Moir, R.D., Yoon, M., Khuon, S., and Goldman, R.D. (2000b). Nuclear lamins A and B1: different pathways of assembly during nuclear envelope formation in living cells. J Cell Biol *151*, 1155-1168.
- Moss, S.F., Krivosheyev, V., de Souza, A., Chin, K., Gaetz, H.P., Chaudhary, N., Worman, H.J., and Holt, P.R. (1999). Decreased and aberrant nuclear lamin expression in gastrointestinal tract neoplasms. Gut *45*, 723-729.
- Mounkes, L.C., Kozlov, S., Hernandez, L., Sullivan, T., and Stewart, C.L. (2003). A progeroid syndrome in mice is caused by defects in A-type lamins. Nature *423*, 298-301.
- Muchir, A., Bonne, G., van der Kooi, A.J., van Meegen, M., Baas, F., Bolhuis, P.A., de Visser, M., and Schwartz, K. (2000). Identification of mutations in the gene encoding lamins A/C in autosomal dominant limb girdle muscular dystrophy with atrioventricular conduction disturbances (LGMD1B). Hum Mol Genet *9*, 1453-1459.
- Muchir, A., van Engelen, B.G., Lammens, M., Mislow, J.M., McNally, E., Schwartz, K., and Bonne, G. (2003). Nuclear envelope alterations in fibroblasts from LGMD1B patients carrying nonsense Y259X heterozygous or homozygous mutation in lamin A/C gene. Exp Cell Res *291*, 352-362.
- Muchir, A., and Worman, H.J. (2004). The nuclear envelope and human disease. Physiology (Bethesda) *19*, 309-314.
- Murphy, M.P. (2009). How mitochondria produce reactive oxygen species. Biochem J *417*, 1-13.
- Navarro, A., Torrejon, R., Bandez, M.J., Lopez-Cepero, J.M., and Boveris, A. (2005). Mitochondrial function and mitochondria-induced apoptosis in an overstimulated rat ovarian cycle. Am J Physiol Endocrinol Metab *289*, E1101-1109.
- Navarro, C.L., De Sandre-Giovannoli, A., Bernard, R., Boccaccio, I., Boyer, A., Genevieve, D., Hadj-Rabia, S., Gaudy-Marqueste, C., Smitt, H.S., Vabres, P., Faivre, L., Verloes, A., Van Essen, T., Flori, E., Hennekam, R., Beemer, F.A., Laurent, N., Le Merrer, M., Cau, P., and Levy, N. (2004). Lamin A and ZMPSTE24 (FACE-1) defects cause nuclear disorganization and identify restrictive dermopathy as a lethal neonatal laminopathy. Hum Mol Genet *13*, 2493-2503.
- Navarro, C.L., Cadinanos, J., De Sandre-Giovannoli, A., Bernard, R., Courrier, S., Boccaccio, I., Boyer, A., Kleijer, W.J., Wagner, A., Giuliano, F., Beemer, F.A., Freije, J.M., Cau, P., Hennekam, R.C., Lopez-Otin, C., Badens, C., and Levy, N. (2005). Loss of ZMPSTE24 (FACE-1) causes autosomal recessive restrictive dermopathy and accumulation of Lamin A precursors. Hum Mol Genet *14*, 1503-1513.
- Newport, J.W., Wilson, K.L., and Dunphy, W.G. (1990). A lamin-independent pathway for nuclear envelope assembly. J Cell Biol *111*, 2247-2259.

- Niemann, A., Ruegg, M., La Padula, V., Schenone, A., and Suter, U. (2005). Ganglioside-induced differentiation associated protein 1 is a regulator of the mitochondrial network: new implications for Charcot-Marie-Tooth disease. J Cell Biol *170*, 1067-1078.
- Nili, E., Cojocaru, G.S., Kalma, Y., Ginsberg, D., Copeland, N.G., Gilbert, D.J., Jenkins, N.A., Berger, R., Shaklai, S., Amariglio, N., Brok-Simoni, F., Simon, A.J., and Rechavi, G. (2001). Nuclear membrane protein LAP2beta mediates transcriptional repression alone and together with its binding partner GCL (germ-cell-less). J Cell Sci *114*, 3297-3307.
- Nishikawa, T., Edelstein, D., Du, X.L., Yamagishi, S., Matsumura, T., Kaneda, Y., Yorek, M.A., Beebe, D., Oates, P.J., Hammes, H.P., Giardino, I., and Brownlee, M. (2000). Normalizing mitochondrial superoxide production blocks three pathways of hyperglycaemic damage. Nature *404*, 787-790.
- Nisoli, E., Clementi, E., Paolucci, C., Cozzi, V., Tonello, C., Sciorati, C., Bracale, R., Valerio, A., Francolini, M., Moncada, S., and Carruba, M.O. (2003). Mitochondrial biogenesis in mammals: the role of endogenous nitric oxide. Science *299*, 896-899.
- Nobrega, M.P., Bandeira, S.C., Beers, J., and Tzagoloff, A. (2002). Characterization of COX19, a widely distributed gene required for expression of mitochondrial cytochrome oxidase. J Biol Chem *277*, 40206-40211.
- Norbury, C.J., and Nurse, P. (1989). Control of the higher eukaryote cell cycle by p34cdc2 homologues. Biochim Biophys Acta *989*, 85-95.
- Nunomura, A., Chiba, S., Lippa, C.F., Cras, P., Kalaria, R.N., Takeda, A., Honda, K., Smith, M.A., and Perry, G. (2004). Neuronal RNA oxidation is a prominent feature of familial Alzheimer's disease. Neurobiol Dis *17*, 108-113.
- Nunomura, A., Perry, G., Pappolla, M.A., Wade, R., Hirai, K., Chiba, S., and Smith, M.A. (1999). RNA oxidation is a prominent feature of vulnerable neurons in Alzheimer's disease. J Neurosci *19*, 1959-1964.
- Okinaga, T., Kasai, H., Tsujisawa, T., and Nishihara, T. (2007). Role of caspases in cleavage of lamin A/C and PARP during apoptosis in macrophages infected with a periodontopathic bacterium. J Med Microbiol *56*, 1399-1404.
- Olichon, A., Emorine, L.J., Descoins, E., Pelloquin, L., Brichese, L., Gas, N., Guillou, E., Delettre, C., Valette, A., Hamel, C.P., Ducommun, B., Lenaers, G., and Belenguer, P. (2002). The human dynamin-related protein OPA1 is anchored to the mitochondrial inner membrane facing the inter-membrane space. FEBS Lett *523*, 171-176.
- Ondrej, V., Lukasova, E., Krejci, J., and Kozubek, S. (2008). Intranuclear trafficking of plasmid DNA is mediated by nuclear polymeric proteins lamins and actin. Acta Biochim Pol *55*, 307-315.
- Ojaimi, J., and Byrne, E. (2001). Mitochondrial function and alzheimer's disease. Biol Signals Recept *10*, 254-262.
- Orth, K., Chinnaiyan, A.M., Garg, M., Froelich, C.J., and Dixit, V.M. (1996). The CED-3/ICE-like protease Mch2 is activated during apoptosis and cleaves the death substrate lamin A. J Biol Chem *271*, 16443-16446.

- Ozaki, T., Saijo, M., Murakami, K., Enomoto, H., Taya, Y., and Sakiyama, S. (1994). Complex formation between lamin A and the retinoblastoma gene product: identification of the domain on lamin A required for its interaction. Oncogene *9*, 2649-2653.
- Padiath, Q.S., Saigoh, K., Schiffmann, R., Asahara, H., Yamada, T., Koeppen, A., Hogan, K., Ptacek, L.J., and Fu, Y.H. (2006). Lamin B1 duplications cause autosomal dominant leukodystrophy. Nat Genet *38*, 1114-1123.
- Padmakumar, V.C., Abraham, S., Braune, S., Noegel, A.A., Tunggal, B., Karakesisoglou, I., and Korenbaum, E. (2004). Enaptin, a giant actin-binding protein, is an element of the nuclear membrane and the actin cytoskeleton. Exp Cell Res *295*, 330-339.
- Padmakumar, V.C., Libotte, T., Lu, W., Zaim, H., Abraham, S., Noegel, A.A., Gotzmann, J., Foisner, R., and Karakesisoglou, I. (2005). The inner nuclear membrane protein Sun1 mediates the anchorage of Nesprin-2 to the nuclear envelope. J Cell Sci *118*, 3419-3430.
- Paglin, S., Hollister, T., Delohery, T., Hackett, N., McMahill, M., Sphicas, E., Domingo, D., and Yahalom, J. (2001). A novel response of cancer cells to radiation involves autophagy and formation of acidic vesicles. Cancer Res *61*, 439-444.
- Pagnamenta, A.T., Taanman, J.W., Wilson, C.J., Anderson, N.E., Marotta, R., Duncan, A.J., Bitner-Glindzicz, M., Taylor, R.W., Laskowski, A., Thorburn, D.R., and Rahman, S. (2006). Dominant inheritance of premature ovarian failure associated with mutant mitochondrial DNA polymerase gamma. Hum Reprod *21*, 2467-2473.
- Papadopoulou, L.C., Sue, C.M., Davidson, M.M., Tanji, K., Nishino, I., Sadlock, J.E., Krishna, S., Walker, W., Selby, J., Glerum, D.M., Coster, R.V., Lyon, G., Scalais, E., Lebel, R., Kaplan, P., Shanske, S., De Vivo, D.C., Bonilla, E., Hirano, M., DiMauro, S., and Schon, E.A. (1999). Fatal infantile cardioencephalomyopathy with COX deficiency and mutations in SCO2, a COX assembly gene. Nat Genet *23*, 333-337.
- Parise, P., Finocchiaro, G., Masciadri, B., Quarto, M., Francois, S., Mancuso, F., and Muller, H. (2006). Lap2alpha expression is controlled by E2F and deregulated in various human tumors. Cell Cycle *5*, 1331-1341.
- Pecina, P., Houstkova, H., Hansikova, H., Zeman, J., and Houstek, J. (2004). Genetic defects of cytochrome c oxidase assembly. Physiol Res *53 Suppl 1*, S213-223.
- Pedrola, L., Espert, A., Wu, X., Claramunt, R., Shy, M.E., and Palau, F. (2005). GDAP1, the protein causing Charcot-Marie-Tooth disease type 4A, is expressed in neurons and is associated with mitochondria. Hum Mol Genet *14*, 1087-1094.
- Pekovic, V., Harborth, J., Broers, J.L., Ramaekers, F.C., van Engelen, B., Lammens, M., von Zglinicki, T., Foisner, R., Hutchison, C., and Markiewicz, E. (2007). Nucleoplasmic LAP2alpha-lamin A complexes are required to maintain a proliferative state in human fibroblasts. J Cell Biol *176*, 163-172.

- Pendas, A.M., Zhou, Z., Cadinanos, J., Freije, J.M., Wang, J., Hultenby, K., Astudillo, A., Wernerson, A., Rodriguez, F., Tryggvason, K., and Lopez-Otin, C. (2002). Defective prelamin A processing and muscular and adipocyte alterations in Zmpste24 metalloproteinase-deficient mice. Nat Genet *31*, 94-99.
- Persichini, T., Mazzone, V., Polticelli, F., Moreno, S., Venturini, G., Clementi, E., and Colasanti, M. (2005). Mitochondrial type I nitric oxide synthase physically interacts with cytochrome c oxidase. Neurosci Lett *384*, 254-259.
- Petak, I., and Houghton, J.A. (2001). Shared pathways: death receptors and cytotoxic drugs in cancer therapy. Pathol Oncol Res *7*, 95-106.
- Peter, M., Nakagawa, J., Doree, M., Labbe, J.C., and Nigg, E.A. (1990). In vitro disassembly of the nuclear lamina and M phase-specific phosphorylation of lamins by cdc2 kinase. Cell *61*, 591-602.
- Petit, A., Kawarai, T., Paitel, E., Sanjo, N., Maj, M., Scheid, M., Chen, F., Gu, Y., Hasegawa, H., Salehi-Rad, S., Wang, L., Rogaeva, E., Fraser, P., Robinson, B., St George-Hyslop, P., and Tandon, A. (2005). Wild-type PINK1 prevents basal and induced neuronal apoptosis, a protective effect abrogated by Parkinson disease-related mutations. J Biol Chem *280*, 34025-34032.
- Petros, J.A., Baumann, A.K., Ruiz-Pesini, E., Amin, M.B., Sun, C.Q., Hall, J., Lim, S., Issa, M.M., Flanders, W.D., Hosseini, S.H., Marshall, F.F., and Wallace, D.C. (2005). mtDNA mutations increase tumorigenicity in prostate cancer. Proc Natl Acad Sci U S A *102*, 719-724.
- Poderoso, J.J., Carreras, M.C., Lisdero, C., Riobo, N., Schopfer, F., and Boveris, A. (1996). Nitric oxide inhibits electron transfer and increases superoxide radical production in rat heart mitochondria and submitochondrial particles. Arch Biochem Biophys *328*, 85-92.
- Postnov Iu, V. (2001). [The role of mitochondrial calcium overload and energy deficiency in pathogenesis of arterial hypertension]. Arkh Patol *63*, 3-10.
- Prendergast, G. C., Davide, J. P., Lebowitz, P. F., Wechsler-Reya, R., and Kohl, N. E. (1996). Resistance of a variant ras-transformed cell line to phenotypic reversion by farnesyl transferase inhibitors. Cancer Res *56*, 2626-2632.
- Pyle, A., Foltynie, T., Tiangyou, W., Lambert, C., Keers, S.M., Allcock, L.M., Davison, J., Lewis, S.J., Perry, R.H., Barker, R., Burn, D.J., and Chinnery, P.F. (2005). Mitochondrial DNA haplogroup cluster UKJT reduces the risk of PD. Ann Neurol *57*, 564-567.
- Rahman, S., Blok, R.B., Dahl, H.H., Danks, D.M., Kirby, D.M., Chow, C.W., Christodoulou, J., and Thorburn, D.R. (1996). Leigh syndrome: clinical features and biochemical and DNA abnormalities. Ann Neurol *39*, 343-351.
- Rahman, S., Taanman, J.W., Cooper, J.M., Nelson, I., Hargreaves, I., Meunier, B., Hanna, M.G., Garcia, J.J., Capaldi, R.A., Lake, B.D., Leonard, J.V., and Schapira, A.H. (1999). A missense mutation of cytochrome oxidase subunit II causes defective assembly and myopathy. Am J Hum Genet *65*, 1030-1039.

- Rassow, J., Hartl, F.U., Guiard, B., Pfanner, N., and Neupert, W. (1990). Polypeptides traverse the mitochondrial envelope in an extended state. FEBS Lett *275*, 190-194.
- Riviere, S., Birlouez-Aragon, I., Nourhashemi, F., and Vellas, B. (1998). Low plasma vitamin C in Alzheimer patients despite an adequate diet. Int J Geriatr Psychiatry *13*, 749-754.
- Rospert, S., Looser, R., Dubaquie, Y., Matouschek, A., Glick, B.S., and Schatz, G. (1996). Hsp60-independent protein folding in the matrix of yeast mitochondria. Embo J *15*, 764-774.
- Rusinol, A.E., and Sinensky, M.S. (2006). Farnesylated lamins, progeroid syndromes and farnesyl transferase inhibitors. J Cell Sci *119*, 3265-3272.
- Salina, D., Bodoor, K., Eckley, D.M., Schroer, T.A., Rattner, J.B., and Burke, B. (2002). Cytoplasmic dynein as a facilitator of nuclear envelope breakdown. Cell *108*, 97-107.
- Salviati, L., Sacconi, S., Rasalan, M.M., Kronn, D.F., Braun, A., Canoll, P., Davidson, M., Shanske, S., Bonilla, E., Hays, A.P., Schon, E.A., and DiMauro, S. (2002). Cytochrome c oxidase deficiency due to a novel SCO2 mutation mimics Werdnig-Hoffmann disease. Arch Neurol *59*, 862-865.
- Sarkar, P.K., and Shinton, R.A. (2001). Hutchinson-Guilford progeria syndrome. Postgrad Med J *77*, 312-317.
- Sayre, L.M., Zelasko, D.A., Harris, P.L., Perry, G., Salomon, R.G., and Smith, M.A. (1997). 4-Hydroxynonenal-derived advanced lipid peroxidation end products are increased in Alzheimer's disease. J Neurochem *68*, 2092-2097.
- Sazanov, L.A., and Hinchliffe, P. (2006). Structure of the hydrophilic domain of respiratory complex I from Thermus thermophilus. Science *311*, 1430-1436.
- Sazanov, L.A. (2007). Respiratory complex I: mechanistic and structural insights provided by the crystal structure of the hydrophilic domain. Biochemistry *46*, 2275-2288.
- Schafer, F.Q., and Buettner, G.R. (2001). Redox environment of the cell as viewed through the redox state of the glutathione disulfide/glutathione couple. Free Radic Biol Med *30*, 1191-1212.
- Schofield, C.J., and Ratcliffe, P.J. (2004). Oxygen sensing by HIF hydroxylases. Nat Rev Mol Cell Biol *5*, 343-354.
- Segura-Totten, M., and Wilson, K.L. (2004). BAF: roles in chromatin, nuclear structure and retrovirus integration. Trends Cell Biol *14*, 261-266.
- Selkoe, D.J. (2001). Alzheimer's disease results from the cerebral accumulation and cytotoxicity of amyloid beta-protein. J Alzheimers Dis *3*, 75-80.
- Semenza, G.L. (2004). Hydroxylation of HIF-1: oxygen sensing at the molecular level. Physiology (Bethesda) *19*, 176-182.
- Semenza, G.L., Shimoda, L.A., and Prabhakar, N.R. (2006). Regulation of gene expression by HIF-1. Novartis Found Symp *272*, 2-8; discussion 8-14, 33-16.
- Sen, C.K. (2000). Cellular thiols and redox-regulated signal transduction. Curr Top Cell Regul *36*, 1-30.

- Seneca, S., Verhelst, H., De Meirleir, L., Meire, F., Ceuterick-De Groote, C., Lissens, W., and Van Coster, R. (2001). A new mitochondrial point mutation in the transfer RNA(Leu) gene in a patient with a clinical phenotype resembling Kearns-Sayre syndrome. Arch Neurol *58*, 1113-1118.
- Shackleton, S., Lloyd, D.J., Jackson, S.N., Evans, R., Niermeijer, M.F., Singh, B.M., Schmidt, H., Brabant, G., Kumar, S., Durrington, P.N., Gregory, S., O'Rahilly, S., and Trembath, R.C. (2000). LMNA, encoding lamin A/C, is mutated in partial lipodystrophy. Nat Genet *24*, 153-156.
- Shaklai, S., Amariglio, N., Rechavi, G., and Simon, A.J. (2007). Gene silencing at the nuclear periphery. Febs J *274*, 1383-1392.
- Sherer, T.B., Kim, J.H., Betarbet, R., and Greenamyre, J.T. (2003). Subcutaneous rotenone exposure causes highly selective dopaminergic degeneration and alpha-synuclein aggregation. Exp Neurol *179*, 9-16.
- Shimura, H., Hattori, N., Kubo, S., Mizuno, Y., Asakawa, S., Minoshima, S., Shimizu, N., Iwai, K., Chiba, T., Tanaka, K., and Suzuki, T. (2000). Familial Parkinson disease gene product, parkin, is a ubiquitin-protein ligase. Nat Genet *25*, 302-305.
- Shoubridge, E.A. (2001). Cytochrome c oxidase deficiency. Am J Med Genet *106*, 46-52.
- Silva, L., Cliffe, A., Chang, L., and Knipe, D.M. (2008). Role for A-type lamins in herpesviral DNA targeting and heterochromatin modulation. PLoS Pathog *4*, e1000071.
- Simha, V., Agarwal, A.K., Oral, E.A., Fryns, J.P., and Garg, A. (2003). Genetic and phenotypic heterogeneity in patients with mandibuloacral dysplasia-associated lipodystrophy. J Clin Endocrinol Metab *88*, 2821-2824.
- Singh, K.K. (2006). Mitochondria damage checkpoint, aging, and cancer. Ann N Y Acad Sci *1067*, 182-190.
- Simonnet, H., Alazard, N., Pfeiffer, K., Gallou, C., Beroud, C., Demont, J., Bouvier, R., Schagger, H., and Godinot, C. (2002). Low mitochondrial respiratory chain content correlates with tumor aggressiveness in renal cell carcinoma. Carcinogenesis *23*, 759-768.
- Smirnova, E., Griparic, L., Shurland, D.L., and van der Bliek, A.M. (2001). Dynamin-related protein Drp1 is required for mitochondrial division in mammalian cells. Mol Biol Cell *12*, 2245-2256.
- Smith, D., Gray, J., Mitchell, L., Antholine, W.E., and Hosler, J.P. (2005). Assembly of cytochrome-c oxidase in the absence of assembly protein Surf1p leads to loss of the active site heme. J Biol Chem *280*, 17652-17656.
- Smith, M.A., Perry, G., Richey, P.L., Sayre, L.M., Anderson, V.E., Beal, M.F., and Kowall, N. (1996). Oxidative damage in Alzheimer's. Nature *382*, 120-121.
- Smith, M.A., Rudnicka-Nawrot, M., Richey, P.L., Praprotnik, D., Mulvihill, P., Miller, C.A., Sayre, L.M., and Perry, G. (1995). Carbonyl-related posttranslational modification of neurofilament protein in the neurofibrillary pathology of Alzheimer's disease. J Neurochem *64*, 2660-2666.
- Smythe, C., Jenkins, H.E., and Hutchison, C.J. (2000). Incorporation of the nuclear pore basket protein nup153 into nuclear pore structures is dependent upon lamina assembly: evidence from cell-free extracts of Xenopus eggs. Embo J *19*, 3918-3931.

- Somech, R., Shaklai, S., Amariglio, N., Rechavi, G., and Simon, A.J. (2005a). Nuclear envelopathies--raising the nuclear veil. Pediatr Res *57*, 8R-15R.
- Somech, R., Shaklai, S., Geller, O., Amariglio, N., Simon, A.J., Rechavi, G., and Gal-Yam, E.N. (2005b). The nuclear-envelope protein and transcriptional repressor LAP2beta interacts with HDAC3 at the nuclear periphery, and induces histone H4 deacetylation. J Cell Sci *118*, 4017-4025.
- Souza-Pinto, N.C., Croteau, D.L., Hudson, E.K., Hansford, R.G., and Bohr, V.A. (1999). Age-associated increase in 8-oxo-deoxyguanosine glycosylase/AP lyase activity in rat mitochondria. Nucleic Acids Res *27*, 1935-1942.
- Spann, T.P., Goldman, A.E., Wang, C., Huang, S., and Goldman, R.D. (2002). Alteration of nuclear lamin organization inhibits RNA polymerase II-dependent transcription. J Cell Biol *156*, 603-608.
- Spann, T.P., Moir, R.D., Goldman, A.E., Stick, R., and Goldman, R.D. (1997). Disruption of nuclear lamin organization alters the distribution of replication factors and inhibits DNA synthesis. J Cell Biol *136*, 1201-1212.
- Starr, D.A., and Han, M. (2002). Role of ANC-1 in tethering nuclei to the actin cytoskeleton. Science *298*, 406-409.
- Starr, D.A., Hermann, G.J., Malone, C.J., Fixsen, W., Priess, J.R., Horvitz, H.R., and Han, M. (2001). unc-83 encodes a novel component of the nuclear envelope and is essential for proper nuclear migration. Development *128*, 5039-5050.
- Stewart, C.L., Kozlov, S., Fong, L.G., and Young, S.G. (2007). Mouse models of the laminopathies. Exp Cell Res *313*, 2144-2156.
- Stiburek, L., Hansikova, H., Tesarova, M., Cerna, L., and Zeman, J. (2006). Biogenesis of eukaryotic cytochrome c oxidase. Physiol Res *55 Suppl 2*, S27-41.
- Stiburek, L., Vesela, K., Hansikova, H., Pecina, P., Tesarova, M., Cerna, L., Houstek, J., and Zeman, J. (2005). Tissue-specific cytochrome c oxidase assembly defects due to mutations in SCO2 and SURF1. Biochem J *392*, 625-632.
- Stowers, R.S., Megeath, L.J., Gorska-Andrzejak, J., Meinertzhagen, I.A., and Schwarz, T.L. (2002). Axonal transport of mitochondria to synapses depends on milton, a novel Drosophila protein. Neuron *36*, 1063-1077.
- Strnad, P., Stumptner, C., Zatloukal, K., and Denk, H. (2008). Intermediate filament cytoskeleton of the liver in health and disease. Histochem Cell Biol *129*, 735-749.
- Stuurman, N., Heins, S., and Aebi, U. (1998). Nuclear lamins: their structure, assembly, and interactions. J Struct Biol *122*, 42-66.
- Summerhayes, I.C., Lampidis, T.J., Bernal, S.D., Nadakavukaren, J.J., Nadakavukaren, K.K., Shepherd, E.L., and Chen, L.B. (1982). Unusual retention of rhodamine 123 by mitochondria in muscle and carcinoma cells. Proc Natl Acad Sci U S A *79*, 5292-5296.
- Sun, A.S., Sepkowitz, K., and Geller, S.A. (1981). A study of some mitochondrial and peroxisomal enzymes in human colonic adenocarcinoma. Lab Invest *44*, 13-17.

- Susin, S.A., Lorenzo, H.K., Zamzami, N., Marzo, I., Snow, B.E., Brothers, G.M., Mangion, J., Jacotot, E., Costantini, P., Loeffler, M., Larochette, N., Goodlett, D.R., Aebersold, R., Siderovski, D.P., Penninger, J.M., and Kroemer, G. (1999). Molecular characterization of mitochondrial apoptosis-inducing factor. Nature *397*, 441-446.
- Suzuki, M., Jeong, S.Y., Karbowski, M., Youle, R.J., and Tjandra, N. (2003). The solution structure of human mitochondria fission protein Fis1 reveals a novel TPR-like helix bundle. J Mol Biol *334*, 445-458.
- Taanman, J.W. (1997). Human cytochrome c oxidase: structure, function, and deficiency. J Bioenerg Biomembr *29*, 151-163.
- Takuma, K., Yan, S.S., Stern, D.M., and Yamada, K. (2005). Mitochondrial dysfunction, endoplasmic reticulum stress, and apoptosis in Alzheimer's disease. J Pharmacol Sci *97*, 312-316.
- Tang, C.W., Maya-Mendoza, A., Martin, C., Zeng, K., Chen, S., Feret, D., Wilson, S.A., and Jackson, D.A. (2008). The integrity of a lamin-B1-dependent nucleoskeleton is a fundamental determinant of RNA synthesis in human cells. J Cell Sci *121*, 1014-1024.
- Taniura, H., Glass, C., and Gerace, L. (1995). A chromatin binding site in the tail domain of nuclear lamins that interacts with core histones. J Cell Biol *131*, 33-44.
- Taylor, B.S., and Geller, D.A. (2000). Molecular regulation of the human inducible nitric oxide synthase (iNOS) gene. Shock *13*, 413-424.
- Thannickal, V.J., and Fanburg, B.L. (2000). Reactive oxygen species in cell signaling. Am J Physiol Lung Cell Mol Physiol *279*, L1005-1028.
- Thomas, T., Thomas, G., McLendon, C., Sutton, T., and Mullan, M. (1996). beta-Amyloid-mediated vasoactivity and vascular endothelial damage. Nature *380*, 168-171.
- Thorburn, A. (2004). Death receptor-induced cell killing. Cell Signal *16*, 139-144.
- Tilli, C.M., Ramaekers, F.C., Broers, J.L., Hutchison, C.J., and Neumann, H.A. (2003). Lamin expression in normal human skin, actinic keratosis, squamous cell carcinoma and basal cell carcinoma. Br J Dermatol *148*, 102-109.
- Tondera, D., Czauderna, F., Paulick, K., Schwarzer, R., Kaufmann, J., and Santel, A. (2005). The mitochondrial protein MTP18 contributes to mitochondrial fission in mammalian cells. J Cell Sci *118*, 3049-3059.
- Tiranti, V., Hoertnagel, K., Carrozzo, R., Galimberti, C., Munaro, M., Granatiero, M., Zelante, L., Gasparini, P., Marzella, R., Rocchi, M., Bayona-Bafaluy, M.P., Enriquez, J.A., Uziel, G., Bertini, E., Dionisi-Vici, C., Franco, B., Meitinger, T., and Zeviani, M. (1998). Mutations of SURF-1 in Leigh disease associated with cytochrome c oxidase deficiency. Am J Hum Genet *63*, 1609-1621.
- Trounce, I., Byrne, E., and Marzuki, S. (1989). Decline in skeletal muscle mitochondrial respiratory chain function: possible factor in ageing. Lancet *1*, 637-639.

- Tsukihara, T., Aoyama, H., Yamashita, E., Tomizaki, T., Yamaguchi, H., Shinzawa-Itoh, K., Nakashima, R., Yaono, R., and Yoshikawa, S. (1996). The whole structure of the 13-subunit oxidized cytochrome c oxidase at 2.8 A. Science *272*, 1136-1144.
- Vaillant, D.C., and Paulin-Levasseur, M. (2008). Evaluation of mammalian cell-free systems of nuclear disassembly and assembly. J Histochem Cytochem *56*, 157-173.
- Valko, M., Rhodes, C.J., Moncol, J., Izakovic, M., and Mazur, M. (2006). Free radicals, metals and antioxidants in oxidative stress-induced cancer. Chem Biol Interact *160*, 1-40.
- Valnot, I., Osmond, S., Gigarel, N., Mehaye, B., Amiel, J., Cormier-Daire, V., Munnich, A., Bonnefont, J.P., Rustin, P., and Rotig, A. (2000a). Mutations of the SCO1 gene in mitochondrial cytochrome c oxidase deficiency with neonatal-onset hepatic failure and encephalopathy. Am J Hum Genet *67*, 1104-1109.
- Valnot, I., von Kleist-Retzow, J.C., Barrientos, A., Gorbatyuk, M., Taanman, J.W., Mehaye, B., Rustin, P., Tzagoloff, A., Munnich, A., and Rotig, A. (2000b). A mutation in the human heme A:farnesyltransferase gene (COX10) causes cytochrome c oxidase deficiency. Hum Mol Genet *9*, 1245-1249.
- van der Bliek, A.M. (2000). A mitochondrial division apparatus takes shape. J Cell Biol *151*, F1-4.
- van der Walt, J.M., Nicodemus, K.K., Martin, E.R., Scott, W.K., Nance, M.A., Watts, R.L., Hubble, J.P., Haines, J.L., Koller, W.C., Lyons, K., Pahwa, R., Stern, M.B., Colcher, A., Hiner, B.C., Jankovic, J., Ondo, W.G., Allen, F.H., Jr., Goetz, C.G., Small, G.W., Mastaglia, F., Stajich, J.M., McLaurin, A.C., Middleton, L.T., Scott, B.L., Schmechel, D.E., Pericak-Vance, M.A., and Vance, J.M. (2003). Mitochondrial polymorphisms significantly reduce the risk of Parkinson disease. Am J Hum Genet *72*, 804-811.
- Venables, R.S., McLean, S., Luny, D., Moteleb, E., Morley, S., Quinlan, R.A., Lane, E.B., and Hutchison, C.J. (2001). Expression of individual lamins in basal cell carcinomas of the skin. Br J Cancer *84*, 512-519.
- Verma, M., Kagan, J., Sidransky, D., and Srivastava, S. (2003). Proteomic analysis of cancer-cell mitochondria. Nat Rev Cancer *3*, 789-795.
- Verstraeten, V.L., Caputo, S., van Steensel, M.A., Duband-Goulet, I., Zinn-Justin, S., Kamps, M., Kuijpers, H.J., Ostlund, C., Worman, H.J., Briede, J.J., Le Dour, C., Marcelis, C.L., van Geel, M., Steijlen, P.M., van den Wijngaard, A., Ramaekers, F.C., and Broers, J.L. (2009). The R439C mutation in LMNA causes lamin oligomerisation and susceptibility to oxidative stress. J Cell Mol Med.
- Vigouroux, C., Auclair, M., Dubosclard, E., Pouchelet, M., Capeau, J., Courvalin, J.C., and Buendia, B. (2001). Nuclear envelope disorganization in fibroblasts from lipodystrophic patients with heterozygous R482Q/W mutations in the lamin A/C gene. J Cell Sci *114*, 4459-4468.
- Vigouroux, C., and Capeau, J. (2005). A-type lamin-linked lipodystrophies. Novartis Found Symp *264*, 166-177; discussion 177-182, 227-130.
- Vila, M., and Przedborski, S. (2003). Targeting programmed cell death in neurodegenerative diseases. Nat Rev Neurosci *4*, 365-375.

- Vindis, C., Elbaz, M., Escargueil-Blanc, I., Auge, N., Heniquez, A., Thiers, J.C., Negre-Salvayre, A., and Salvayre, R. (2005). Two distinct calcium-dependent mitochondrial pathways are involved in oxidized LDL-induced apoptosis. Arterioscler Thromb Vasc Biol *25*, 639-645.
- Wallace, D.C. (1999). Mitochondrial diseases in man and mouse. Science *283*, 1482-1488.
- Wallace, D.C. (2005). Mitochondria and cancer: Warburg addressed. Cold Spring Harb Symp Quant Biol *70*, 363-374.
- Wang, X., McCullough, K.D., Franke, T.F., and Holbrook, N.J. (2000). Epidermal growth factor receptor-dependent Akt activation by oxidative stress enhances cell survival. J Biol Chem *275*, 14624-14631.
- Weber, J. (2006). ATP synthase: subunit-subunit interactions in the stator stalk. Biochim Biophys Acta *1757*, 1162-1170.
- Wielburski, A., Kuzela, S., and Nelson, B.D. (1982). Studies on the assembly of cytochrome oxidase in isolated rat hepatocytes. Biochem J *204*, 239-245.
- Wielburski, A., and Nelson, B.D. (1983). Evidence for the sequential assembly of cytochrome oxidase subunits in rat liver mitochondria. Biochem J *212*, 829-834.
- Wikstrom, M. (2000). Proton translocation by cytochrome c oxidase: a rejoinder to recent criticism. Biochemistry *39*, 3515-3519.
- Wiese, C., Goldberg, M.W., Allen, T.D., and Wilson, K.L. (1997). Nuclear envelope assembly in Xenopus extracts visualized by scanning EM reveals a transport-dependent 'envelope smoothing' event. J Cell Sci *110 (Pt 13)*, 1489-1502.
- Wilhelmsen, K., Litjens, S.H., Kuikman, I., Tshimbalanga, N., Janssen, H., van den Bout, I., Raymond, K., and Sonnenberg, A. (2005). Nesprin-3, a novel outer nuclear membrane protein, associates with the cytoskeletal linker protein plectin. J Cell Biol *171*, 799-810.
- Williams, S.L., Valnot, I., Rustin, P., and Taanman, J.W. (2004). Cytochrome c oxidase subassemblies in fibroblast cultures from patients carrying mutations in COX10, SCO1, or SURF1. J Biol Chem *279*, 7462-7469.
- Willis, N.D., Cox, T.R., Rahman-Casans, S.F., Smits, K., Przyborski, S.A., van den Brandt, P., van Engeland, M., Weijenberg, M., Wilson, R.G., de Bruine, A., and Hutchison, C.J. (2008). Lamin A/C is a risk biomarker in colorectal cancer. PLoS ONE *3*, e2988.
- Willsie, J.K., and Clegg, J.S. (2002). Small heat shock protein p26 associates with nuclear lamins and HSP70 in nuclei and nuclear matrix fractions from stressed cells. J Cell Biochem *84*, 601-614.
- Wilson, F.H., Hariri, A., Farhi, A., Zhao, H., Petersen, K.F., Toka, H.R., Nelson-Williams, C., Raja, K.M., Kashgarian, M., Shulman, G.I., Scheinman, S.J., and Lifton, R.P. (2004). A cluster of metabolic defects caused by mutation in a mitochondrial tRNA. Science *306*, 1190-1194.
- Wilson, K.L., Zastrow, M.S., and Lee, K.K. (2001). Lamins and disease: insights into nuclear infrastructure. Cell *104*, 647-650.
- Worman, H.J., and Courvalin, J.C. (2002). The nuclear lamina and inherited disease. Trends Cell Biol *12*, 591-598.

- Worman, H.J., and Courvalin, J.C. (2004). How do mutations in lamins A and C cause disease? J Clin Invest *113*, 349-351.
- Wredenberg, A., Wibom, R., Wilhelmsson, H., Graff, C., Wiener, H.H., Burden, S.J., Oldfors, A., Westerblad, H., and Larsson, N.G. (2002). Increased mitochondrial mass in mitochondrial myopathy mice. Proc Natl Acad Sci U S A *99*, 15066-15071.
- Yakes, F.M., and Van Houten, B. (1997). Mitochondrial DNA damage is more extensive and persists longer than nuclear DNA damage in human cells following oxidative stress. Proc Natl Acad Sci U S A *94*, 514-519.
- Yang, L., Guan, T., and Gerace, L. (1997a). Integral membrane proteins of the nuclear envelope are dispersed throughout the endoplasmic reticulum during mitosis. J Cell Biol *137*, 1199-1210.
- Yang, L., Guan, T., and Gerace, L. (1997b). Lamin-binding fragment of LAP2 inhibits increase in nuclear volume during the cell cycle and progression into S phase. J Cell Biol *139*, 1077-1087.
- Yao, J., and Shoubridge, E.A. (1999). Expression and functional analysis of SURF1 in Leigh syndrome patients with cytochrome c oxidase deficiency. Hum Mol Genet *8*, 2541-2549.
- Yorifuji, H., Tadano, Y., Tsuchiya, Y., Ogawa, M., Goto, K., Umetani, A., Asaka, Y., and Arahata, K. (1997). Emerin, deficiency of which causes Emery-Dreifuss muscular dystrophy, is localized at the inner nuclear membrane. Neurogenetics *1*, 135-140.
- Yoshikawa, S., Shinzawa-Itoh, K., and Tsukihara, T. (1998). Crystal structure of bovine heart cytochrome c oxidase at 2.8 A resolution. J Bioenerg Biomembr *30*, 7-14.
- Yu, J., Zhang, L., Hwang, P.M., Rago, C., Kinzler, K.W., and Vogelstein, B. (1999). Identification and classification of p53-regulated genes. Proc Natl Acad Sci U S A *96*, 14517-14522.
- Young, J., Morbois-Trabut, L., Couzinet, B., Lascols, O., Dion, E., Bereziat, V., Feve, B., Richard, I., Capeau, J., Chanson, P., and Vigouroux, C. (2005). Type A insulin resistance syndrome revealing a novel lamin A mutation. Diabetes *54*, 1873-1878.
- Young, S.G., Meta, M., Yang, S.H., and Fong, L.G. (2006). Prelamin A farnesylation and progeroid syndromes. J Biol Chem *281*, 39741-39745.
- Zastrow, M.S., Vlcek, S., and Wilson, K.L. (2004). Proteins that bind A-type lamins: integrating isolated clues. J Cell Sci *117*, 979-987.
- Zermati, Y., Garrido, C., Amsellem, S., Fishelson, S., Bouscary, D., Valensi, F., Varet, B., Solary, E., and Hermine, O. (2001). Caspase activation is required for terminal erythroid differentiation. J Exp Med *193*, 247-254.
- Zhang, Q., Ragnauth, C.D., Skepper, J.N., Worth, N.F., Warren, D.T., Roberts, R.G., Weissberg, P.L., Ellis, J.A., and Shanahan, C.M. (2005). Nesprin-2 is a multi-isomeric protein that binds lamin and emerin at the nuclear envelope and forms a subcellular network in skeletal muscle. J Cell Sci *118*, 673-687.
- Zhang, X., Sejas, D.P., Qiu, Y., Williams, D.A., and Pang, Q. (2007). Inflammatory ROS promote and cooperate with the Fanconi anemia mutation for hematopoietic senescence. J Cell Sci *120*, 1572-1583.

- Zhang, Y., McLaughlin, R., Goodyer, C., and LeBlanc, A. (2002). Selective cytotoxicity of intracellular amyloid beta peptide1-42 through p53 and Bax in cultured primary human neurons. J Cell Biol *156*, 519-529.
- Zhang, Y.Q., and Sarge, K.D. (2008). Sumoylation regulates lamin A function and is lost in lamin A mutants associated with familial cardiomyopathies. J Cell Biol *182*, 35-39.
- Zhou, S., Kachhap, S., and Singh, K.K. (2003). Mitochondrial impairment in p53-deficient human cancer cells. Mutagenesis *18*, 287-292.
- Zhu, X., Lee, H.G., Casadesus, G., Avila, J., Drew, K., Perry, G., and Smith, M.A. (2005). Oxidative imbalance in Alzheimer's disease. Mol Neurobiol *31*, 205-217.
- Zhu, X., Smith, M.A., Honda, K., Aliev, G., Moreira, P.I., Nunomura, A., Casadesus, G., Harris, P.L., Siedlak, S.L., and Perry, G. (2007). Vascular oxidative stress in Alzheimer disease. J Neurol Sci *257*, 240-246.
- Zhu, Z., Yao, J., Johns, T., Fu, K., De Bie, I., Macmillan, C., Cuthbert, A.P., Newbold, R.F., Wang, J., Chevrette, M., Brown, G.K., Brown, R.M., and Shoubridge, E.A. (1998). SURF1, encoding a factor involved in the biogenesis of cytochrome c oxidase, is mutated in Leigh syndrome. Nat Genet *20*, 337-343.
- Zuchner, S., Mersiyanova, I.V., Muglia, M., Bissar-Tadmouri, N., Rochelle, J., Dadali, E.L., Zappia, M., Nelis, E., Patitucci, A., Senderek, J., Parman, Y., Evgrafov, O., Jonghe, P.D., Takahashi, Y., Tsuji, S., Pericak-Vance, M.A., Quattrone, A., Battaloglu, E., Polyakov, A.V., Timmerman, V., Schroder, J.M., and Vance, J.M. (2004). Mutations in the mitochondrial GTPase mitofusin 2 cause Charcot-Marie-Tooth neuropathy type 2A. Nat Genet *36*, 449-451.